SOME PHYSICS RESULTS & BOSE-EINSTEIN CORRELATIONS STUDY AT 13 TeV WITH ATLAS

BEC@13: ATL-COM-PHYS-2016-1621; ATL-COM-PHYS-2018-044

Yuri Kulchitsky[1),2)], Pavel Tsiareshka[1),2)]

[1)] Institute of Physics, National Academy of Sciences of Belarus, Minsk, Belarus
[2)] JINR, Dubna, Russia

27.02.2018, LHC Days in Belarus 2018, Minsk, Belarus

A TOROIDAL LHC APPARATUS (ATLAS)

Muon spectrometer

(*μ Trigger/tracking and Toroid Magnets*)

Precision Tracking:

- **MDT** (Monitored Drift Tubes)
- **CSC** (Cathode Strip Chambers) |η| >2.4

Trigger:

- **RPC** (Resistive Plate Chamber) barrel
- **TGC** (Thin Gas Chamber) endcap

Calorimeter: EM and Hadronic energy

- **Liquid Ar** (LAr) EM barrel and End-cap & Hadronic End-cap
- **Tile** calorimeter (Fe-scintillator) Hadronic barrel

Inner Detector (ID)

Tracking; 2T Solenoid Magnet

- **Silicon Pixels** 50 x 400 μm^2
- **Silicon Strips** (SCT) 40 μm rad stereo strips
- **Transition Radiation Tracker** (**TRT**) up to 36 points/track

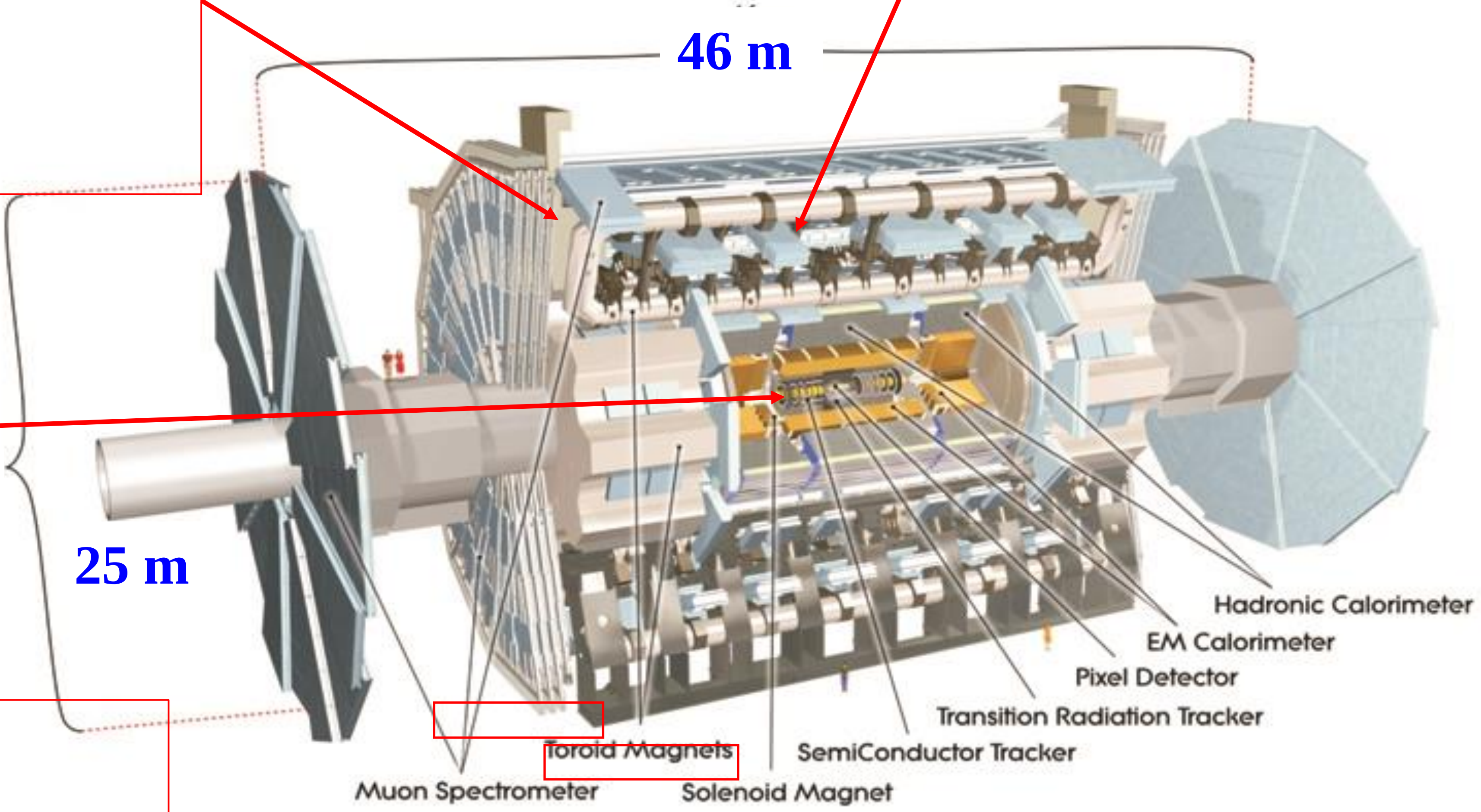

7 000 tons

Two Level Trigger system

- **L1 – hardware**: **100 kHz**, **2.5 μs** latency
- **HLT – farm**: merge the former **L2** and **Event Filter 1.5 kHz**, **0.2 s** latency

STANDARD MODEL

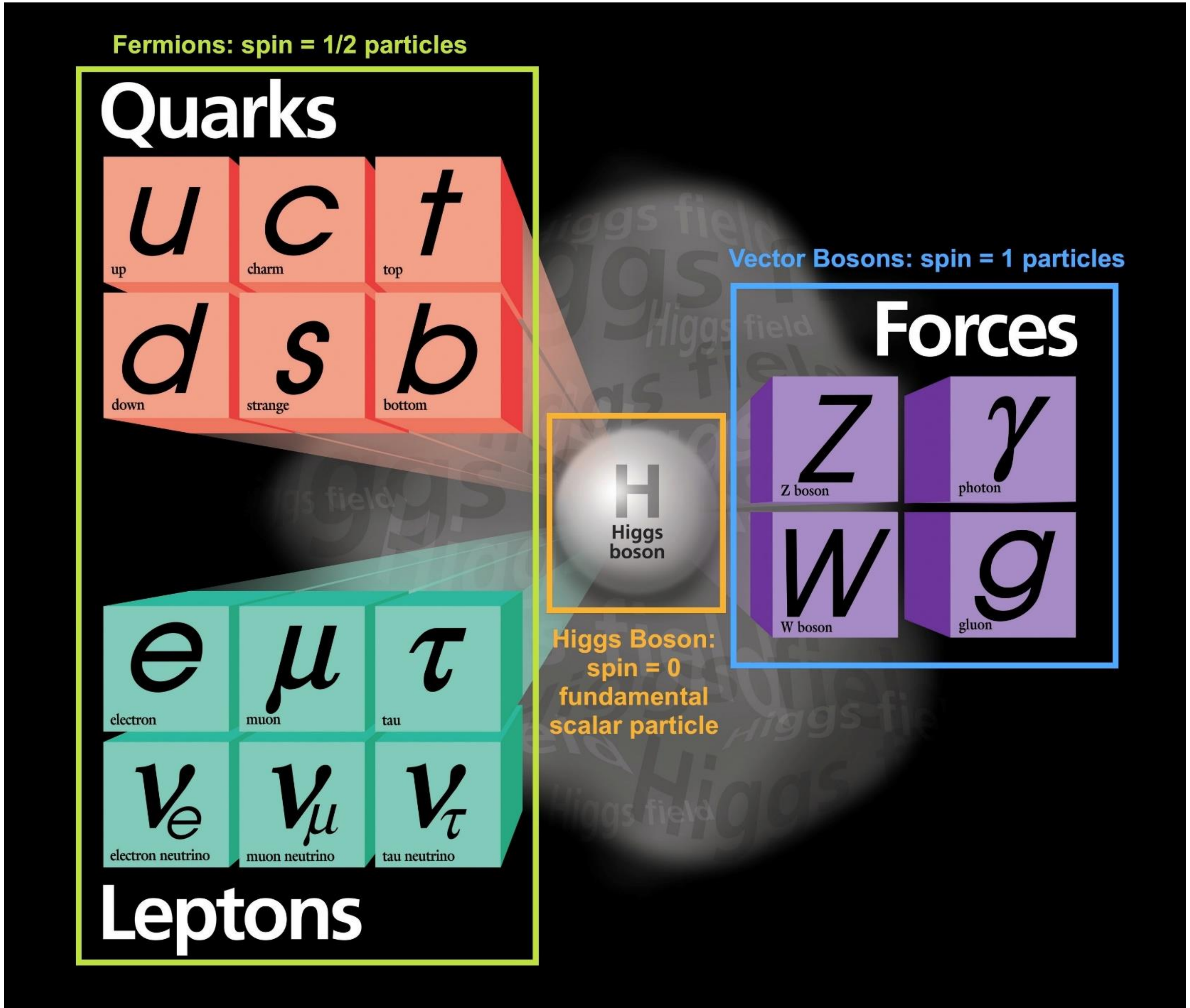

Mass of the Higgs boson was not predicted!

Higgs Decay Channels prediction for Higgs boson mass from 90 to 250 GeV

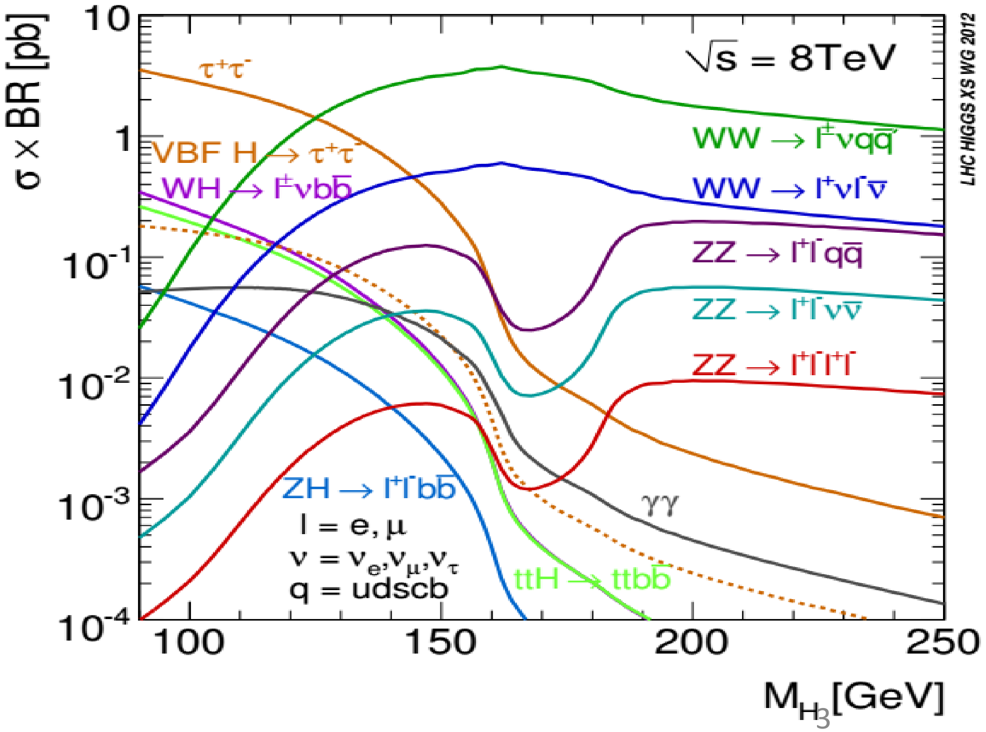

DISCOVERY OF HIGGS BOSON

arxiv:1708.02810
ATLAS-CONF-2017-045
ATLAS-CONF-2017-047

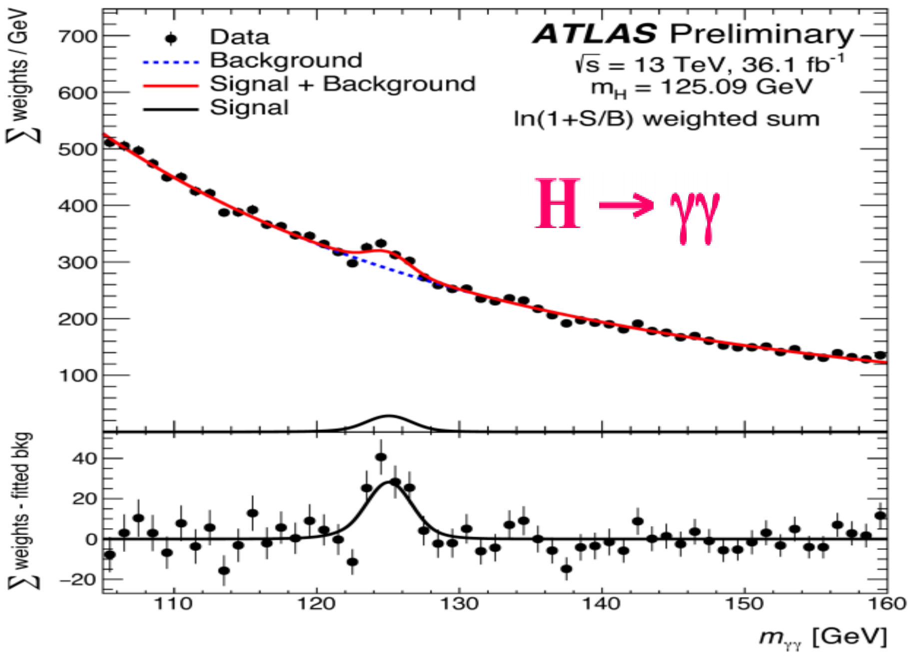

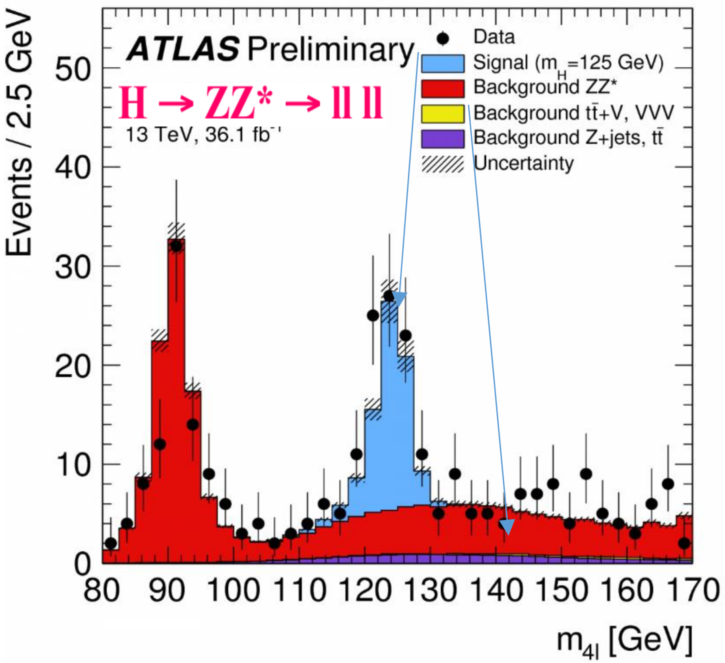

New results in the

- ➢ H→ZZ*→4ℓ &
- ➢ H→γγ channels.
- ➢ Combined measurements of fiducial and total production cross sections (assuming SM branching ratios)

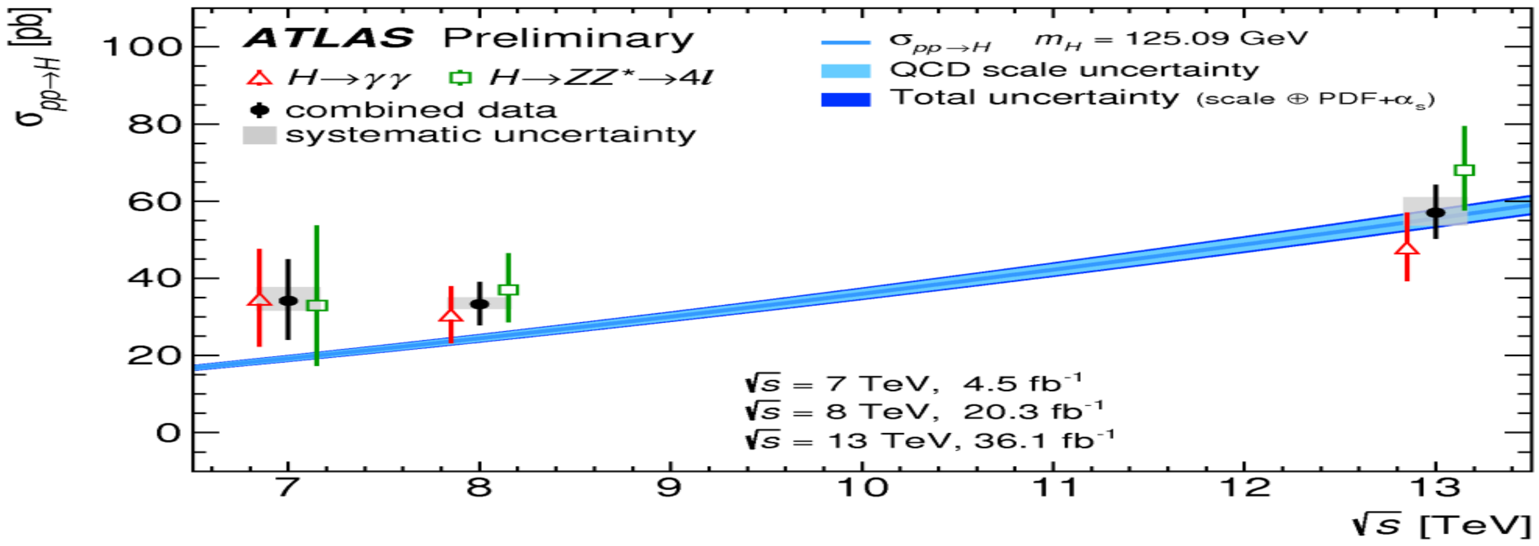

m_H=125.09±0.24 GeV

Combined global signal strength compatible with the Standard Model:

$$\mu = 1.09 \pm 0.12$$
$$= 1.09 \pm 0.09\,(\text{stat.})\,^{+0.06}_{-0.05}\,(\text{exp.})\,^{+0.06}_{-0.05}\,(\text{th.}).$$

Total pp→H+X cross sections measured at √s= 7, 8, and 13 TeV, compared to SM predictions

HIGGS BOSON CROSS SECTIONS

ATLAS-CONF-2017-045
ATLAS-CONF-2017-047

- The increased collision energy and large integrated luminosity provides the opportunity to measure Higgs differential cross sections
- Combinations of measurements in different kinematical regions can be used to probe different production modes, *notably gluon-gluon fusion (ggF), vector boson fusion (VBF)*
- Results also interpreted using new simplified template cross section framework, reducing theoretical systematic uncertainties

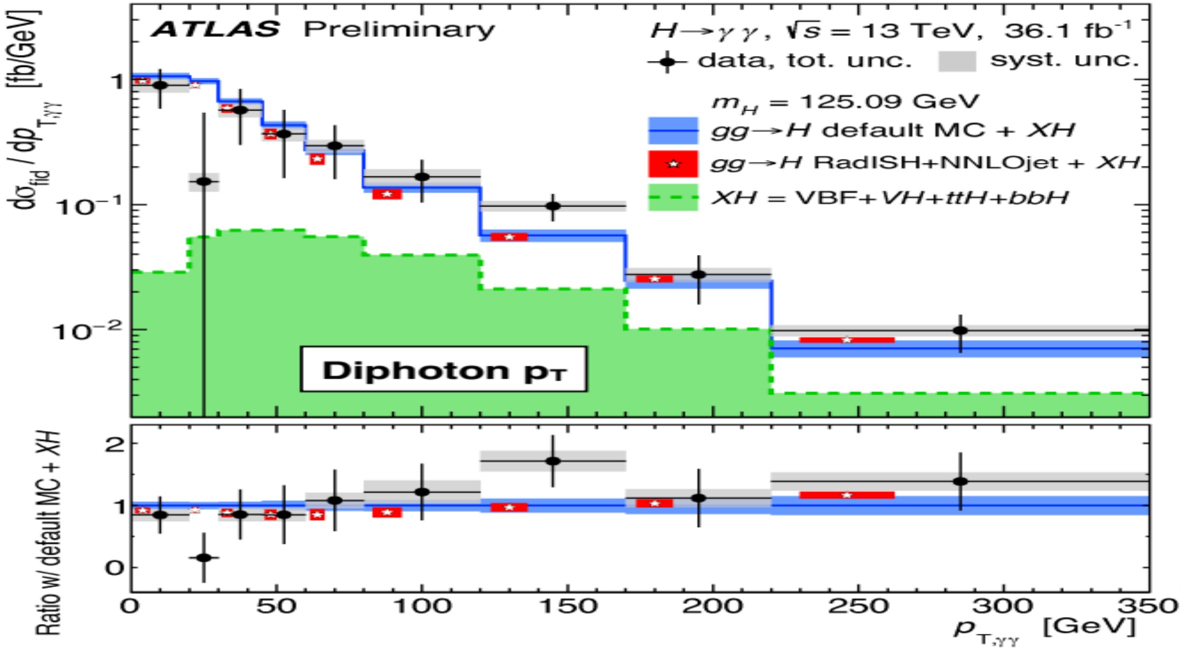

The differential cross section for pp→H→γγ as a function of $p_T^{\gamma\gamma}$ and compared to SM expectation

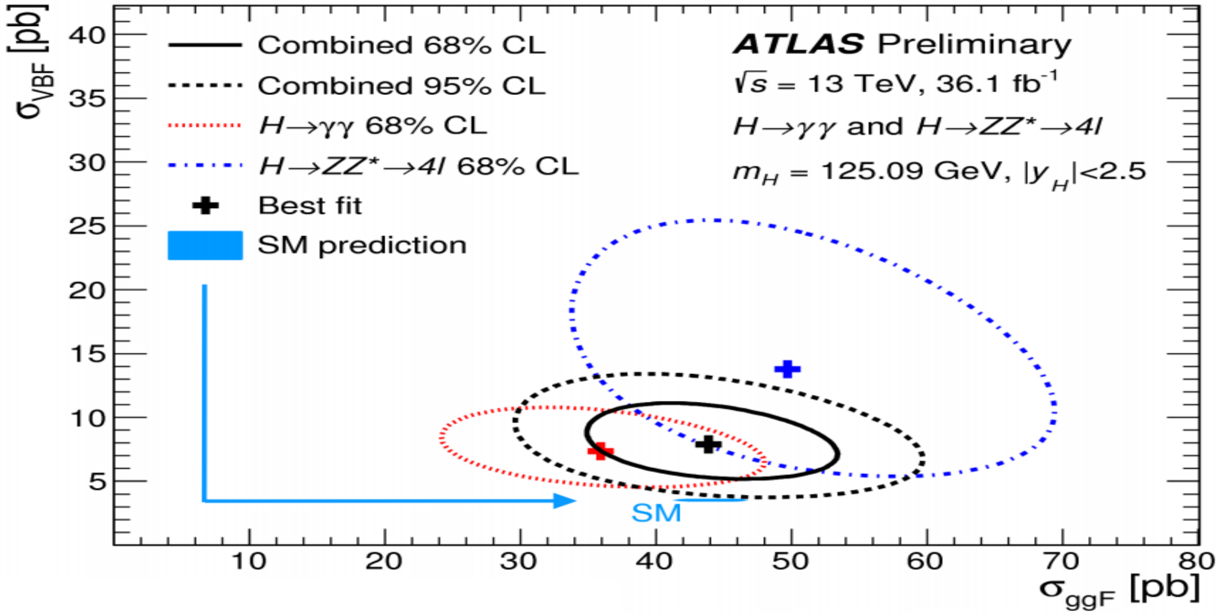

Likelihood contours in σ_{VBF} vs. σ_{ggF} plane in H→γγ (red) and H→ZZ*→4l (blue), their combination (black), SM prediction (light blue)

HIGGS BOSON MASS

ATLAS-CONF-2017-046

- Higgs boson mass measurements in the **H→ ZZ*→4ℓ** & **H→γγ** channels complementary
  - 4ℓ channel the stat uncertainty dominates
  - γγ channel dominated by systematic uncertainties (most notably the γ energy scale calibration)
- Measurements consistent between sub-channels, and consistent with the Run 1 combined result

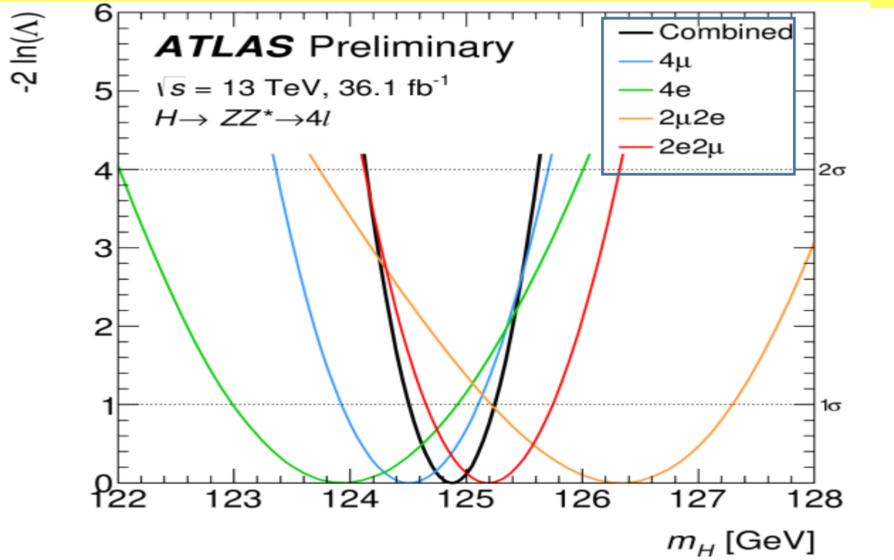

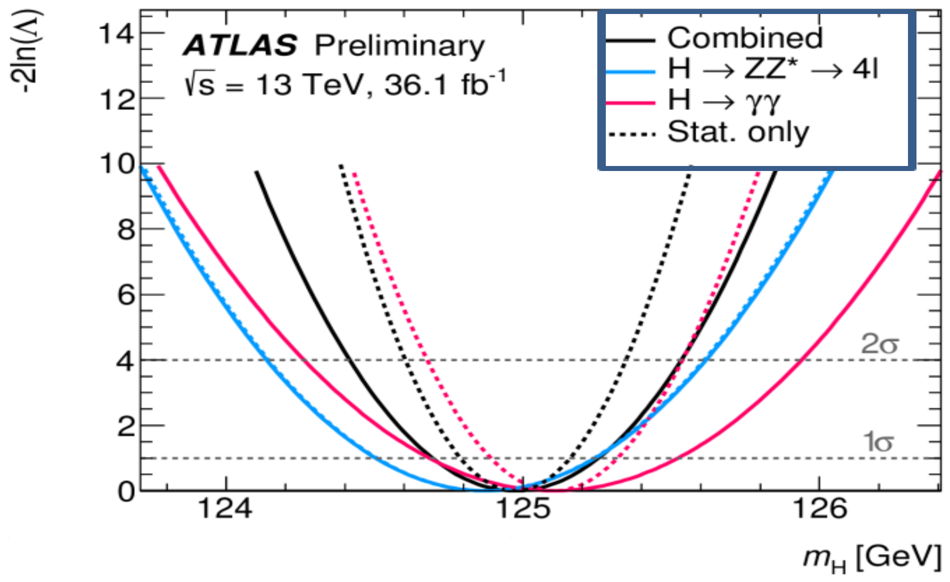

The value of $-2\ln\Lambda$ as a function of m_H for the individual channels & their combination

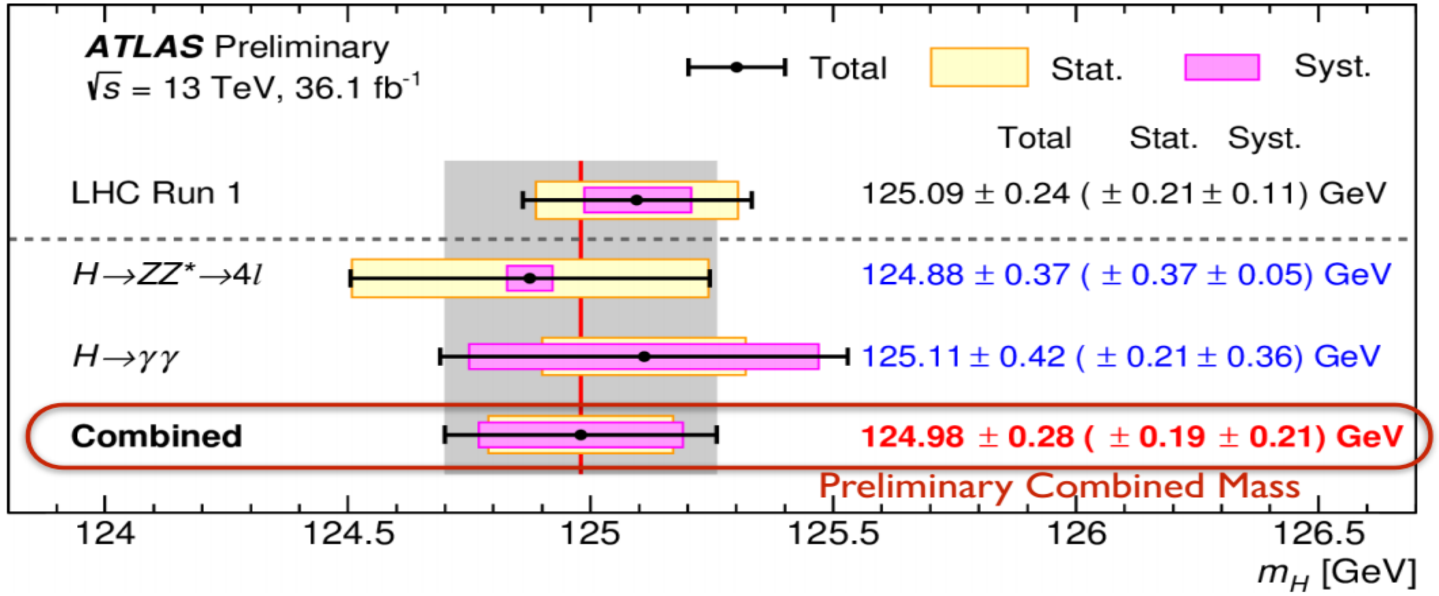

The Higgs boson mass measurements from the individual and combined analyses, compared to the combined *Run 1 measurement by ATLAS & CMS*

Higgs boson production: $q\bar{q} \to W^* \to WH$, $W \to \nu\mu$, $H \to b\bar{b}$

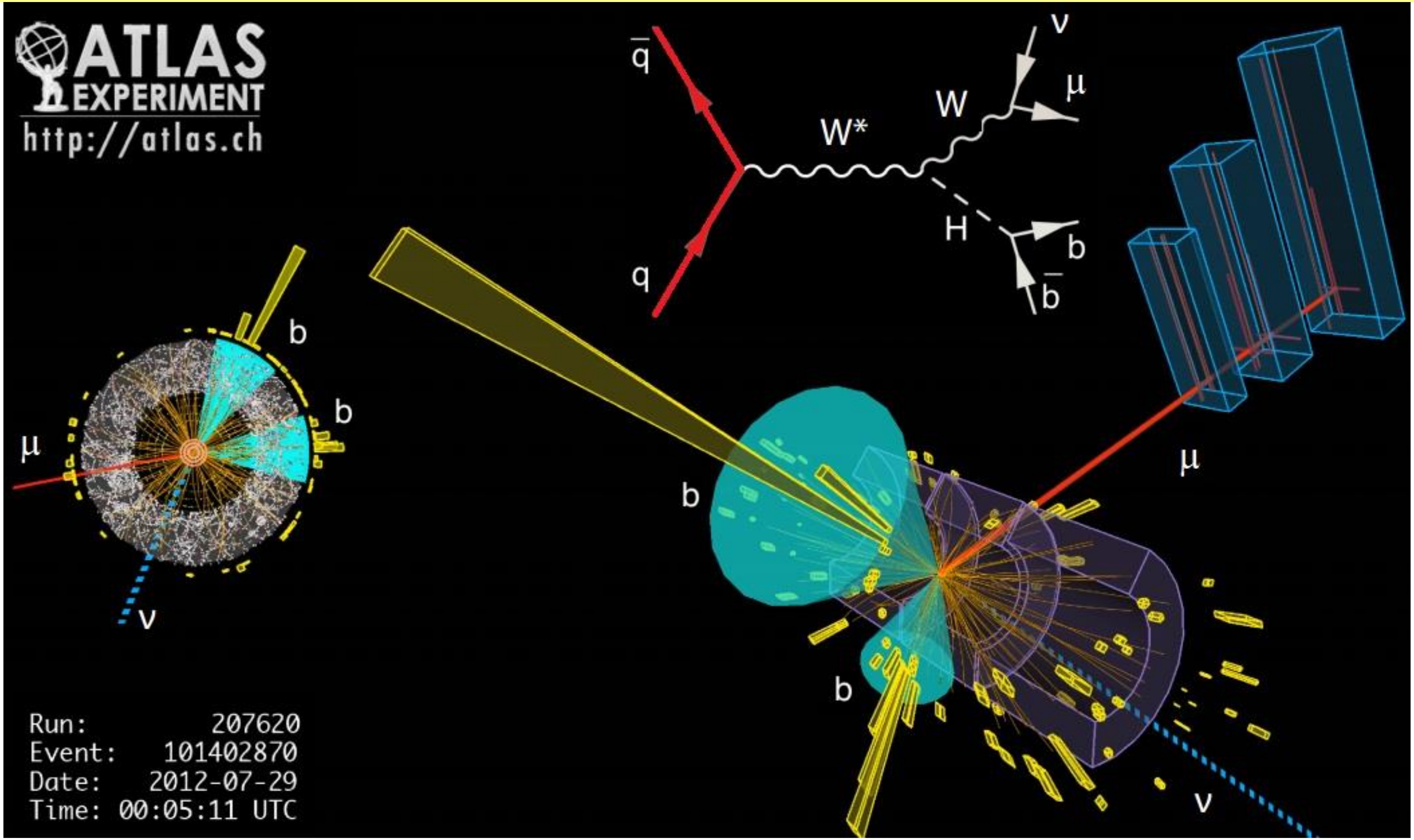

SEARCHES FOR HIGGS BOSON DECAYS TO $\bar{b}b$

arxiv:1708.03299

- Most sensitive channel to look for the decay **H→$\bar{b}$b** is associated production, **VH** (V= W/Z) with **H→ $\bar{b}$b**
- Largest Higgs branching ratio **BR(H→ $\bar{b}$b) ≈ 58%**
- ATLAS analysis combines **Z & W** final states, channels characterized by lepton multiplicity:
  - 2 lepton (Z→ℓℓ), 1-lepton (W→ℓν), 0-lepton (Z→νν)
- Validation of performance and systematics understanding of the Boosted Decision Trees (BDTs) analysis from an independent search for **VZ, Z→ $\bar{b}$b**
- Observed (expected) significance: **5.8σ (5.3σ)**

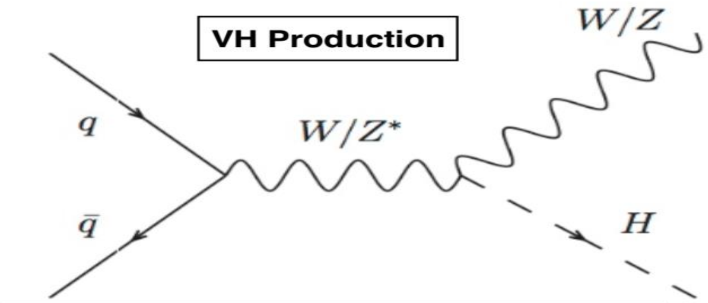

$$\mu_{VZ} = 1.11^{+0.12}_{-0.11}(\text{stat.})^{+0.22}_{-0.19}(\text{syst.})$$

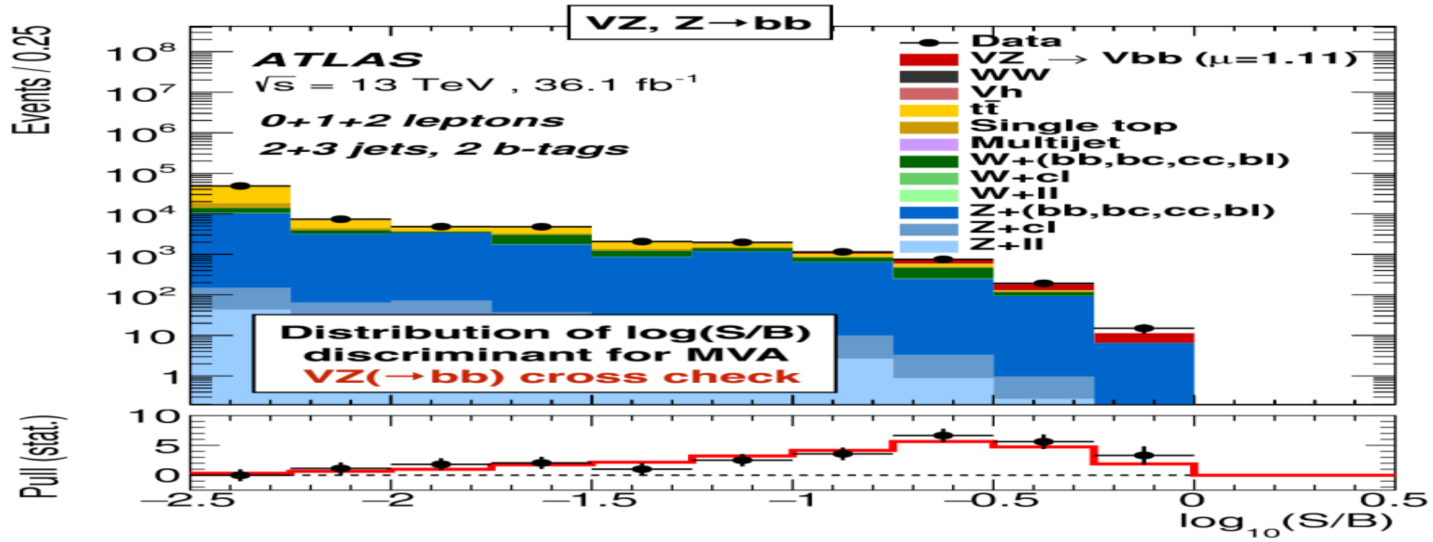

Event yields as a function of $\log_{10}$(S/B) for data, background and a Higgs boson signal with m_H=125 GeV

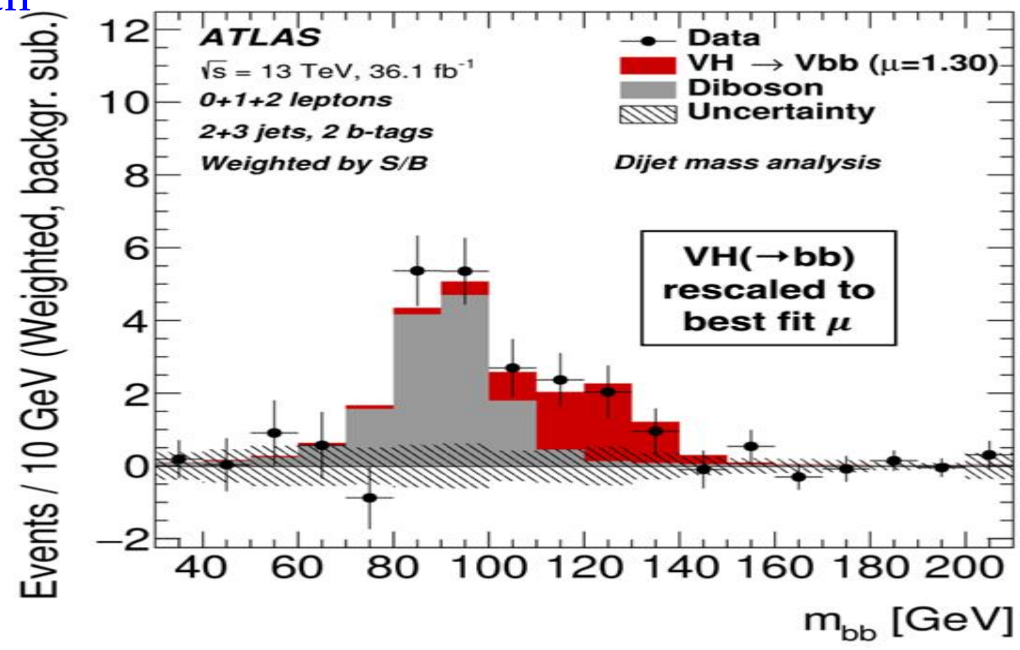

The distribution of m_{bb} after subtraction of backgrounds, except for the *WZ* and *ZZ* dibosons proc.

itsk,

STANDARD MODEL MEASUREMENTS

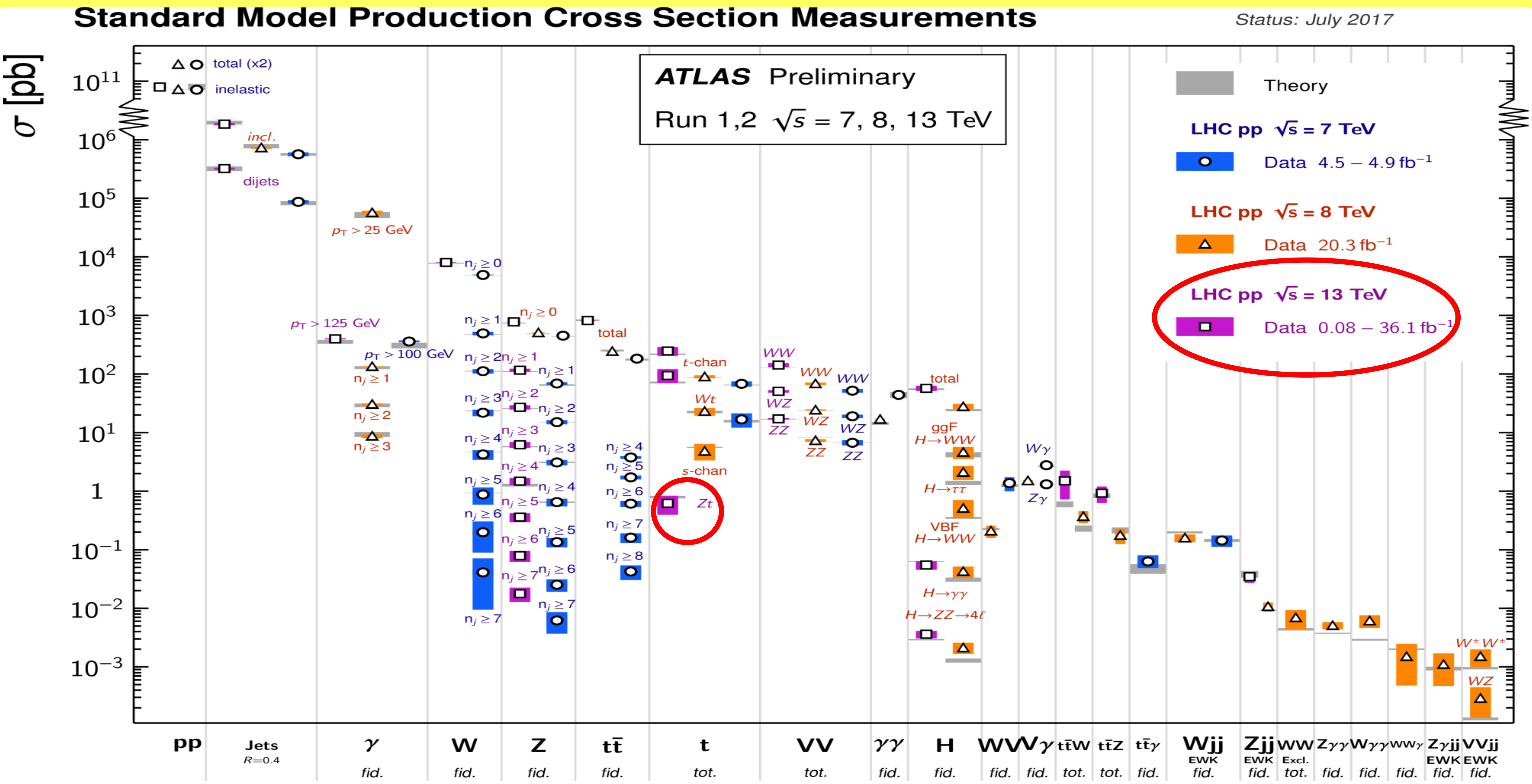

Summary of several **SM total and fiducial production cross section** measurements, corrected for leptonic branching fractions, compared to the theoretical expectations

EVIDENCE FOR Zt PRODUCTION

ATLAS-CONF-2017-052

- Events selected by requiring:
  - 3 identified leptons
  - 2 jets, out of which one should be b-tagged
- **A *Neural Net*** is trained to separate the signal events from the background
- Evidence for **Zt** production:
  - Significance **4.2σ (5.4σ** expected)
  - Cross section **620±170±140 fb**
  - ✓ Consistent with the SM expectation

Evidence of the production of a single t-quark in association with a Z boson in the ***pp→tZq***

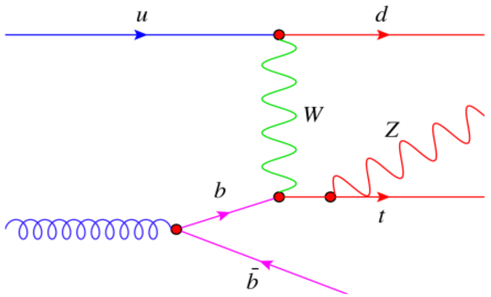

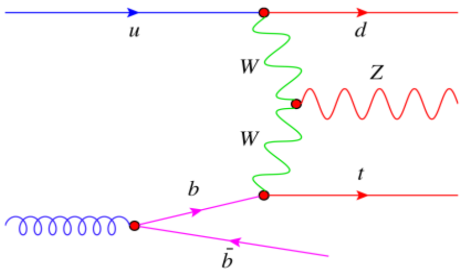

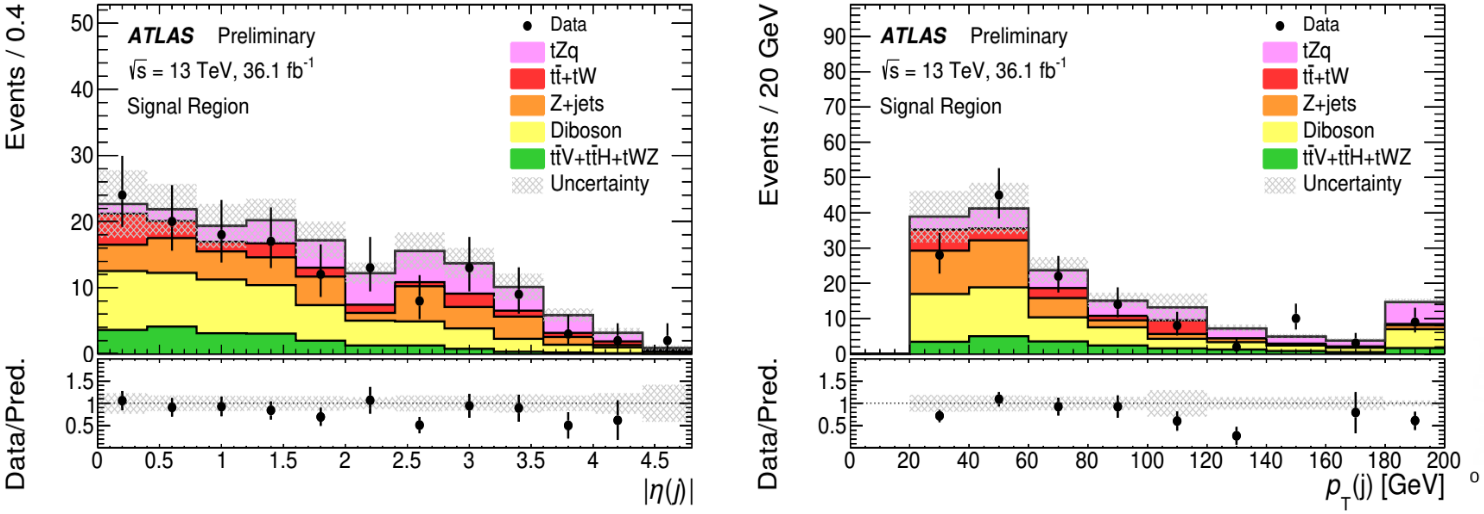

Comparison of Data and Signal + Background model of the neural-network training variables

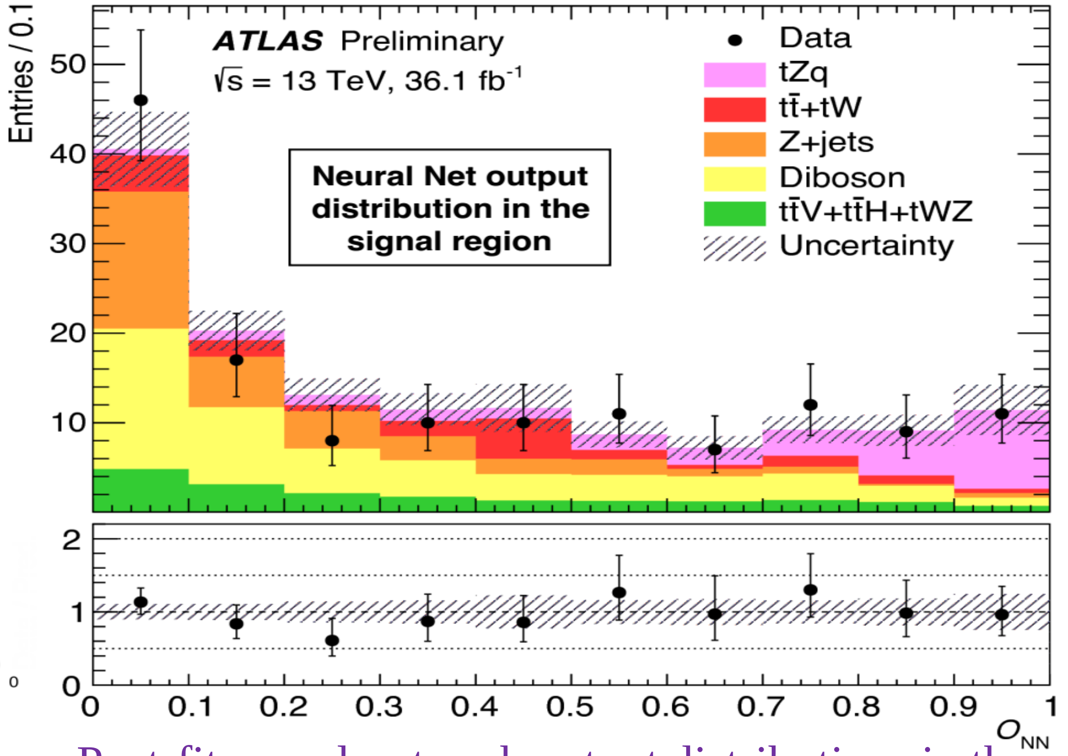

Post-fit neural-network output distributions in the signal region

STANDARD MODEL MEASUREMENTS

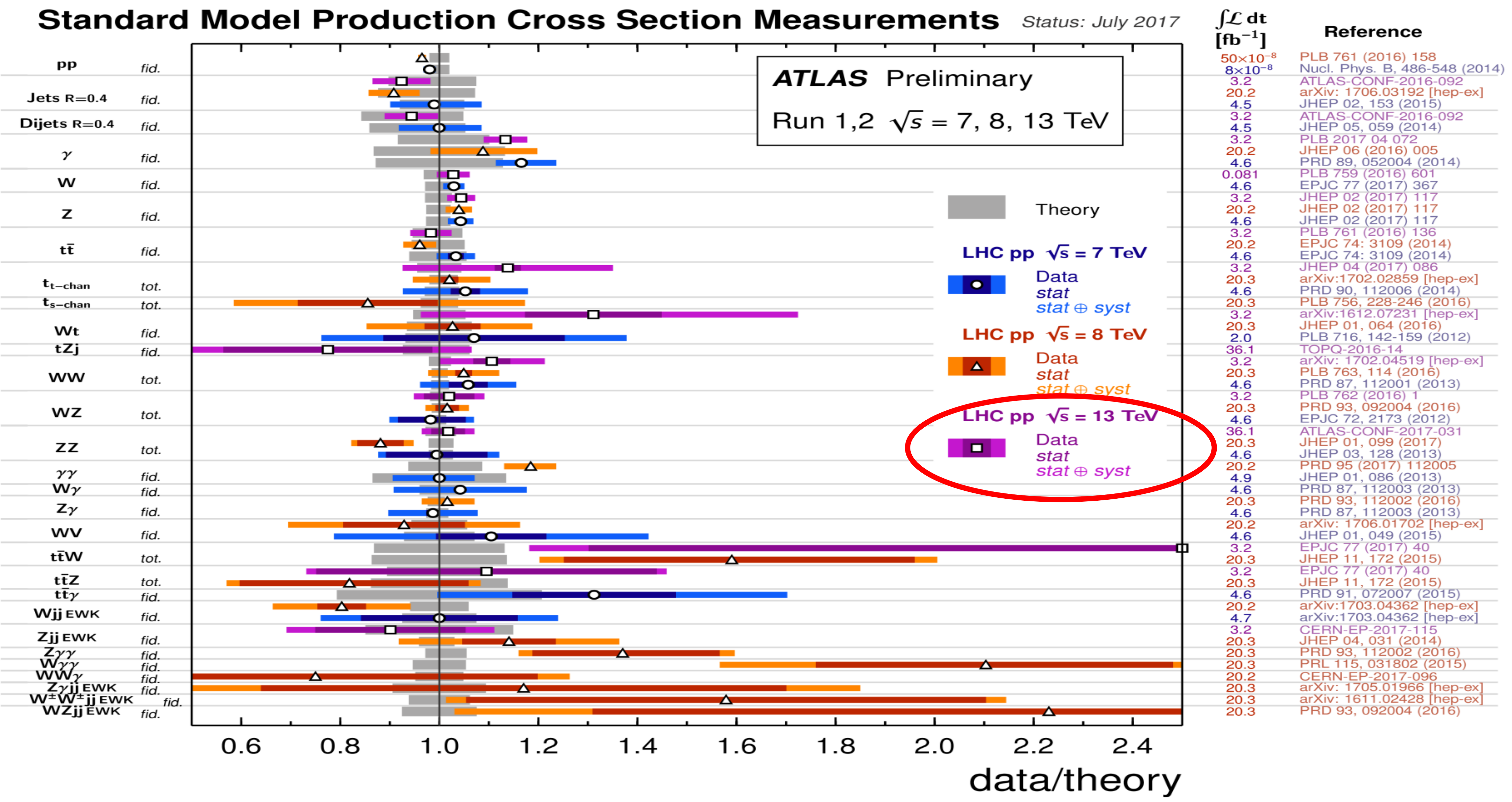

Ratio of SM cross section measurements to theory

STUDY OF MINIMUM-BIAS EVENTS WITH ATLAS

Understanding of soft-QCD interactions has direct impact on

1. **precision measurements**
2. **searches for new physics**

Studies include:

- **Charged-particle distributions in pp interactions at 0.9 – 13 TeV**
- **Bose-Einstein correlations** (BEC)
  - represent a unique probe of the *space-time geometry* of the *hadronization region*
  - allow the *determination the size and shape of the source* from which particles are *emitted*
- **Underlying events distributions in pp interactions**

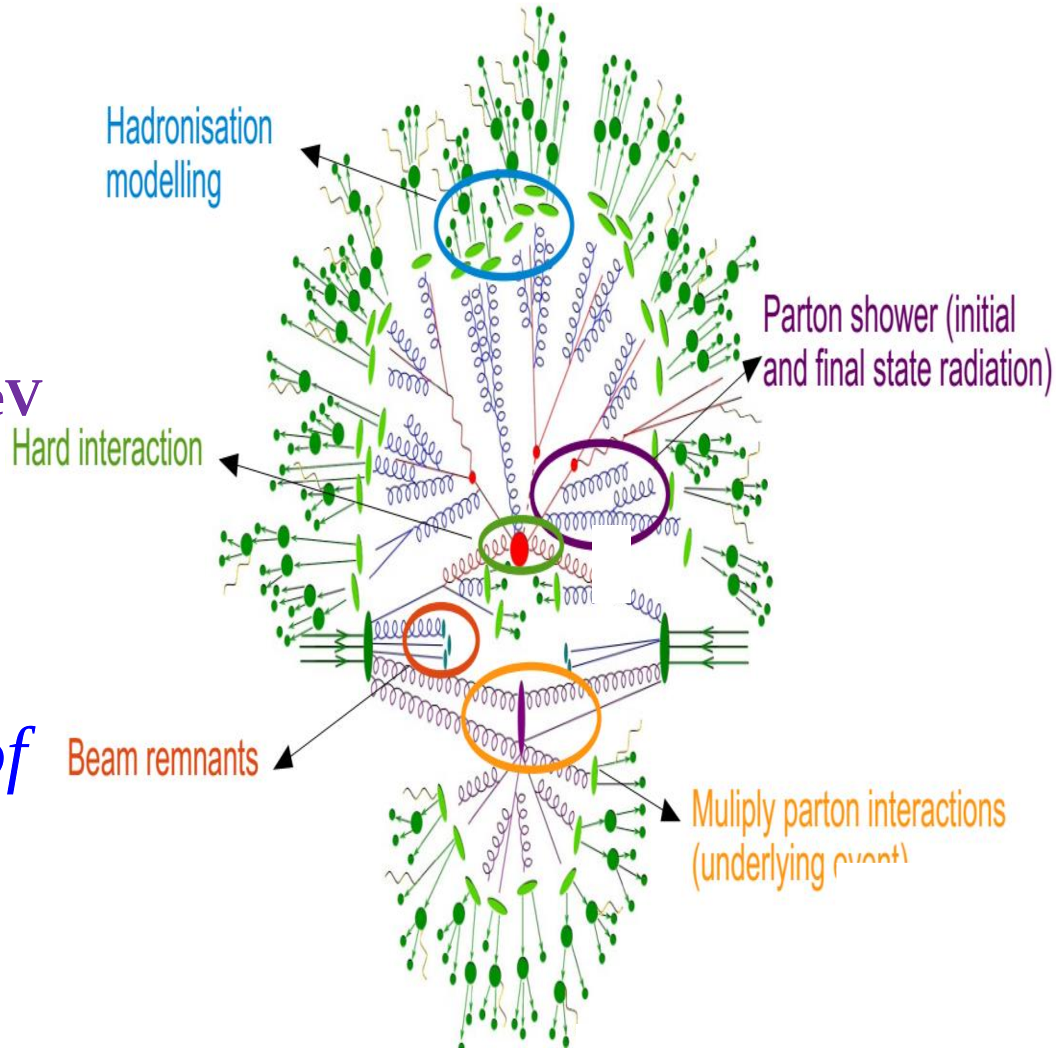

Provides insight into strong interactions in non-perturbative QCD regime:

- Soft QCD results used in Monte-Carlo generators tuning,
- Low energy QCD description essential for simulating multiple pp interactions

EXAMPLE OF VERY-HIGH-MULTIPLICITY EVENT

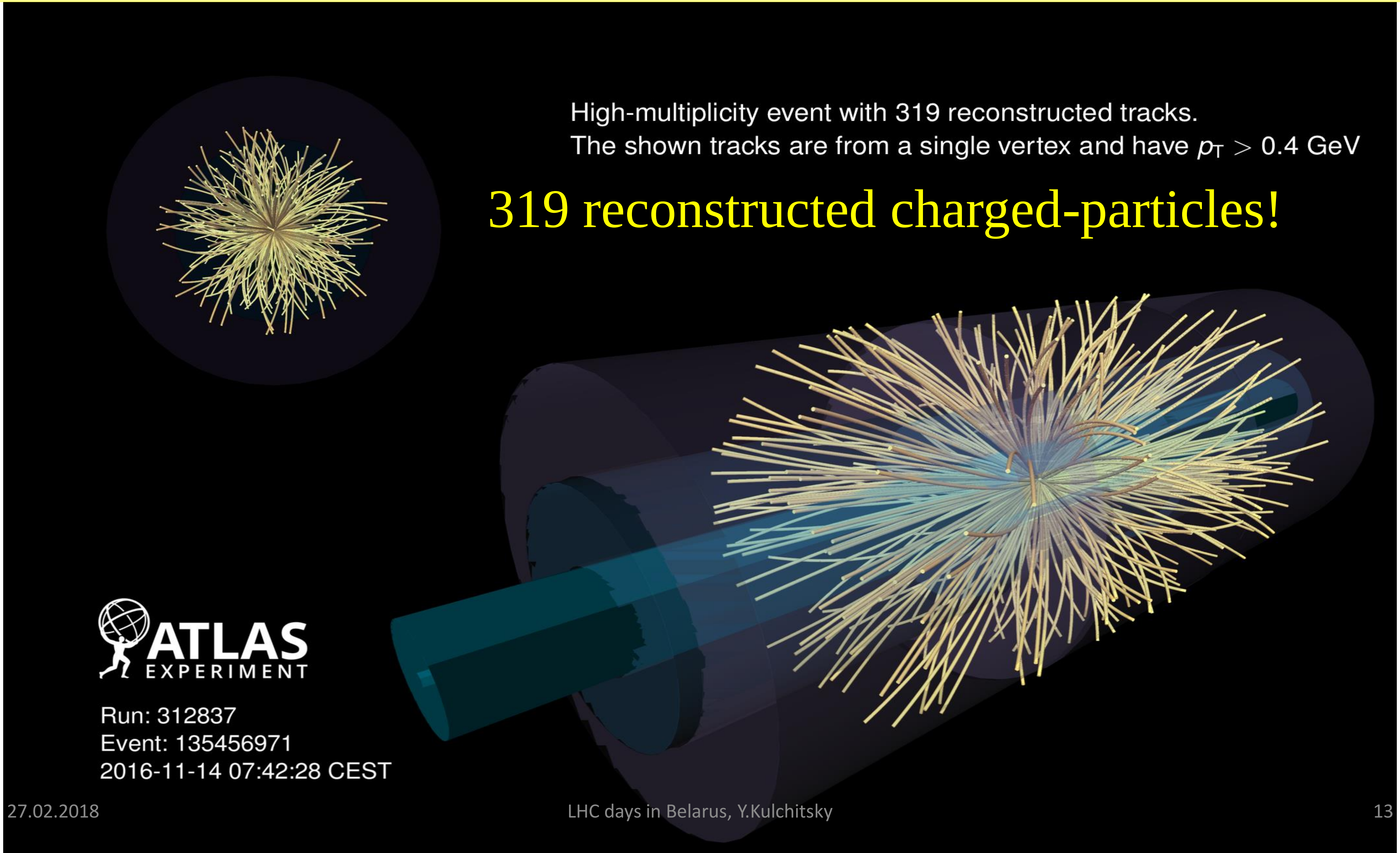

EXAMPLE OF VERY-HIGH-MULTIPLICITY EVENT

319 reconstructed charged-particles

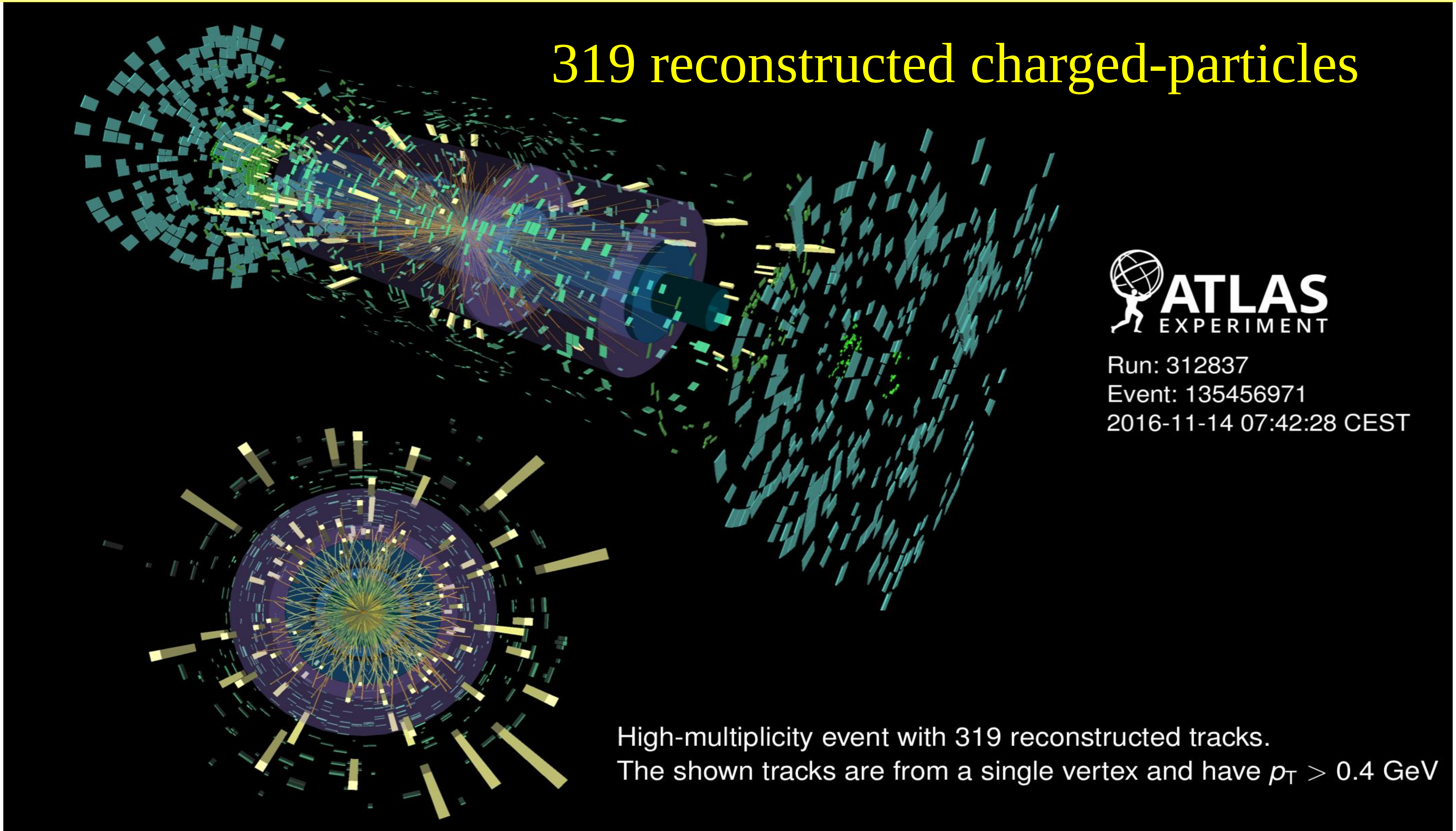

BOSE-EINSTEIN CORRELATIONS

Correlations in phase space **between two identical bosons** from symmetry of wave functions.

► Enhances likelihood of two particles close in phase space

► Allows one to ‘probe’ the source of the bosons in size and shape

► Dependence on particle multiplicity and transverse momentum probes the production mechanism

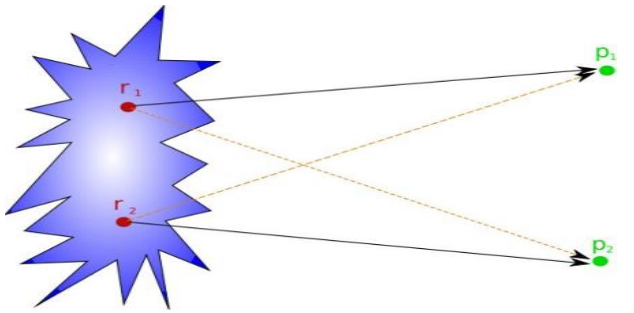

Correlation function $C_2(Q)$ a ratio of probabilities:

$$C_2(Q) = \frac{\rho(p_1, p_2)}{\rho_0(p_1, p_2)} = C_0\left(1+\Omega(\lambda, RQ)\right)\cdot\left(1+Q\varepsilon\right), \quad Q^2 = -(p_1 - p_2)^2$$

$$\Omega^G(\lambda, RQ) = \lambda e^{-R^2Q^2}$$

$$\Omega^E(\lambda, RQ) = \lambda e^{-RQ}$$

$\mathbf{C_0}$ is a normalisation, **ε** accounts for long range effects, **R** is the effective radius parameter of the source, **λ** is the strength of the effect parameter, 0/1 for coherent/chaotic source. Two possible parameterisation: Gaussian and Exponential.

$$C_2(Q) = \frac{N^{++,--}(Q)}{N^{ref}(Q)}$$

$\mathbf{N_{ref}}$ **without BEC effect from:** unlike-charge particles (UCP), opposite hemispheres, event mixing. **Basic Reference**: distribution of UCP pairs of non-identical particle taken from the same event.

$$R_2(Q) = \frac{C_2^{Data}(Q)}{C_2^{MC}(Q)} = \frac{\rho(++,--)\big/\rho(+-)}{\rho^{MC}(++,--)\big/\rho^{MC}(+-)}$$

The studies are carried out using the **double ratio correlation function**. The $\mathbf{R_2(Q)}$ eliminates problems with energy-momentum conservation, topology, resonances etc.
MC without BEC.

HIGH MULTIPLICITY TRACK TRIGGER EFFICIENCY

- High multiplicity track trigger (**HLT_mb_sp900_trk60_hmt_L1MBTS_1_1**) efficiency calculation as difference the HMT trigger to minimum-bias trigger (**L1MBTS_1_1**)

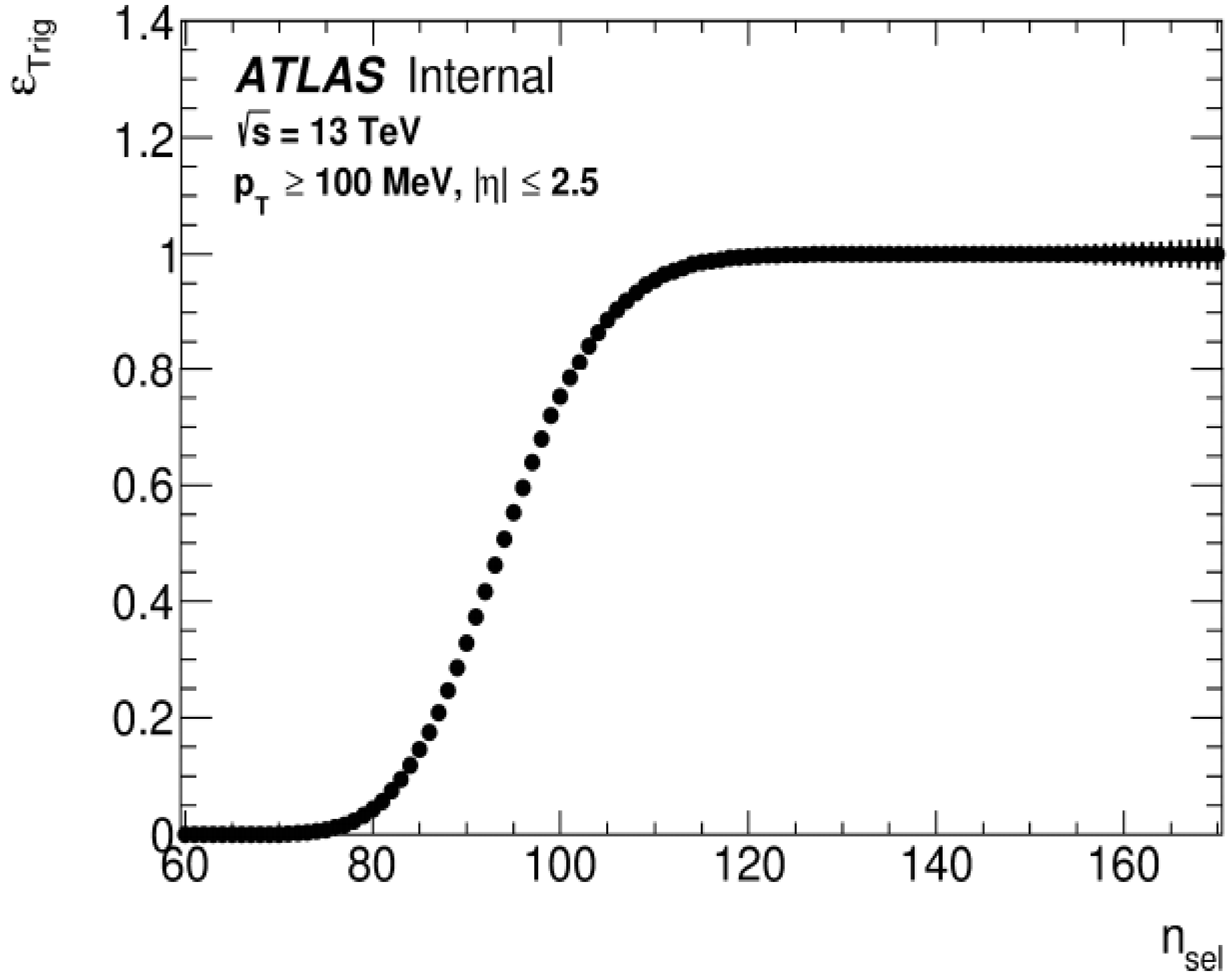

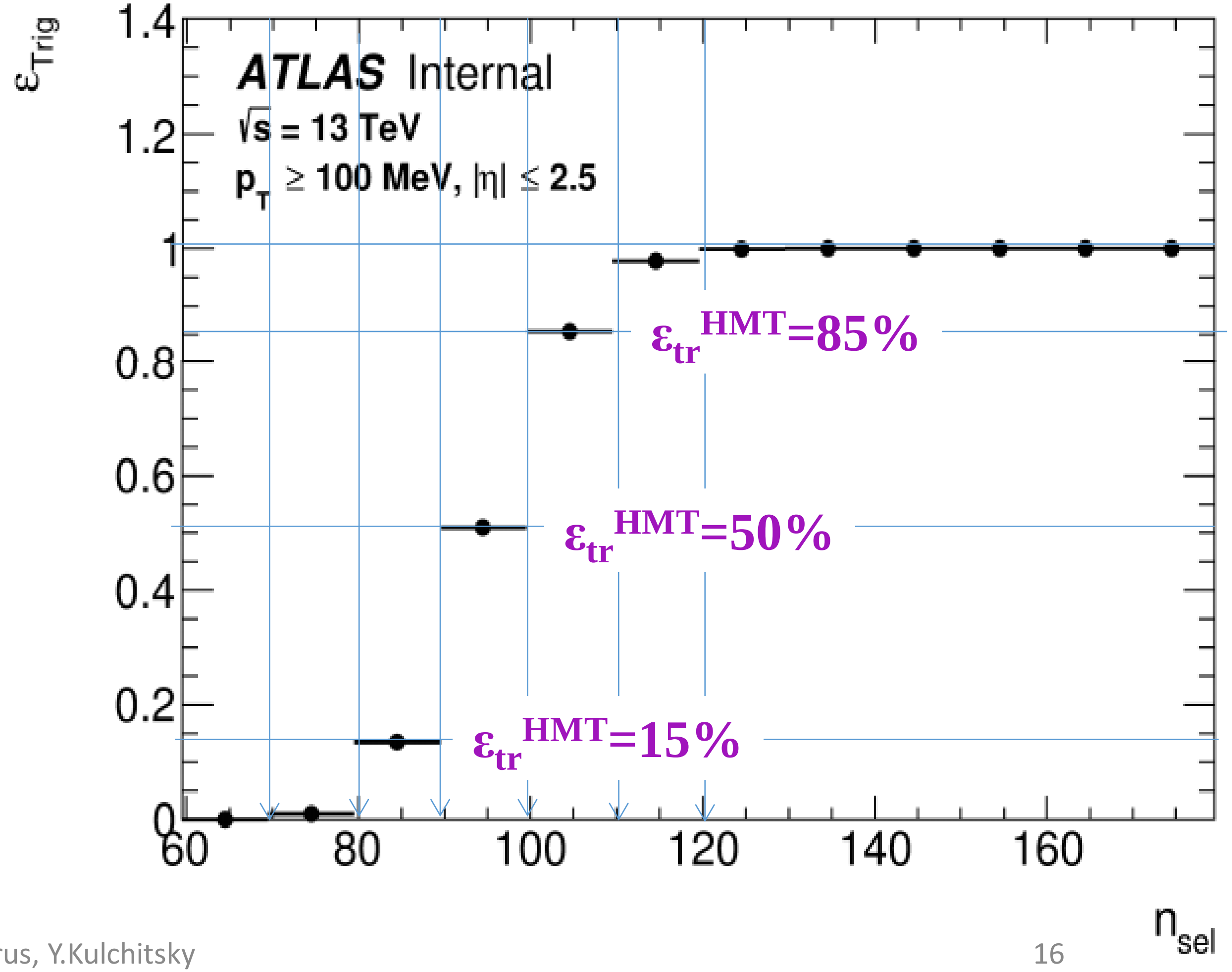

SUMMARY: CORRECTION OF R_2 CORRELATION FUNCTION

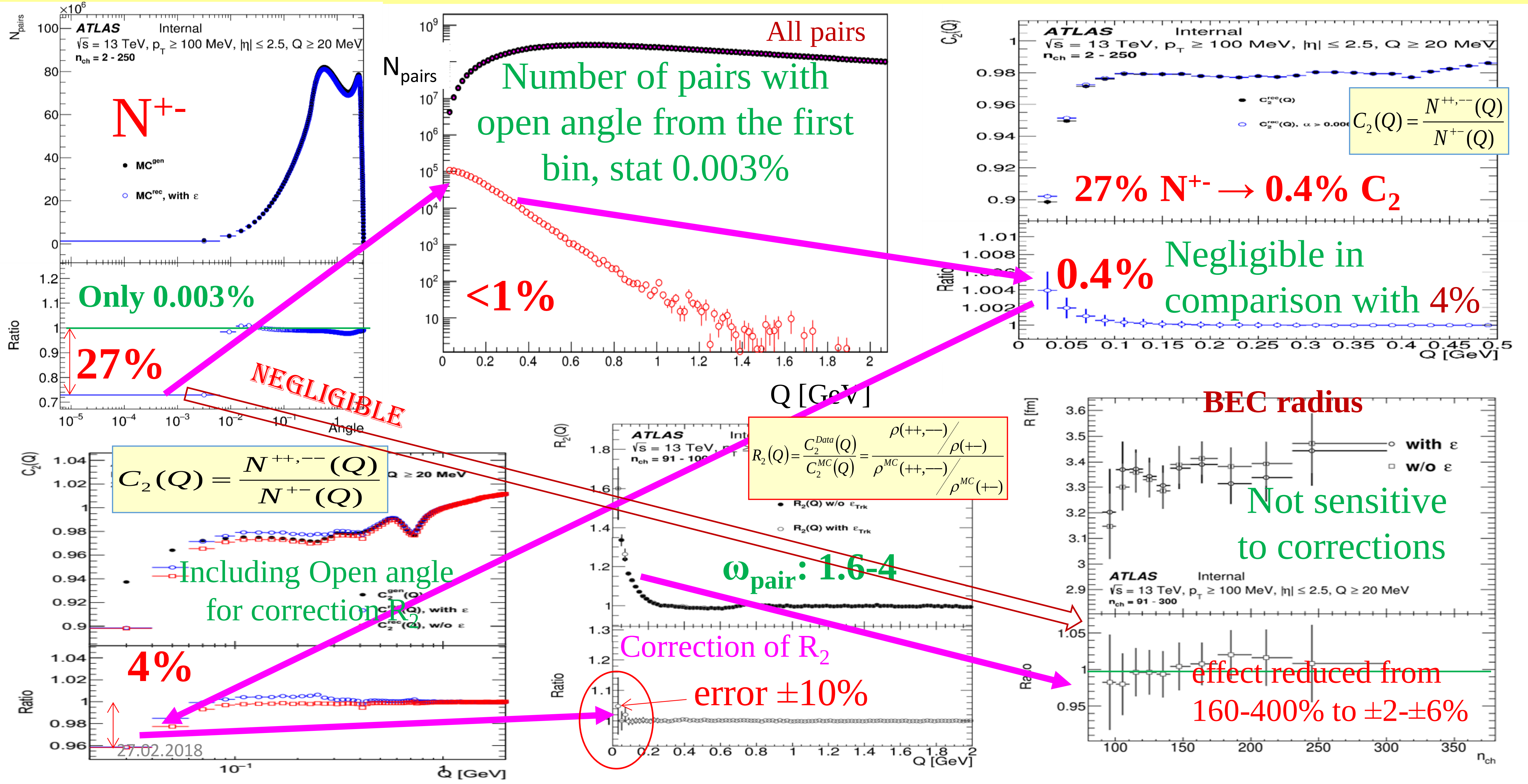

COULOMB CORRECTION

The measured N(Q) distribution for like or unlike signed particle (track) pairs in presence of the Coulomb interaction is given by:

$$N_{meas}(Q) = G(Q)N(Q)$$

where $N_{meas}(Q)$ is the measured distribution, *N(Q) is the distribution free of Coulomb correlations.*

Gamow penetration G(Q) factor $G(Q) = \frac{2\pi\eta}{e^{2\pi\eta} - 1}$

Sommerfeld parameter η $\eta = \frac{\pm\alpha_m}{|Q|}$

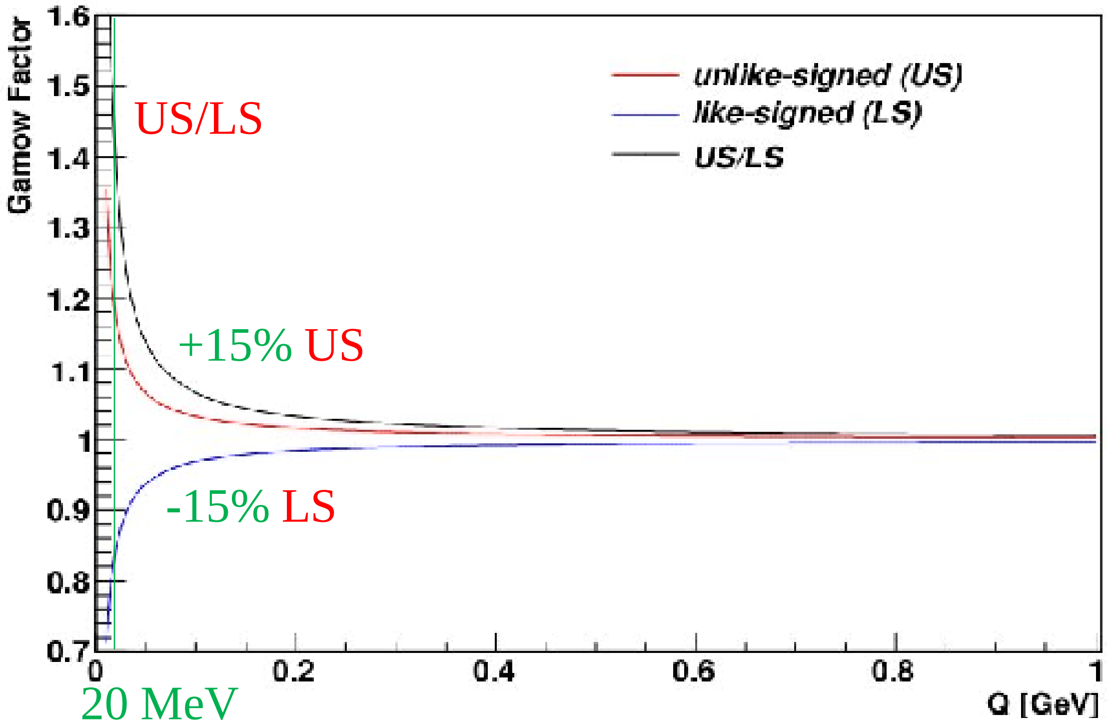

Gamow factor: **blue curve** – like-signed (LS) particle pairs,
red curve – unlike-signed (US) particle pairs,
black curve – US/LS

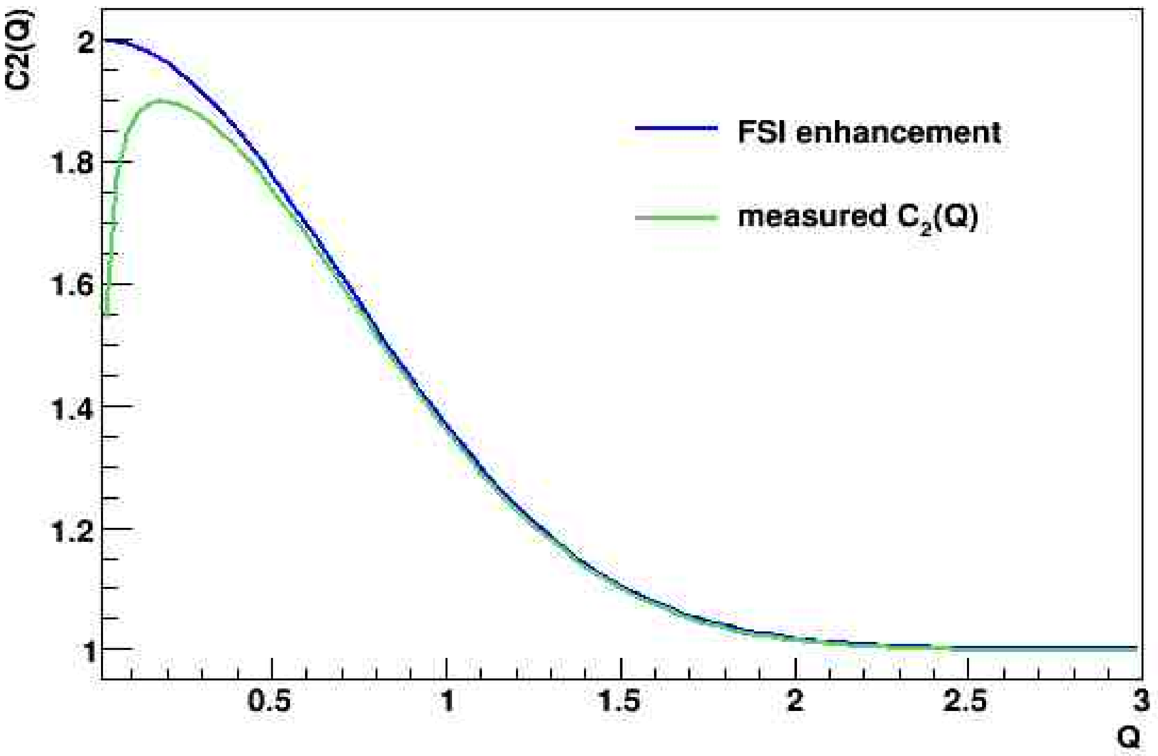

Ratio of the same $C_2(Q)$ function – with and without correction on Coulomb correction. FSI – final state interactions.

SYSTEMATIC UNCERTAINTIES FOR BEC AT 13 TeV

The systematic uncertainties of the spread for n_{ch} distribution and inclusive fit parameters, *R* and *λ*, of the exponential model are summarized in the Table. The systematic uncertainties are combined by adding them in quadrature and the resulting values are given in the bottom row of the Table. The same sources of uncertainty are considered for the differential measurements in n_{ch}; the average transverse momentum k_T of a pair; the two-differential measurements in intervals of (n_{ch}; k_T), and their impact on the fit parameters is found to be similar in size.

1. Track reconstruction efficiency: ω±δω
2. Monte Carlo: EPOS, Pythia8 Monash
3. Coulomb correction: ±15%
4. Fitted range of Q: 2 GeV±3σ_Q (100 MeV)
5. Starting value, Q_{min}: 10, 20, 30 MeV
6. Bin size: 10, 20, 30 MeV
7. Excluded intervals: ±20 MeV

Sources	13 TeV				13 TeV (HMT)			
	λ (%)	R (%)	λ (%)	R (%)	λ (%)	R (%)	λ (%)	R (%)
	n_{ch} – spread		Inclusive		n_{ch} – spread		Inclusive	
Track reconstr. efficiency	0.0–0.4	0.1–0.4	0.3	0.1	0.1–0.2	0.01–0.1	0.2	0.01
Track splitting and merging	negligible				negligible			
Monte Carlo samples	0.0–6.9	0.5–7.0	1.1	1.4	1.0–16.	1.0–14.	1.4	0.7
Coulomb correction	1.3–2.0	0.01–0.6	1.8	0.1	1.7–1.9	0.2–0.4	1.8	0.3
Fitted range of Q	0.0–0.5	0.02–0.9	0.2	0.3	0.0–0.2	0.0–0.2	0.02	0.03
Starting value of Q	0.0–1.9	0.01–1.1	0.3	0.2	0.5–1.4	0.3–0.7	0.7	0.4
Bin size	0.0–2.4	0.1–1.5	0.8	0.4	1.0–1.7	0.4–0.9	1.3	0.6
Exclusion intervals	0.0–1.1	0.3–0.8	0.1	0.3	0.4–0.6	0.3–0.6	0.5	0.5
Total	1.3–7.9	0.9–7.2	2.4	1.5	3.0–17.	1.0–15.	2.8	1.2

MULTIPLICITY DEPENDENCE OF BEC PARAMETERS AT 13 TEV

ATL-COM-PHYS-2016-1621

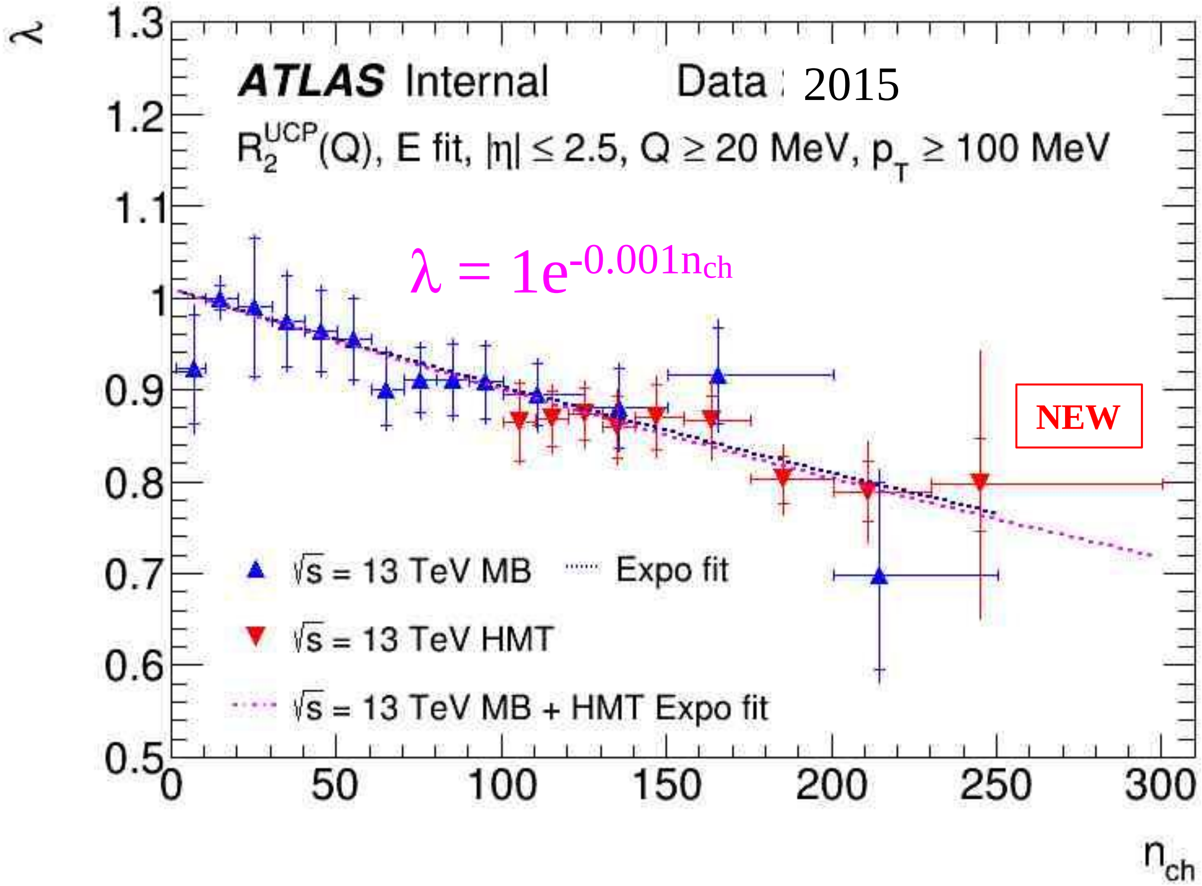

N_{mean}=32.5 for $\sum|\eta|$=5

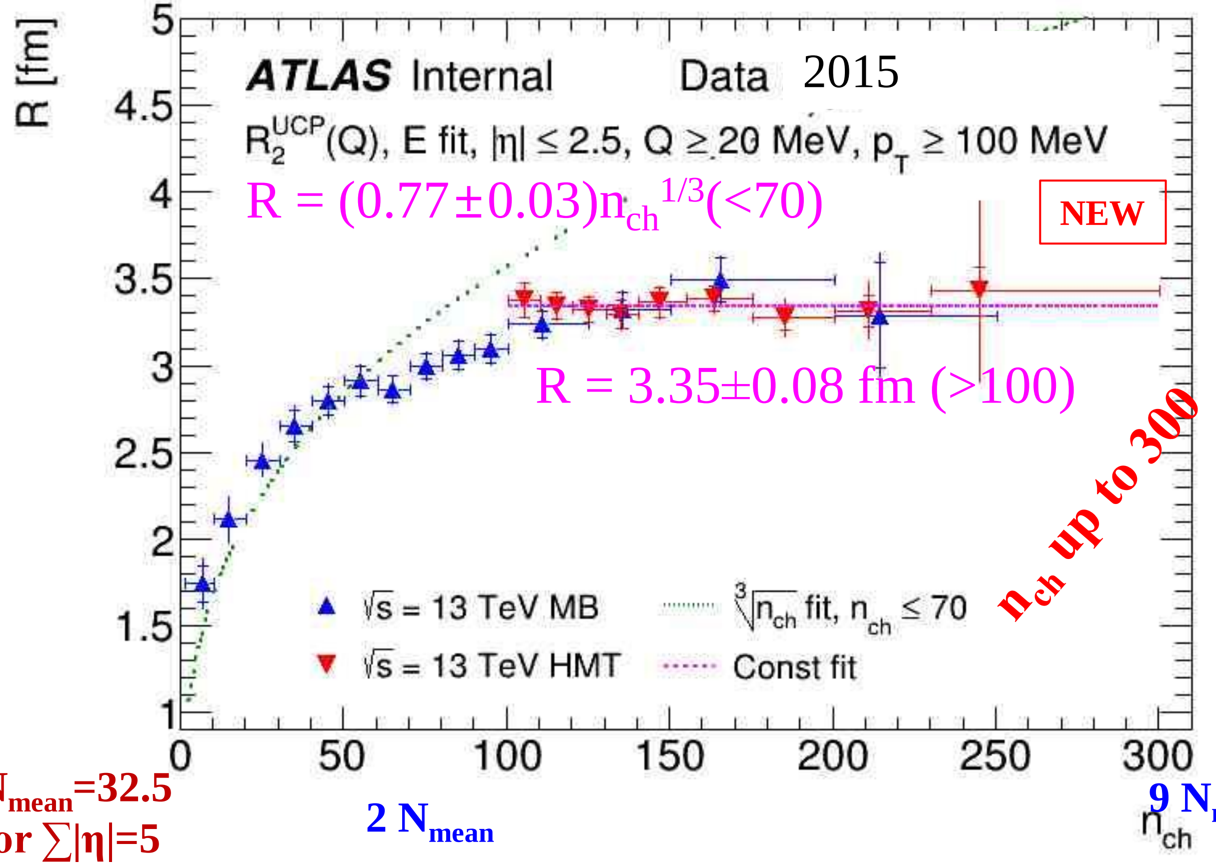

The results for Bose-Einstein Correlations for pairs of like-sign charged particles measured in the kinematic range p_T >100 MeV and $|\eta|$<2.5 in pp collisions at energy 13 TeV

- The multiplicity dependence of the BEC parameters characterizing the ***correlation strength*** and the ***correlation source size*** are investigated for multiplicities of up to ***very-high number of charged-particles***, $n_{ch} \approx 300$
- A ***saturation effect*** in the multiplicity dependence of the correlation source-size parameter is observed at 13 TeV

MULTIPLICITY DEPENDENCE OF BEC PARAMETERS AT 0.9 –13 TEV

EPJC 75 (2015) 10, 466; ATL-COM-PHYS-2016-1621

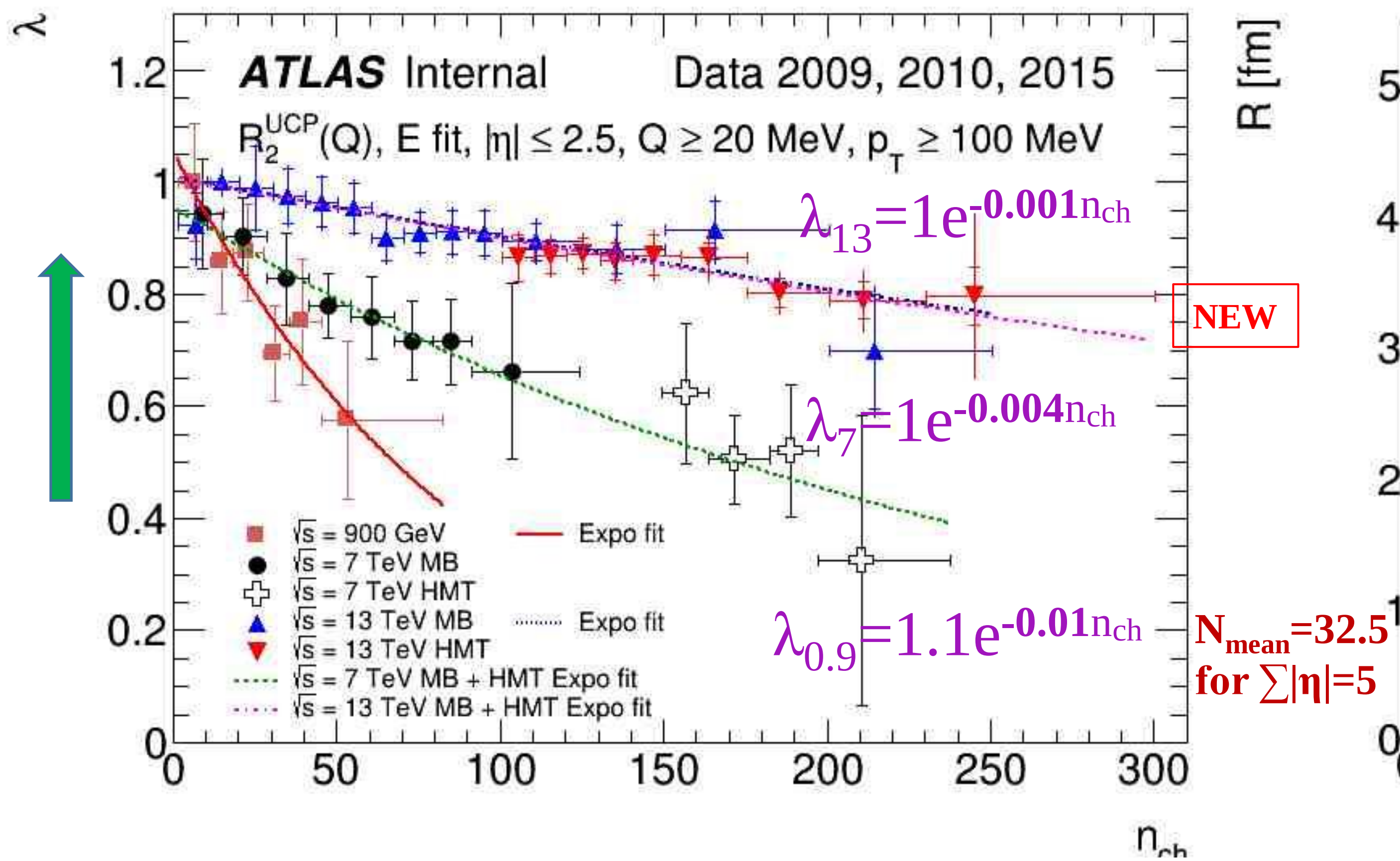

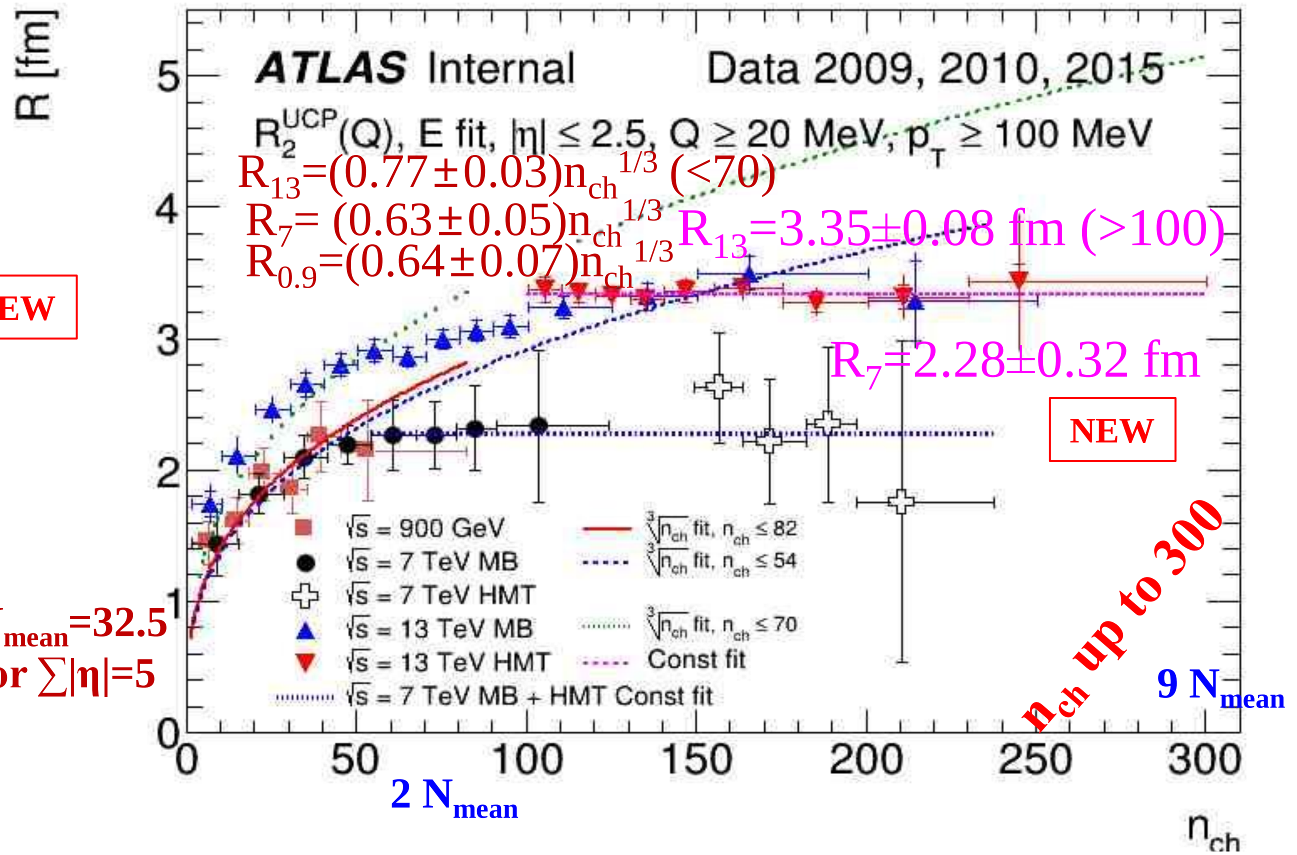

- The slope of an exponential fit of the λ vs n_{ch} distributions decrease with increasing of energy.
- The parameters α of the $\alpha \cdot n_{ch}^{1/3}$ fit of R vs n_{ch} for $n_{ch} \le 55$ at 0.9 TeV is α=0.64±0.07 fm, 7 TeV is α=0.63±0.05 fm and for $n_{ch} \le 70$ at 13 TeV is α=0.77±0.03 fm.

  For multiplicity region $n_{ch} \le 70$, the R values are systematically higher at 13 TeV than at 7 TeV.
- The R is a constant for $n_{ch}>55$ at 7 TeV R=2.28±0.32 fm and for $n_{ch}>100$ at 13 TeV R=3.35±0.08 fm.

  The R is systematically higher at 13 TeV than at 7 TeV but in the error bars is in agreement.

k_T dependence of BEC parameters

ATL-COM-PHYS-2016-1621

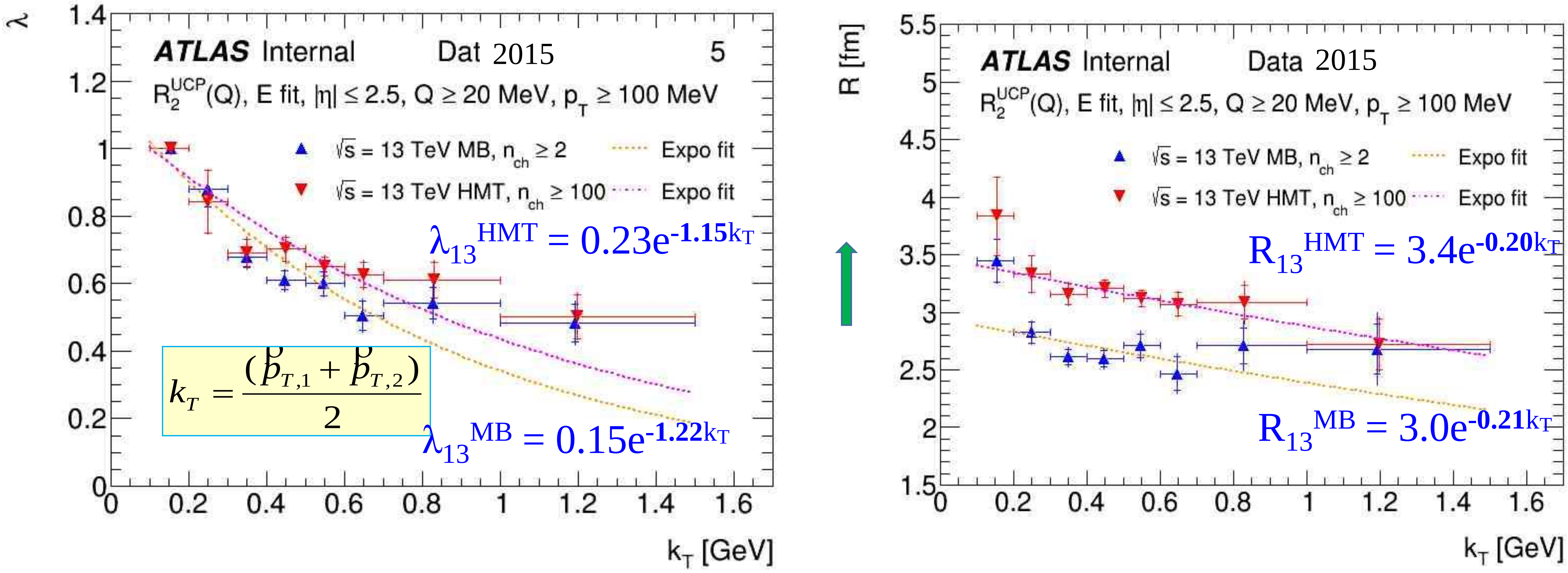

- **The λ values are (trigger) multiplicity-independent within uncertainties at 13 TeV**
- **The R values increase with increasing (trigger) multiplicity region**
- **The λ values decrease exponentially with k_T**
- **The R values decrease exponentially with k_T for HMT events**

k_T DEPENDENCE OF BEC PARAMETERS AT 0.9 –13 TEV

EPJC 75 (2015) 10, 466; ATL-COM-PHYS-2016-1621

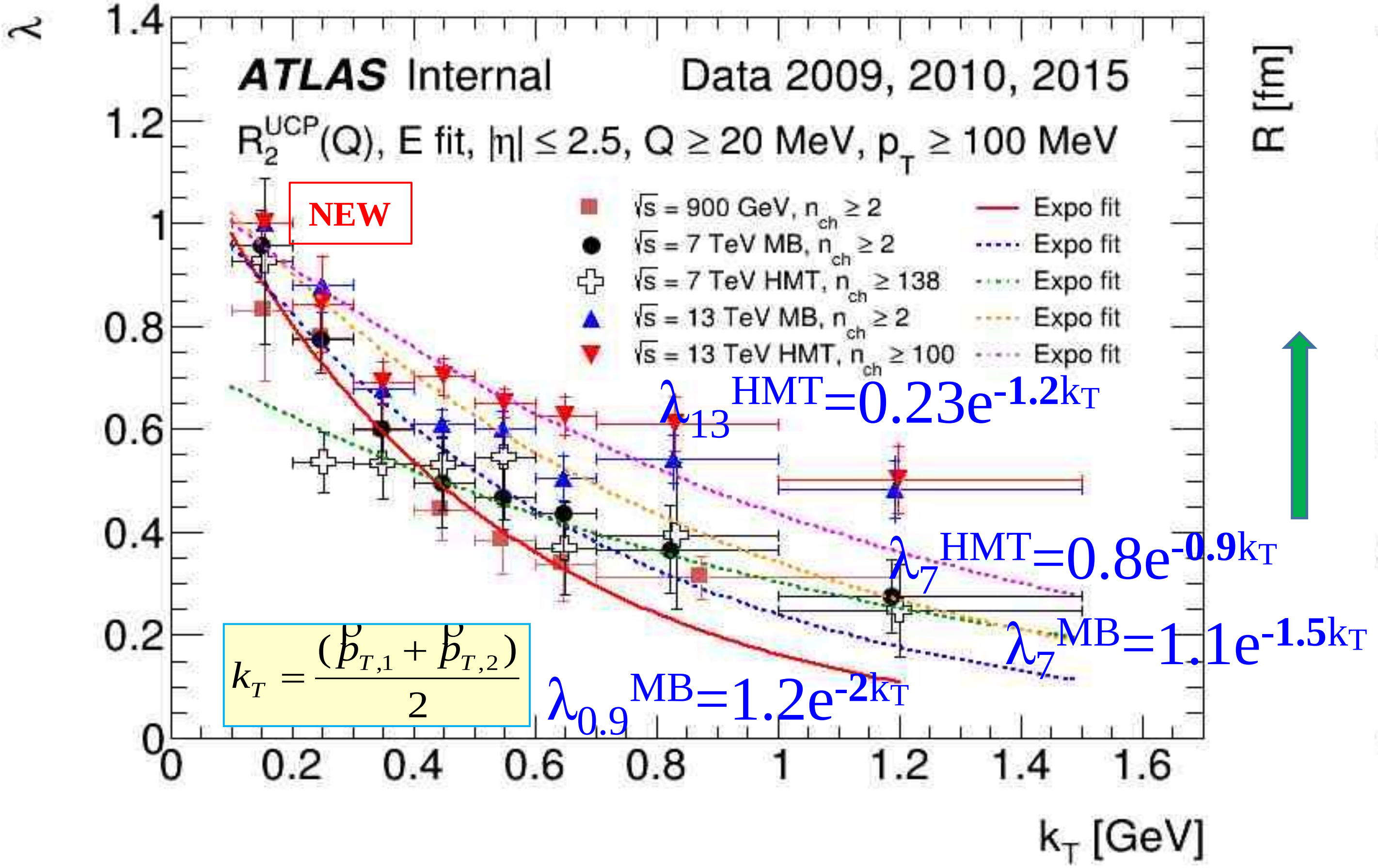

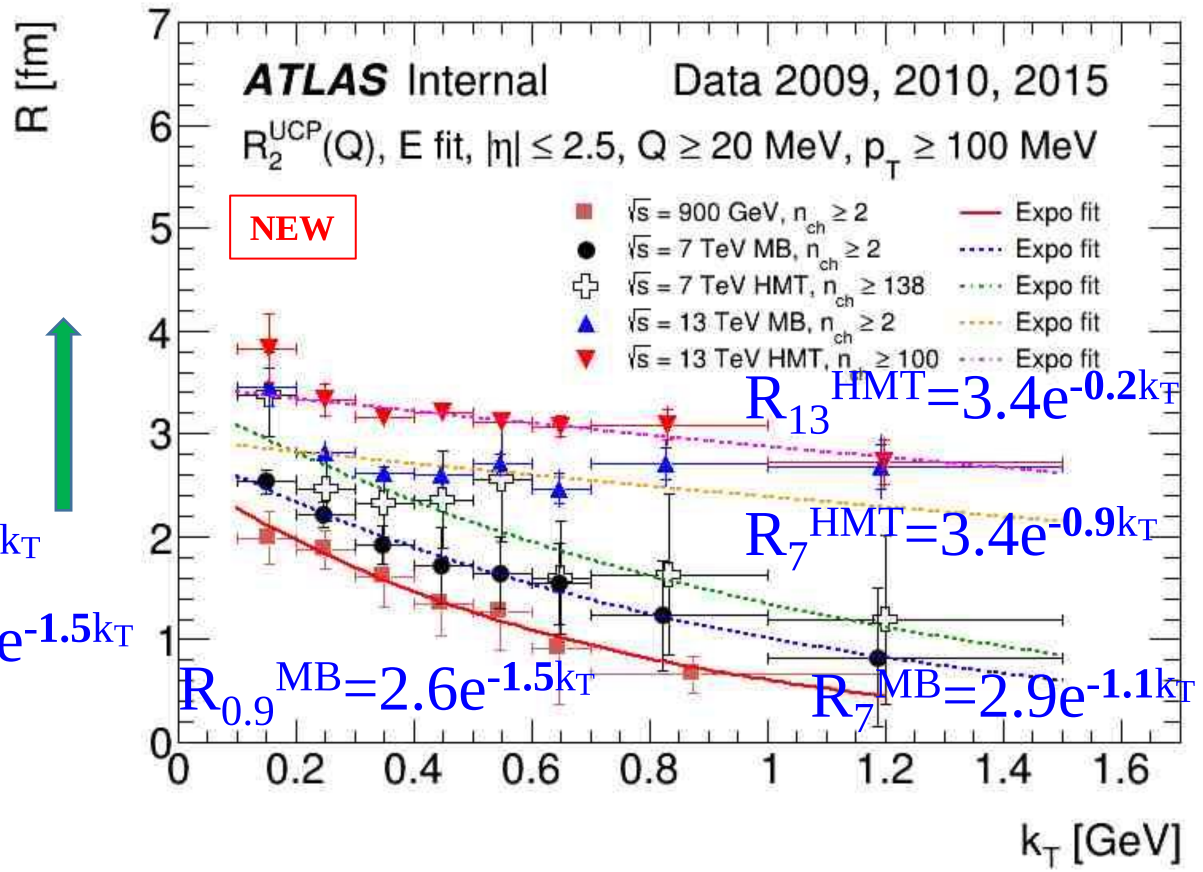

- The amplitude of fit of λ^{MB} vs k_T distributions is decrease from 1.2 to 0.23 with energy increasing.
- The slope of exponential fit of the R values vs k_T distributions decrease from 1.5 to 0.2 with increasing of energy.

MULTIPLICITY DEPENDENCE OF BEC PARAMETERS FOR (N_{CH}, K_T) INTERVALS

MB trigger

λ distribution at 13 TeV

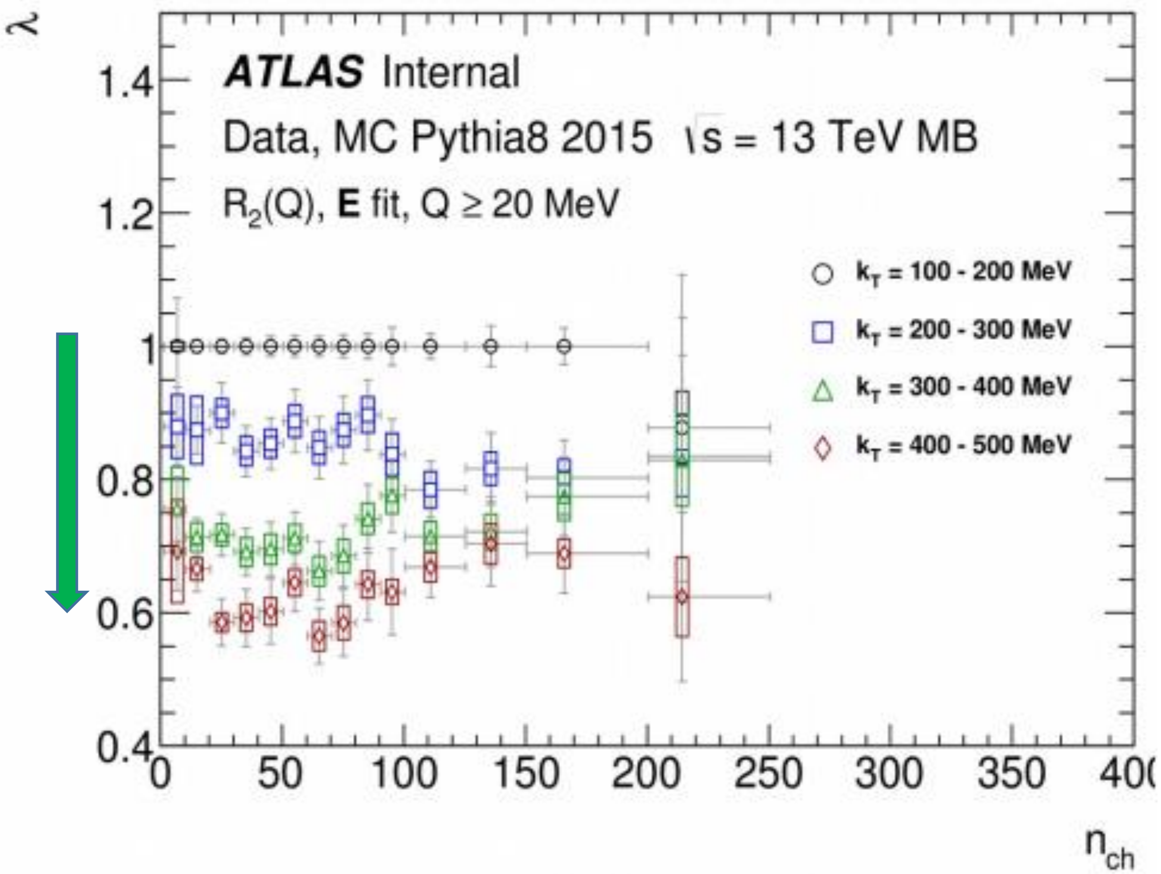

R distribution at 13 TeV

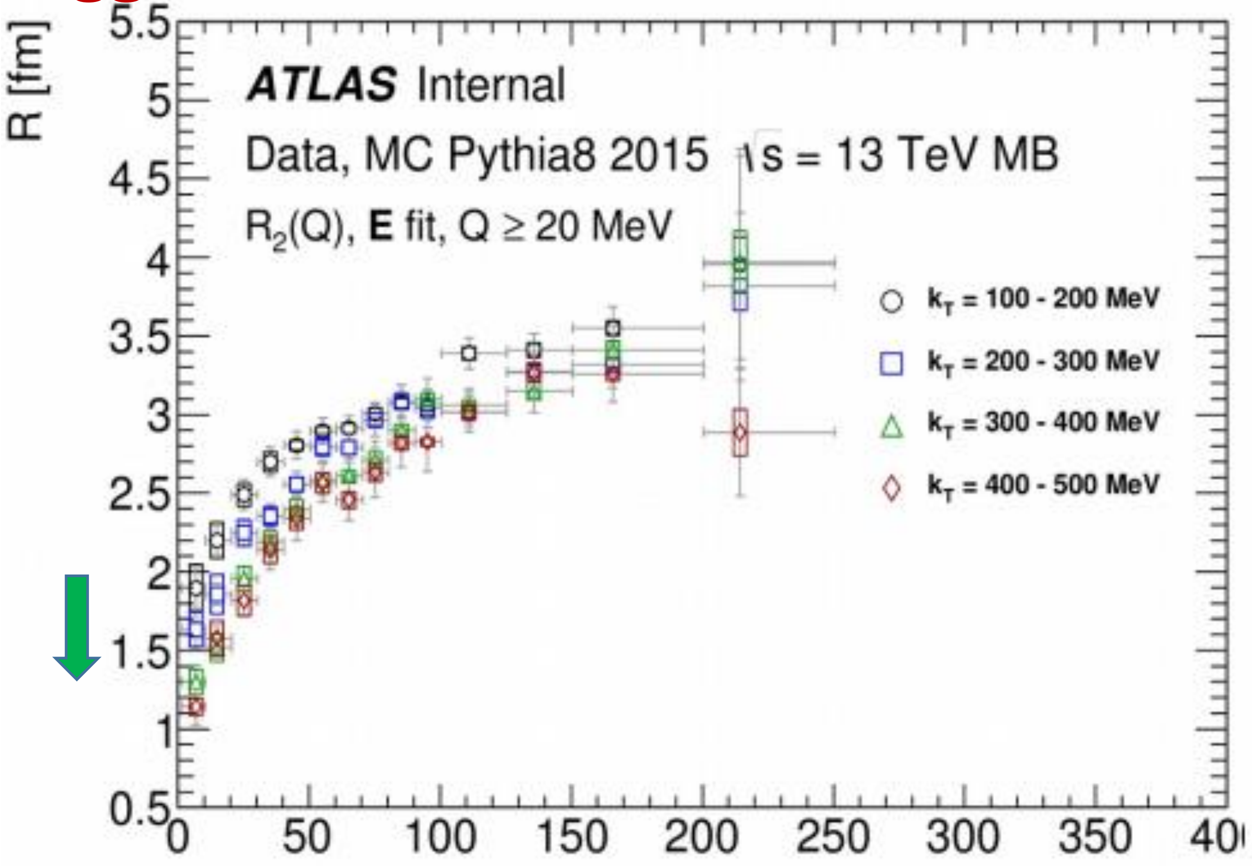

- The λ values are constant and decrease with k_T increasing
- The R values are decrease with k_T increasing
- The R values are increase as $\sim\alpha \cdot n_{ch}^{1/3}$ with multiplicity

MULTIPLICITY DEPENDENCE OF BEC PARAMETERS

λ distribution at 13 TeV **MB + HMT triggers** R distribution at 13 TeV

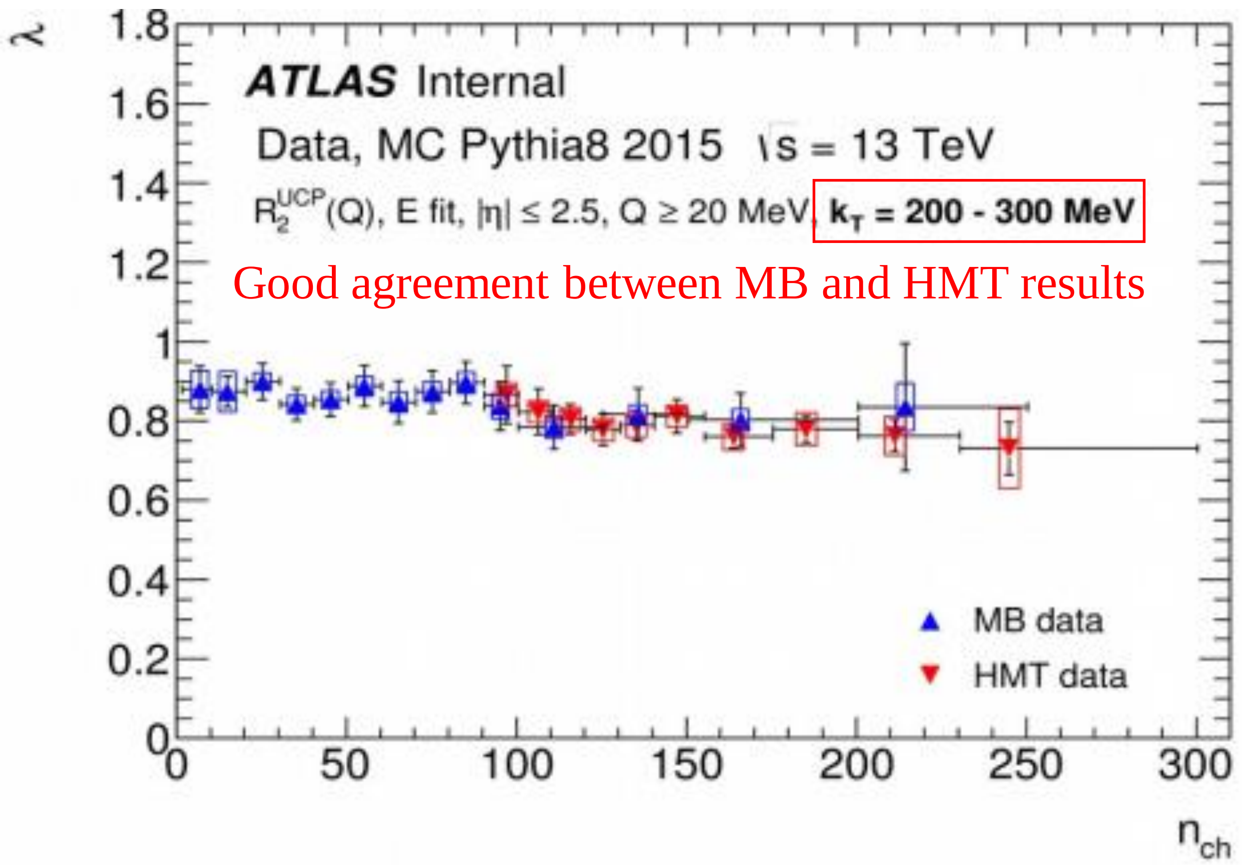

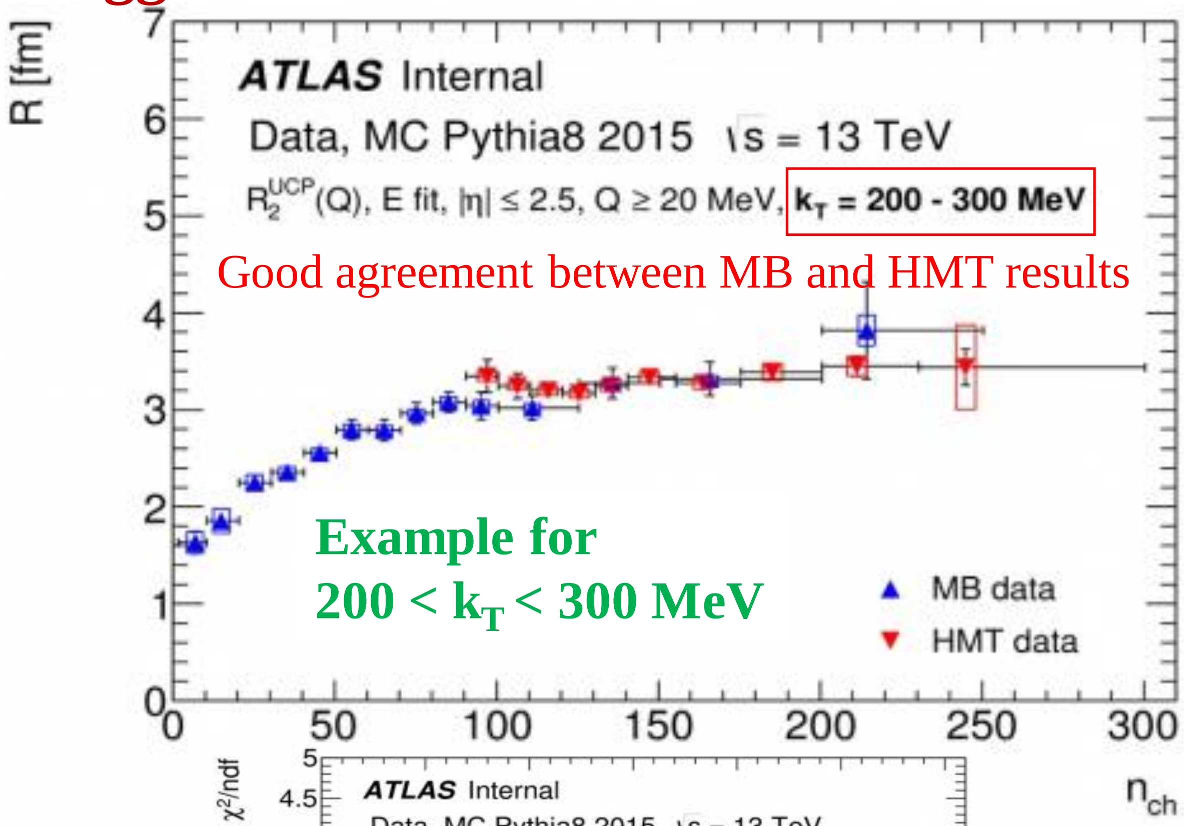

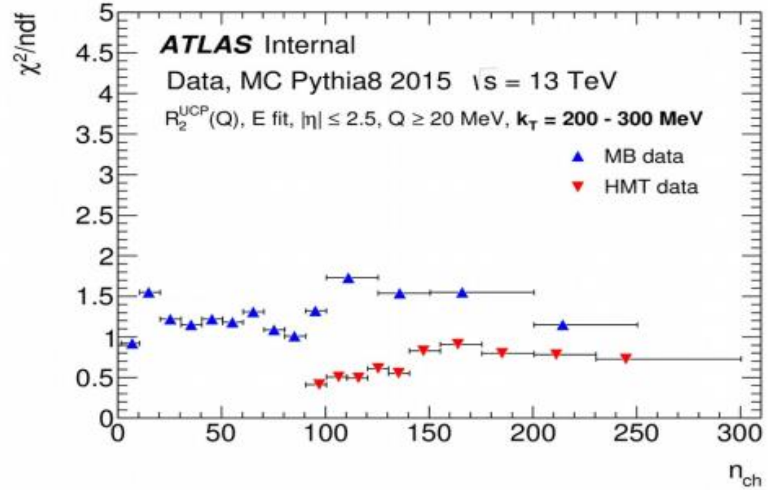

- Good connection between MB and HMT results
- The λ values slowly decreases in dependence of multiplicity
- The R values increases as $\sim\alpha\cdot n_{ch}^{1/3}$ with multiplicity for n_{ch} <100
- The R are constant in dependence of multiplicity for n_{ch} >100

MULTIPLICITY DEPENDENCE OF BEC PARAMETERS FOR (N_{CH}, K_T) INTERVALS - II

MB trigger

λ distribution at 13 TeV

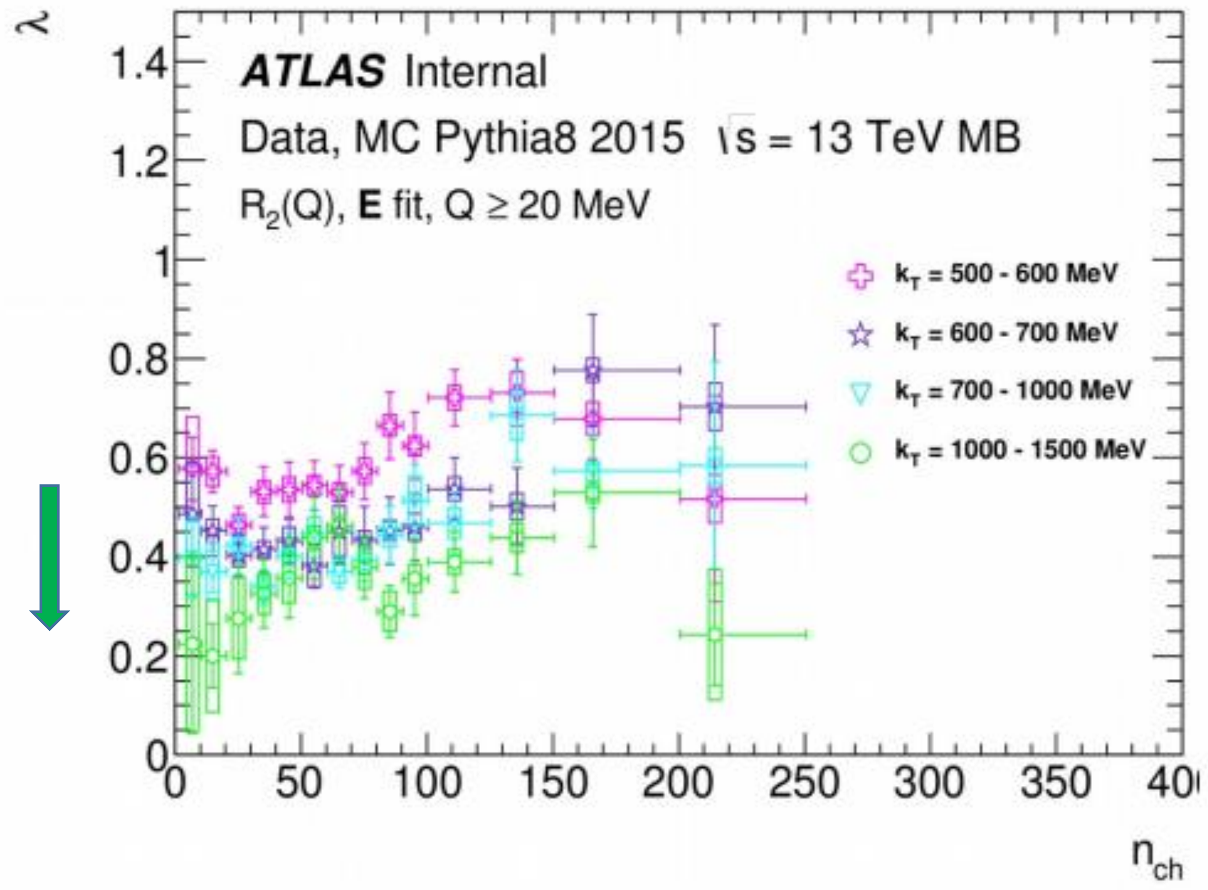

R distribution at 13 TeV

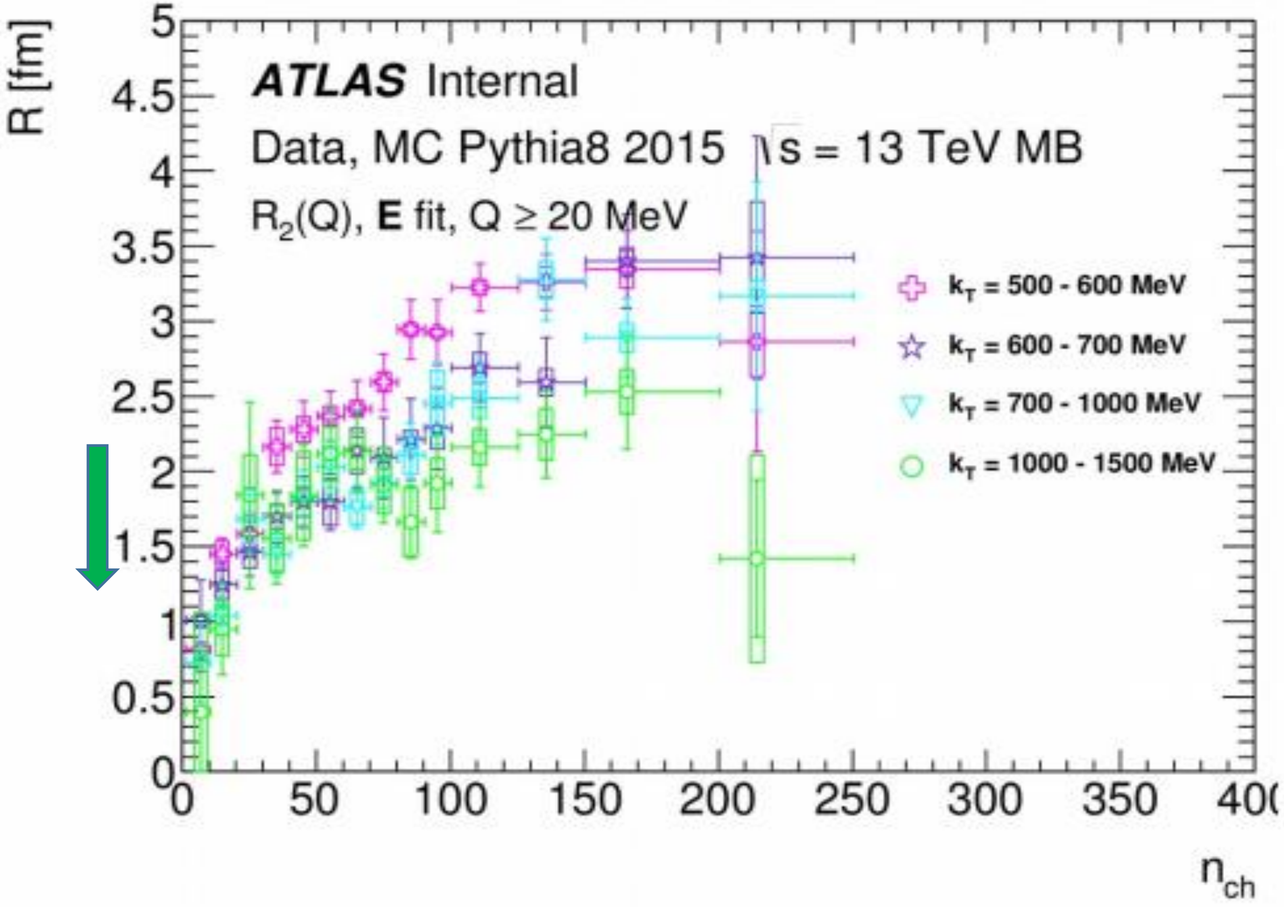

- The λ values are increase with multiplicity and decrease with k_T increasing
- The R values are decrease with k_T increasing
- The R values increases as $\sim\alpha \cdot n_{ch}^{1/3}$ with multiplicity

MULTIPLICITY DEPENDENCE OF BEC PARAMETERS FOR (N_{CH}, K_T) INTERVALS

HMT trigger

λ distribution at 13 TeV

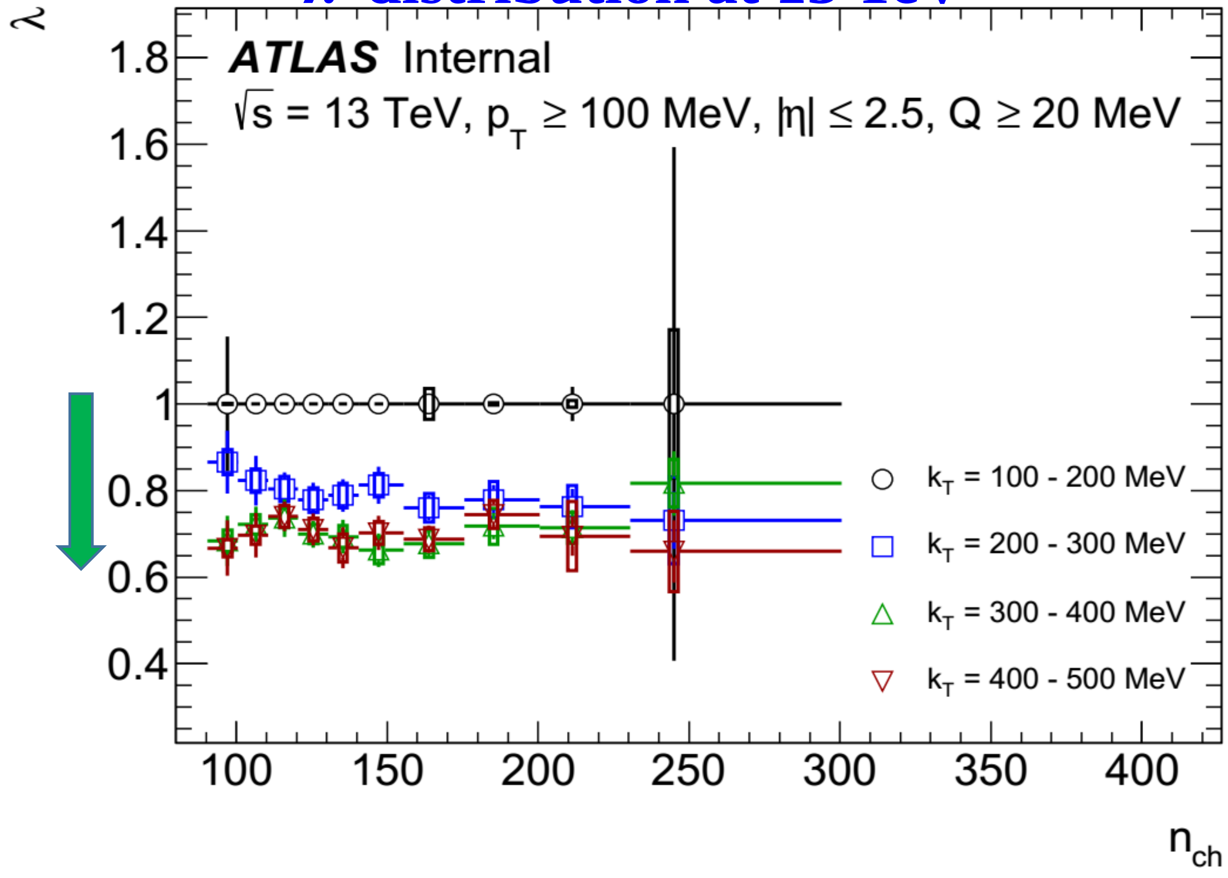

R distribution at 13 TeV

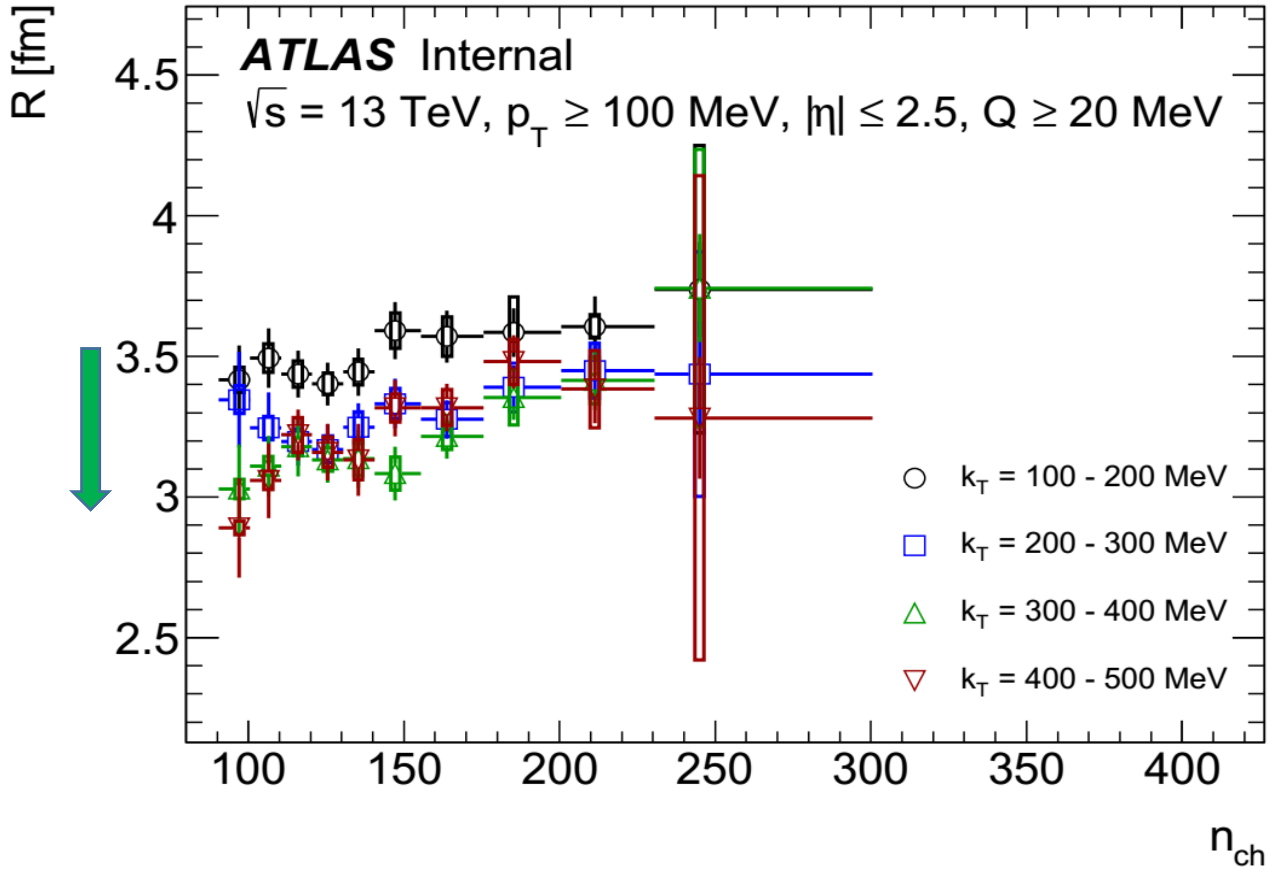

- The λ values are constant in dependence of multiplicity and decrease with k_T increasing
- The R values are constant in dependence of multiplicity and decrease with k_T increasing

λ distribution at 13 TeV **HMT trigger** **R distribution at 13 TeV**

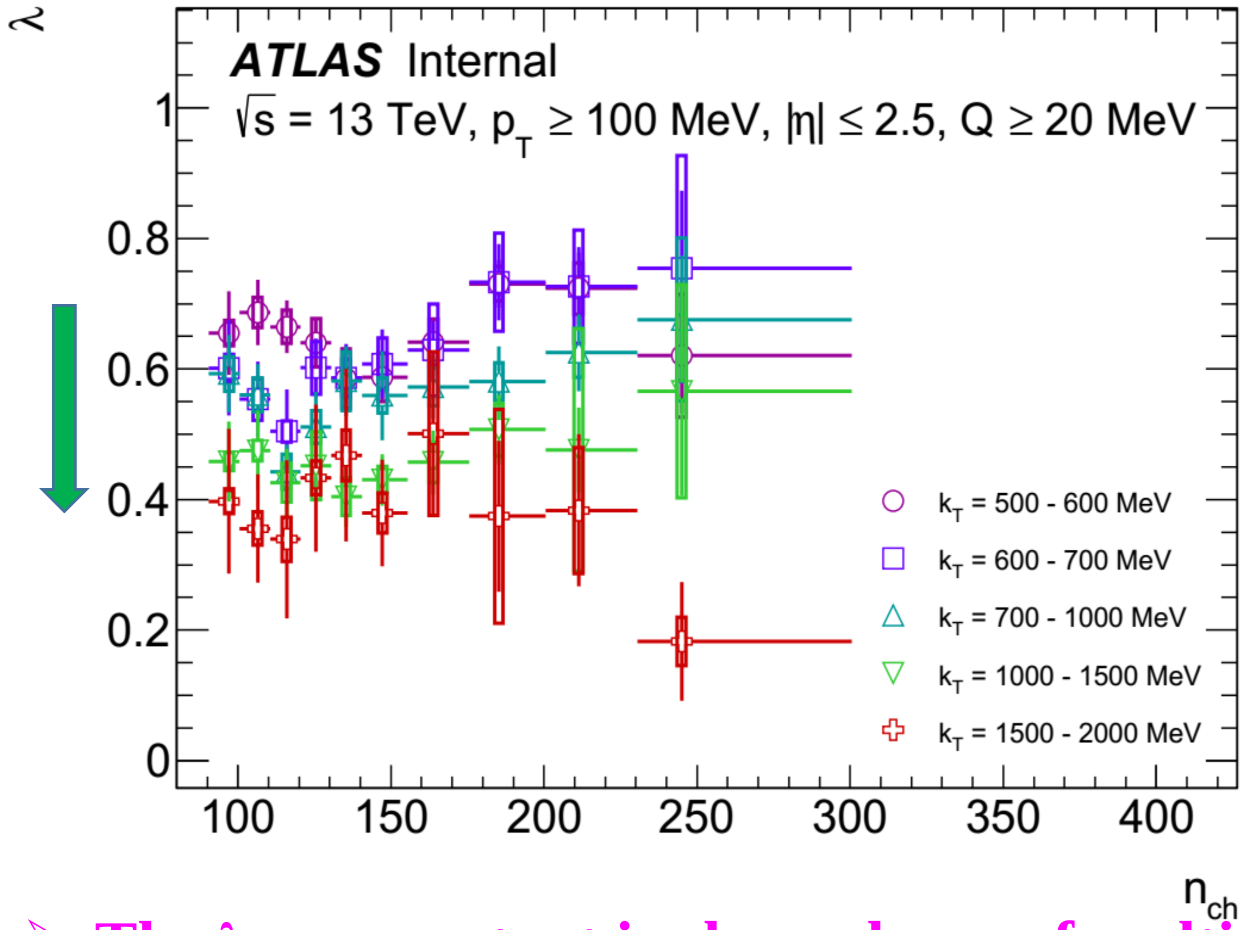

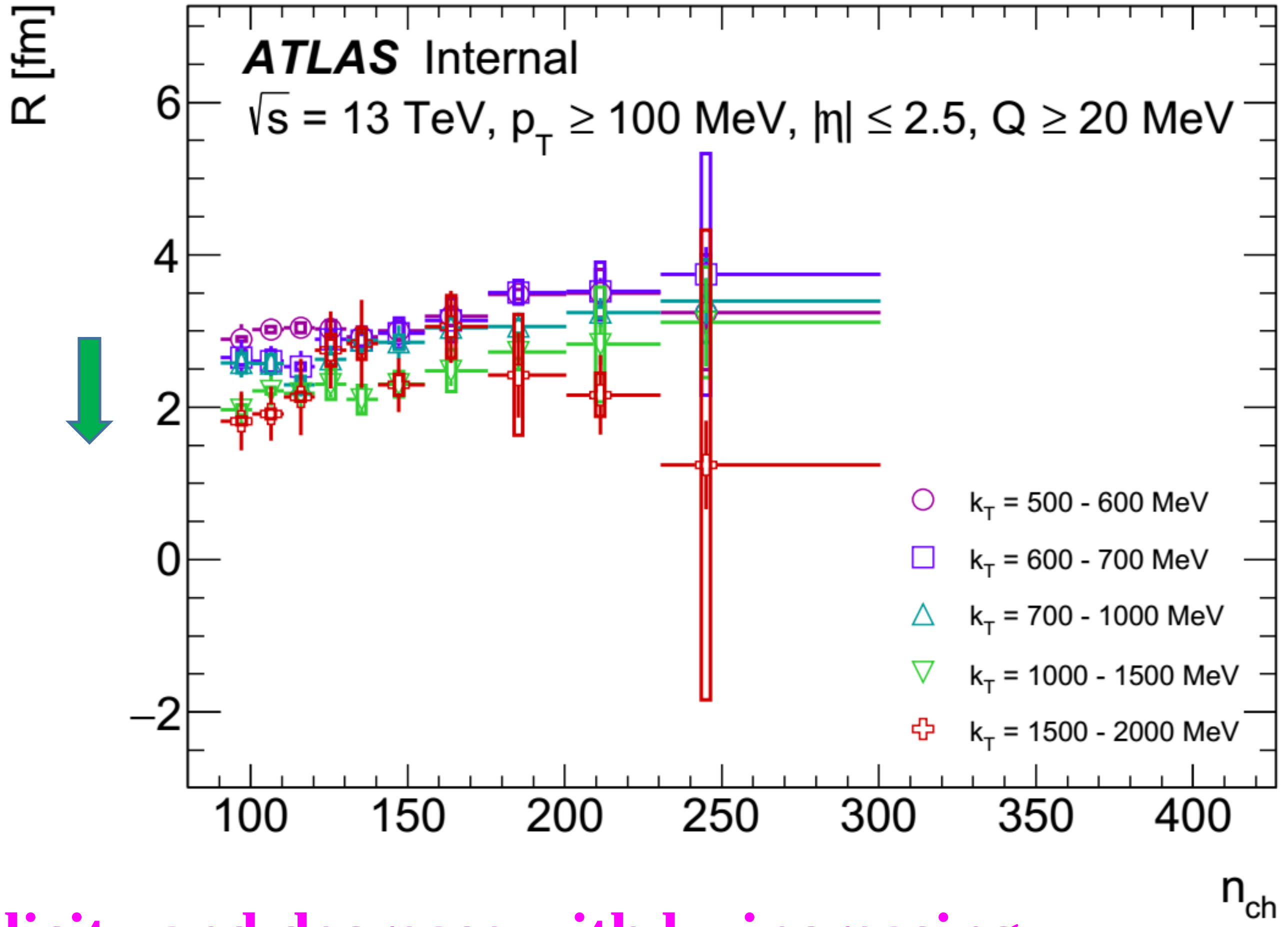

- **The λ are constant in dependence of multiplicity and decrease with k_T increasing**
- **The R are constant in dependence of multiplicity and decrease with k_T increasing**

k_T DEPENDENCE OF BEC PARAMETERS FOR (N_{CH}, K_T) INTERVALS AT 7 TEV

EPJC 75 (2015) 466

λ distribution at 7 TeV **MB trigger** **R distribution at 7 TeV**

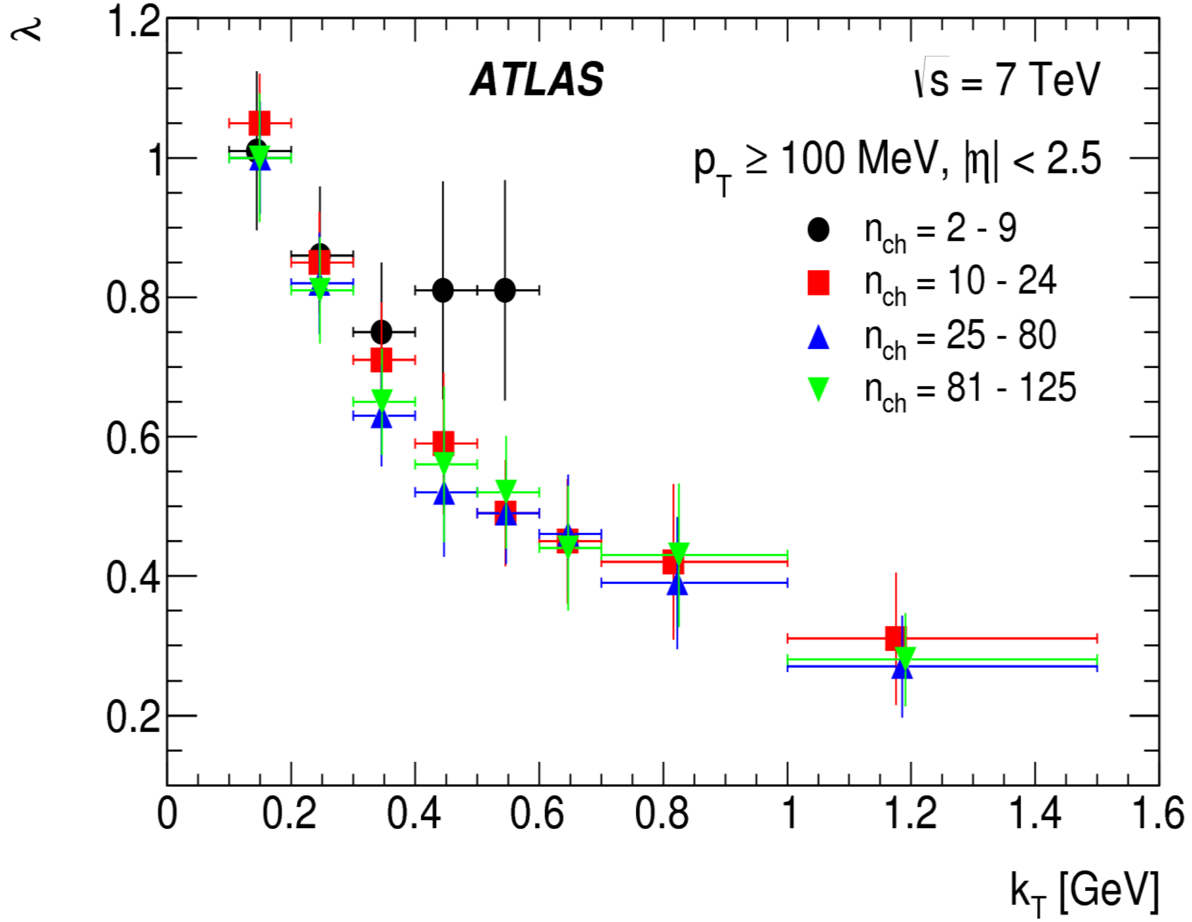

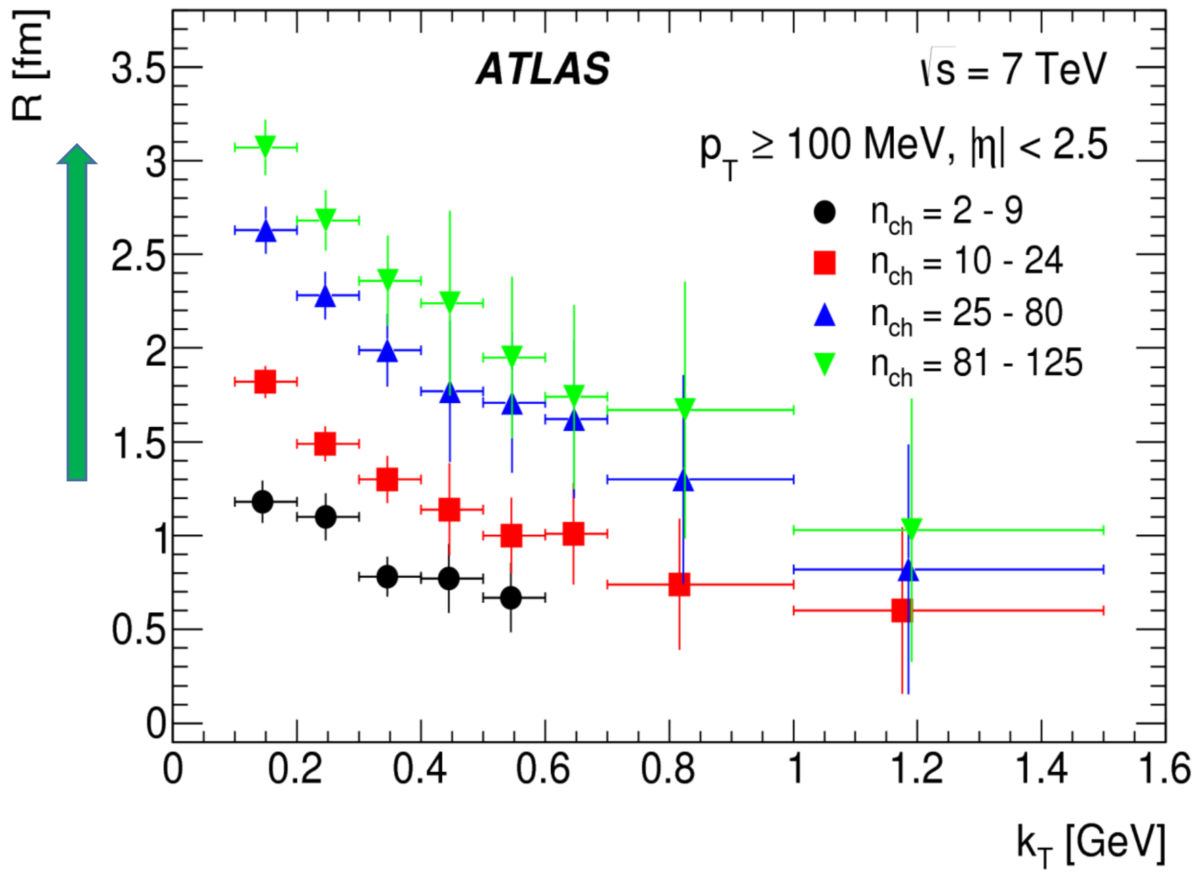

- The λ values are independent of multiplicity within uncertainties
- The R values increase with increasing multiplicity
- The λ and R values decrease exponentially with k_T

k_T DEPENDENCE OF BEC PARAMETERS FOR (N_{CH}, k_T) INTERVALS

λ distribution at 13 TeV **MB trigger** **R distribution at 13 TeV**

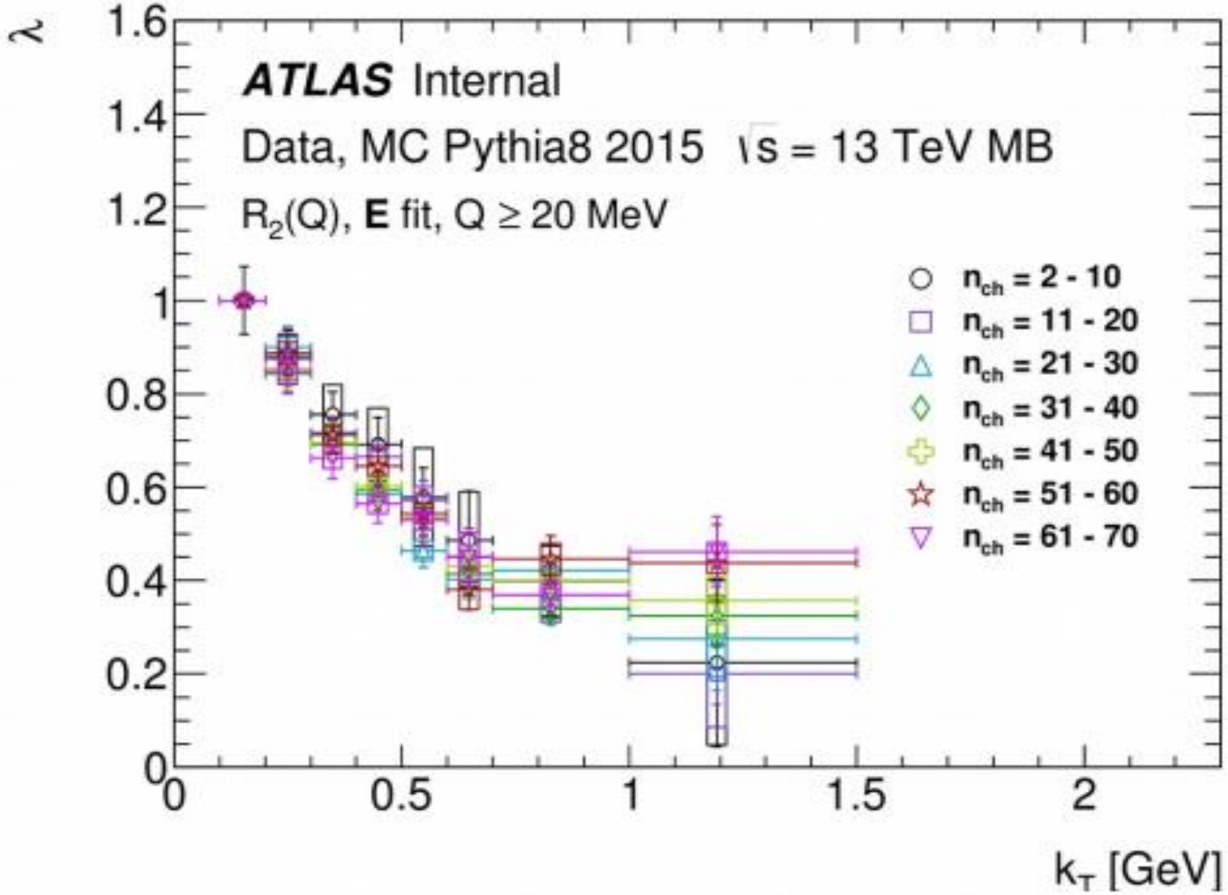

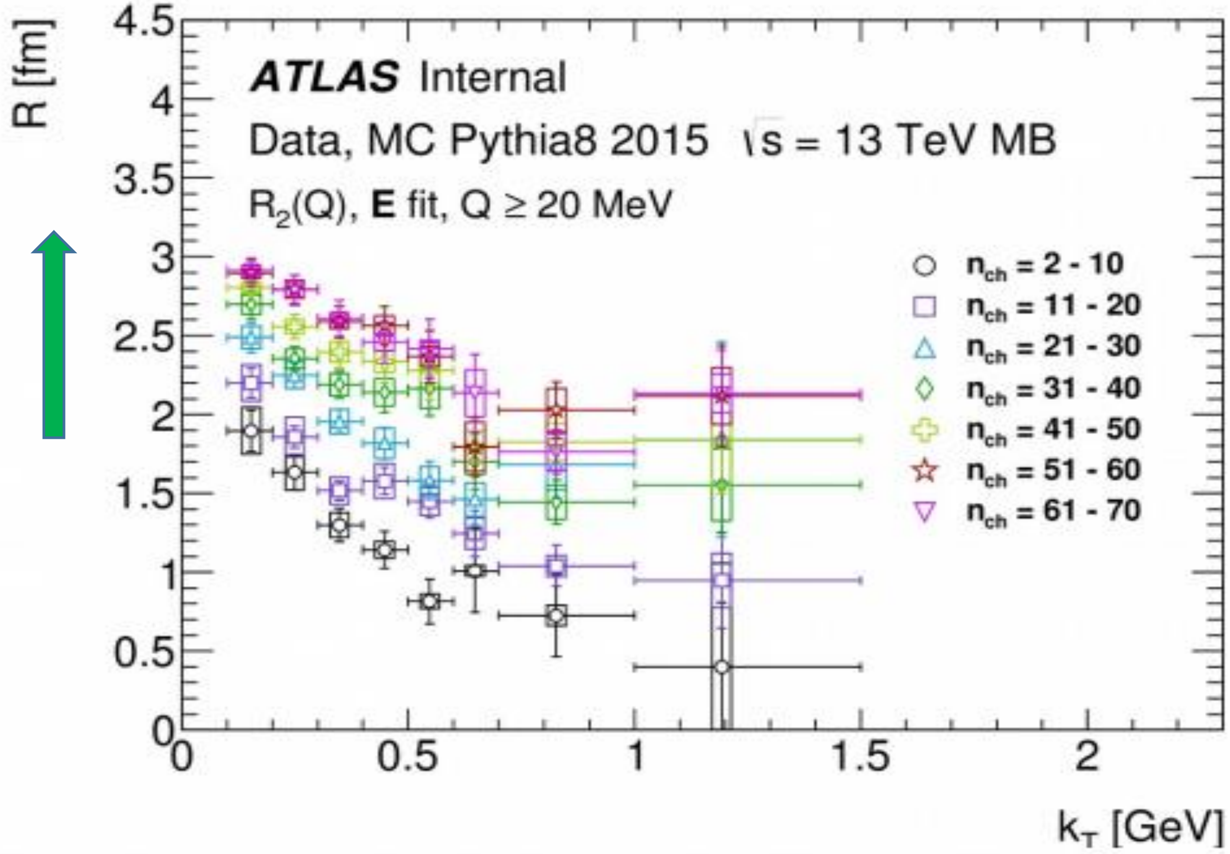

- The λ values are independent of multiplicity within uncertainties
- The R values increase with increasing multiplicity
- The λ and R values decrease exponentially with k_T

The effects similar to that observed for 7 TeV (see Backup slides)

k_T dependence of BEC parameters for (n_{ch}, k_T) intervals (cont.)

λ distribution at 13 TeV **MB trigger** **R distribution at 13 TeV**

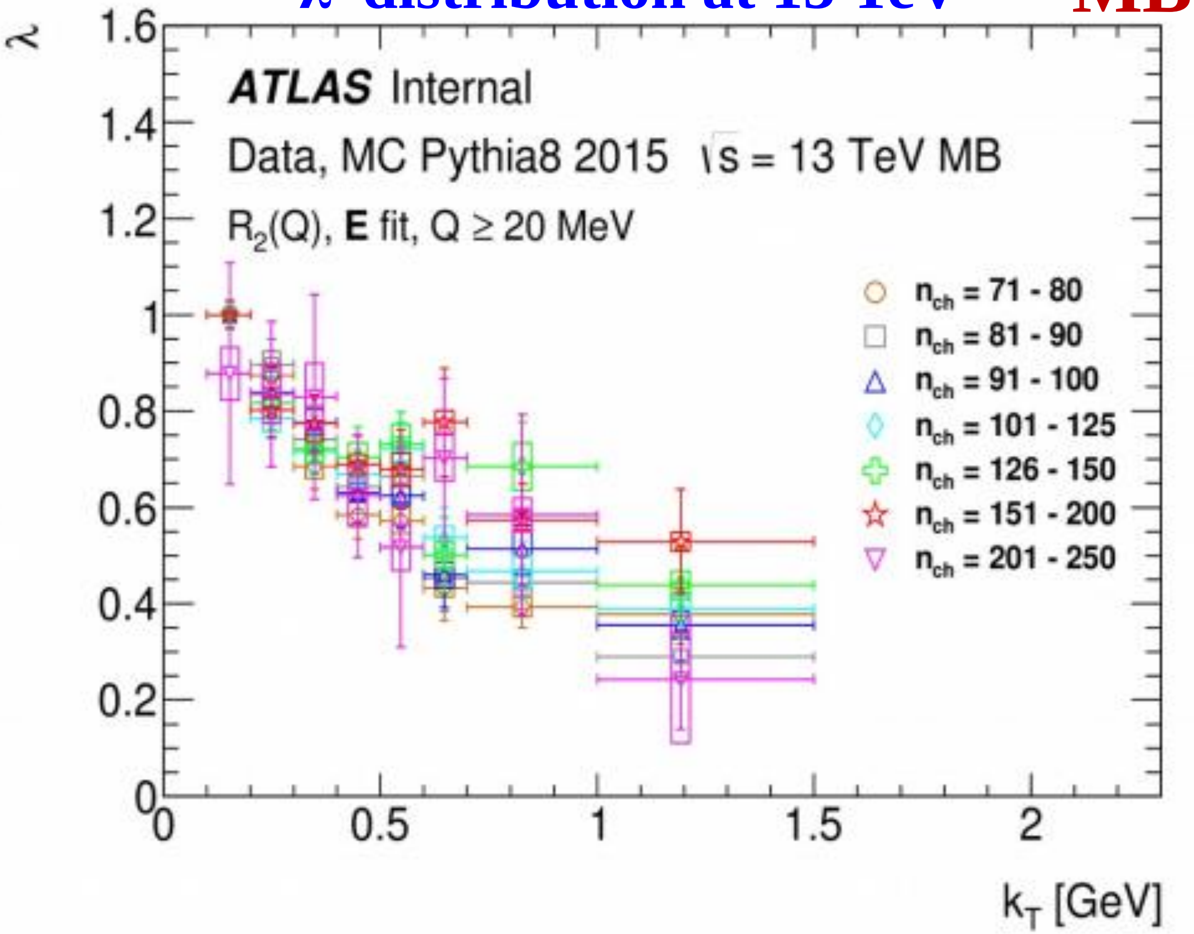

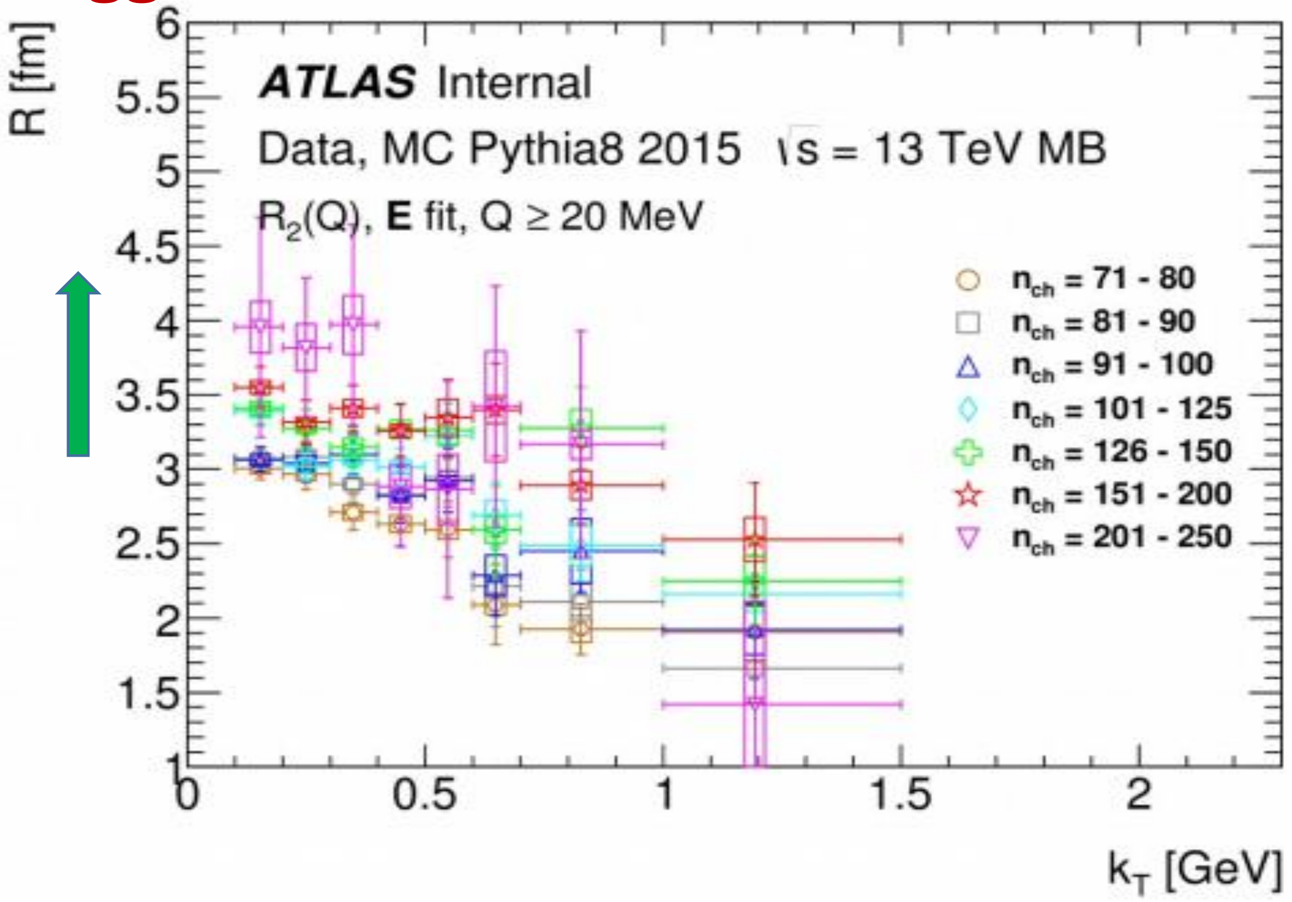

- The λ and R values are independent of multiplicity within uncertainties
- The λ and R values decrease exponentially with k_T

k_T DEPENDENCE OF BEC PARAMETERS

λ distribution at 13 TeV **MB + HMT triggers** **R distribution at 13 TeV**

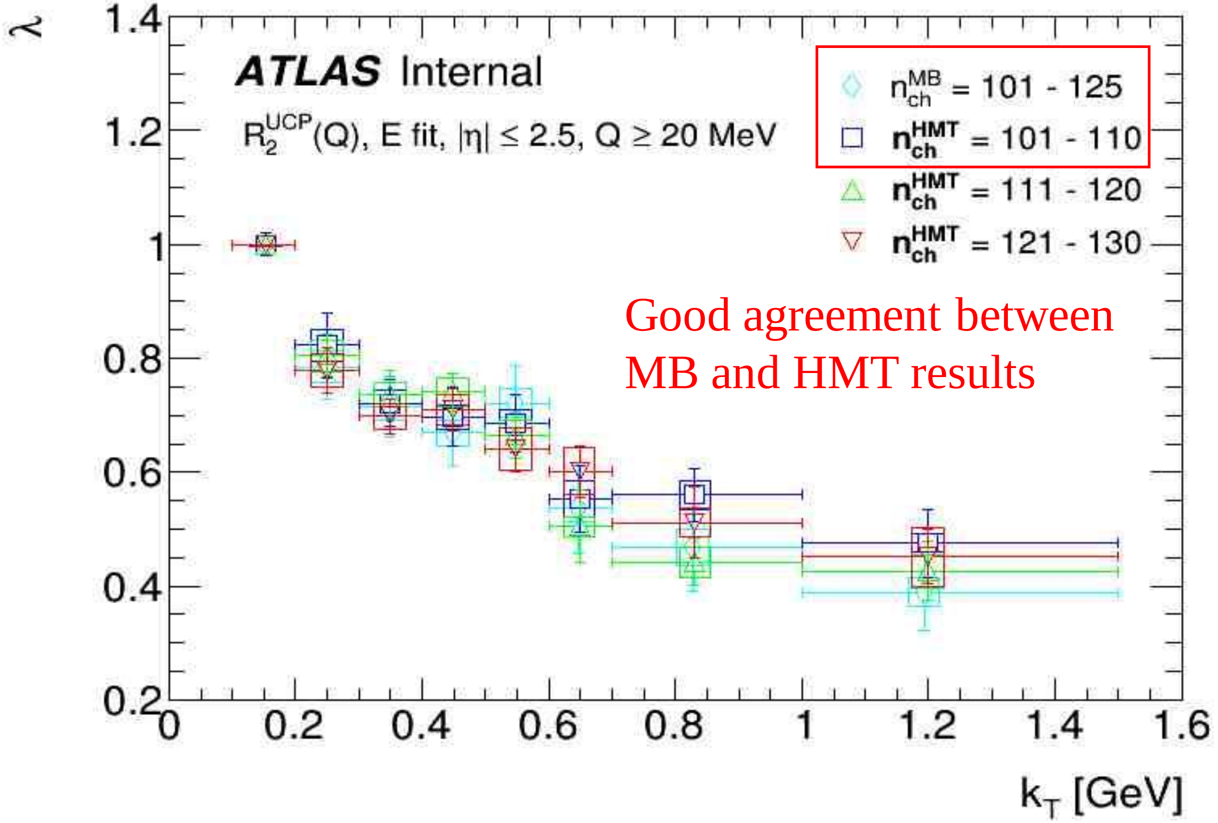

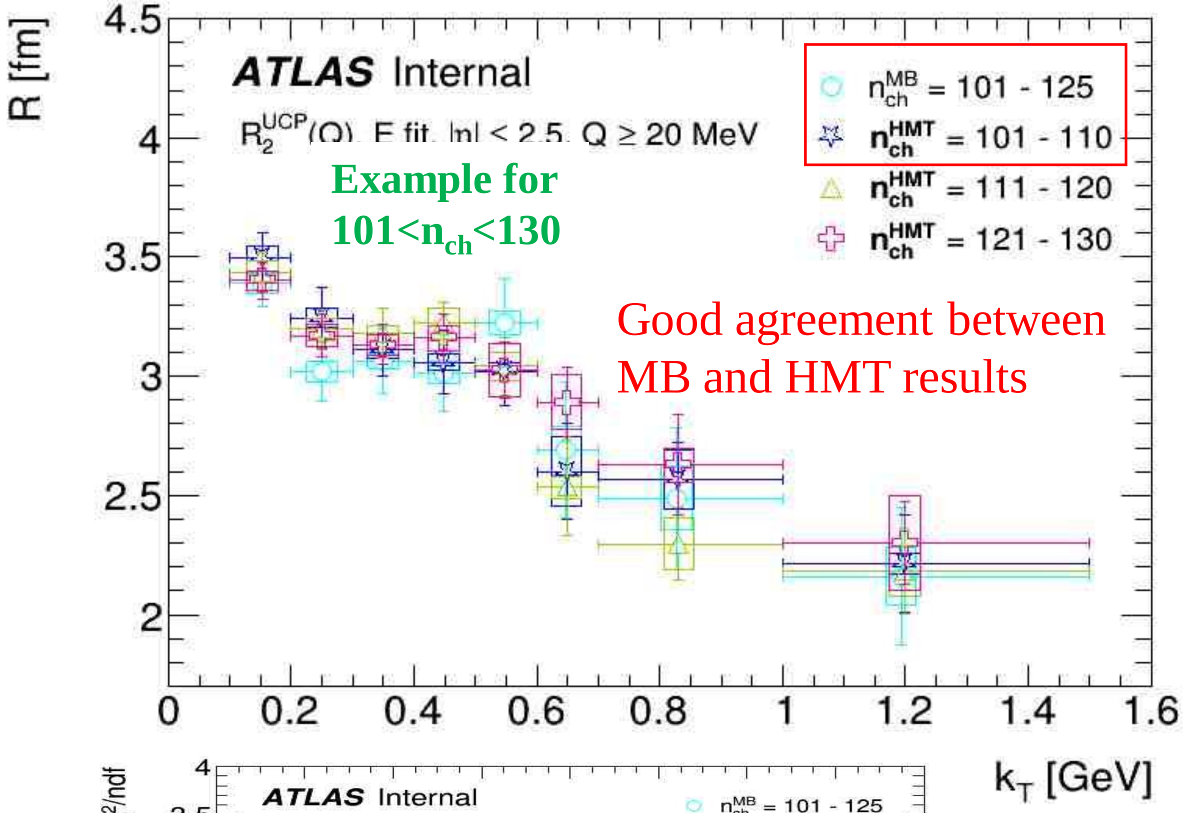

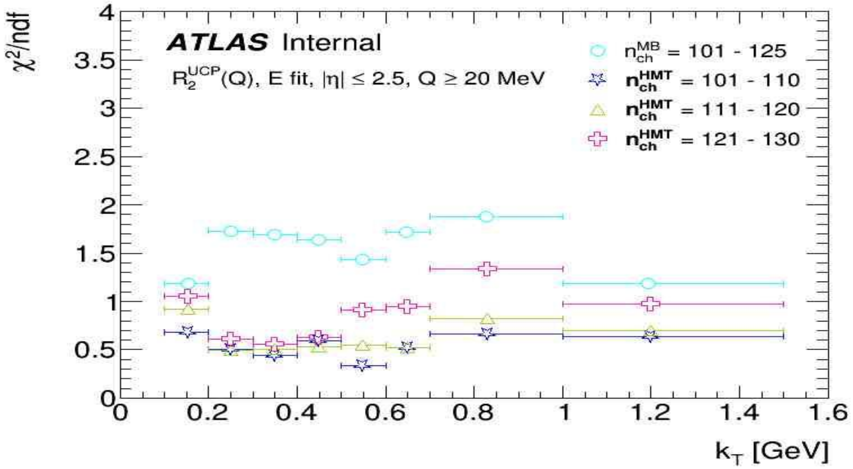

- Agreement between MB and HMT results
- The λ values decreases exponentially in dependence of k_T
- The R values decreases exponentially in dependence of k_T

k_T DEPENDENCE OF BEC PARAMETERS FOR (N_{CH}, k_T) INTERVALS

HMT trigger

λ distribution at 13 TeV

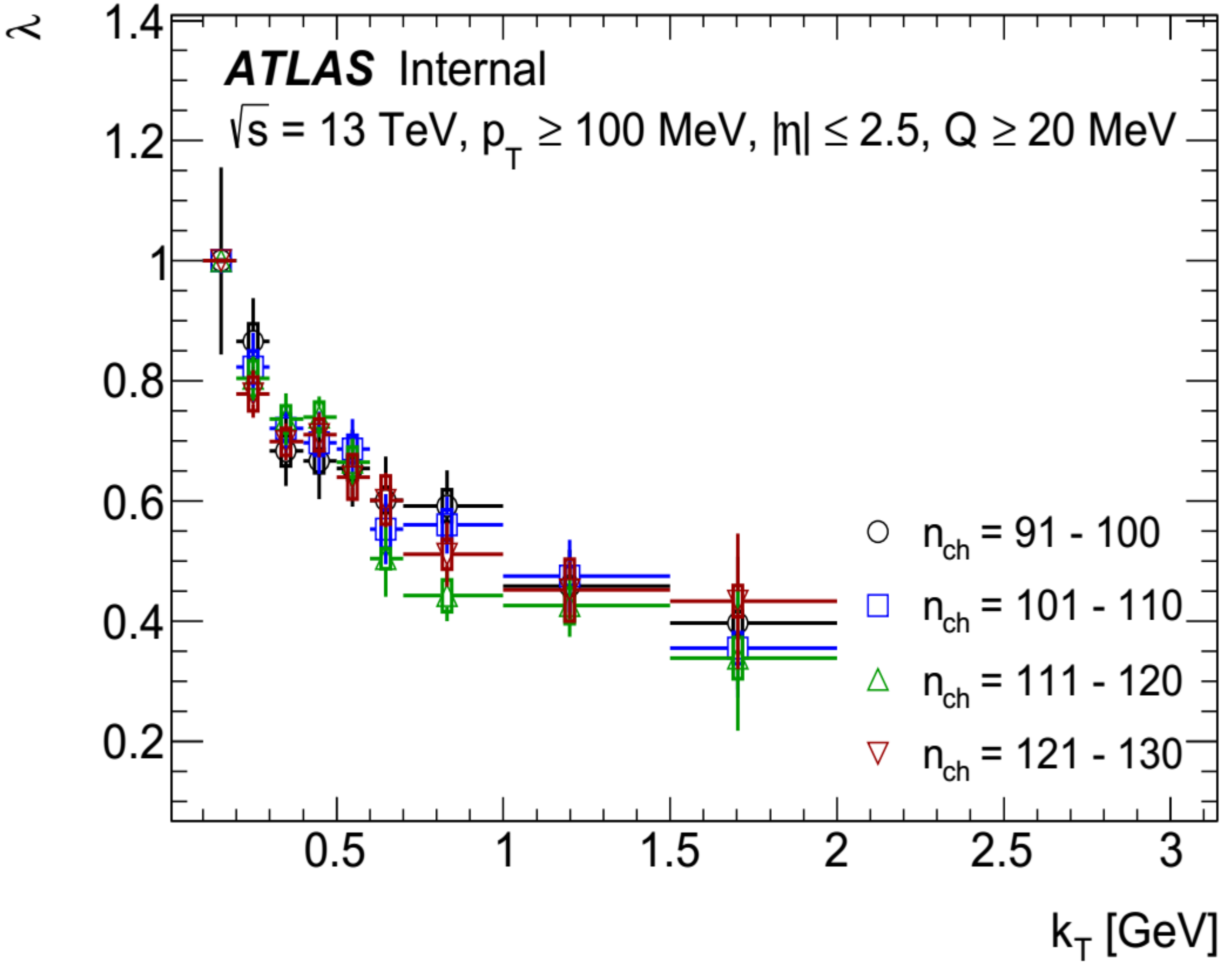

R distribution at 13 TeV

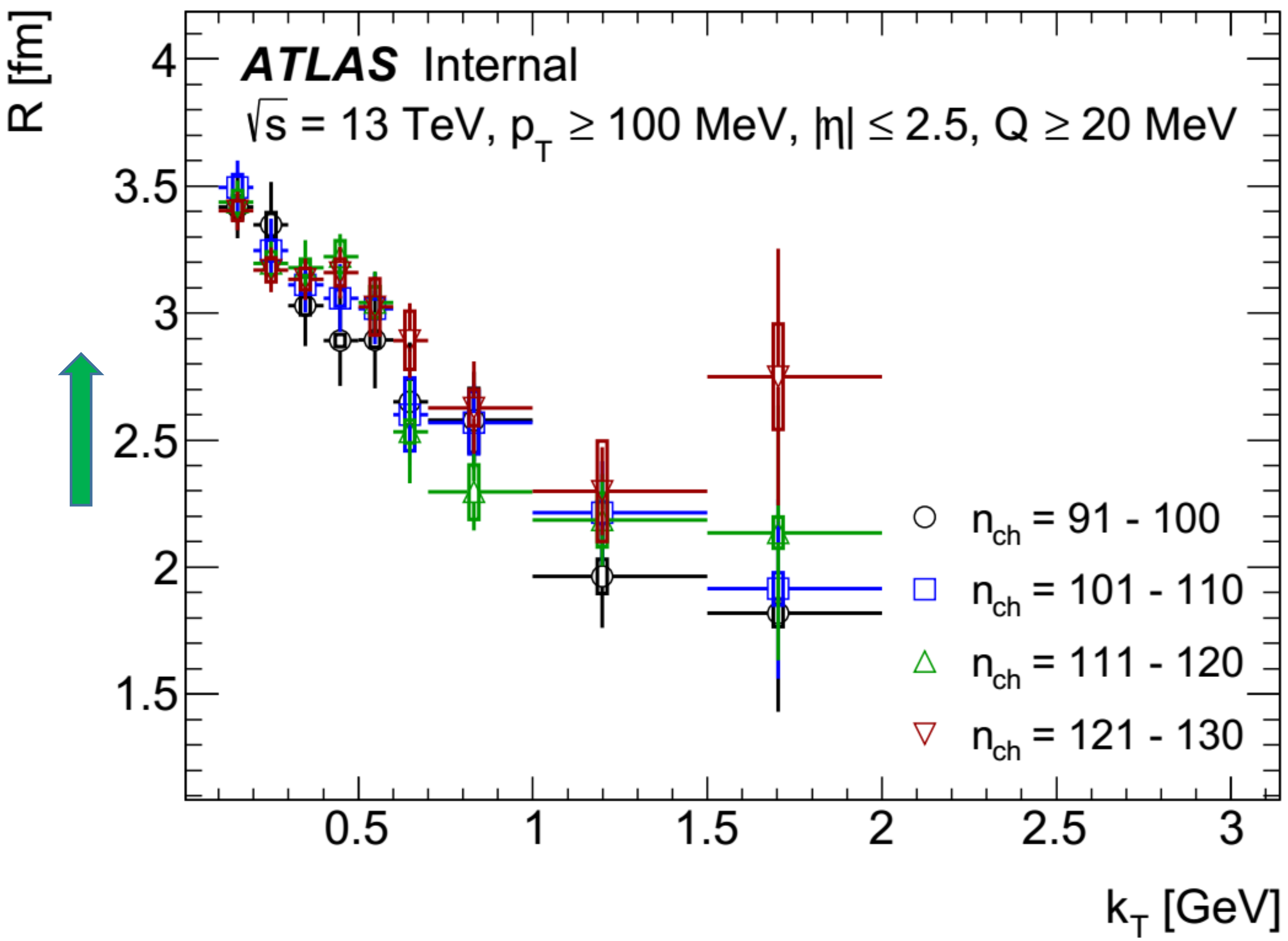

- **The λ and R values are independent of multiplicity within uncertainties**
- **The λ and R values decrease exponentially with k_T**

k_T DEPENDENCE OF BEC PARAMETERS FOR (n_{CH}, k_T) INTERVALS (CONT.)

λ distribution at 13 TeV **HMT trigger** **R distribution at 13 TeV**

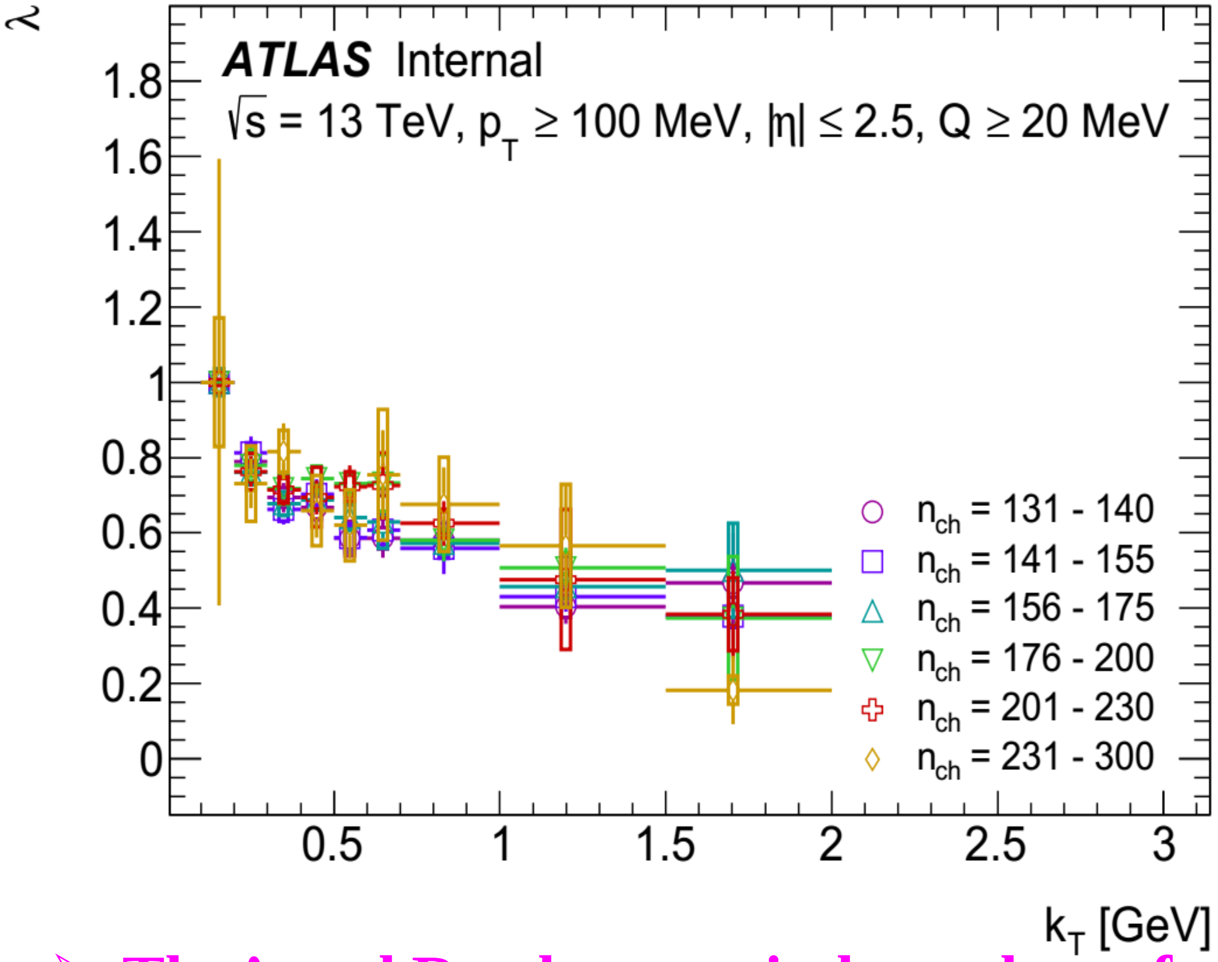

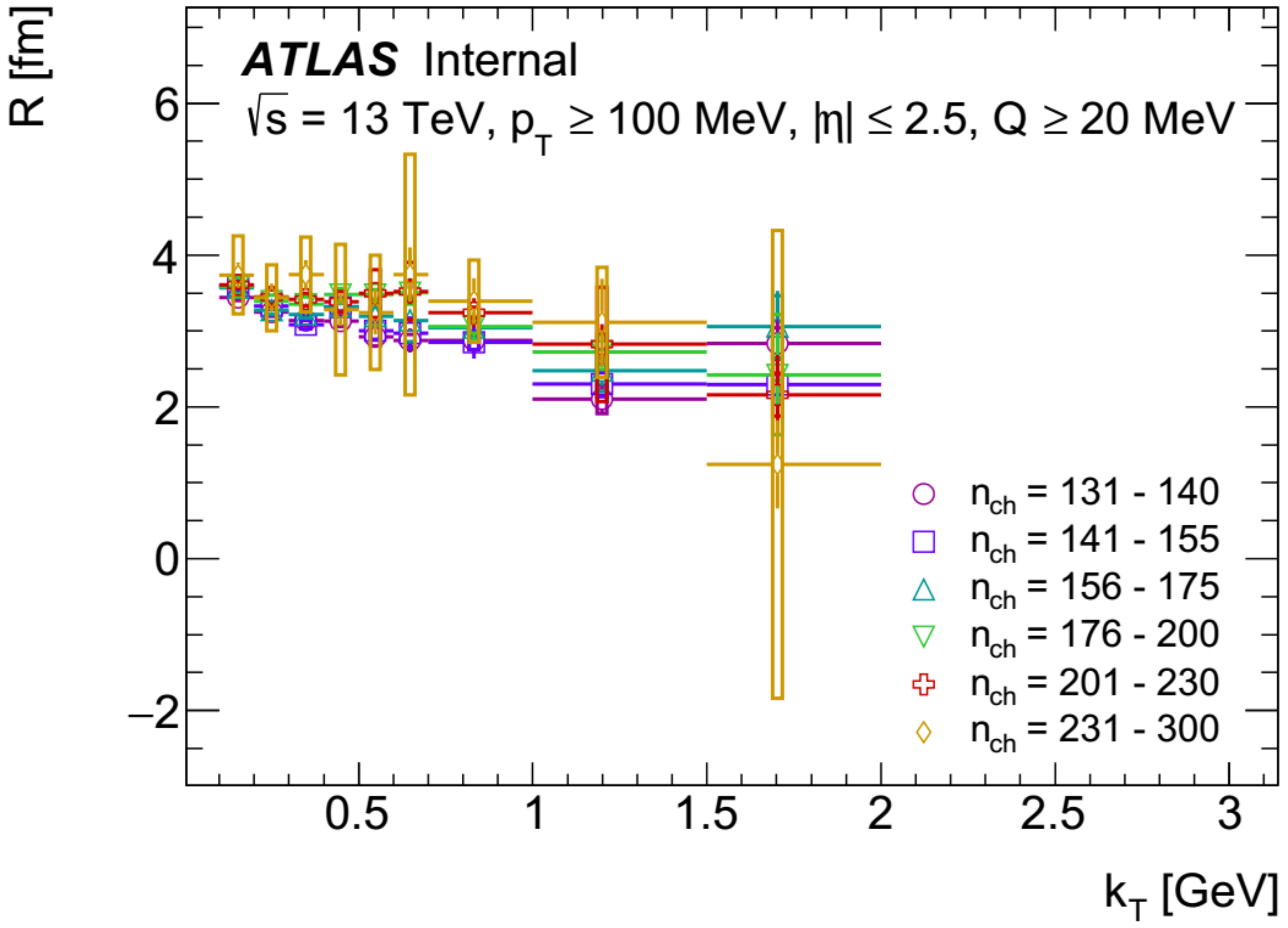

- **The λ and R values are independent of multiplicity within uncertainties**
- **The λ and R values decrease exponentially with k_T**

CONCLUSIONS

- ATLAS data taking in Run 2 is going very well. Good data taking efficiency and Data Quality
- A rich set of new physics results:
  - Evidence for Higgs bosons decaying to a pair of b-quarks
  - Evidence for Zt production, rate consistent with the SM
  - A first study of Bose-Einstein correlations in pp collisions at 13 TeV
    - ✓Confirmation of the BEC radius saturation effect for high multiplicity region. The feature for the first time observed by ATLAS at 7 TeV
    - ✓Energy dependence of λ

THANK YOU VERY MUCH FOR ATTENTION!

BACKUP SLIDES

EXOTIC SEARCHES

ATLAS Exotics Searches* - 95% CL Upper Exclusion Limits

Status: July 2017

ATLAS Preliminary

$\int \mathcal{L}\,dt = (3.2 - 37.0)\ \text{fb}^{-1}$ $\sqrt{s} = 8, 13$ TeV

	Model	ℓ, γ	Jets†	E_T^{miss}	$\int \mathcal{L}\,dt[\text{fb}^{-1}]$	Limit		Reference
Extra dimensions	ADD $G_{KK} + g/q$	$0\ e, \mu$	$1-4$ j	Yes	36.1	M_D 7.75 TeV	$n = 2$	ATLAS-CONF-2017-060
	ADD non-resonant $\gamma\gamma$	$2\ \gamma$	–	–	36.7	M_S 8.6 TeV	$n = 3$ HLZ NLO	CERN-EP-2017-132
	ADD QBH	–	2 j	–	37.0	M_{th} 8.9 TeV	$n = 6$	1703.09217
	ADD BH high $\sum p_T$	$\geq 1\ e, \mu$	≥ 2 j	–	3.2	M_{th} 8.2 TeV	$n = 6$, $M_D = 3$ TeV, rot BH	1606.02265
	ADD BH multijet	–	≥ 3 j	–	3.6	M_{th} 9.55 TeV	$n = 6$, $M_D = 3$ TeV, rot BH	1512.02586
	RS1 $G_{KK} \to \gamma\gamma$	$2\ \gamma$	–	–	36.7	G_{KK} mass 4.1 TeV	$k/\overline{M}_{Pl} = 0.1$	CERN-EP-2017-132
	Bulk RS $G_{KK} \to WW \to qq\ell\nu$	$1\ e, \mu$	1 J	Yes	36.1	G_{KK} mass 1.75 TeV	$k/\overline{M}_{Pl} = 1.0$	ATLAS-CONF-2017-051
	2UED / RPP	$1\ e, \mu$	≥ 2 b, ≥ 3 j	Yes	13.2	KK mass 1.6 TeV	Tier (1,1), $\mathcal{B}(A^{(1,1)} \to tt) = 1$	ATLAS-CONF-2016-104
Gauge bosons	SSM $Z' \to \ell\ell$	$2\ e, \mu$	–	–	36.1	Z' mass 4.5 TeV		ATLAS-CONF-2017-027
	SSM $Z' \to \tau\tau$	$2\ \tau$	–	–	36.1	Z' mass 2.4 TeV		ATLAS-CONF-2017-050
	Leptophobic $Z' \to bb$	–	2 b	–	3.2	Z' mass 1.5 TeV		1603.08791
	Leptophobic $Z' \to tt$	$1\ e, \mu$	≥ 1 b, ≥ 1J/2j	Yes	3.2	Z' mass 2.0 TeV	$\Gamma/m = 3\%$	ATLAS-CONF-2016-014
	SSM $W' \to \ell\nu$	$1\ e, \mu$	–	Yes	36.1	W' mass 5.1 TeV		1706.04786
	HVT $V' \to WV \to qqqq$ model B	$0\ e, \mu$	2 J	–	36.7	V' mass 3.5 TeV	$g_V = 3$	CERN-EP-2017-147
	HVT $V' \to WH/ZH$ model B	multi-channel			36.1	V' mass 2.93 TeV	$g_V = 3$	ATLAS-CONF-2017-055
	LRSM $W'_R \to tb$	$1\ e, \mu$	2 b, 0-1 j	Yes	20.3	W' mass 1.92 TeV		1410.4103
	LRSM $W'_R \to tb$	$0\ e, \mu$	≥ 1 b, 1 J	–	20.3	W' mass 1.76 TeV		1408.0886
CI	CI $qqqq$	–	2 j	–	37.0	Λ 21.8 TeV η_{LL}^-		1703.09217
	CI $\ell\ell qq$	$2\ e, \mu$	–	–	36.1	Λ 40.1 TeV η_{LL}^-		ATLAS-CONF-2017-027
	CI $uutt$	2(SS)/$\geq$3 e,μ	≥ 1 b, ≥ 1 j	Yes	20.3	Λ 4.9 TeV	$\lvert C_{RR}\rvert = 1$	1504.04605
DM	Axial-vector mediator (Dirac DM)	$0\ e, \mu$	$1-4$ j	Yes	36.1	m_{med} 1.5 TeV	g_q=0.25, g_χ=1.0, $m(\chi) < 400$ GeV	ATLAS-CONF-2017-060
	Vector mediator (Dirac DM)	$0\ e, \mu$, $1\ \gamma$	≤ 1 j	Yes	36.1	m_{med} 1.2 TeV	g_q=0.25, g_χ=1.0, $m(\chi) < 480$ GeV	1704.03848
	$VV\chi\chi$ EFT (Dirac DM)	$0\ e, \mu$	1 J, ≤ 1 j	Yes	3.2	M_* 700 GeV	$m(\chi) < 150$ GeV	1608.02372
LQ	Scalar LQ 1st gen	$2\ e$	≥ 2 j	–	3.2	LQ mass 1.1 TeV	$\beta = 1$	1605.06035
	Scalar LQ 2nd gen	$2\ \mu$	≥ 2 j	–	3.2	LQ mass 1.05 TeV	$\beta = 1$	1605.06035
	Scalar LQ 3rd gen	$1\ e, \mu$	$\geq$1 b, $\geq$3 j	Yes	20.3	LQ mass 640 GeV	$\beta = 0$	1508.04735
Heavy quarks	VLQ $TT \to Ht + X$	0 or 1 e, μ	≥ 2 b, ≥ 3 j	Yes	13.2	T mass 1.2 TeV	$\mathcal{B}(T \to Ht) = 1$	ATLAS-CONF-2016-104
	VLQ $TT \to Zt + X$	$1\ e, \mu$	≥ 1 b, ≥ 3 j	Yes	36.1	T mass 1.16 TeV	$\mathcal{B}(T \to Zt) = 1$	1705.10751
	VLQ $TT \to Wb + X$	$1\ e, \mu$	≥ 1 b, ≥ 1J/2j	Yes	36.1	T mass 1.35 TeV	$\mathcal{B}(T \to Wb) = 1$	CERN-EP-2017-094
	VLQ $BB \to Hb + X$	$1\ e, \mu$	≥ 2 b, ≥ 3 j	Yes	20.3	B mass 700 GeV	$\mathcal{B}(B \to Hb) = 1$	1505.04306
	VLQ $BB \to Zb + X$	2/$\geq$3 e, μ	$\geq$2/$\geq$1 b	–	20.3	B mass 790 GeV	$\mathcal{B}(B \to Zb) = 1$	1409.5500
	VLQ $BB \to Wt + X$	$1\ e, \mu$	≥ 1 b, ≥ 1J/2j	Yes	36.1	B mass 1.25 TeV	$\mathcal{B}(B \to Wt) = 1$	CERN-EP-2017-094
	VLQ $QQ \to WqWq$	$1\ e, \mu$	≥ 4 j	Yes	20.3	Q mass 690 GeV		1509.04261
Excited fermions	Excited quark $q^* \to qg$	–	2 j	–	37.0	q^* mass 6.0 TeV	only u^* and d^*, $\Lambda = m(q^*)$	1703.09127
	Excited quark $q^* \to q\gamma$	$1\ \gamma$	1 j	–	36.7	q^* mass 5.3 TeV	only u^* and d^*, $\Lambda = m(q^*)$	CERN-EP-2017-148
	Excited quark $b^* \to bg$	–	1 b, 1 j	–	13.3	b^* mass 2.3 TeV		ATLAS-CONF-2016-060
	Excited quark $b^* \to Wt$	1 or 2 e, μ	1 b, 2-0 j	Yes	20.3	b^* mass 1.5 TeV	$f_g = f_L = f_R = 1$	1510.02664
	Excited lepton ℓ^*	$3\ e, \mu$	–	–	20.3	ℓ^* mass 3.0 TeV	$\Lambda = 3.0$ TeV	1411.2921
	Excited lepton ν^*	$3\ e, \mu, \tau$	–	–	20.3	ν^* mass 1.6 TeV	$\Lambda = 1.6$ TeV	1411.2921
Other	LRSM Majorana ν	$2\ e, \mu$	2 j	–	20.3	N^0 mass 2.0 TeV	$m(W_R) = 2.4$ TeV, no mixing	1506.06020
	Higgs triplet $H^{\pm\pm} \to \ell\ell$	2,3,4 e, μ (SS)	–	–	36.1	$H^{\pm\pm}$ mass 870 GeV	DY production	ATLAS-CONF-2017-053
	Higgs triplet $H^{\pm\pm} \to \ell\tau$	$3\ e, \mu, \tau$	–	–	20.3	$H^{\pm\pm}$ mass 400 GeV	DY production, $\mathcal{B}(H_L^{\pm\pm} \to \ell\tau) = 1$	1411.2921
	Monotop (non-res prod)	$1\ e, \mu$	1 b	Yes	20.3	spin-1 invisible particle mass 657 GeV	$a_{non-res} = 0.2$	1410.5404
	Multi-charged particles	–	–	–	20.3	multi-charged particle mass 785 GeV	DY production, $\lvert q\rvert = 5e$	1504.04188
	Magnetic monopoles	–	–	–	7.0	monopole mass 1.34 TeV	DY production, $\lvert g\rvert = 1g_D$, spin 1/2	1509.08059

Limit axis: 10^{-1}, 1, 10 — Mass scale [TeV]

$\sqrt{s} = 8$ TeV $\sqrt{s} = 13$ TeV

*Only a selection of the available mass limits on new states or phenomena is shown.

†Small-radius (large-radius) jets are denoted by the letter j (J).

RESONANCE SEARCHES (DIBOSON)

- Searches for new resonances decaying to a pair of W, Z or H bosons. At the time of the LHCC in May, only the VH→qqbb result was ready. Now:
  - VV→qqqq/qq$\ell\nu$/qq$\ell\ell$/qq$\nu\nu$, VH→qqbb/$\ell\nu$bb/$\ell\ell$bb.
- Reconstruct merged jets at high pT for resonances at the highest mass, using substructure techniques ('boson-tagging').
- No significant excess observed over the SM expectations.
- Set limits in framework of Heavy Vector Triplet (HVT) model*.

* JHEP 09 (2014) 060, JHEP 01 (2013) 166

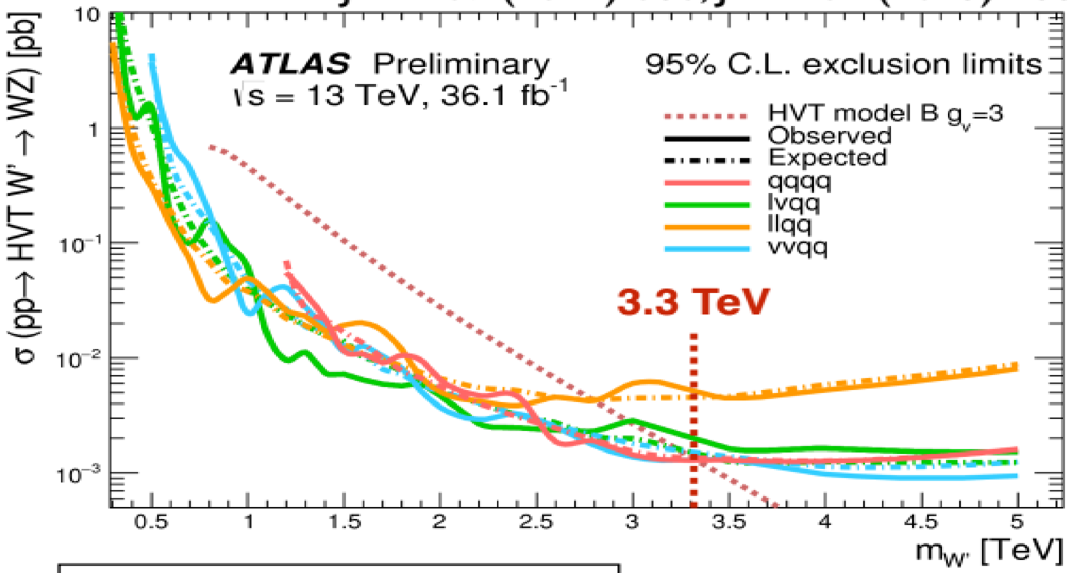

ATLAS-CONF-2017-051, arxiv:1708.09638

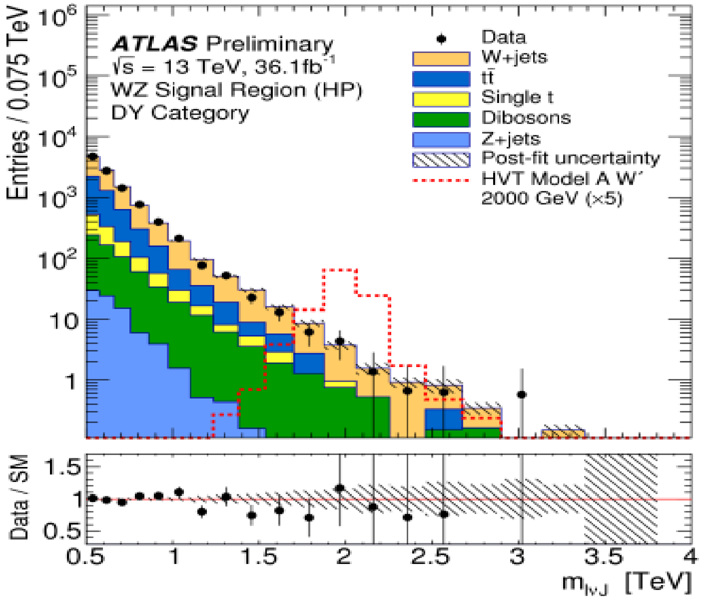

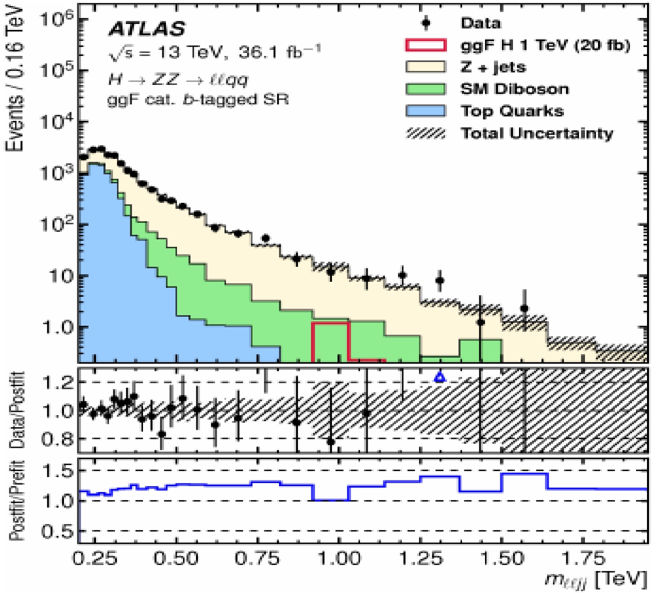

RESONANCE SEARCHES (γγ, ττ)

- Diphoton and ditau searches sensitive to new heavy scalars, e.g. Higgs bosons.
  - γγ search also targets spin-2 (graviton) production with a dedicated selection.
  - ττ searches sensitive to SUSY Higgs (H/A).
- No significant excess over the SM expectation.

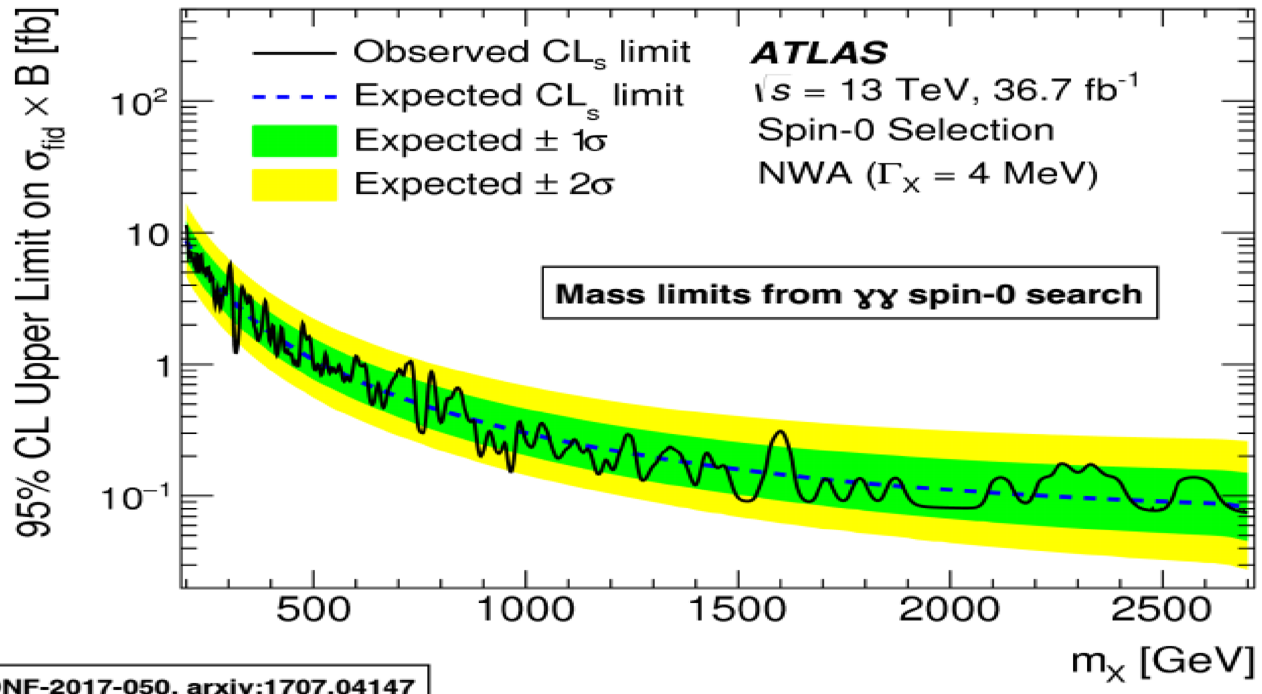

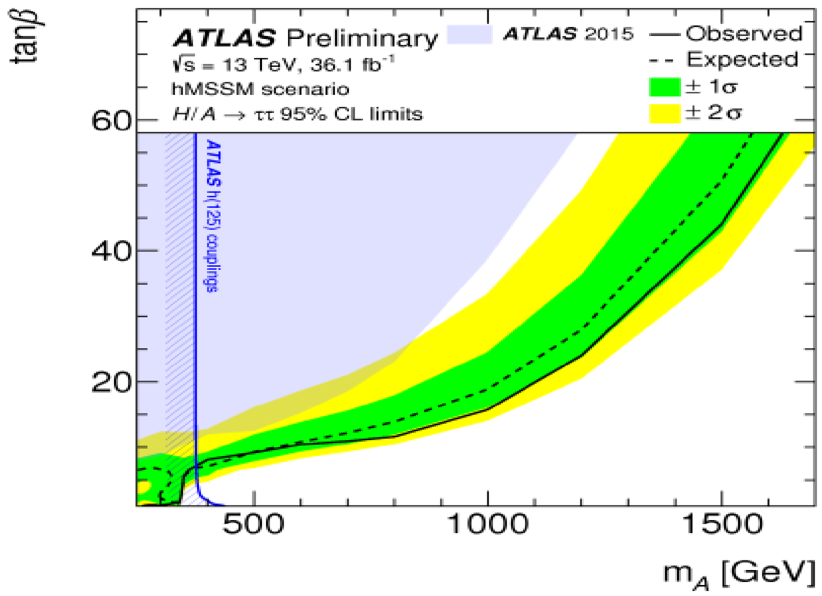

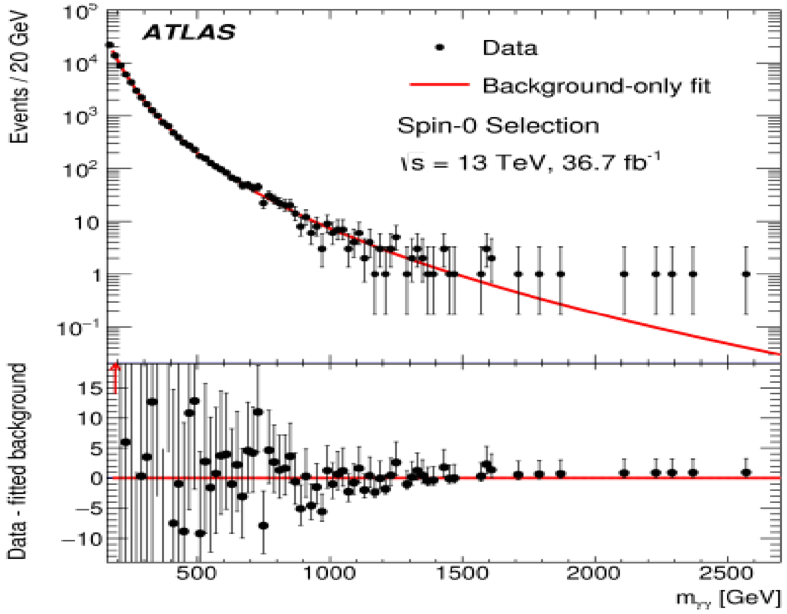

ATLAS-CONF-2017-050, arxiv:1707.04147

SEARCHES FOR DARK MATTER

- Generic dark matter models tested with searches for mono-jet/γ/Z/H(→γγ/bb)+E_T^{miss}, with recoil against invisible dark matter particle(s).
  - Complementary to direct dark matter searches, and direct searches for the mediator decaying to e.g. a pair of jets.
- Phenomenology depends on mass of DM, mass of heavy mediator and value and type of couplings.
- No significant excesses over the SM predictions.

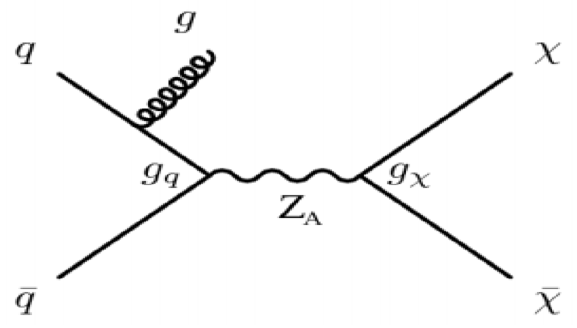

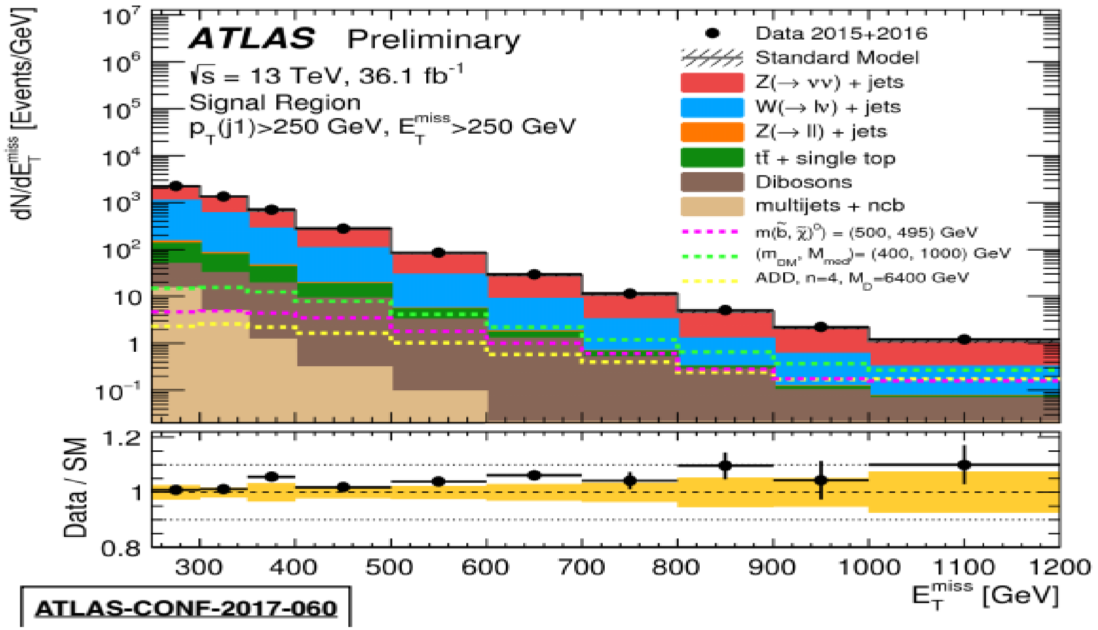

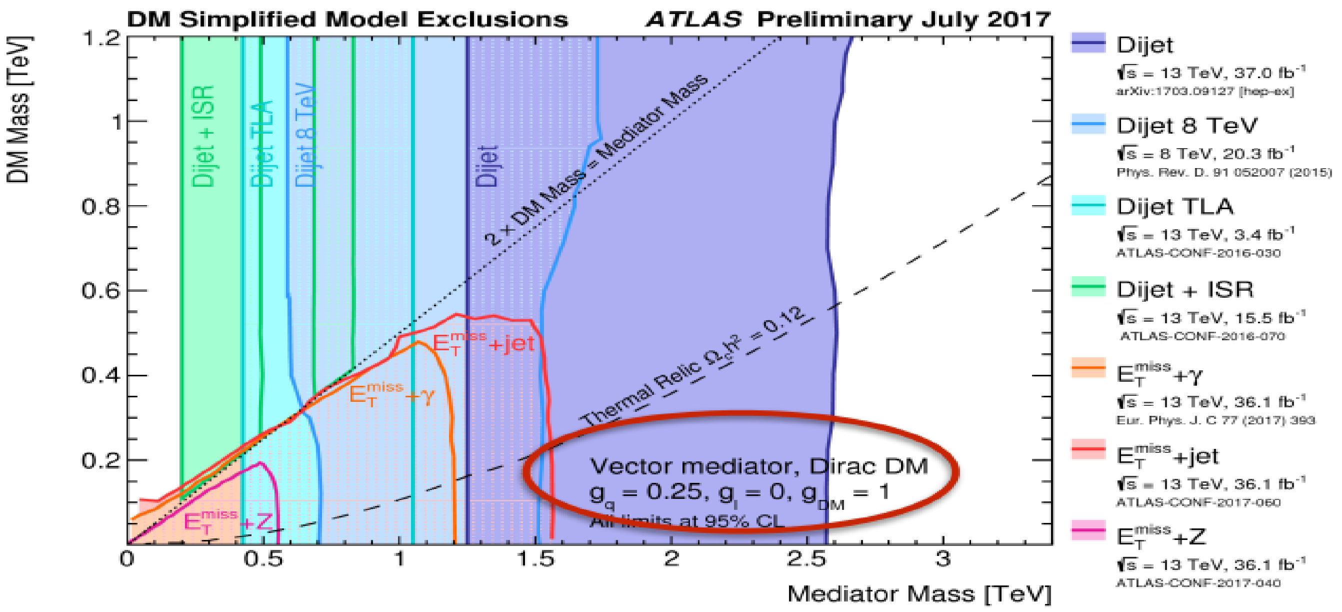

SEARCHES FOR SUPERSYMMETRY

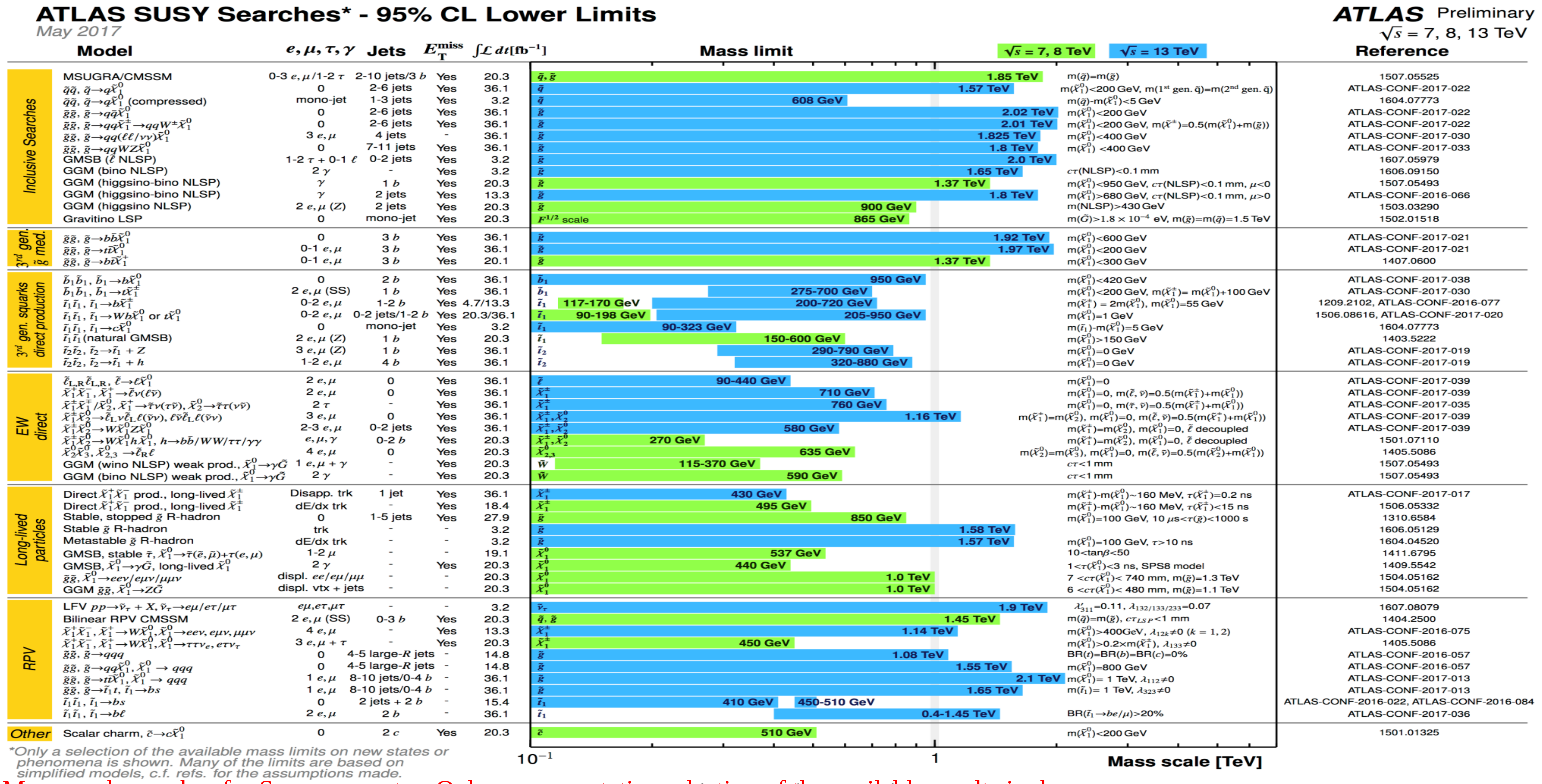

Mass reach searches for Supersymmetry. Only a representative selection of the available results is shown.

OVERVIEW

The focus of ATLAS is high-p_T physics, and also provides a window onto important soft QCD processes.

These have intrinsic interest but also the understanding of underpins searches for new physics.

Task ►Bose Einstein Correlations

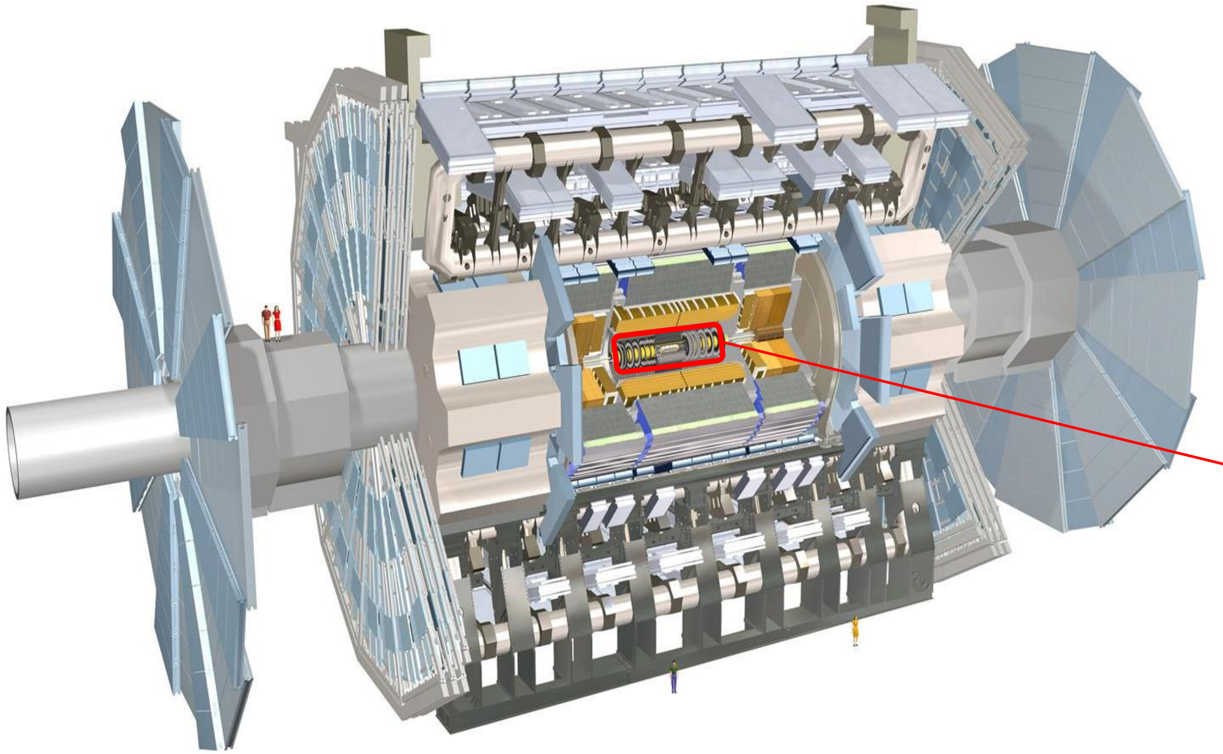

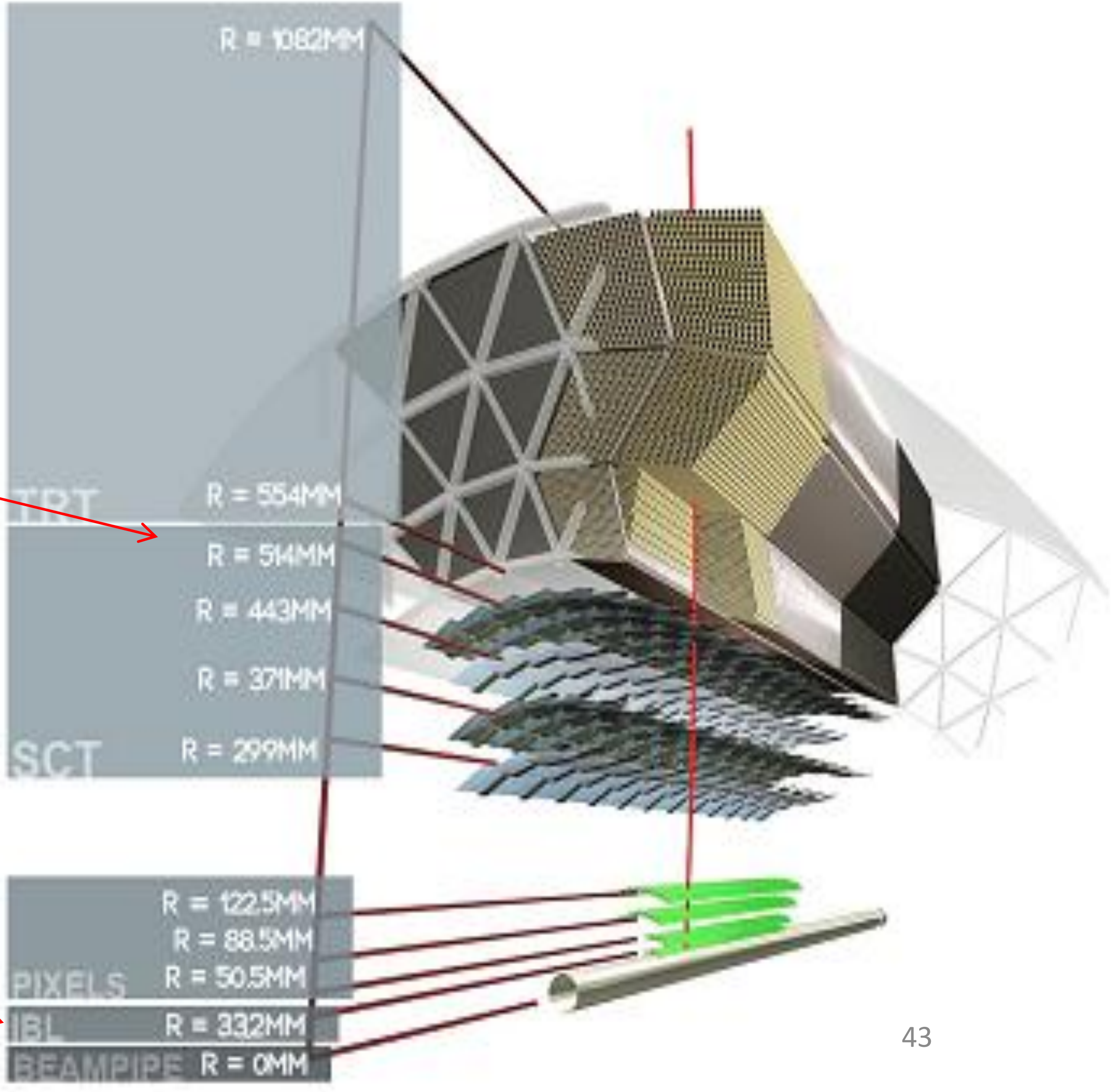

ATLAS Inner Detector (ID) **main tracking device**:

Consists of **Pixel, Silicon strip (SCT) and drift tube (TRT) detectors.** Single hit resolution between 10 μm (Pixel) and 1 μm (TRT). New: *Insertable B-Layer* (IBL) in the Pixel

INNER DETECTORS (ID)

ATLAS tracking detectors:
Pixels, SCT & TRT

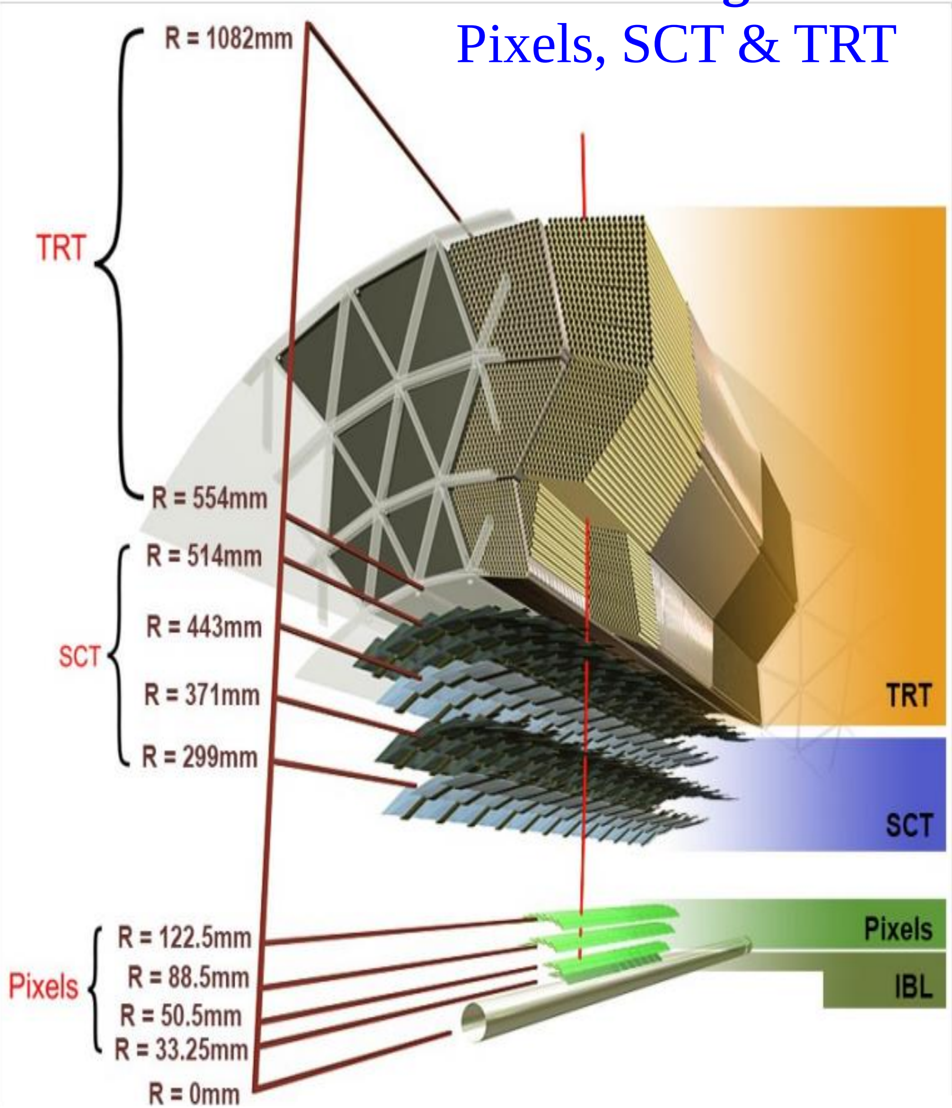

- ❑ **New innermost 4-th layer** for the Pixel detector [**IBL** = Insertable B-Layer]
- ❑ Required complete removal of the ATLAS Pixel volume
- ❑ IBL fully operational

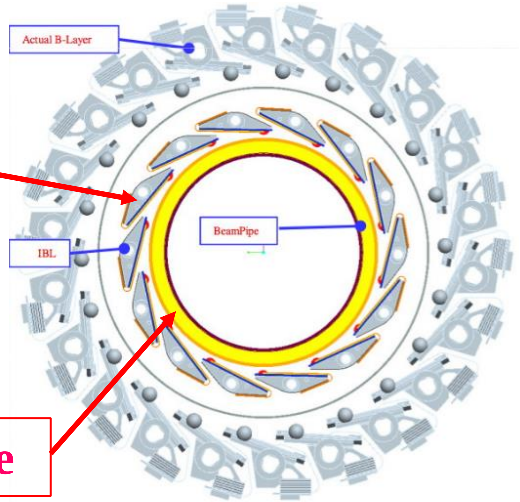

New Be beam pipe

Two times better tracks impact parameters resolution at 13 TeV!

MINIMUM BIAS TRIGGER SCINTILLATOR

24 independent wedge-shaped plastic scintillators (12 per side) read out by PMTs,

$2.08<|\eta|<3.86$*

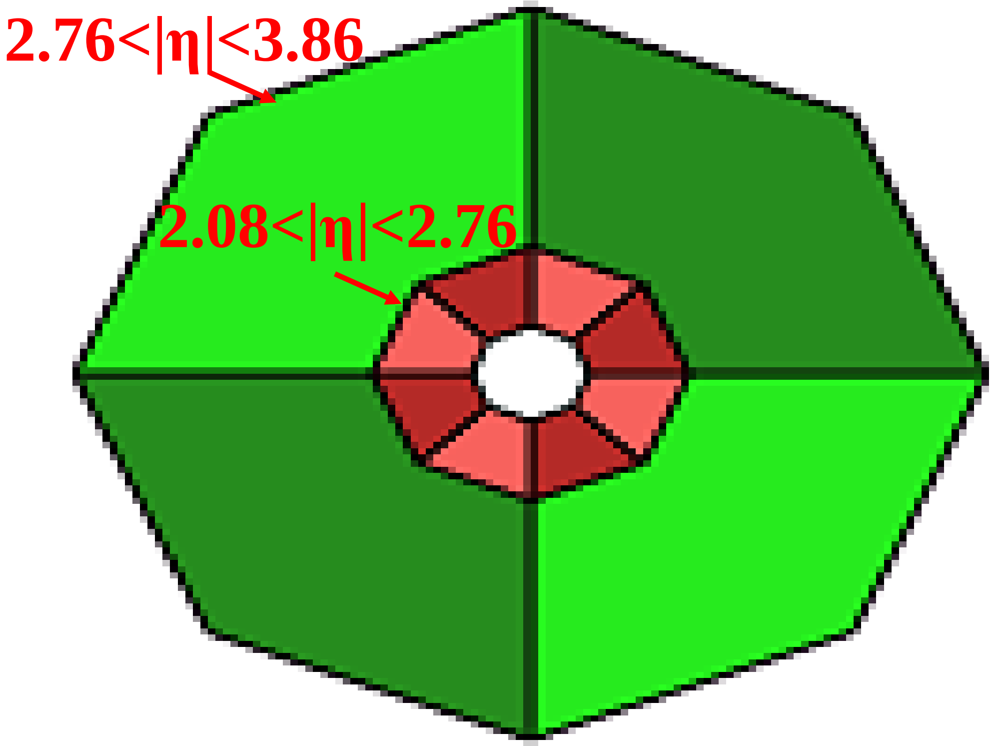

* Pseudorapidity is defined as $\eta = -\frac{1}{2} \ln(\tan(\theta/2))$, θ is the polar angle with respect to the beam.

- Designed for triggering on min bias events, >99% efficiency
- MBTS timing used to veto halo and beam gas events
- Also being used as gap trigger for various diffractive subjects

MINIMUM-BIAS AND HIGH MULTIPLICITY TRACK TRIGGERS

- For these analysis the events collected with **Minimum-bias** (MB) trigger named as ***HLT_noalg_mb_L1MBTS _1*** were used.
  - This trigger required at least one hit in one of the 12+12 sectors (A and C sides) of the MBTS detector.

✓ Integral Luminosity ~151 μb^{-1}; Statistic: 9.6×10^{6} events with 2.8×10^{8} tracks

- For these analysis the events collected with **High multiplicity track** (HMT) trigger named as ***HLT_mb_sp900_trk60_hmt_L1MBTS_1_1*** were used.
  - High-multiplicity track (HMT) events were collected at 13 TeV using a dedicated high-multiplicity track trigger:
    - requires more than 900 SCT space-points,
    - more than 60 reconstructed good quality charged tracks with p_T>0.4 GeV associated with the primary vertex.

✓ Integral Luminosity ~8.4 nb^{-1}; Statistic: 9.1×10^{6} events with 9.8×10^{8} tracks

MOTIVATION FOR BOSE-EINSTEIN CORRELATIONS

- Bose-Einstein correlations (BEC) represent a unique probe of the *space-time geometry* of the *hadronization region* and allow the *determination the size and shape of the source* from which particles are *emitted*.

- Studies of the dependence of BEC on *particle multiplicity* and *transverse momentum* are of special interest. They help in the understanding of multiparticle production mechanisms.

- High-multiplicity data in proton interactions can serve as a reference for studies in nucleus-nucleus collisions. The effect is reproduced in hydrodynamical and Pomeron-based approaches for hadronic interactions where high multiplicities play a crucial role.

BOSE-EINSTEIN CORRELATIONS AND HANBURY BROWN –TWISS INTERFEROMETRY

Bose-Einstein correlations (BEC) are often considered to be the analogue of the **Hanbury Brown and Twiss effect** in astronomy, describing the interference of incoherently-emitted identical bosons.

Intensity interferometry of photons in radio-astronomy: measures angular diameter of two stars, so the physical size of the source

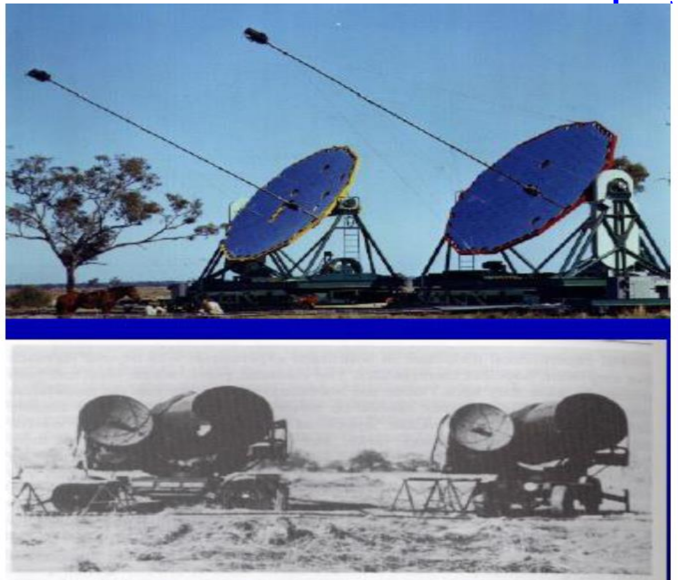

Figure 10.1 The first stellar intensity interferometer; the pilot model of the stellar intensity interferometer at Jodrell Bank in 1955. Two Army searchlights were used to make the first measurement of the angular diameter of a main sequence star (Sirius).

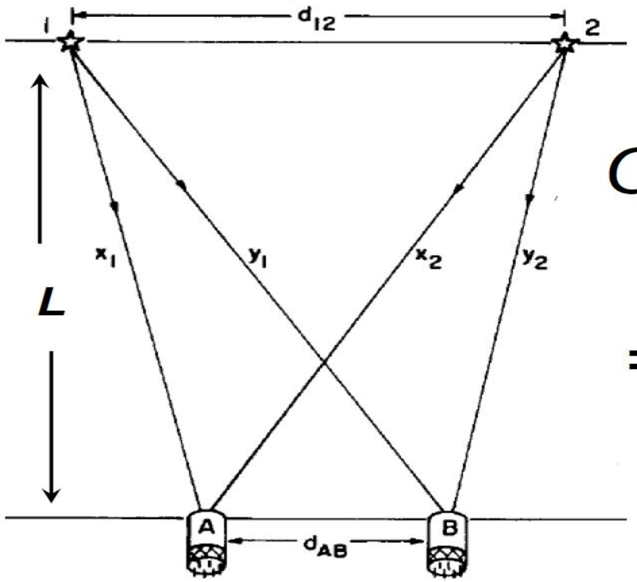

$$C(d) = \frac{\langle I_1 I_2 \rangle}{\langle I_1 \rangle \langle I_2 \rangle}$$

$$= 1 + A\cos(d_{AB})$$

$$d_{AB} = \lambda/\theta$$

$I_{1(2)}$ - intensities, $<x>$ - averaging over random phases

λ is the wavelength of the light, $\theta = d_{12}/L$

Varying d_{AB} one learns the angle, and using the individual wave vectors, the physical size of the source

We correct the events on:

$$w(n) = \frac{1}{\varepsilon_{trig}(n) \cdot \varepsilon_{vert}(n)}$$

The trigger efficiency – $\varepsilon_{trig}(n)$, The vertex reconstruction efficiency – $\varepsilon_{vert}(n)$

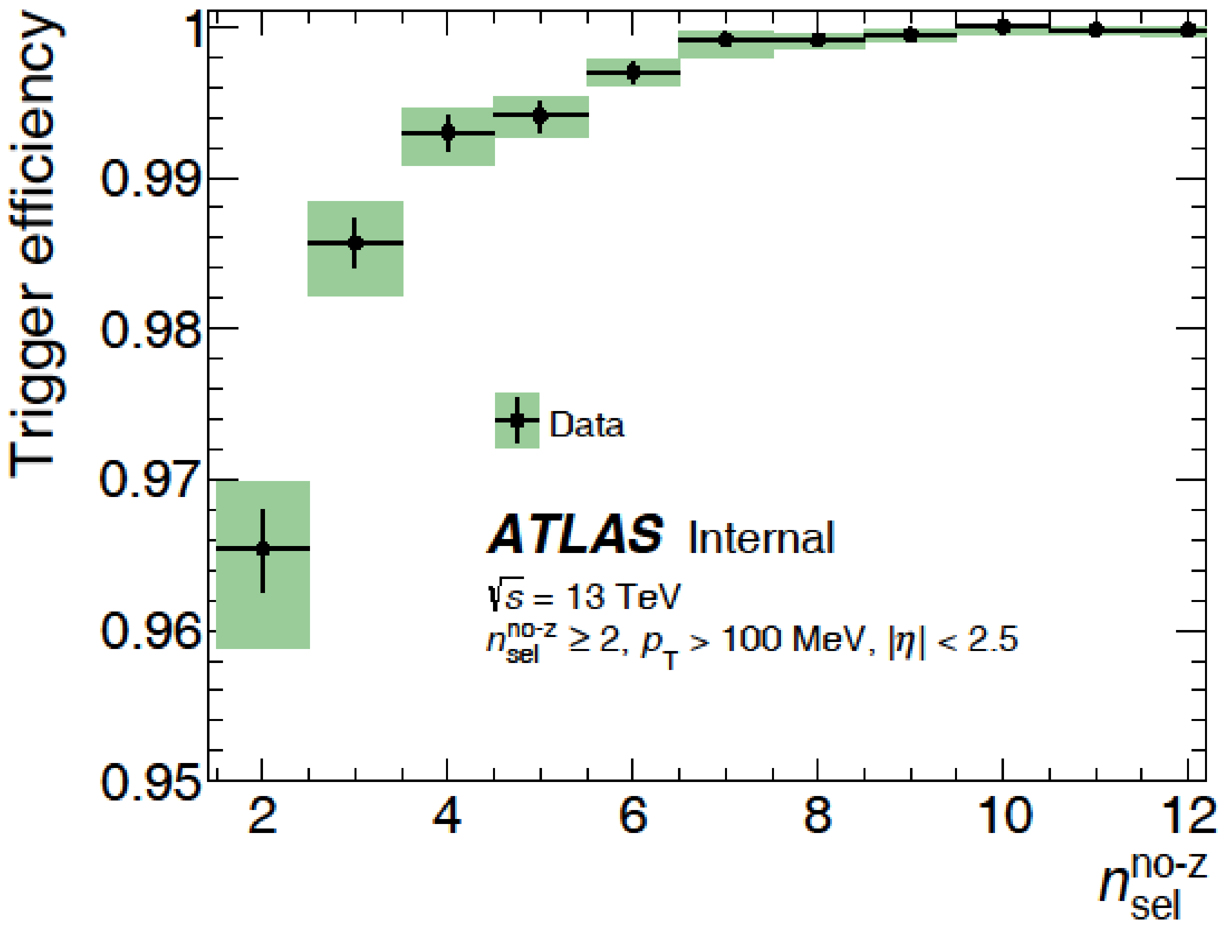

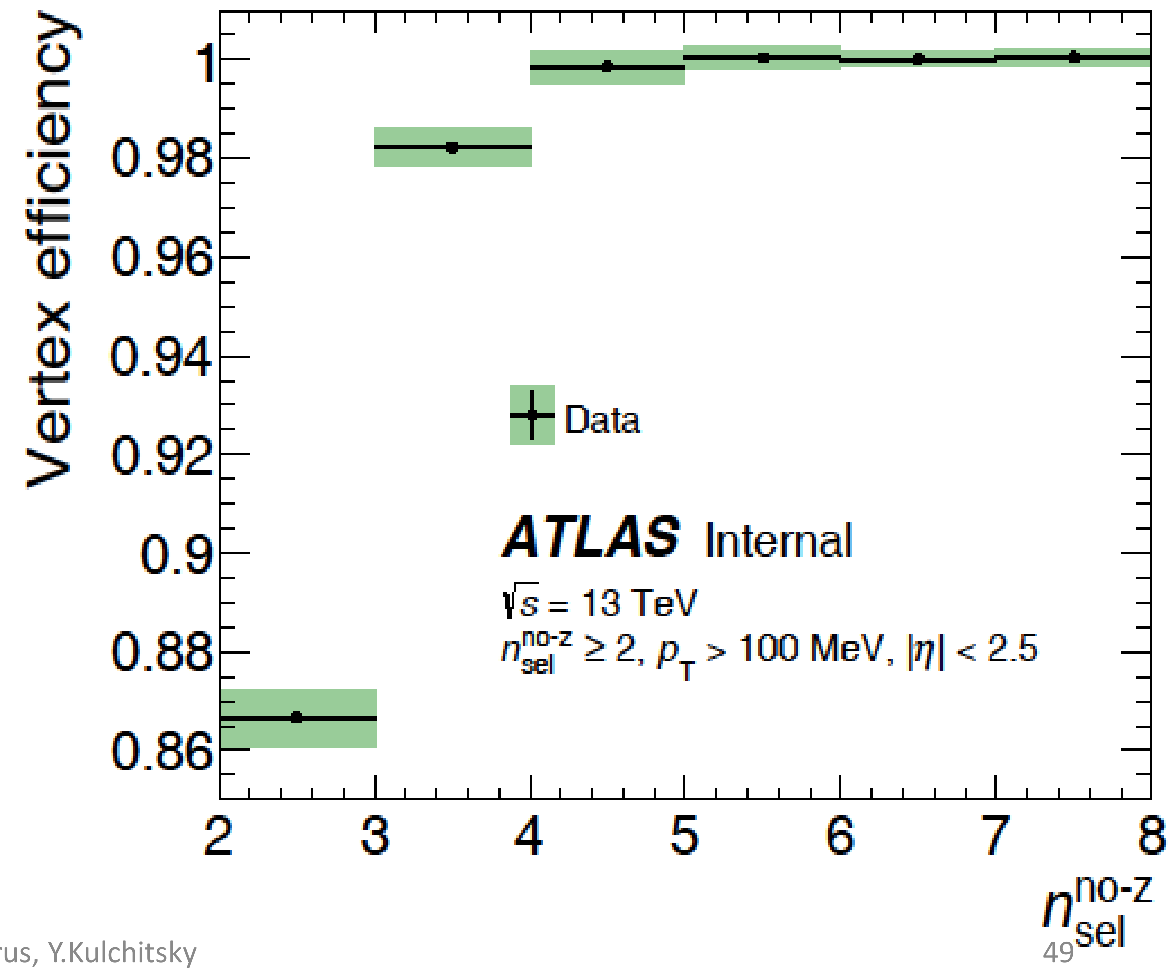

DATA SAMPLES

Information from ATL-COM-PHYS-2015-1379 p.51

Run	μ	Events in MinBias Stream	L1MBTS_1_1 Prescales	sp900_trk60 Prescales
267358	0.003	8.6	2	
267359	0.007	12.3	2	
267360	0.03-0.04	12.5	LB:294-296, 100	
			LB:297-444, 1	1
267367	0.03	17.1	LB:328-329, 100	1
			LB:330-393, 1	1
			LB:393-396, 200	1
			LB:397-399, 2	
			LB:400-405, 10	
			LB:406-420, 4	
			LB:465-500, 3	1
			LB:502-505, 3	1
267385	0.04	71.2	LB:241-584, 3	1
			LB:870-908, 1	1
			LB:910, 1	1
267599	0.01	105.6	LB:289-482, 1	1
	0.03		LB:483-495, 1.9	1
	0.03		LB:496-500, 1.4	1
	0.03		LB:501-1130, 1	1

Low μ

20.9 millions of triggers

High μ

206.4 millions of triggers

Minimum-Bias trigger
Events: 9.6×10^{6};
Tracks: 2.8×10^{8}

High Multiplicity Tracks trigger
Events: 9.1×10^{6};
Tracks: 9.8×10^{8}

This data can be used for pile-up study for runs with higher μ

MONTE-CARLO SAMPLES

Generator	Version	Tune	PDF
Pythia8	8.185	A2	MSTW2008LO
Pythia8	8.186	Monash	NNPDF2.3LO
EPOS	LHCv3400	LHC	—

Monte-Carlo	Name of dataset: *mc15_13TeV : mc15_13TeV.*	Stat. [mil]
Pythia8 A2	361203.*Pythia8_A2_MSTW2008LO_ND_minbias.merge.AOD.e3639_a782_a787_r6264*	30
	361204.*Pythia8_A2_MSTW2008LO_SD_minbias.merge.AOD.e3639_a782_a787_r6264*	
	361205.*Pythia8_A2_MSTW2008LO_DD_minbias.merge.AOD.e3639_a782_a787_r6264*	
Pythia8 A2 Filtered	361214.*Pythia8_A2MSTW2008LO_minbias_NDnch120.merge.AOD.e3908_a782_a787_r6264*	1
	361215.*Pythia8_A2MSTW2008LO_minbias_NDnch160.merge.AOD.e3908_a782_a787_r6264*	1
	361216.*Pythia8_A2MSTW2008LO_minbias_NDnch200.merge.AOD.e3908_a782_a787_r6264*	1
Pythia8 Monash	361200.*Pythia8_Monash_NNPDF23LO_ND_minbias.merge.AOD.e3639_s2601_s2132_r6616_r6270*	16
	361201.*Pythia8_Monash_NNPDF23LO_SD_minbias.merge.AOD.e3639_s2601_s2132_r6616_r6264*	
	361202.*Pythia8_Monash_NNPDF23LO_DD_minbias.merge.AOD.e3639_s2601_s2132_r6616_r6264*	
EPOS	361224.*Epos_minbias_inelastic.merge.AOD.e3908_a782_s2183_a787_r6264mc15*	20

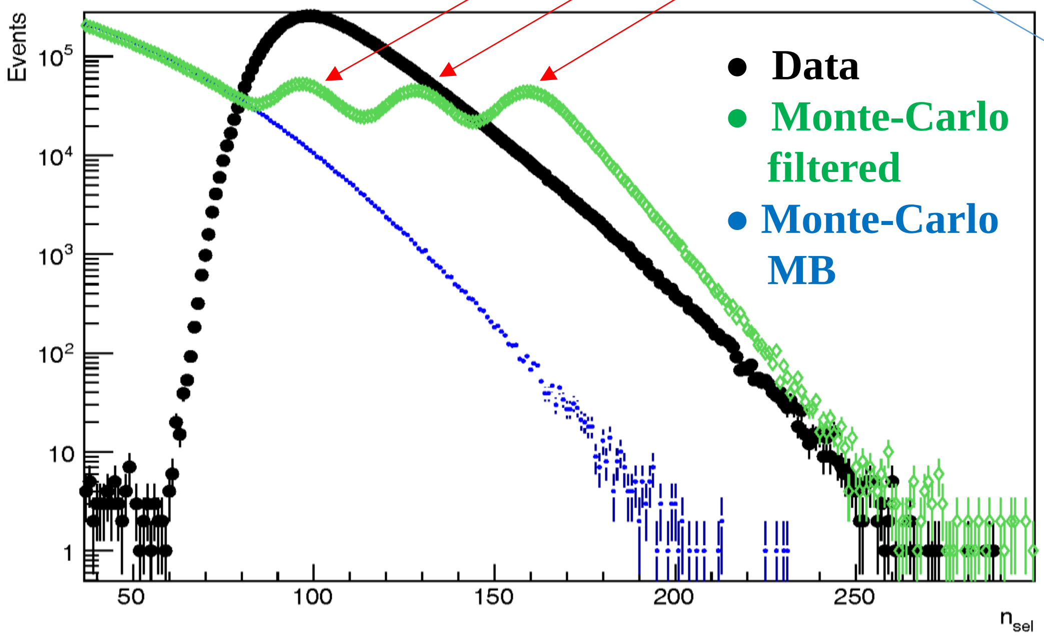

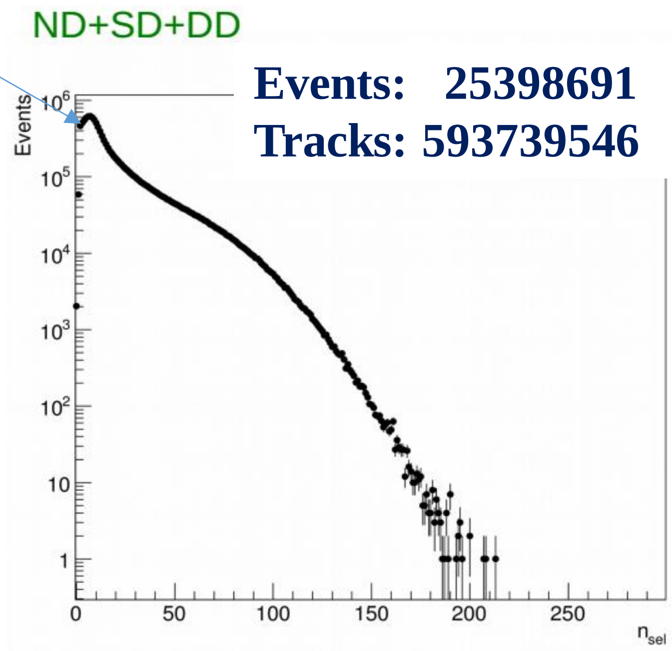

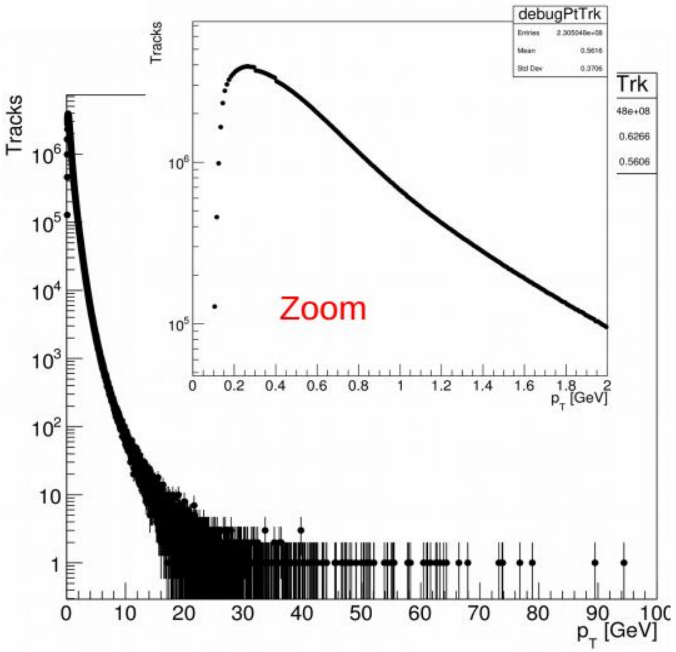

Pile-up for HMT and MB events

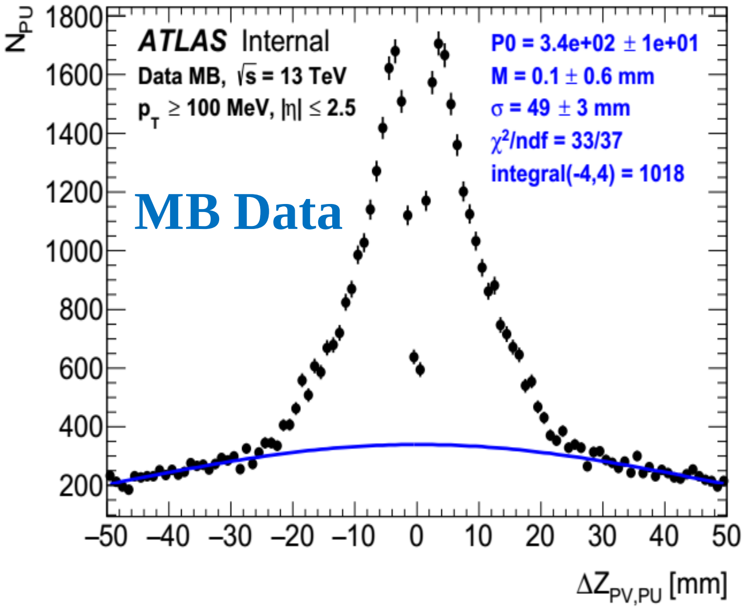

MB trigger

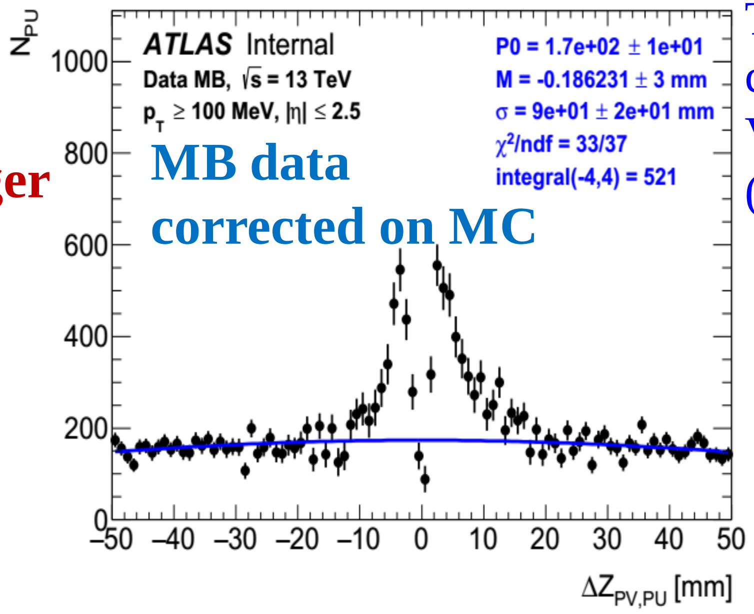

The distribution of the distance between Z coordinates of Primary Vertex and Pile-Up Vertexes for MB and HMT events for Data (left) and Data corrected on MC (right)

For MB events the number of pile-up vertexes in the Primary Vertex (PV) region ±4 mm is ~520 after correction on MC, and the number of tracks in Pile-up vertex is 9.4. Therefore the fraction of pile-up tracks in MB events is **0.002%**

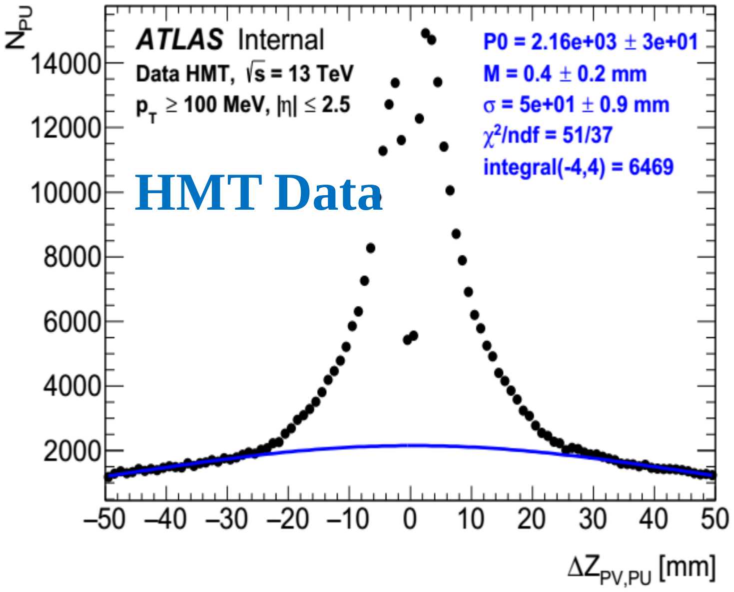

HMT trigger

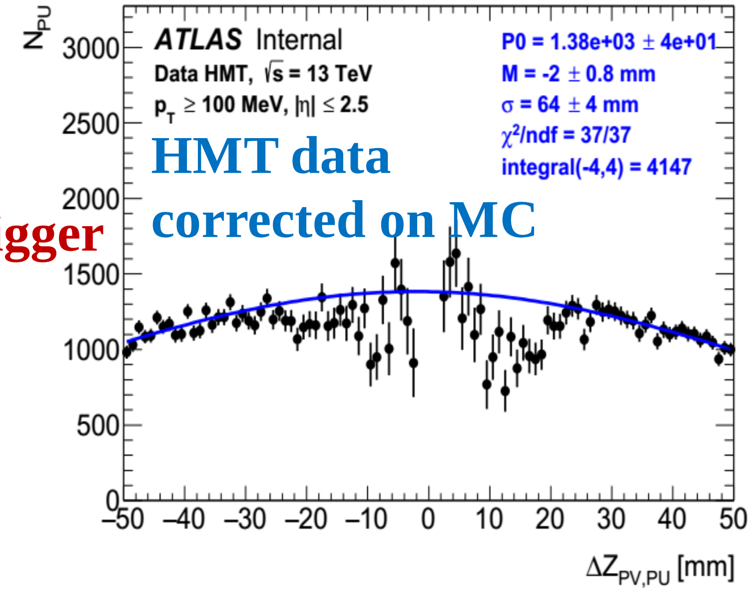

For HMT events the number of pile-up vertexes in the Primary Vertex (PV) region ±4 mm is ~4150, after correction on MC, and the number of tracks in Pile-up vertex is 23. Therefore the fraction of pile-up tracks in MB events is **0.01%**

We can conclude that mean number of pile-up tracks per MB or HMT event is negligible

Mean number of tracks (pile-up tracks) per event: MB – 26 (0.0005) tracks/event; HMT – 108 (0.01) tracks/event

CLOSURE TEST FOR TWO-PARTICLES C_2 CORRELATION FUNCTION

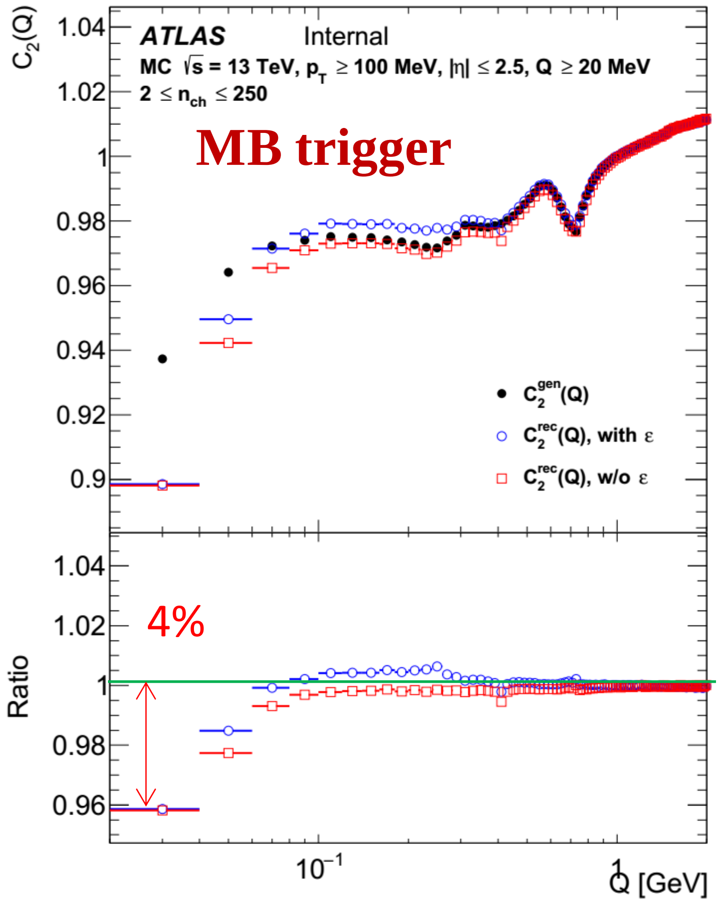

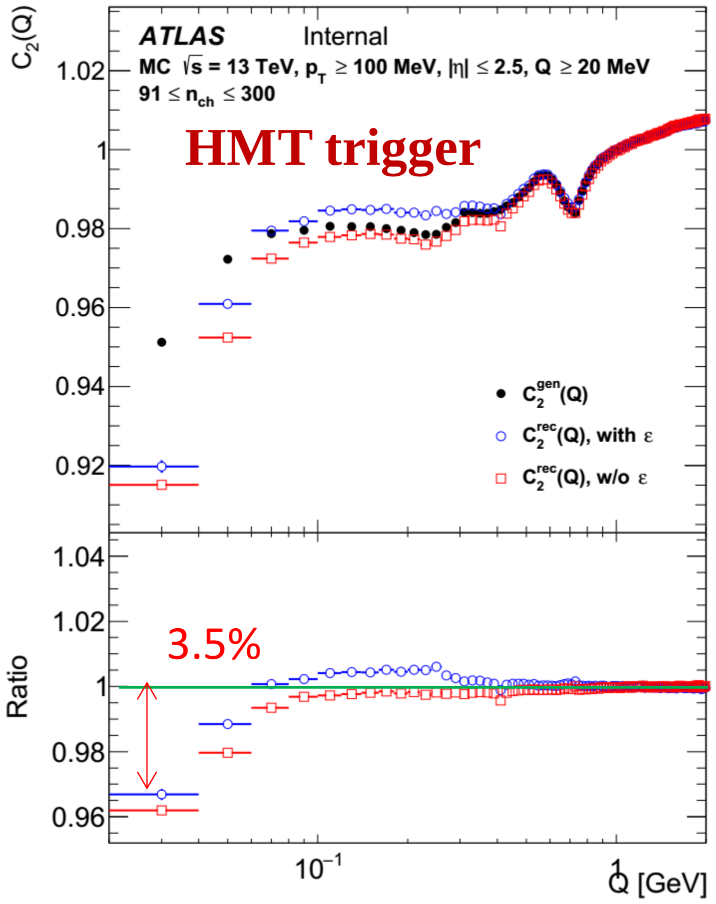

Un-closure between for reconstruction efficiency correction important only for smallest ***k_T region from 100 to 200 MeV and high multiplicity region n_{ch}>60*** on the level up to 2%.

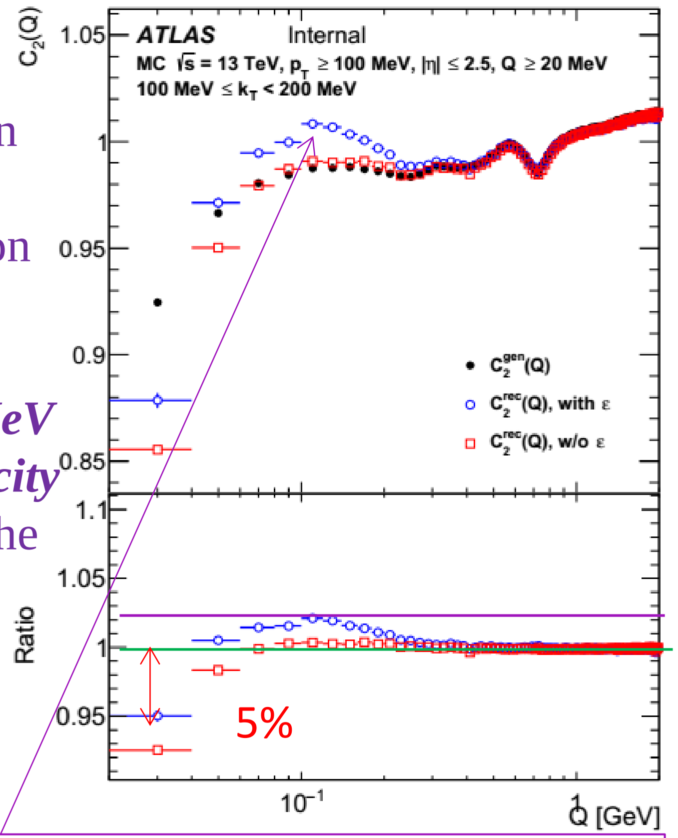

Only for 100<k_T<200 MeV and n_{ch}>60

The closure tests for $C_2(Q)$ correlation function of Pythia8 A2 datasets at 13 TeV MB events for multiplicity region $2 \le n_{ch} \le 250$ and HMT events for multiplicity region $91 \le n_{ch} \le 300$ built using the unlike-sign pair reference sample.

The differences between the particle level distributions and the reconstructed distributions after unfolding are assigned to the full error for bins of $R_2(Q)$ correlation functions and included in the final fitting error of the BEC parameters

Minimum-Bias Event Selection Criteria

Events pass the data quality criteria ("good events": all ID sub-systems nominal cond., stable beam, defined beam spot)

- Accept on signal-arm Minimum Bias Trigger scintillator,
- Primary vertex (2 tracks with p_T>100 MeV),
- Veto to any additional vertices with ≥4 tracks,
- At least 2 tracks with p_T>100 MeV, $|\eta|$<2.5,
- At least 1 first Pixel layer hit & 2, 4, or 6 SCT hits for p_T>100, 300, 400 MeV respectively,
- IBL hit required if expected (if not expected, next to innermost hit required if expected),
- Cuts on the transverse impact parameter: $|d_0^{BL}|$<1.5 mm (w.r.t beam line),
- Cuts on the longitudinal impact parameter: $|\Delta z_0 \sin\Theta|$<1.5 mm (Δz_0 is difference between tracks z_0 and vertex z position),
- Track fit χ^2 probability >0.01 for tracks with p_T>10 GeV.

Correct distributions for detector effects:

- where possible the data used to reduce the MC dependencies
- Monte Carlo derived corrections for tracking

TRACK RECONSTRUCTION CORRECTIONS

Performed corrections on:

1. The reconstruction track efficiency – ε (pt,η),
2. The fraction of non-primary (secondaries and fake) tracks – f_{nonp}(pt,η),
3. The fraction of tracks for which the corresponding primary particles are outside the kinematic range – f_{okr}(pt,η),
4. The strange barion tracks – f_{sb}(pt,η),

We use the formula, as earlier and as in MB studies:

$$w_i(p_t,\eta) = \frac{\left(1 - f_{nonp}(p_t,\eta) - f_{okr}(p_t,\eta) - f_{sb}(p_t,\eta)\right)}{\varepsilon(p_t,\eta)}$$

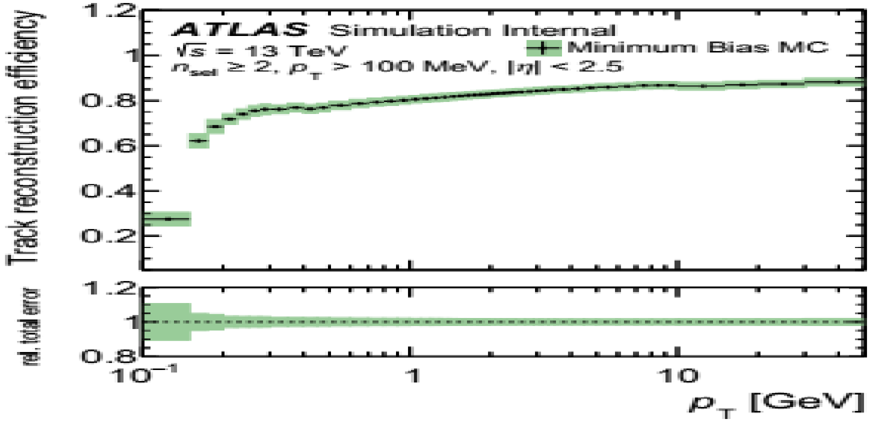

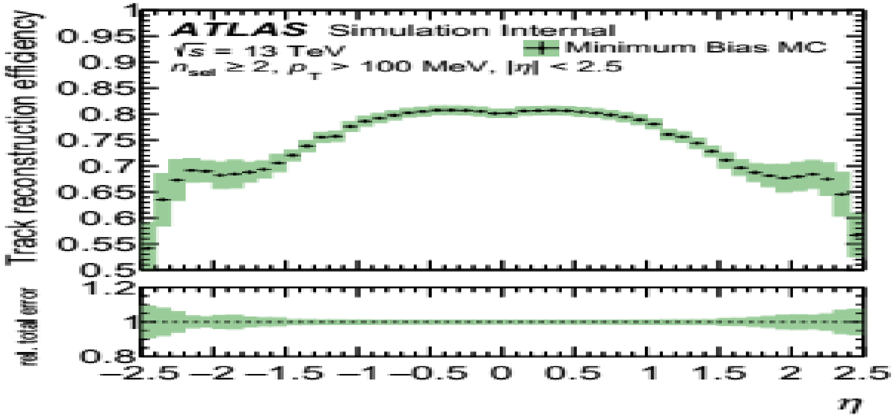

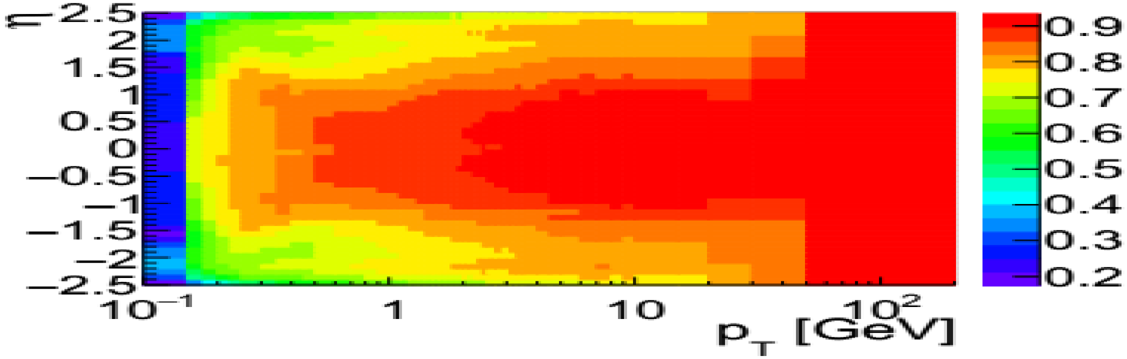

THE PHASE SPACE CORRECTION

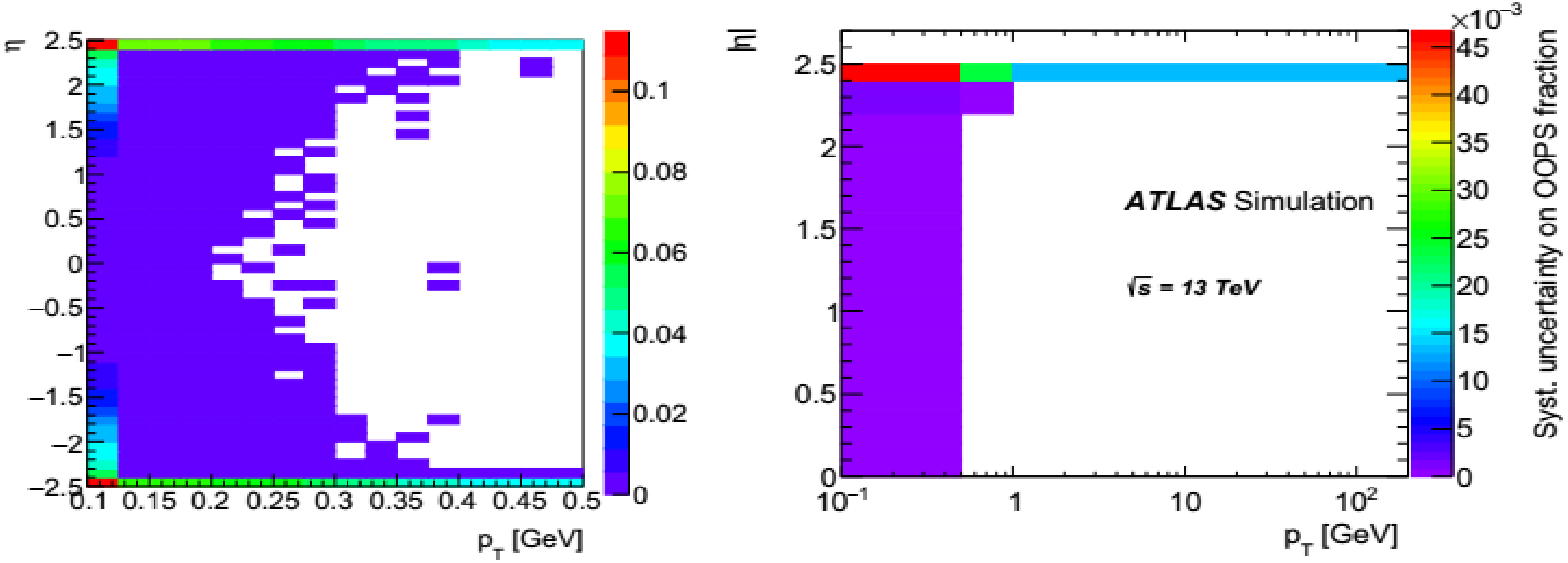

Figure 16: The out of phase space correction (OOPS) in p_T and η bins (left) and the systematic uncertainty on the out of phase space correction fractions (b). The systematic is made up of several contributions added up in quadrature, where each contribution is calculated as the difference in migration fractions between samples (see body text for further explanation).

FAKE TRACK CORRECTION

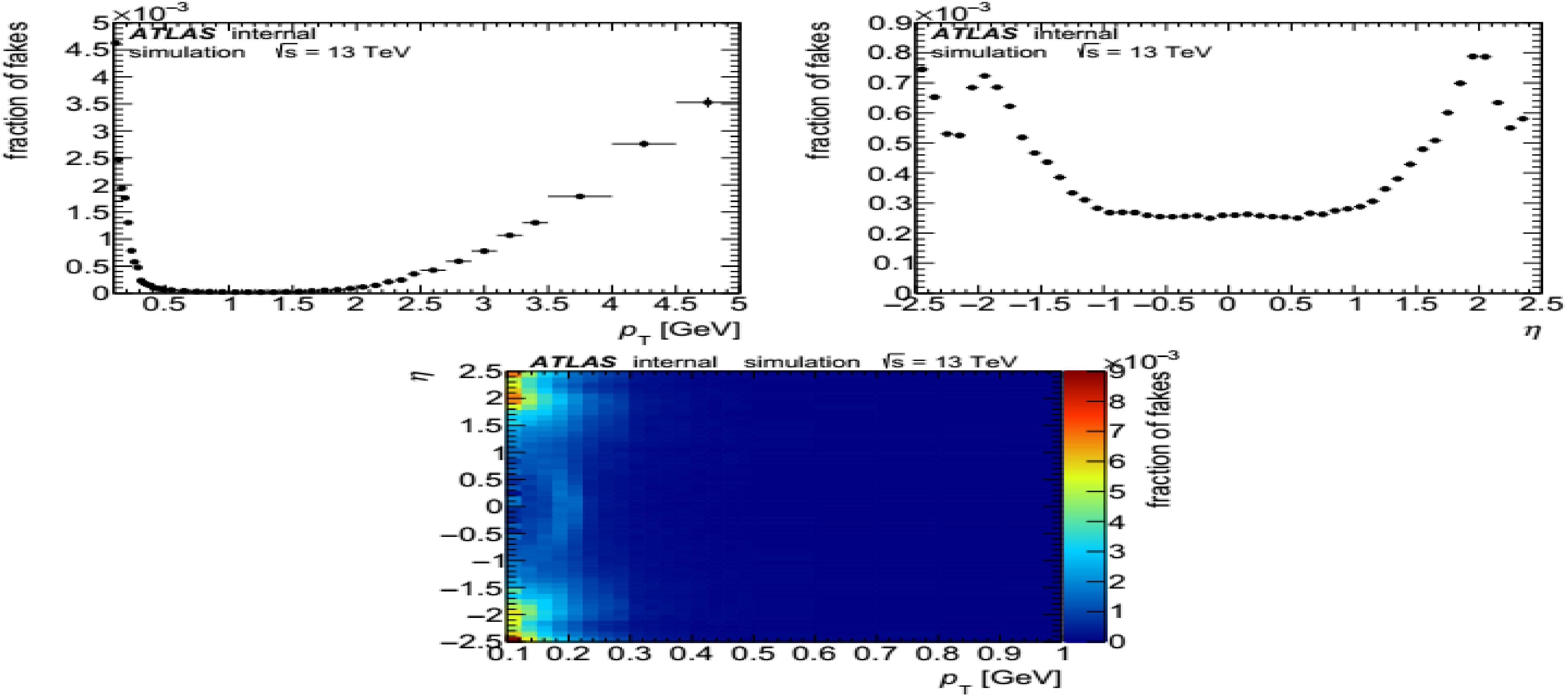

Figure 9: The fraction of fakes after applying the full event selection (see Section 3) as a function of p_T (left top) or η (right top) and the two-dimensional dependency of p_T and η (bottom). The fraction is below 1% and therefore negligible for the analysis.

STRANGE BARYONS

- **Particles with lifetime 30 ps < τ < 300 ps are no longer considered primary particles in the analysis, decay products are treated like secondary particles.**
- All of these particles were **strange baryons:** with low reconstruction efficiency (<0.1%) and large variations in predicted rates lead to a model dependence
- Primary particles have τ > 300 ps

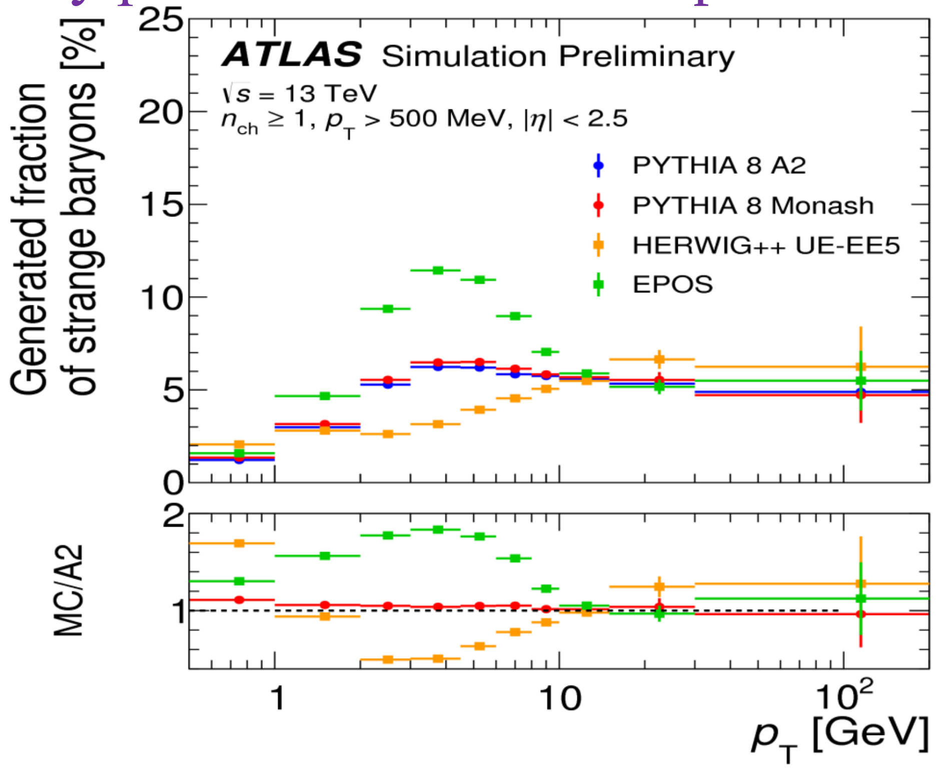

The fraction of strange baryons in generated particles as a function of particle p_T as predicted by various generators.

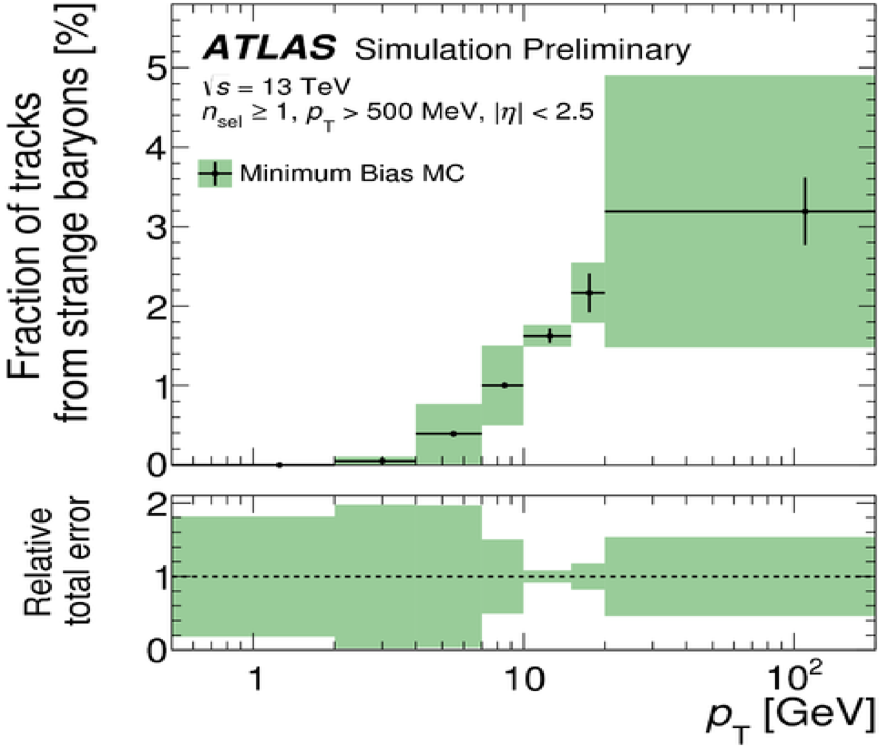

The fraction of reconstructed tracks coming from strange baryons as a function of track p_T as predicted by PYTHIA8 A2.

MULTIPLICITY UNFOLDING

- **Multiplicity unfolding** is the same like for Minimum-bias analysis
- For High multiplicity track events the Multiplicity unfolding matrix additionally included the MC with filters: more 120, 160, 200

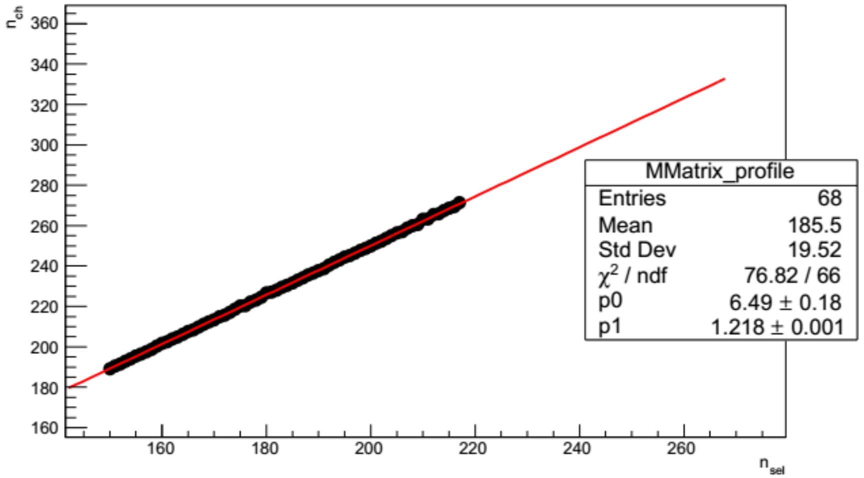

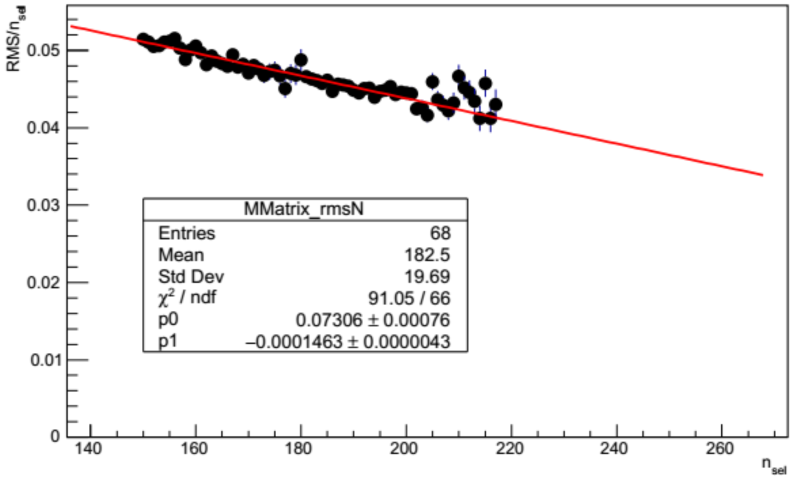

MB unfolding matrix

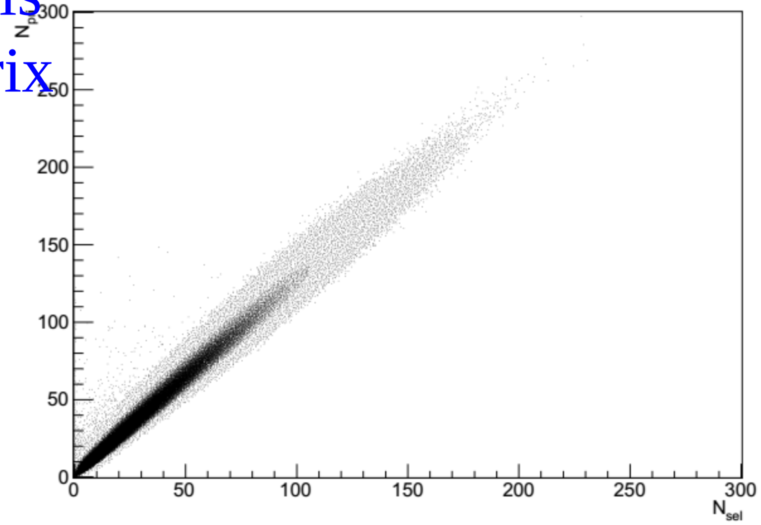

MB + HMT unfolding matrix

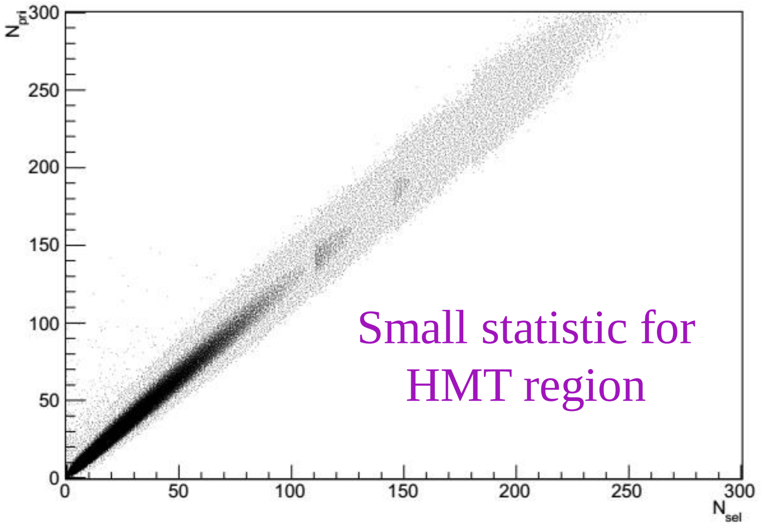

Small statistic for HMT region

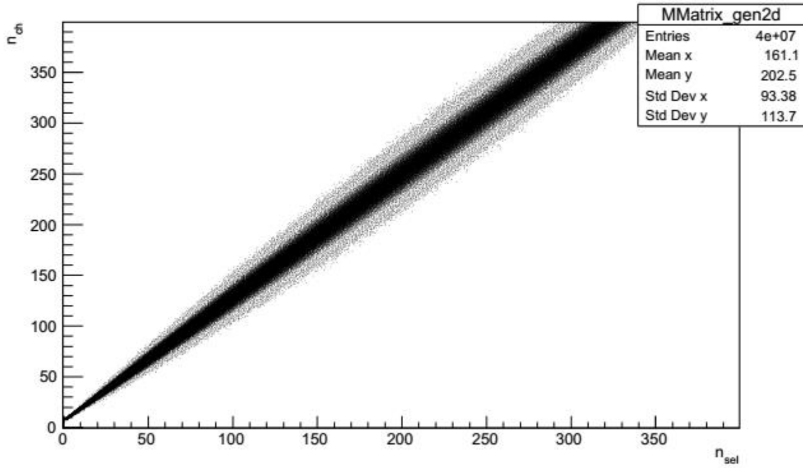

For high multiplicity region n_{sel} >140 with small statistic the calculation of mean and RMS/n_{sel} of unfolding matrix were done and used for calculation of unfolding matrix for high multiplicity region

RESONANCES STUDY

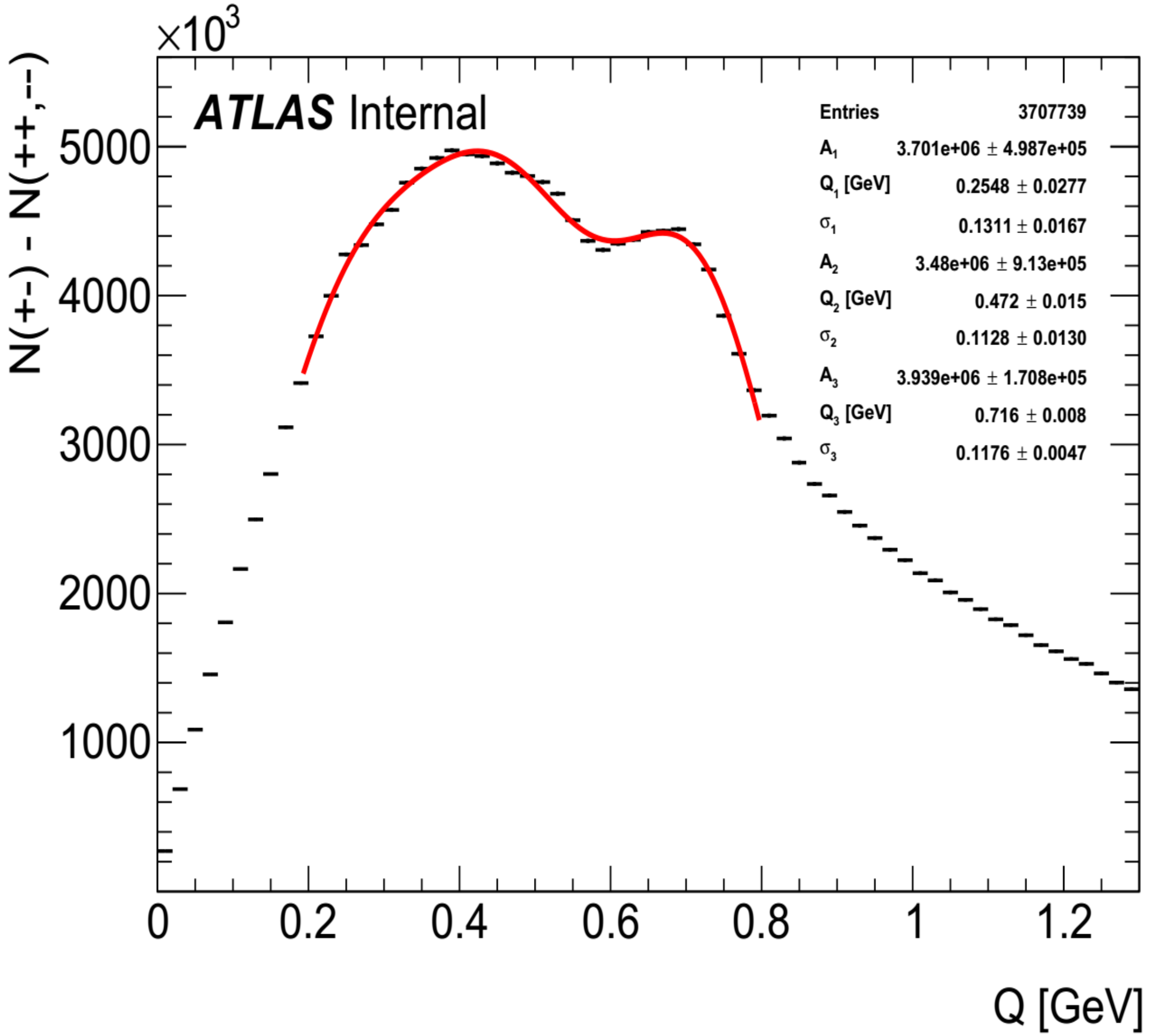

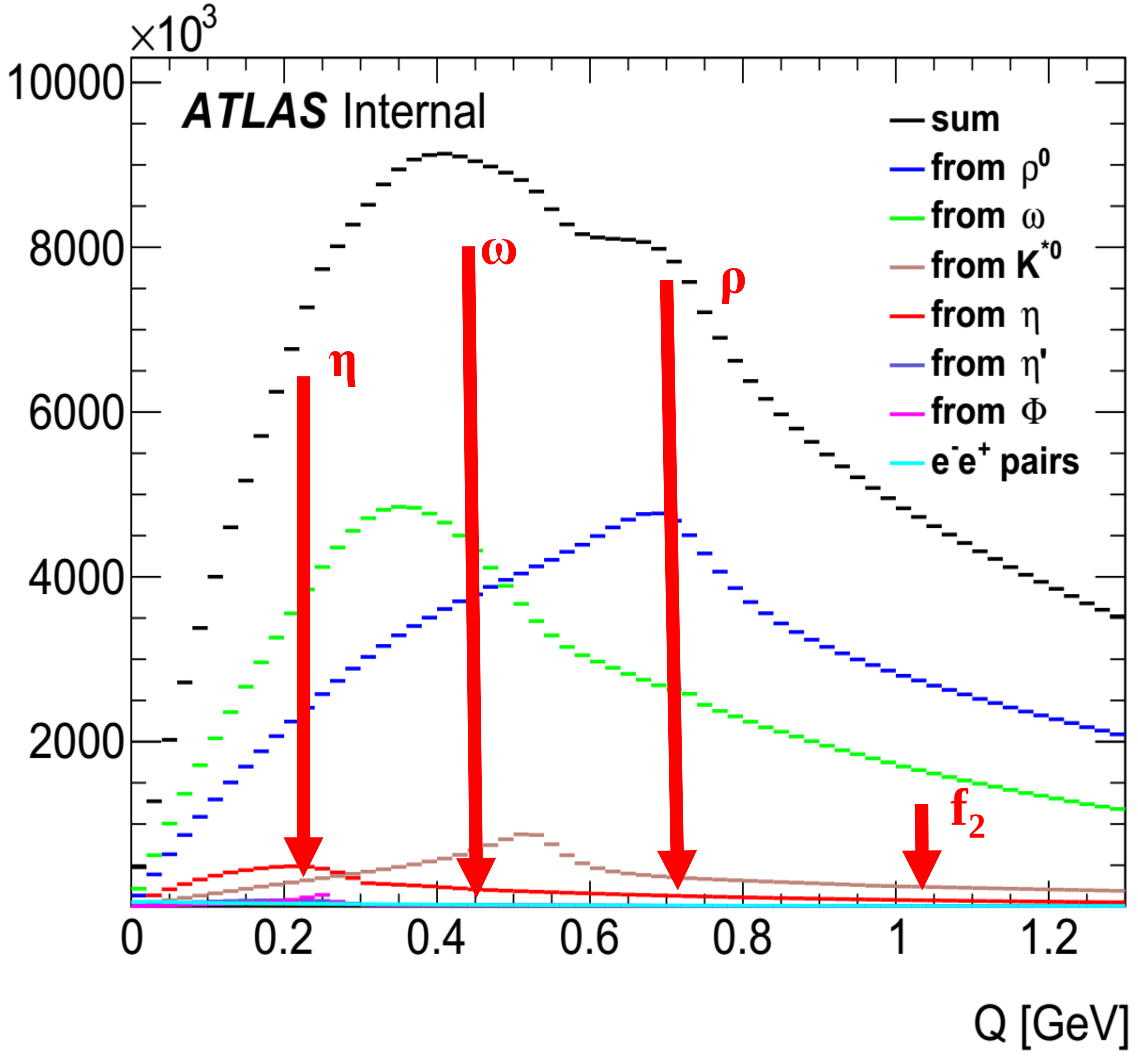

The Q spectrum generated by Pythia8 and the decomposition of its resonant part into leading contributions.

ZOOM OF INCLUSIVE R_2 DISTRIBUTION

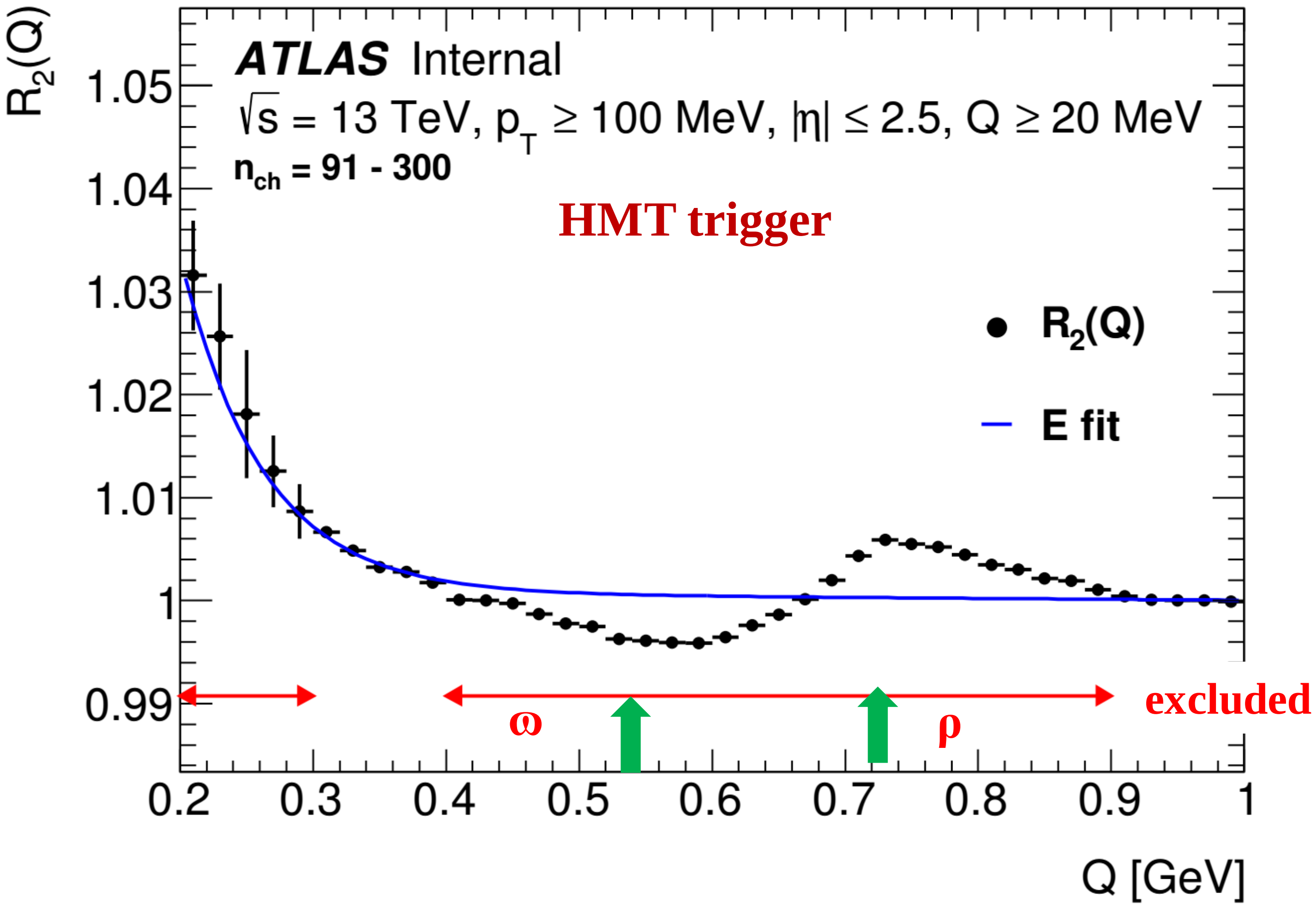

Inclusive HMT two particles R_2 correlation function

$R_2 = C_2^{data}/C_2^{MC} = N_{data}^{\pm\pm}/N_{MC}^{\pm\pm}\ \ N_{MC}^{+-}/N_{data}^{+-}$

Three bump regions because MC underestimated or overestimates:

1) $\eta \to \pi^+\pi^-\pi^o$ and $\eta' \to \pi^+\pi^-\gamma$;
2) $\omega \to \pi^+\pi^-\pi^o$ and $\rho \to \pi^+\pi^-$,
3) $f_2 \to \pi^+\pi^-$;

The excluded regions at 13 TeV

1) 0.2–0.3 GeV – not important after non-closure correction;
2) 0.4–0.9 GeV – important;
3) 1.0–1.16 GeV (only for $2 \le n_{ch} \le 40$ and $100 \le k_T \le 200$ MeV) – not important for BEC.

The excluded region at 7 TeV was 0.5–0.9 GeV.

HOW COMES THAT THE ρ- AND ω-MESONS ARE SO BADLY MODELED?

1. There are not MC, which is in agreement with all charged-particle distributions at 0.9 – 13 TeV.
2. The MC description of resonances are not so badly in scale of MC description of charged-particle distributions.
3. In R_2 correlation functions the ratio of experimental N_{data}^{+-} to MC N_{MC}^{+-} unlike sign particles distribution are used:

$$R_2=C_2^{data}/C_2^{MC} = N_{data}^{\pm\pm}/N_{MC}^{\pm\pm}\ N_{MC}^{+-}/N_{data}^{+-}$$

4. One can see in Figure on previous page that MC little bit underestimate ω-meson and little bit overestimate ρ-meson. We excluded region of these mesons because of small statistical errors and therefore large χ^2/ndf for this region.
5. The situation as we have in our analysis is standard for similar analysis at other energies.

INCLUSIVE R_2 DISTRIBUTIONS

Inclusive MB two particles R_2 correlation function

Lum. ~151 μb^{-1}; Statistic: 9.6×10^6 events with 2.8×10^8 tracks

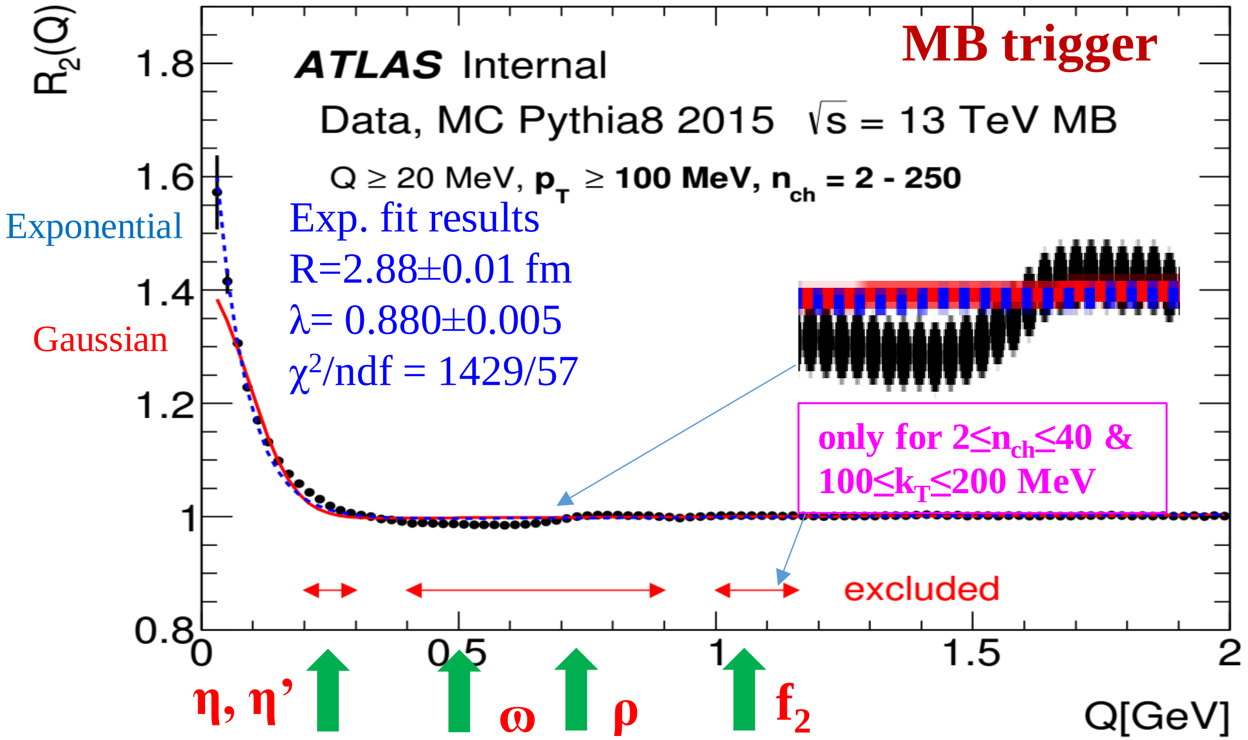

Inclusive HMT two particles R_2 correlation function

Lum. ~8.4 nb^{-1}; Statistic: 9.1×10^6 events with 9.8×10^8 tracks

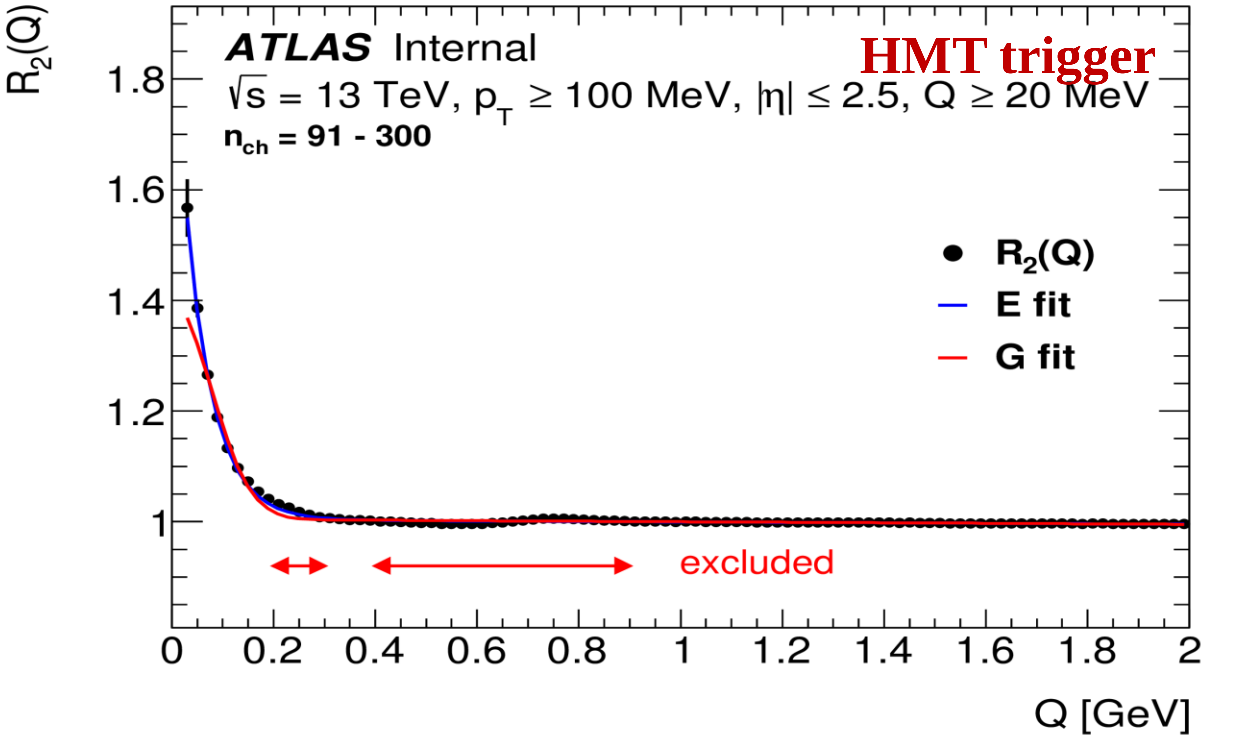

Fit to extract strength and source size. Goldhaber spherical shape with a Gaussian distribution of the source. Exponential, radial Lorentzian distribution of the source -> much better at low Q. Three bumps regions because MC overestimates: 1) $\eta\to\pi^+\pi^-\pi^o$ or $\eta\to\pi^+\pi^-\gamma$; 2) $\omega\to\pi^+\pi^-\pi^o$ and $\rho\to\pi^+\pi^-$, 3) $f_2\to\pi^+\pi^-$; Therefore regions 0.2–0.3 GeV; 0.4–0.9 GeV and 1.0–1.16 GeV (only for $2\leq n_{ch}\leq40$ and $100\leq k_T\leq200$ MeV) excluded from the fit. Q region is from 0.02 to 2 GeV.

Fit function: $\mathbf{R_2(Q)= C_0[1+\lambda\,\Omega(QR)](1+\varepsilon Q)}$, **ε**-term counts for the *long-range* correlations

Studies of one-dimensional BEC effects in pp collisions for p_T>100 MeV and $|\eta|$ < 2.5 at 13 TeV

COULOMB CORRECTION

The measured N(Q) distribution for like or unlike signed particle (track) pairs in presence of the Coulomb interaction is given by:

where $N_{meas}(Q)$ is the measured distribution, N(Q) is the distribution free of Coulomb correlations.

$$N_{meas}(Q) = G(Q)N(Q)$$

Gamow penetration G(Q) factor

$$G(Q) = \frac{2\pi\eta}{e^{2\pi\eta} - 1}$$

Sommerfeld parameter η

$$\eta = \frac{\pm\alpha_m}{|Q|}$$

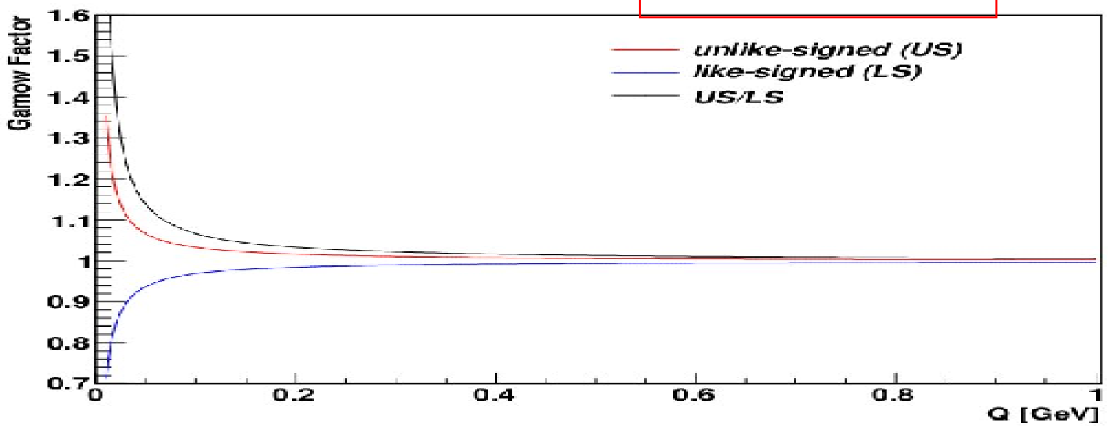

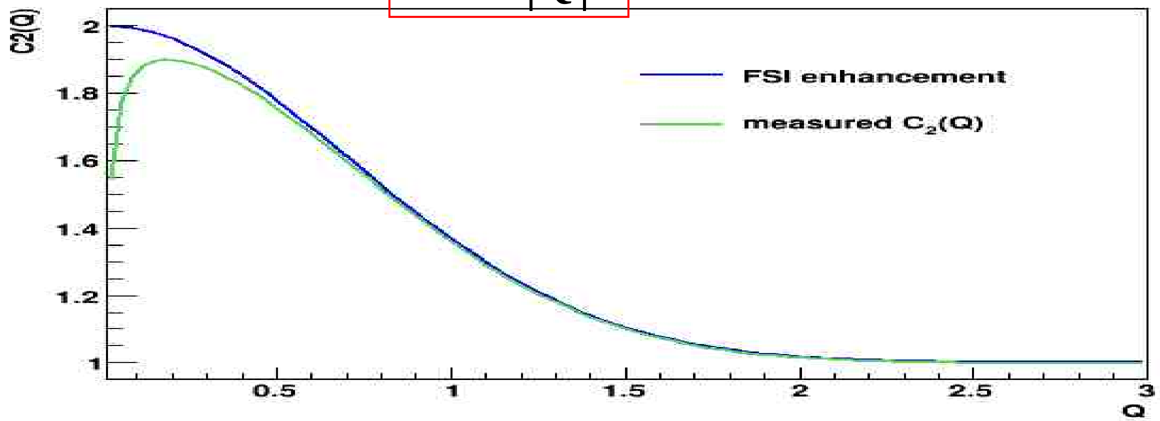

Comparison of the same $C_2(Q)$ function: blue – primary data $C_2(Q)$, red – $C_2(Q)$ corrected to Coulomb correction

Ratio of the same $C_2(Q)$ function – with and without correction on Coulomb correction

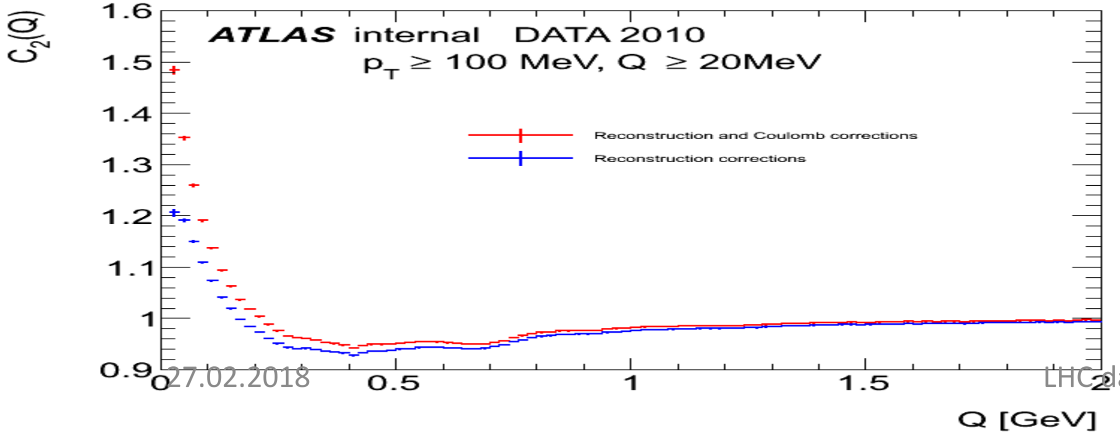

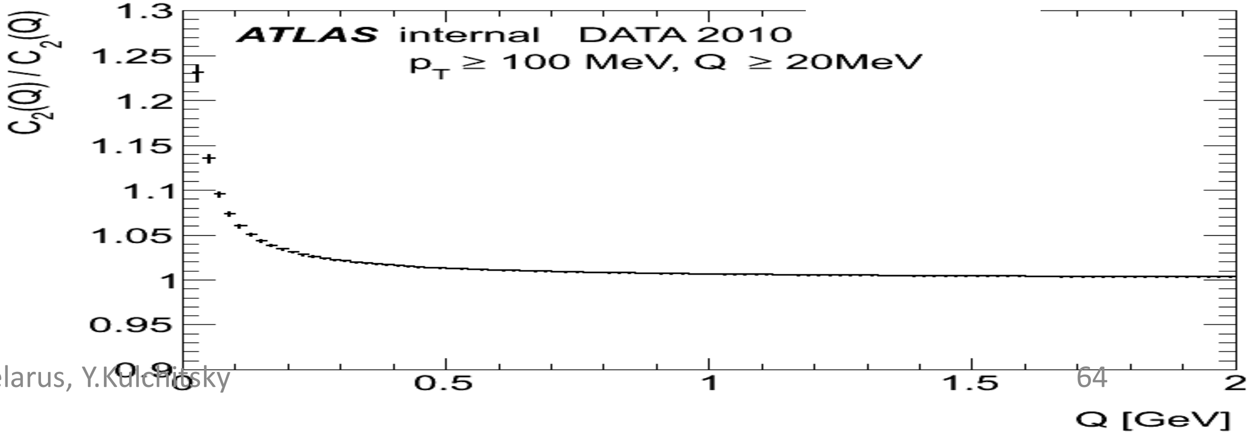

OHP (MIX) AND UCP REFERENCE SAMPLES: k_T

The two-particle correlation function C_2 (Q) for different k_T intervals using the opposite-hemisphere reference sample for data (red) and MC (blue)

Artificial peak in C_2 in BEC region

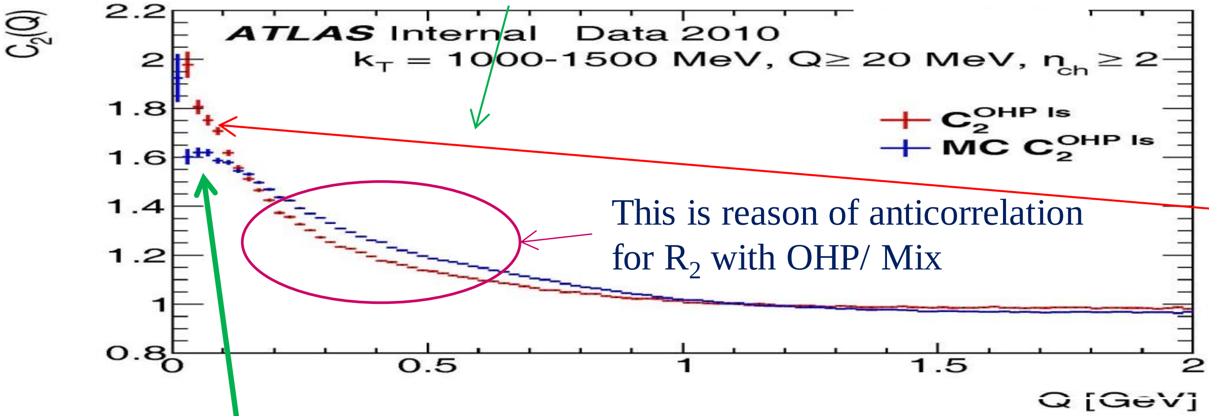

This is reason of anticorrelation for R_2 with OHP/ Mix

Small BEC peak for R_2 OHP

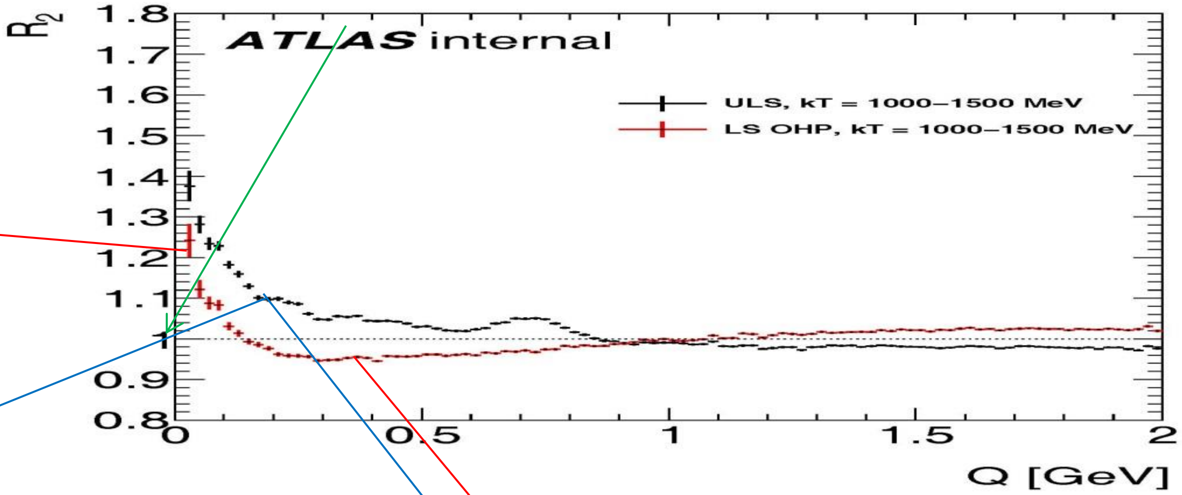

Reflection of resonances in C_2 UCP

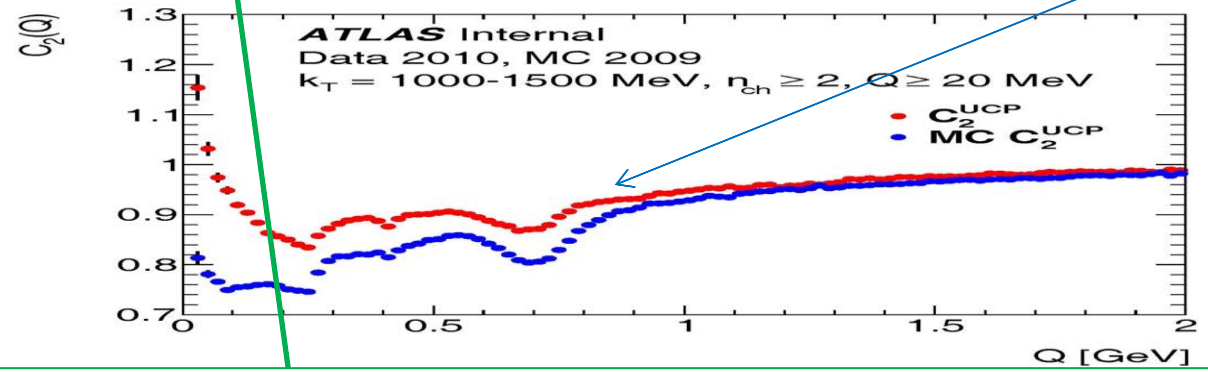

k_T dependences for R for R_2 with different reference

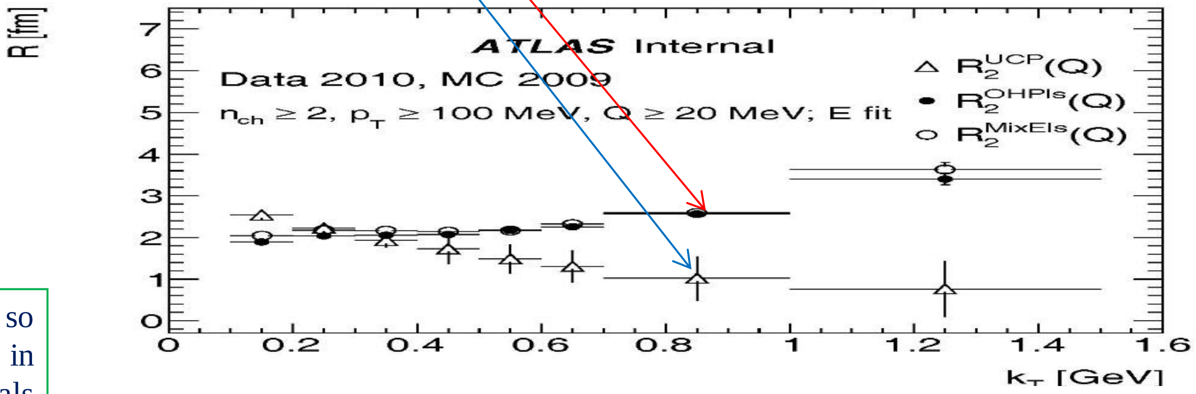

To note is that the slope in the MC can be explained by the fact that MC is tuned to the data and so reflects different dynamical constraints, but MC has no possibility to reproduce a peak at small Q as in the data but shows a broad enhancement.. The additional correlations in large multiplicity intervals seem to be due to multi-jet events in MC where the correlations between particles within the same jet can contribute to the region of low-Qs. In this case, the single-ratio C_2(Q) correlation function numerator contains contributions from multi-jets, while the denominator does not have this effect as no correlations are expected in randomly paired particles.

Disadvantage for OHP/MIX: violation of energy-momentum constraint, event topology, destroying other features such as non-BEC etc.

Inclusive R_2 distribution for p_T>100 MeV: 2 ≤ N_{CH}

χ^2 vs Q distribution

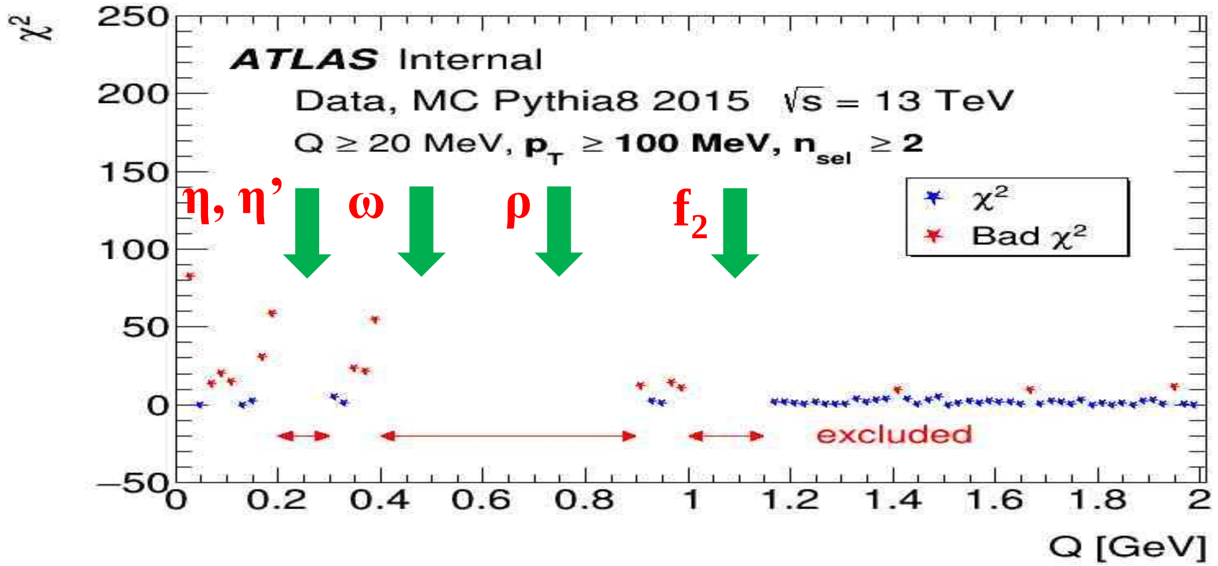

Comparison of C2 and R_2 distributions

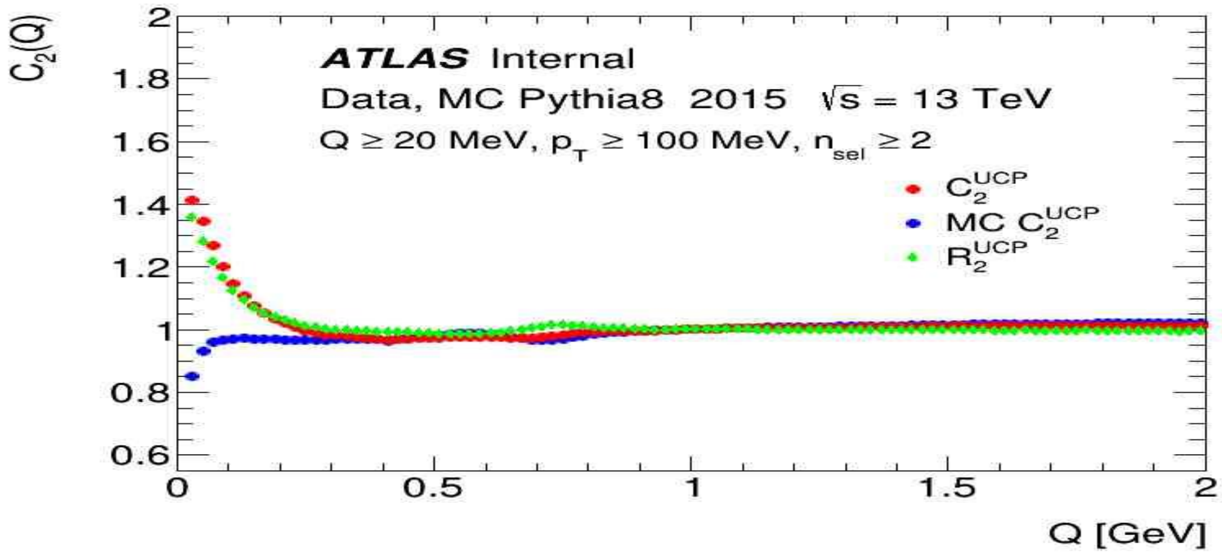

Exponential fit results comparison for R_2

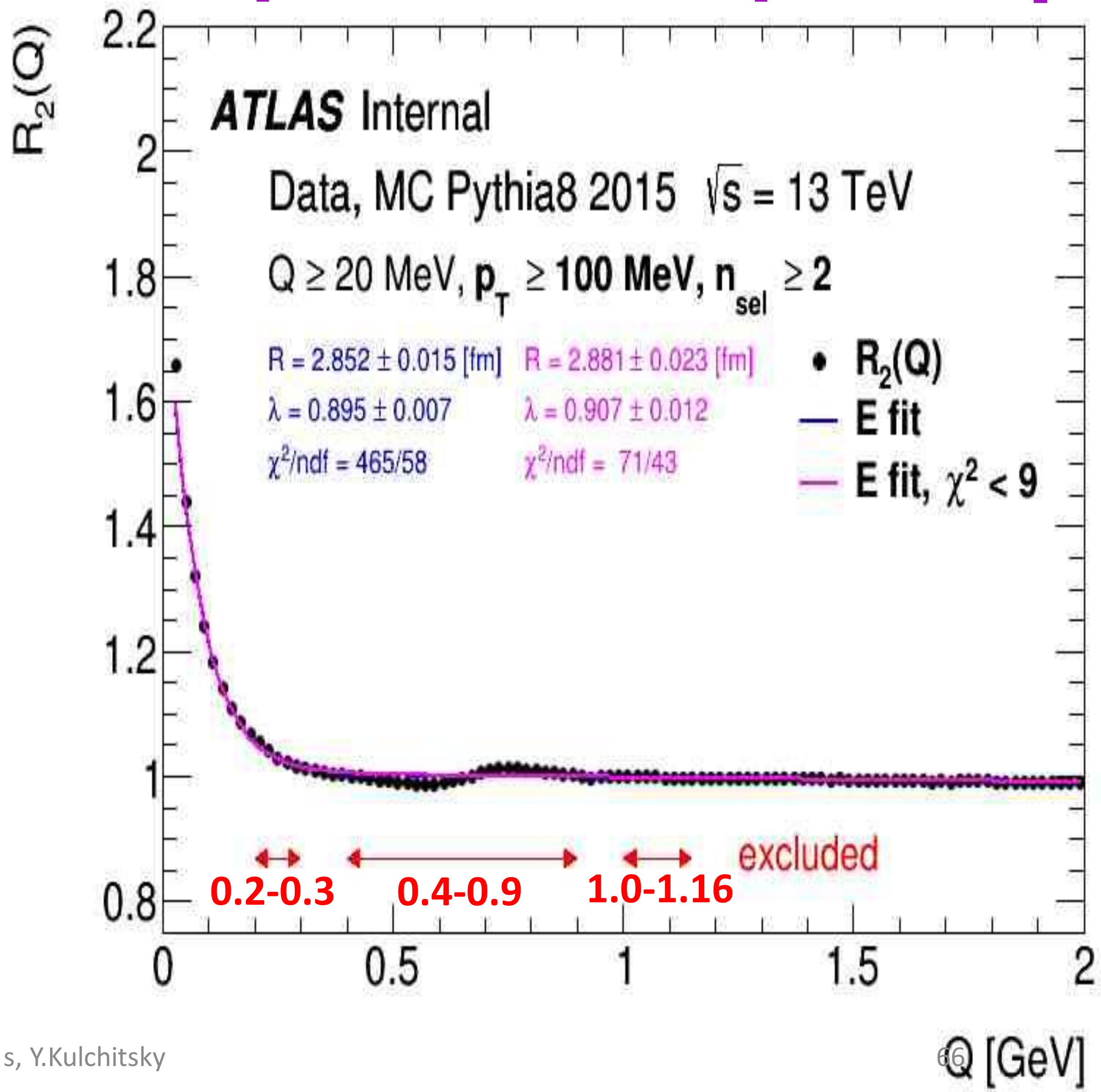

TYPICAL TWO-PARTICLE R_2 CORRELATION FUNCTIONS

MB two particles R_2 correlation function

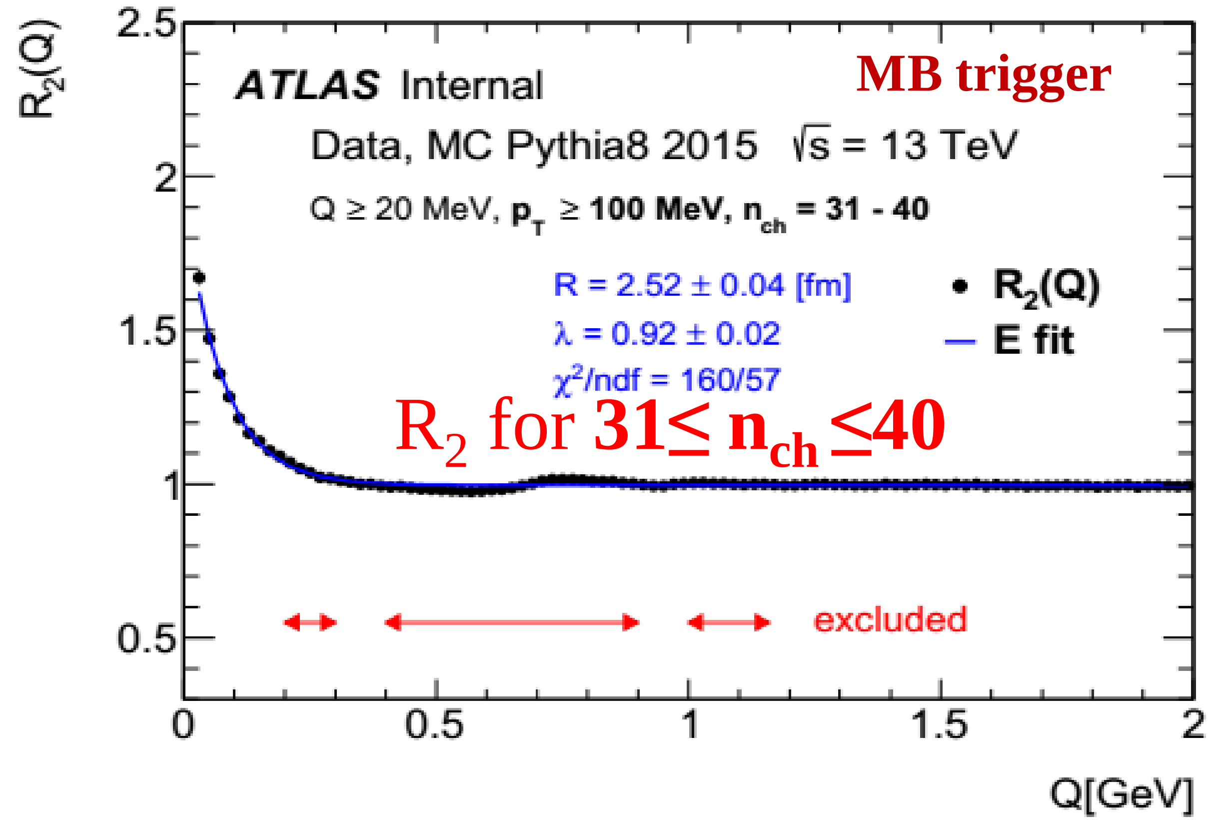

HMT two particles R_2 correlation function

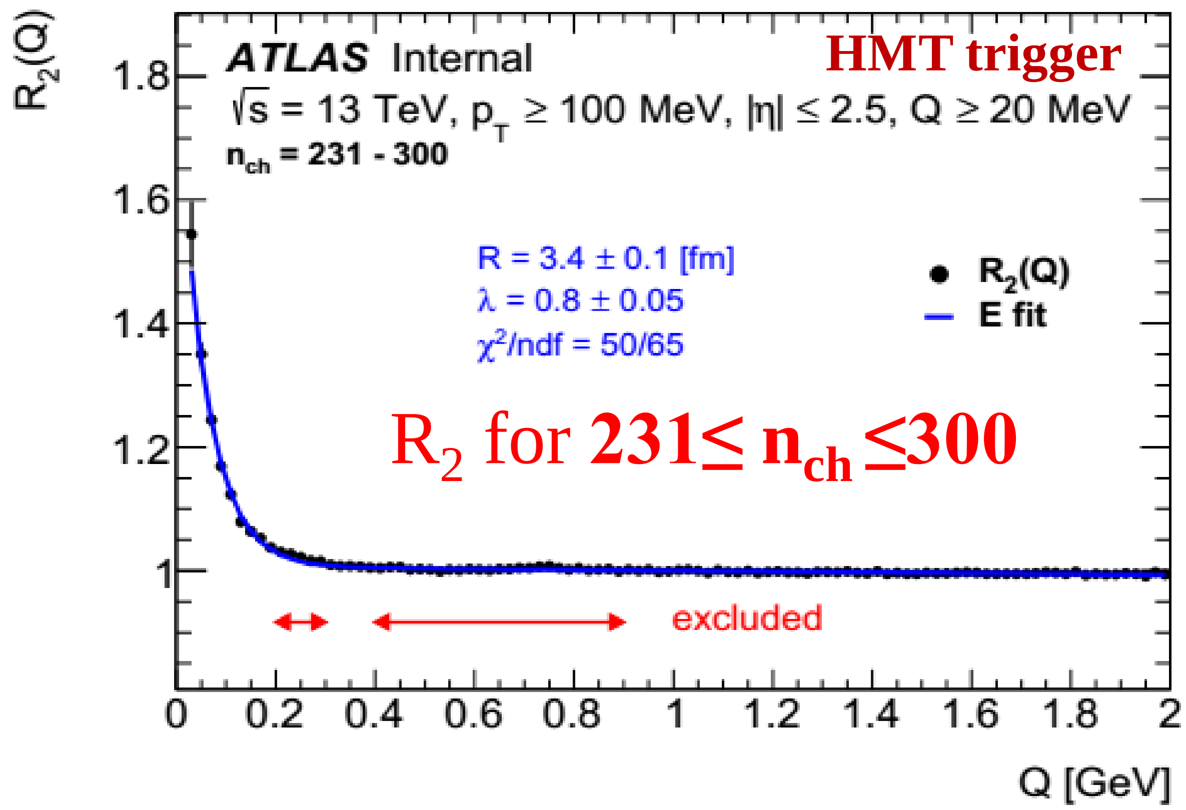

Fit to extract strength and source size. Goldhaber spherical shape with a Gaussian distribution of the source. Exponential, radial Lorentzian distribution of the source -> much better at low Q. Three bumps regions because MC overestimates: 1) $\eta\to\pi^+\pi^-\pi^o$ or $\eta\to\pi^+\pi^-\gamma$; 2) $\omega\to\pi^+\pi^-\pi^o$ and $\rho\to\pi^+\pi^-$, 3) $f_2\to\pi^+\pi^-$; Therefore regions 0.2–0.3 GeV; 0.4–0.9 GeV and 1.0–1.16 GeV (only for $2\le n_{ch}\le 40$ and $100\le k_T\le 200$ MeV) excluded from the fit. Q region is from 0.02 to 2 GeV.

Fit function: $\mathbf{R_2(Q)= C_0[1+\lambda\,\Omega(QR)](1+\varepsilon Q)}$, **ε**-term counts for the *long-range* correlations

Studies of one-dimensional BEC effects in pp collisions for p_T>100 MeV and |η| < 2.5 at 13 TeV

OPEN ANGLE AND NON-CLOSURE FOR TWO PARTICLES

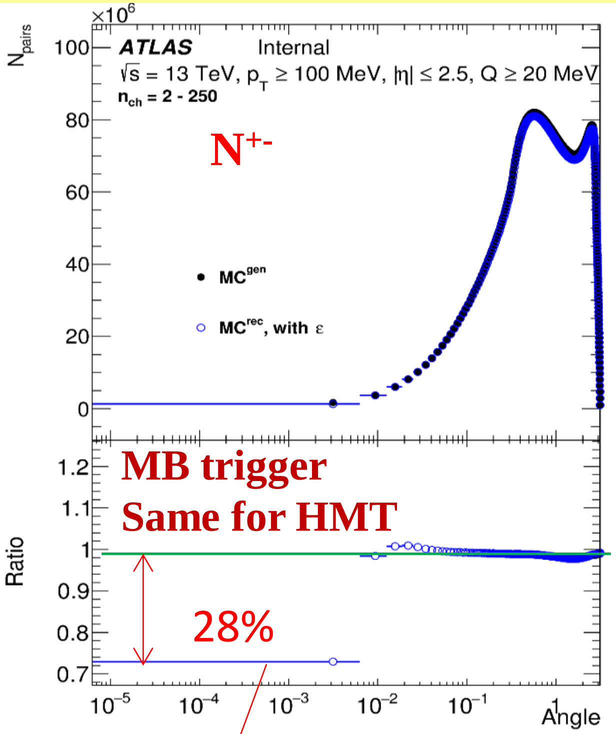

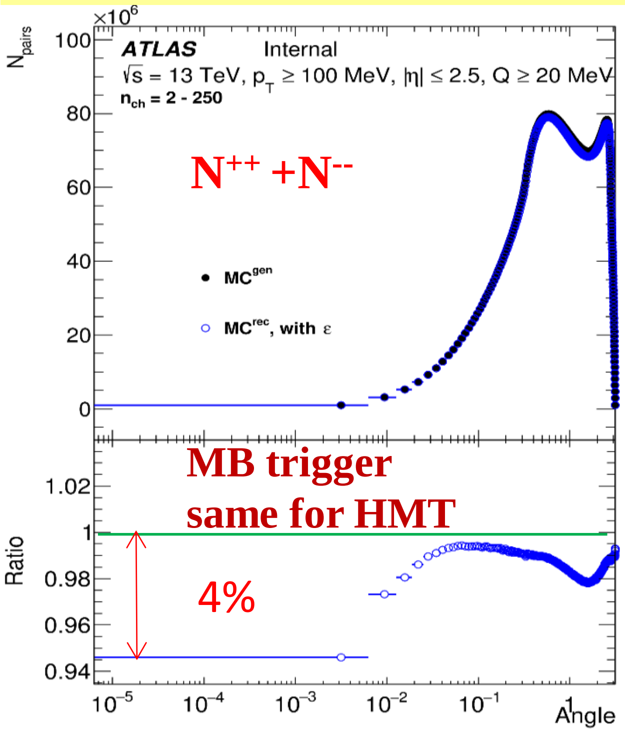

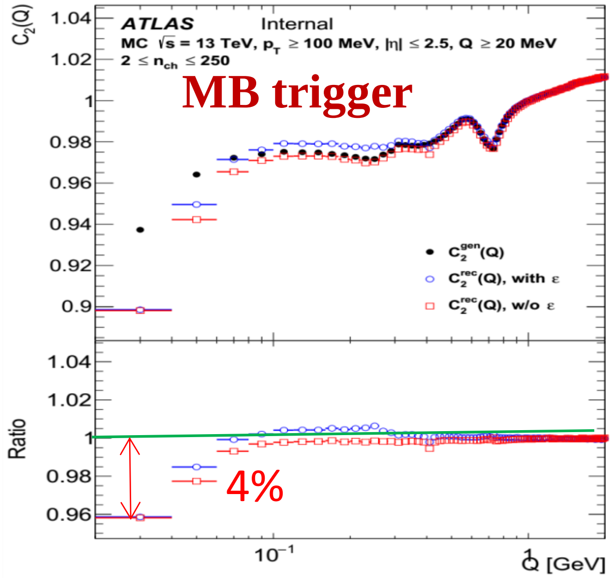

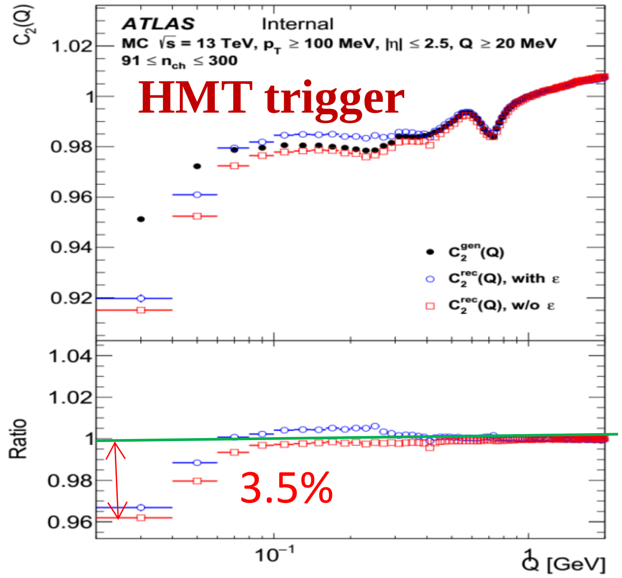

Closure test for C_2 correlation functions for MB/HMT events

Open angle distributions N^{+-} and $N^{\pm\pm}$ particle pairs

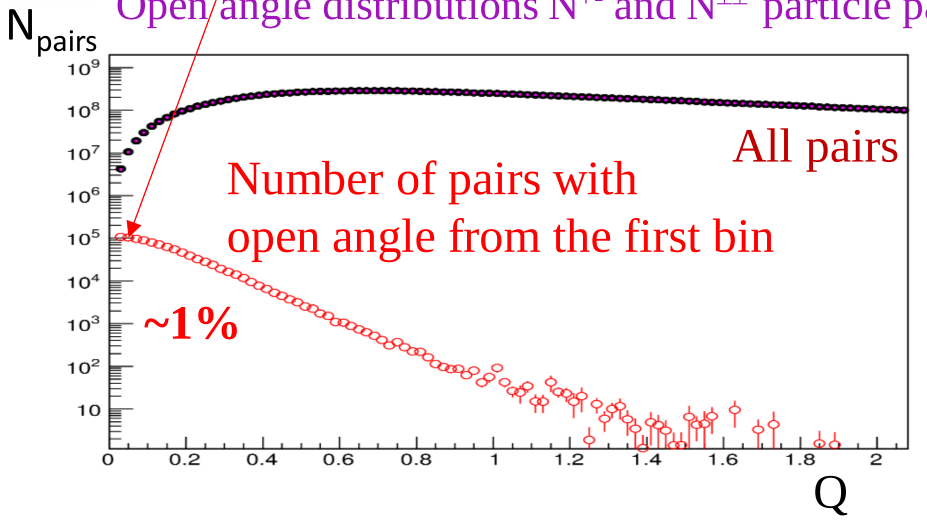

Q-distributions of N^{+-} and $N^{\pm\pm}$ particle pairs with all open angles (black circles), OA, an with open angles from the firs bin (red circles). The fraction the last is on the level of ~1% for the 0.02<Q<0.06 GeV region

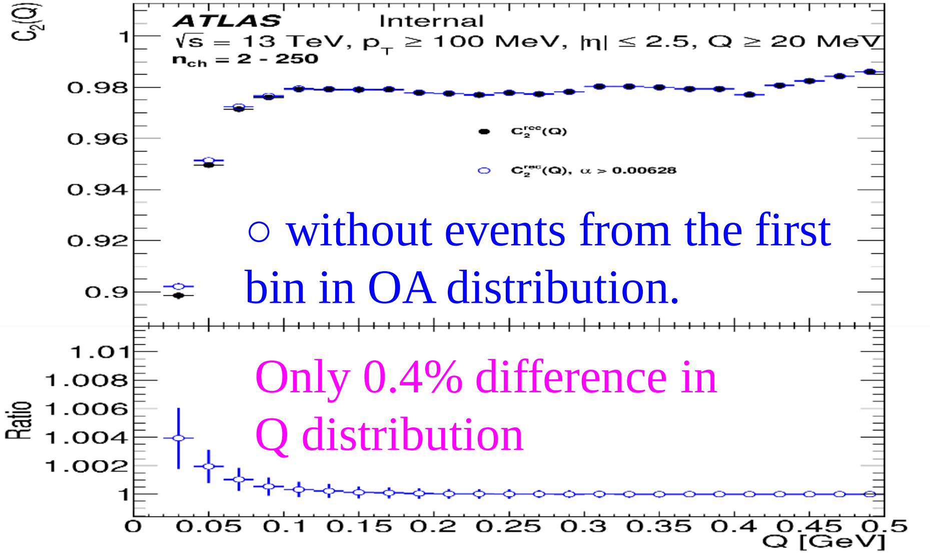

MULTIPLICITY DEPENDENCE OF BEC PARAMETERS

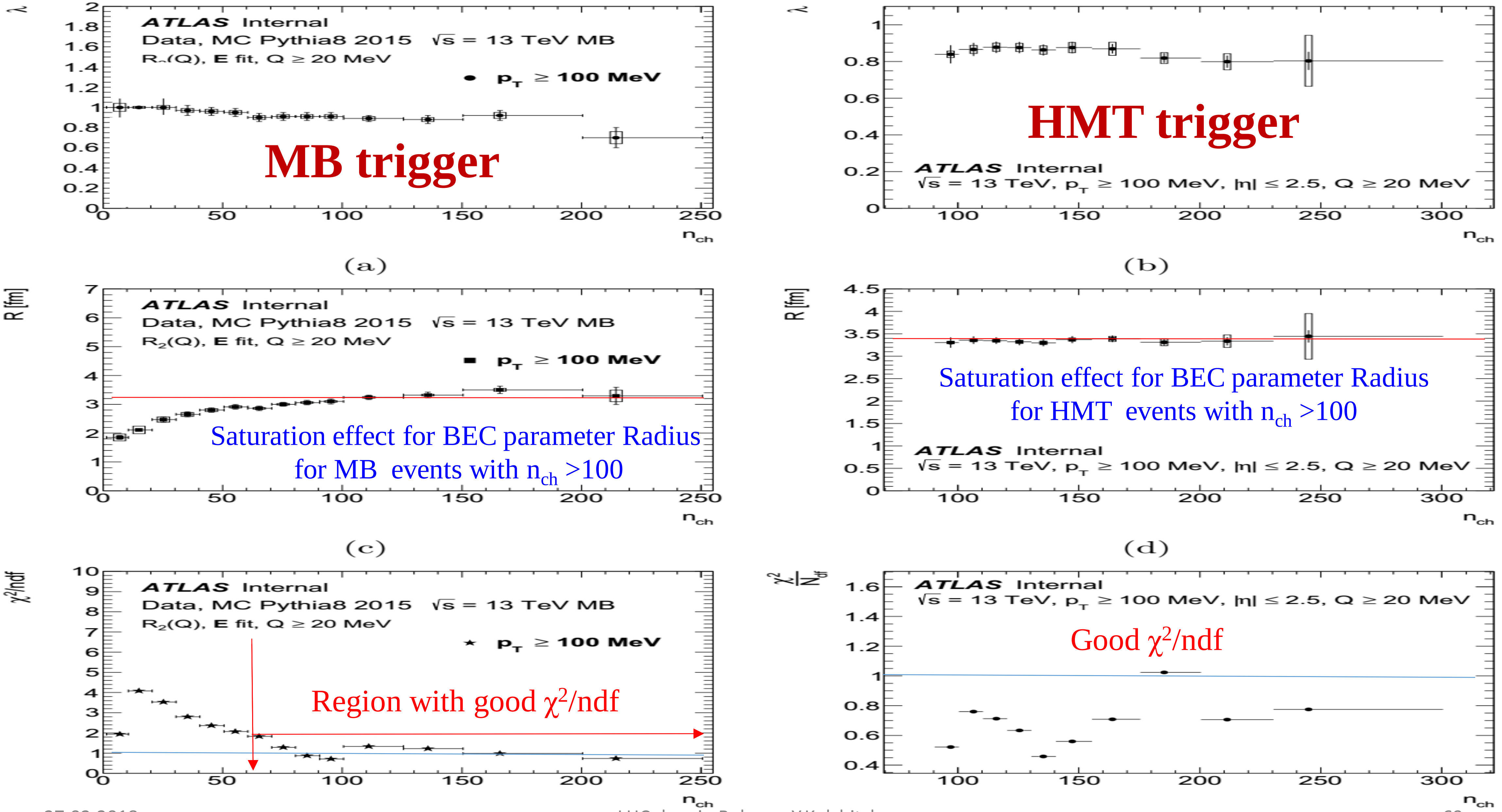

K_T DEPENDENCE OF BEC PARAMETERS

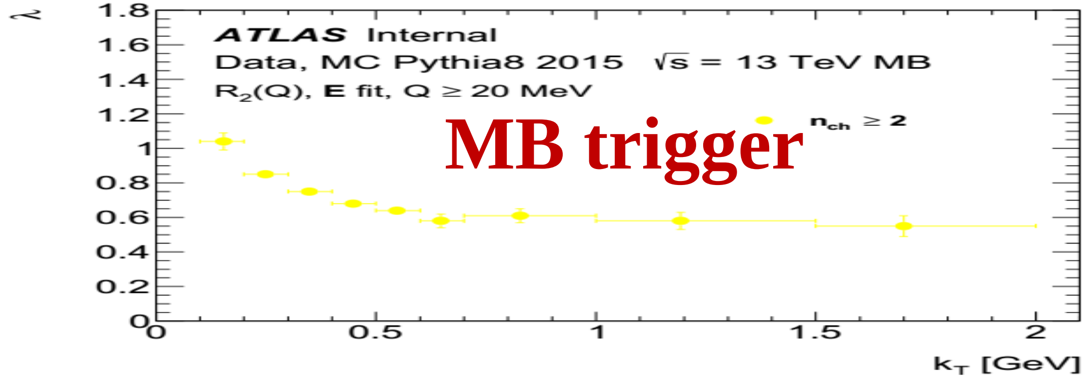

(a)

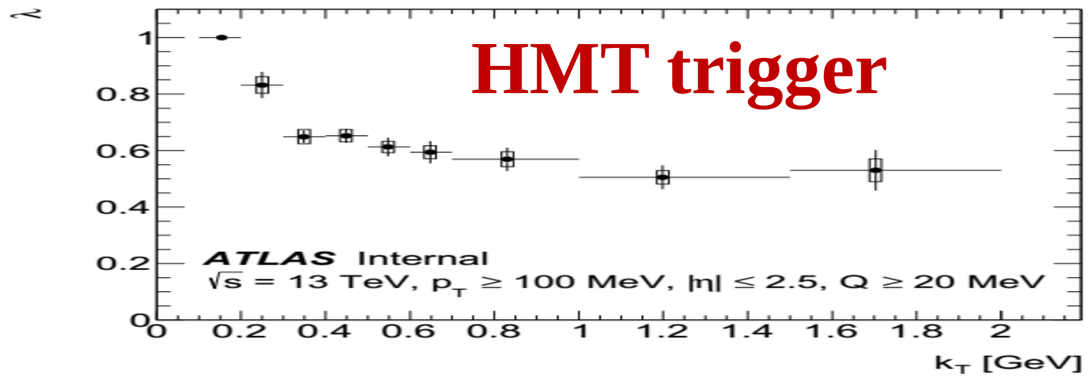

(b)

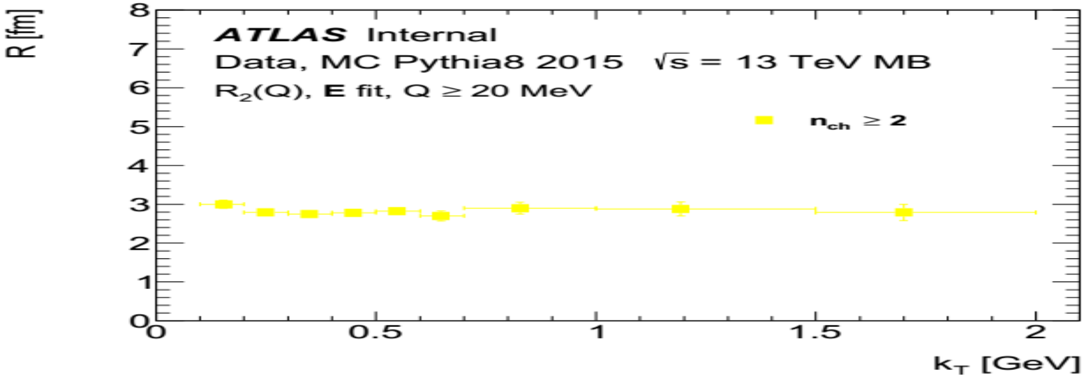

(c)

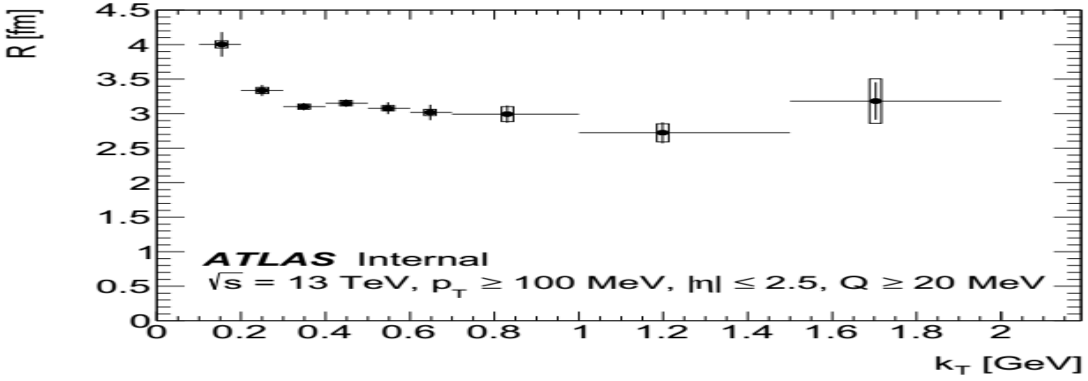

(d)

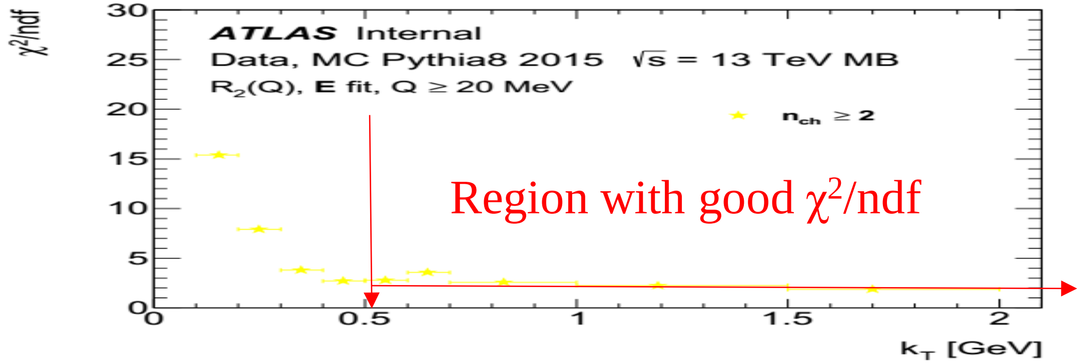

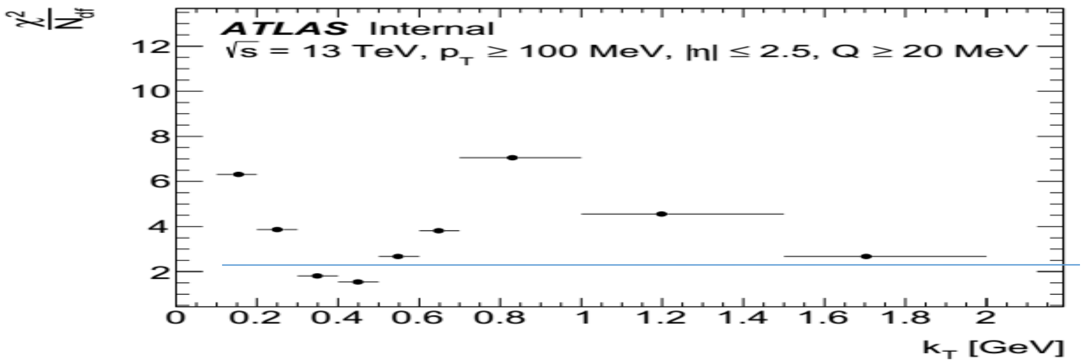

Region with good χ^2/ndf

FIT RESULTS FOR BEC PARAMETERS AT 13 TEV

The fit results of the BEC parameters R and λ dependence on the multiplicity, n_{ch}, and the transverse momentum of the pair, k_T, for different functional forms and for different data samples at 13 TeV. The errors represent the statistical and systematical uncertainties.

BEC param.	Fit function	13 TeV Minimum-bias events		13 TeV High-multiplicity track events
$R(n_{ch})$	$\alpha \sqrt[3]{n_{ch}}$	$\alpha = 0.77 \pm 0.02 \pm 0.02$ fm $(n_{ch} \leq 70)$		—
	β	$\beta = 3.35 \pm 0.03 \pm 0.07$ fm $(n_{ch} \geq 100)$		
$\lambda(n_{ch})$	$\gamma\, e^{-\delta n_{ch}}$	$\gamma = 1.01 \pm 0.01 \pm 0.02$		
		$\delta = 0.0011 \pm 0.0001 \pm 0.0002$		
$R(k_T)$	$\xi\, e^{-\kappa k_T}$	$\xi = 2.95 \pm 0.31 \pm 0.10$ fm		$\xi = 3.42 \pm 0.19 \pm 0.01$ fm
		$\kappa = 0.21 \pm 0.24 \pm 0.13$ GeV^{-1}	same	$\kappa = 0.20 \pm 0.12 \pm 0.03$ GeV^{-1}
$\lambda(k_T)$	$\mu\, e^{-\nu k_T}$	$\mu = 1.15 \pm 0.09 \pm 0.01$		$\mu = 1.23 \pm 0.10 \pm 0.01$
		$\nu = 1.22 \pm 0.19 \pm 0.07$ GeV^{-1}	similar	$\nu = 1.15 \pm 0.21 \pm 0.09$ GeV^{-1}

FIT RESULTS FOR BEC PARAMETERS AT 0.9 – 7 TEV

The fit results of the BEC parameters R and λ dependence on the multiplicity, n_{ch}, and the transverse momentum of the pair, k_T, for different functional forms and for different data samples at 0.9 –7 TeV. The errors represent the quadratic sum of the statistical and systematical uncertainties.

BEC param.	Fit function	0.9 TeV	7 TeV Minimum-bias events	7 TeV High-multiplicity events
$R(n_{ch})$	$\alpha \sqrt[3]{n_{ch}}$	$\alpha = 0.64 \pm 0.07$ fm $(n_{ch} \leq 82)$	$\alpha = 0.63 \pm 0.05$ fm $(n_{ch} < 55)$	—
	β	—	$\beta = 2.28 \pm 0.32$ fm $(n_{ch} \geq 55)$	
$\lambda(n_{ch})$	$\gamma\, e^{-\delta n_{ch}}$	$\gamma = 1.06 \pm 0.10$ $\delta = 0.011 \pm 0.004$	$\gamma = 0.96 \pm 0.07$ $\delta = 0.0038 \pm 0.0008$	
$R(k_T)$	$\xi\, e^{-\kappa k_T}$	$\xi = 2.64 \pm 0.33$ fm $\kappa = 1.48 \pm 0.67$ GeV^{-1}	$\xi = 2.88 \pm 0.27$ fm $\kappa = 1.05 \pm 0.58$ GeV^{-1}	$\xi = 3.39 \pm 0.54$ fm $\kappa = 0.92 \pm 0.73$ GeV^{-1}
$\lambda(k_T)$	$\mu\, e^{-\nu k_T}$	$\mu = 1.20 \pm 0.18$ $\nu = 2.00 \pm 0.35$ GeV^{-1}	$\mu = 1.12 \pm 0.10$ $\nu = 1.54 \pm 0.26$ GeV^{-1}	$\mu = 0.75 \pm 0.10$ $\nu = 0.91 \pm 0.45$ GeV^{-1}

SYSTEMATIC UNCERTAINTIES FOR BEC AT 0.9 – 7 TeV

EPJC 75 (2015) 466

- The systematic uncertainties of the inclusive Bose-Einstein correlation parameters, **R** (the effective radius parameter of the source) and **λ** (the strength of the effect parameter), of the *fit of $R_2(Q)$ correlation functions with exponential model* are summarized in the Table.
- The systematic uncertainties are combined by adding them in quadrature and the resulting values are given in the bottom row.
- The same sources of uncertainty are considered for the differential measurements in n_{ch} and the average transverse momentum k_T of a pair, and their impact on the fit parameters is found to be similar in size.

	0.9 TeV		7 TeV		7 TeV (HM)	
Source	λ	R	λ	R	λ	R
Track reconstruction efficiency	0.6%	0.7%	0.3%	0.2%	1.3%	0.3%
Track splitting and merging	negligible		negligible		negligible	
Monte Carlo samples	14.5%	12.9%	7.6%	10.4%	5.1%	8.4%
Coulomb correction	2.6%	0.1%	5.5%	0.1%	3.7%	0.5%
Fitted range of Q	1.0%	1.6%	1.6%	2.2%	5.5%	6.0%
Starting value of Q	0.4%	0.3%	0.9%	0.6%	0.5%	0.3%
Bin size	0.2%	0.2%	0.9%	0.5%	4.1%	3.4%
Exclusion interval	0.2%	0.2%	1%	0.6%	0.7%	1.1%
Total	14.8%	13.0%	9.6%	10.7%	9.4%	10.9%

COMPARISON WITH OTHER EXPERIMENTS

The results of BEC parameters for

Exponential fits of R_2 used total uncertainties

Statistical uncertainties are below 2–4 %

Energy [GeV]	n_{ch}	λ	$R^{(E)}$ [fm]
0.9	≥2	0.74 ± 0.10	1.83 ± 0.25
7	≥2	0.71 ± 0.07	2.06 ± 0.22
7 (HMT)	≥150	0.74 ± 0.06	2.36 ± 0.30
13	≥2	0.88±0.05	2.88±0.05
13 (HMT)	≥93	0.86±0.02	3.31±0.04

Comparison with results of previous experiments

$$R^{(G)} = R^{(E)} / \sqrt{\pi}$$

Energy [GeV]	n_{ch}	$R^{(G)}$ [fm]
0.9	≥2	1.03 ± 0.14
7	≥2	1.16 ± 0.12
7 (HMT)	≥150	1.33 ± 0.17
13	≥2	1.58±0.03
13 (HMT)	≥93	1.87±0.02

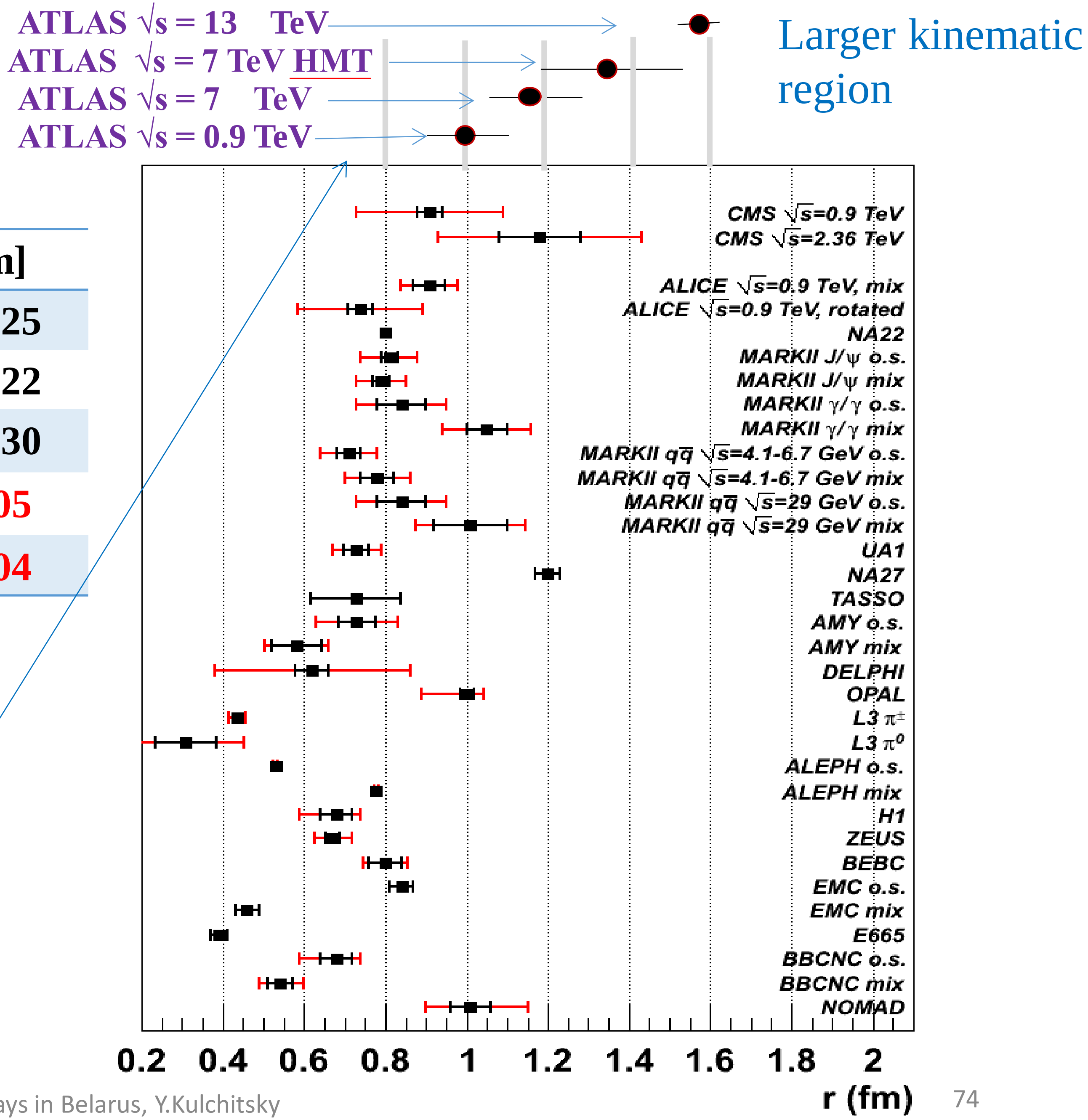

Comparison of multiplicity results with one excluded region 0.5 – 0.9 GeV

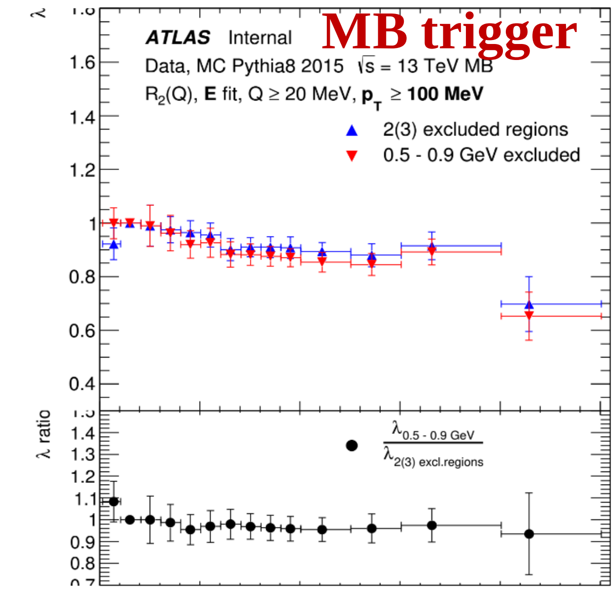

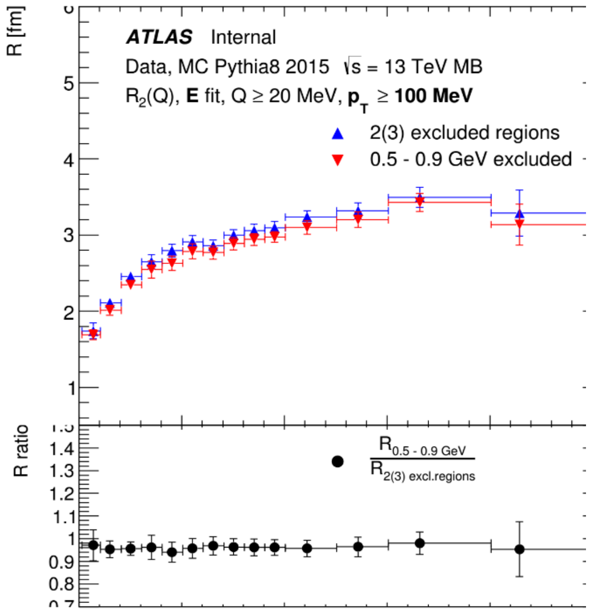

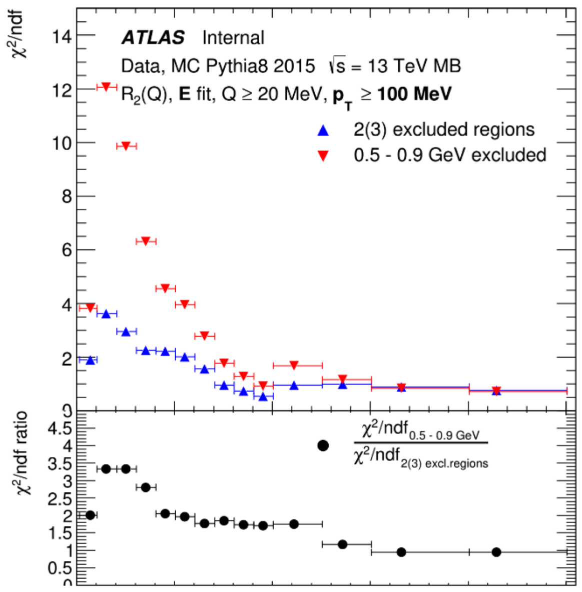

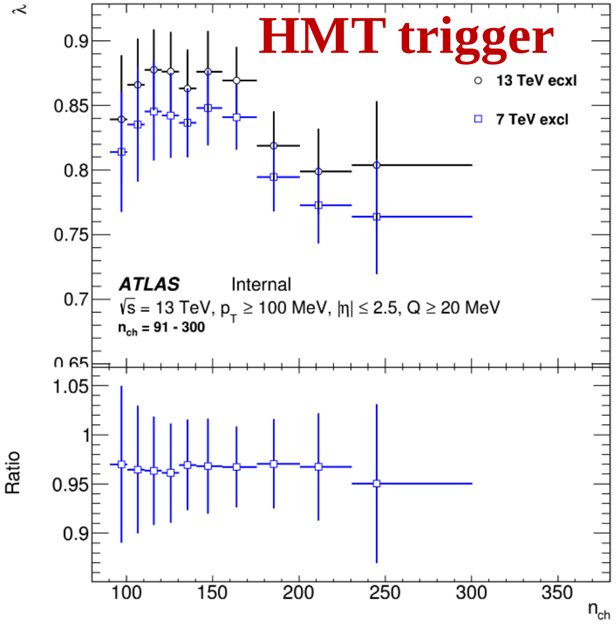

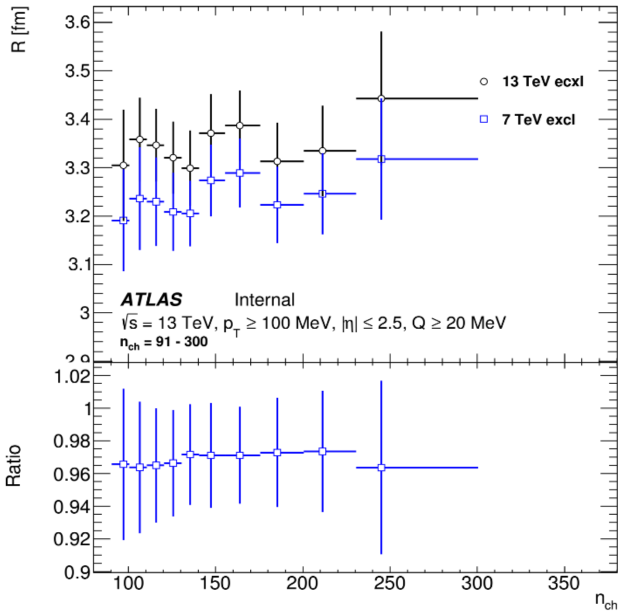

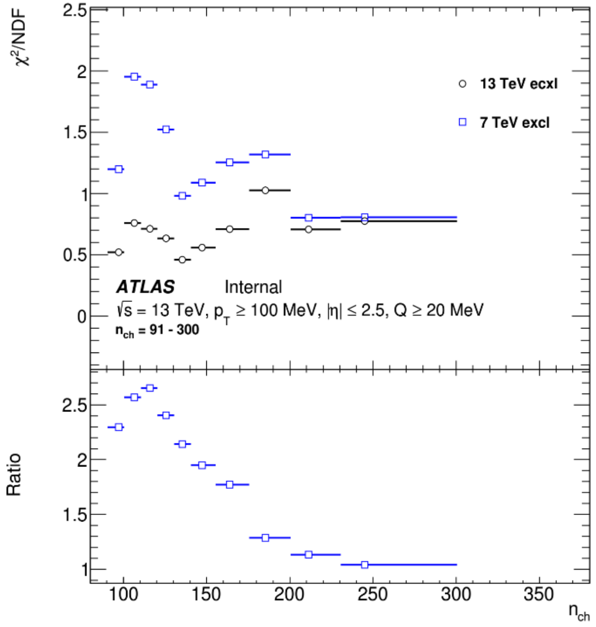

Three bump regions because MC underestimated or overestimates:

1. $\eta \to \pi^+\pi^-\pi^o$ and $\eta' \to \pi^+\pi^-\gamma$;
2. $\omega \to \pi^+\pi^-\pi^o$ and $\rho \to \pi^+\pi^-$,
3. $f_2 \to \pi^+\pi^-$;

The excluded regions at 13 TeV are

1. 0.2–0.3 GeV – not important after non-closure correction;
2. 0.4–0.9 GeV – important;
3. 1.0–1.16 GeV (only for $2 \leq n_{ch} \leq 40$ and $100 \leq k_T \leq 200$ MeV) – not important for BEC.

The excluded region at 7 TeV is 0.5–0.9 GeV.

BEC parameters are in a good agreement in error bars but χ^2/ndf more higher

MULTIPLICITY DEPENDENCE OF BEC PARAMETERS FOR DIFFERENT MC

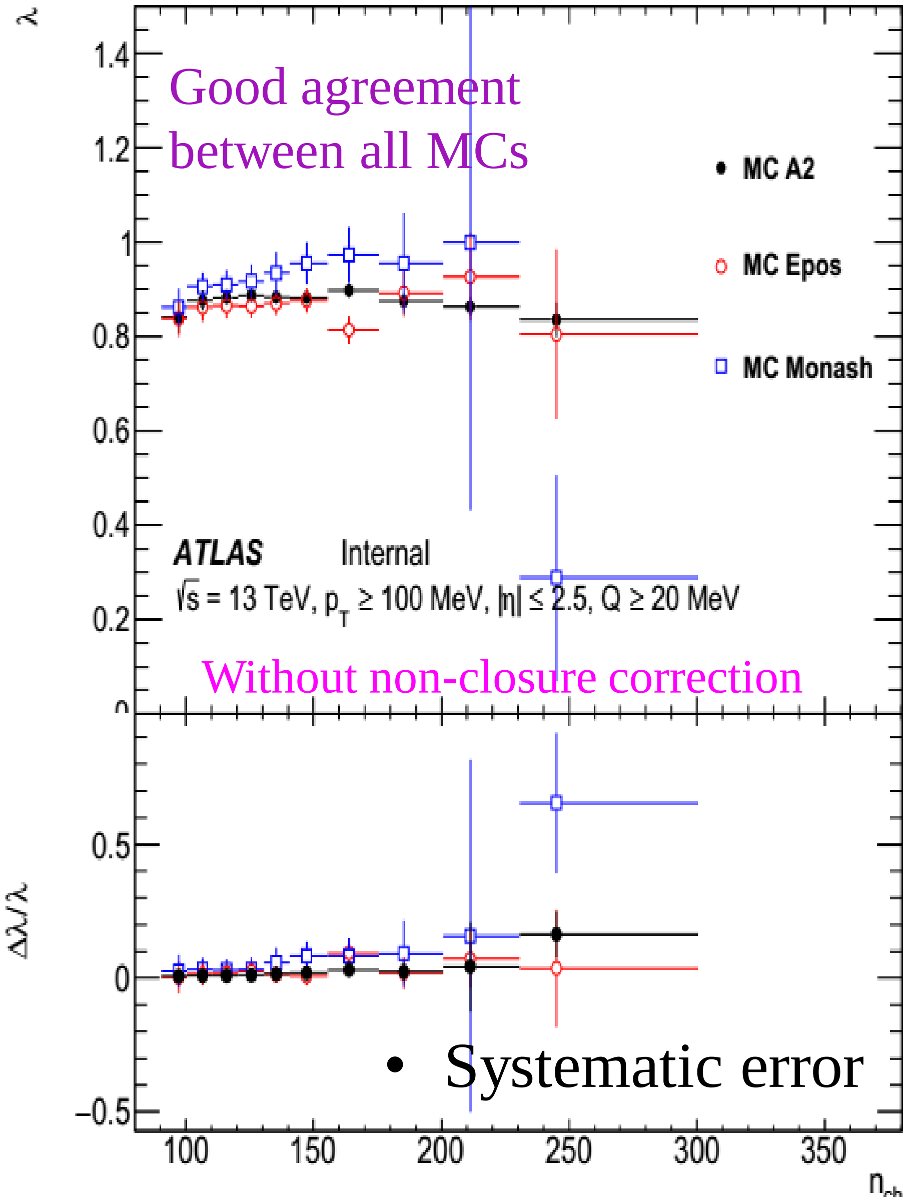

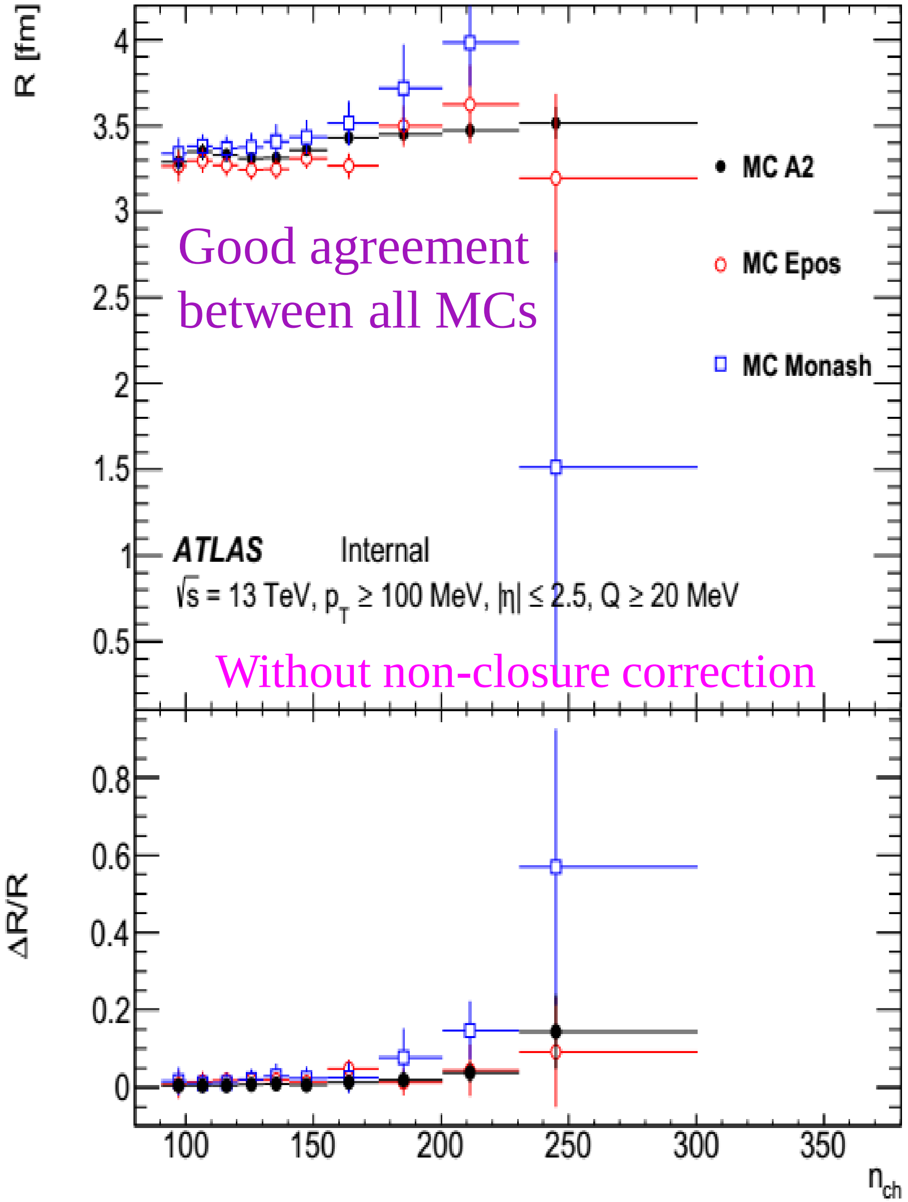

HMT trigger

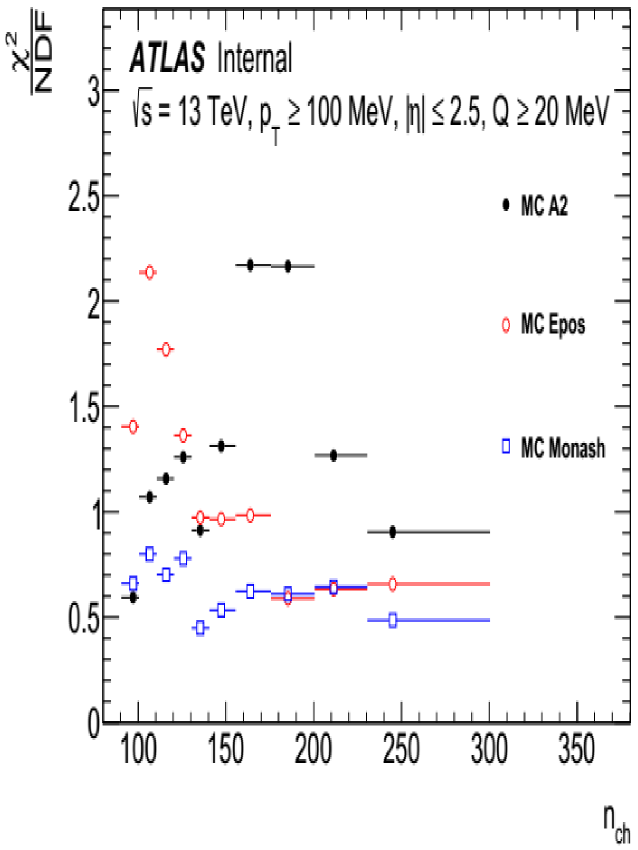

Radius **saturation effect** for all MCs for high multiplicity region

Information about MC samples are given in the Backup slides

Comparison of k_T results with one excluded region 0.5 – 0.9 GeV

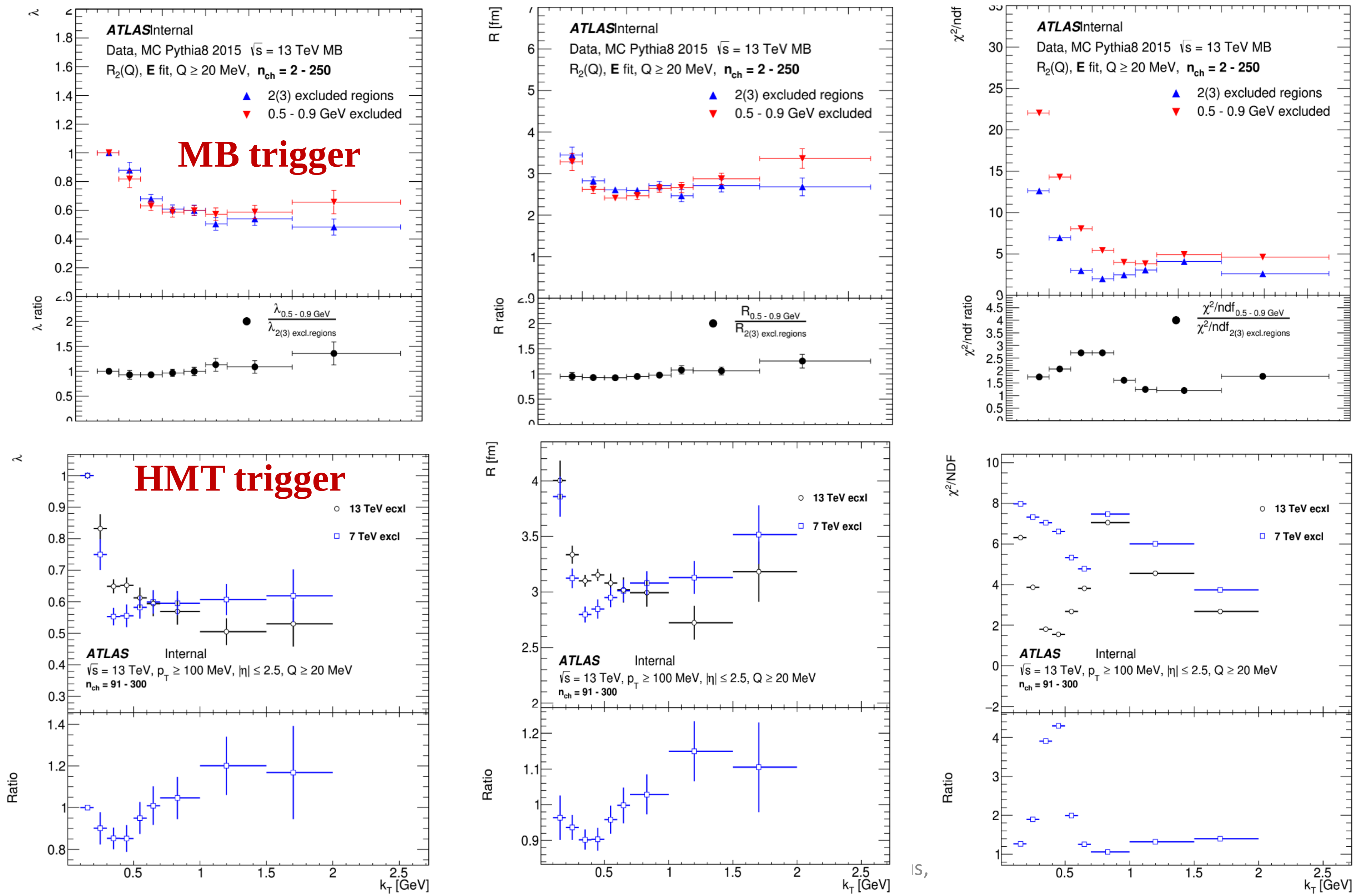

Three bump regions because MC underestimated or overestimates:

1. $\eta \to \pi^+\pi^-\pi^o$ and $\eta' \to \pi^+\pi^-\gamma$;
2. $\omega \to \pi^+\pi^-\pi^o$ and $\rho \to \pi^+\pi^-$,
3. $f_2 \to \pi^+\pi^-$;

The excluded regions at 13 TeV are

1. 0.2–0.3 GeV – not important after non-closure correction;
2. 0.4–0.9 GeV – important;
3. 1.0–1.16 GeV (only for $2 \leq n_{ch} \leq 40$ and $100 \leq k_T \leq 200$ MeV) – not important for BEC.

The excluded region at 7 TeV is 0.5–0.9 GeV.

BEC parameters are in a good agreement in error bars but χ^2/ndf more higher

k_T DEPENDENCE OF BEC PARAMETERS FOR DIFFERENT MC

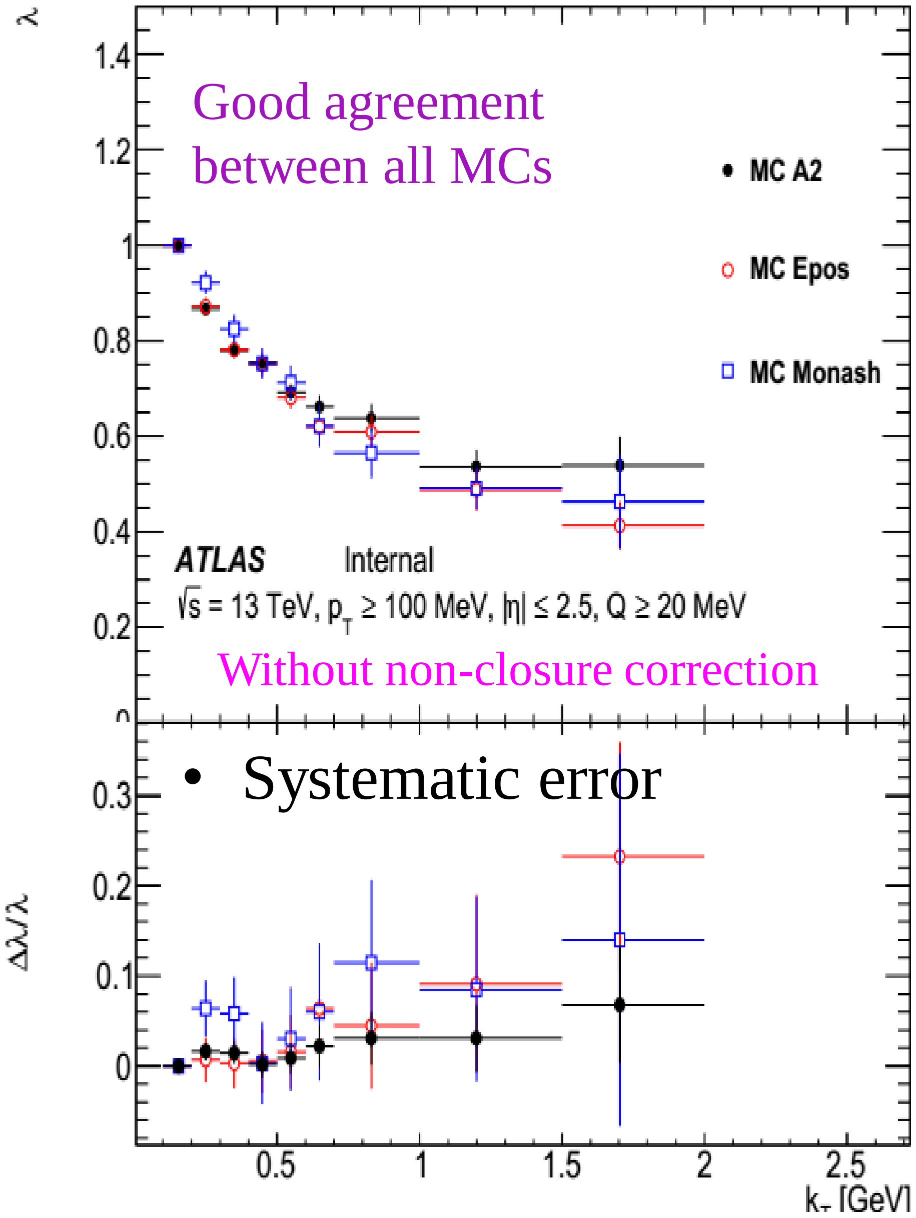

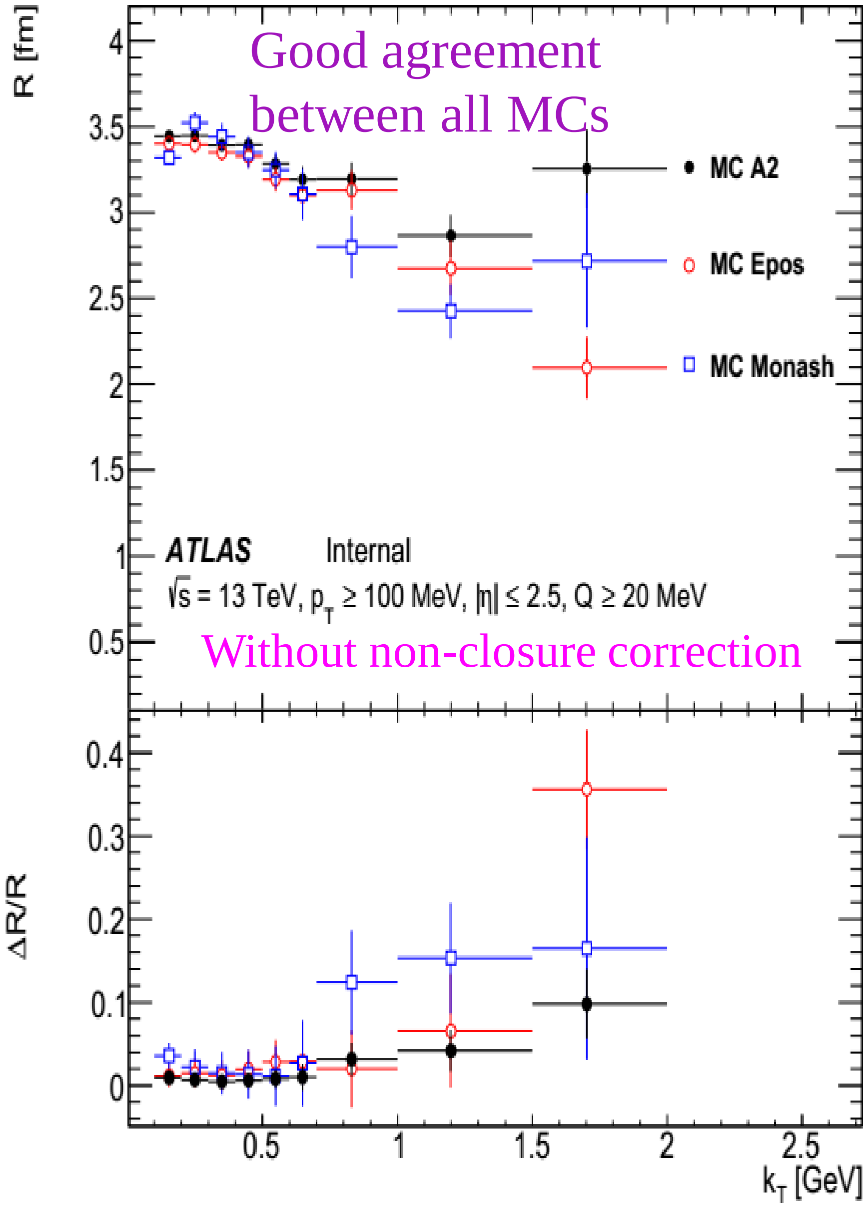

HMT trigger

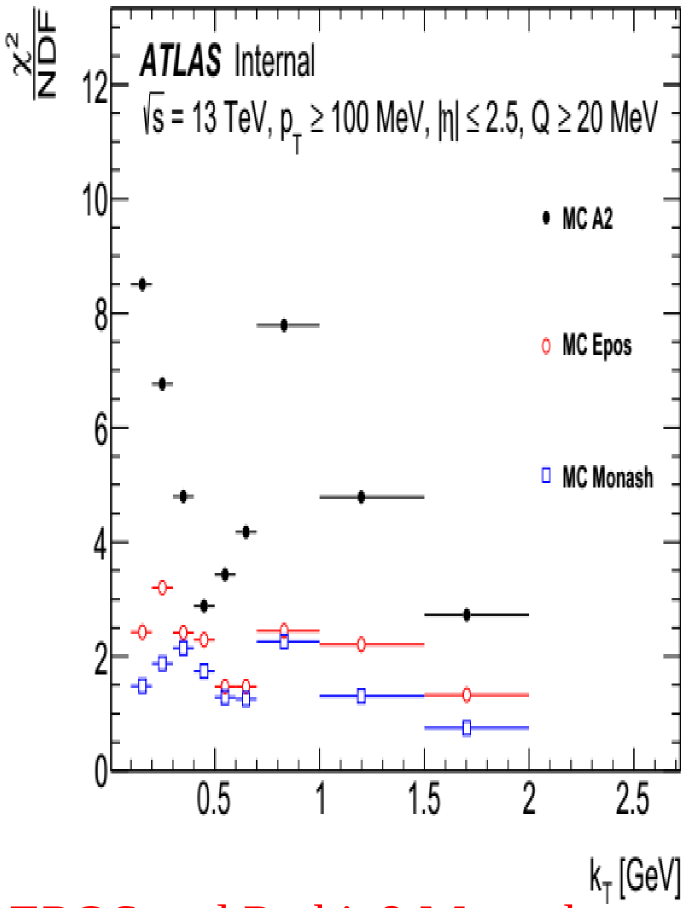

EPOS and Pythia8 Monash – more exponential distribution for BEC radius for high multiplicity region

Information about MC samples are given in the Backup slides

MULTIPLICITY DEPENDENCE OF λ AND R BEC PARAMETERS AT 0.9, 7 TEV

EPJC 75 (2015) 466

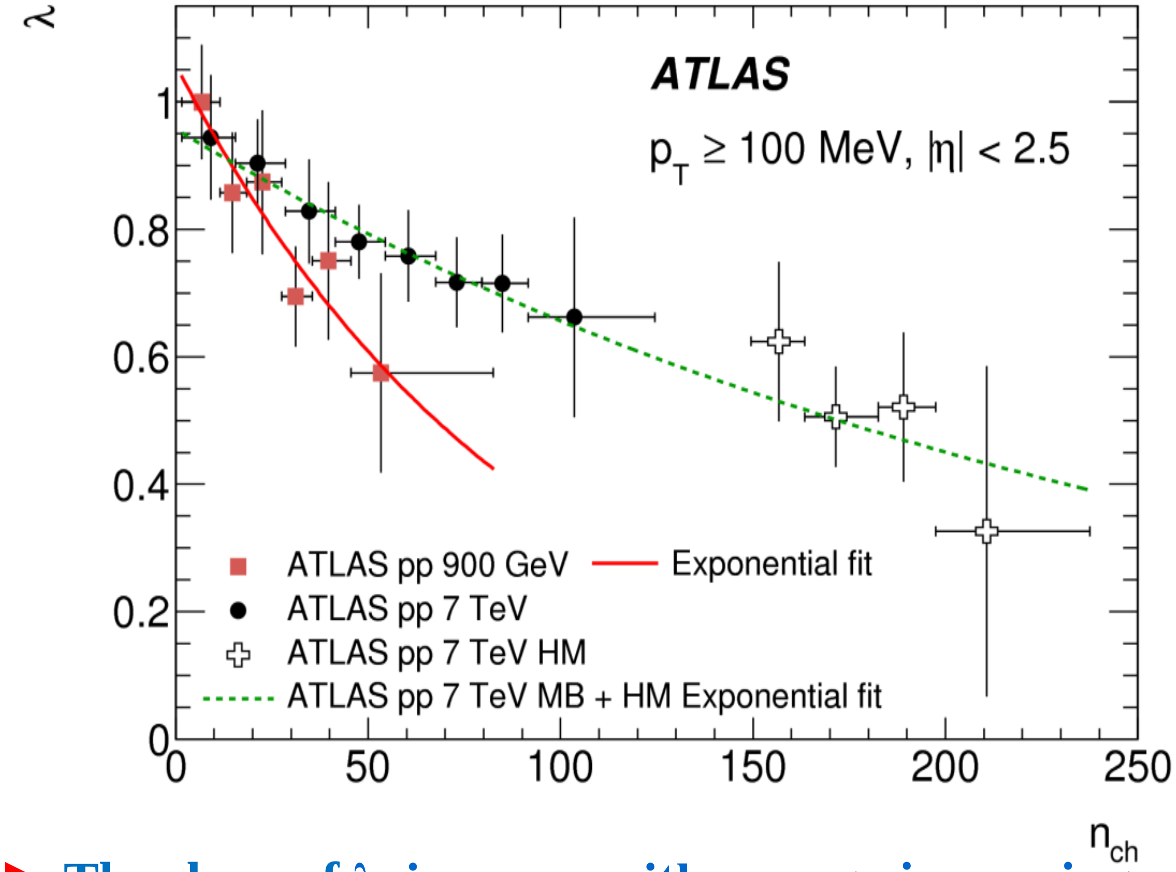

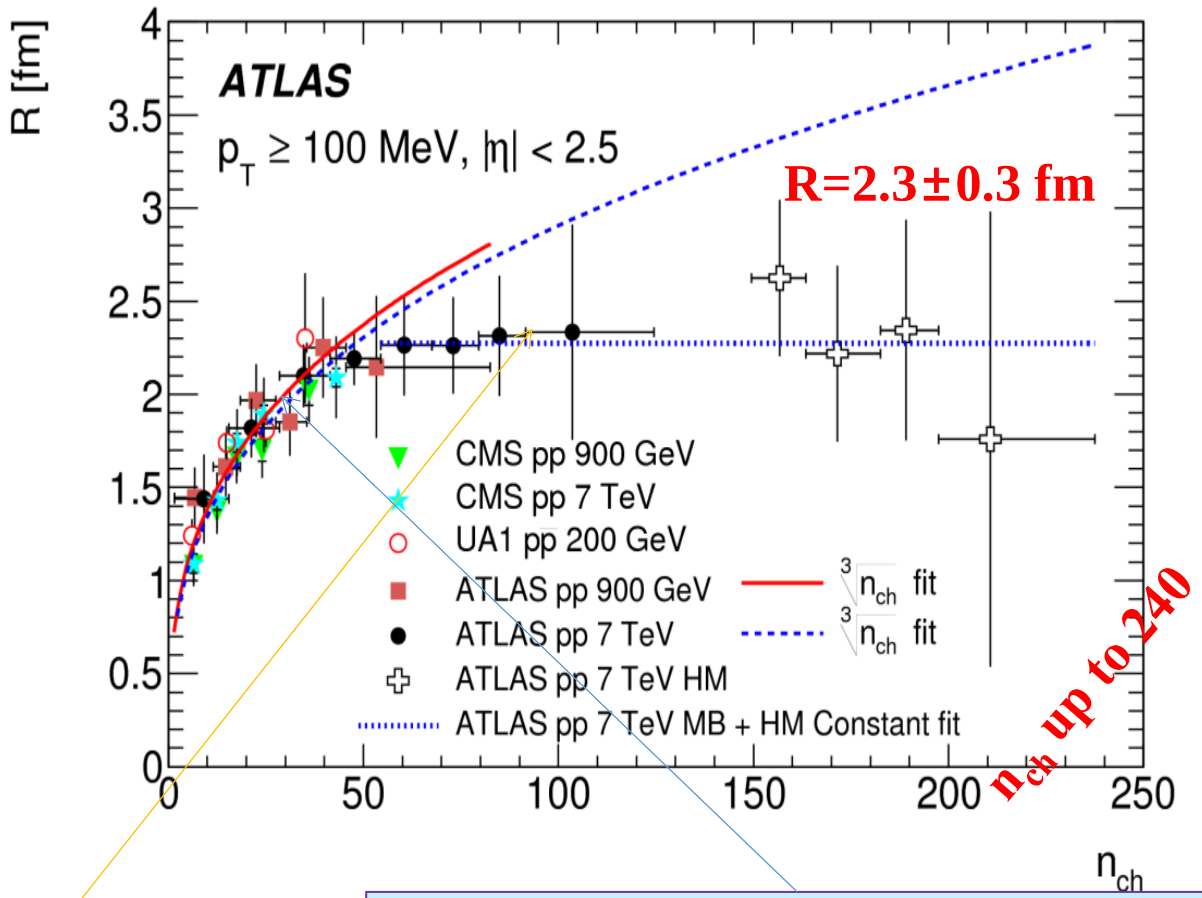

- ► **The slope of λ increase with energy increasing**
- ► **The R are energy independent within the uncertainties**
- ► The λ **exponentially decrease with multiplicity**

Good Agreement with CMS & UA1

- ► R of the **$\alpha \cdot n_{ch}^{1/3}$** fit for ***$n_{ch} \leq 55$: 0.9 TeV is α=0.64 ±0.07 fm, 7 TeV is α=0.63 ±0.05 fm***
- ► **R** is a ***Constant*** for **n_{ch}>55** at 7 TeV ***R=2.28 ±0.32 fm*** **observed for the first time**

THEORY PREDICTION FOR R PARAMETER OF BEC

V.A.Shegelsky, et al, Pomeron universality from identical pion correlations at the LHC, Phys.Letter B703 (2011) 288.
M.G.Ryskin, V.A.Shegelsky, Nucl.Phys B219 (2011) 10.

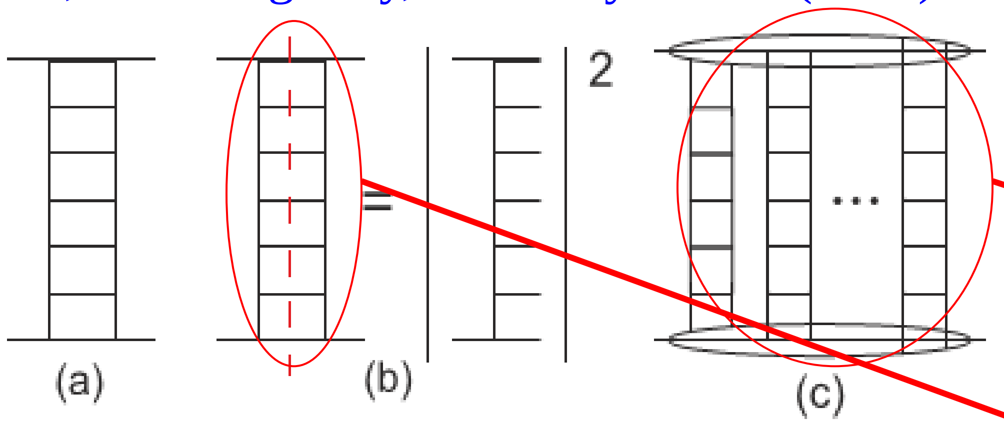

The ladder diagram for one-Pomeron exchange; (b) cutting one-Pomeron exchange leads to the multiperipheral chain of final state particles; (c) a multi-Pomeron exchange diagram.

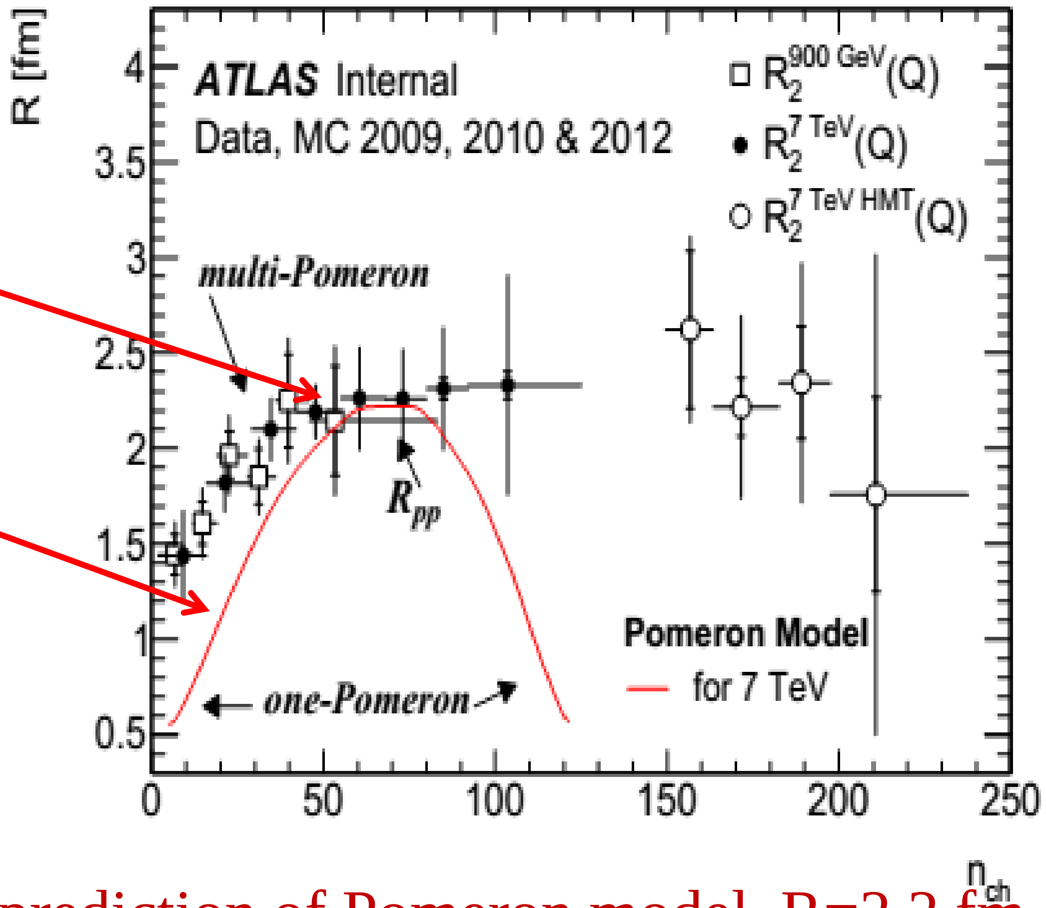

Interpretation: ► The BEC radius for one parton-parton interaction (underline events, cut Pomeron) is ~1 fm, like for smallest multiplicity. ►For high multiplicity events we see BEC signal from some parton-parton interactions. ►The radius for high multiplicity can be interpret as an average distance between separate parton-parton interactions is ~2 fm.

The prediction of Pomeron model R=2.2 fm is in agreement with saturated radius R=2.3 fm at 7 TeV for middle multiplicity region. There is not agreement with data for n_{ch}>80.

BEC PARAMETERS R AND λ VS k_T AT 0.9, 7 TEV

EPJC 75 (2015) 466

λ distribution at 7 TeV

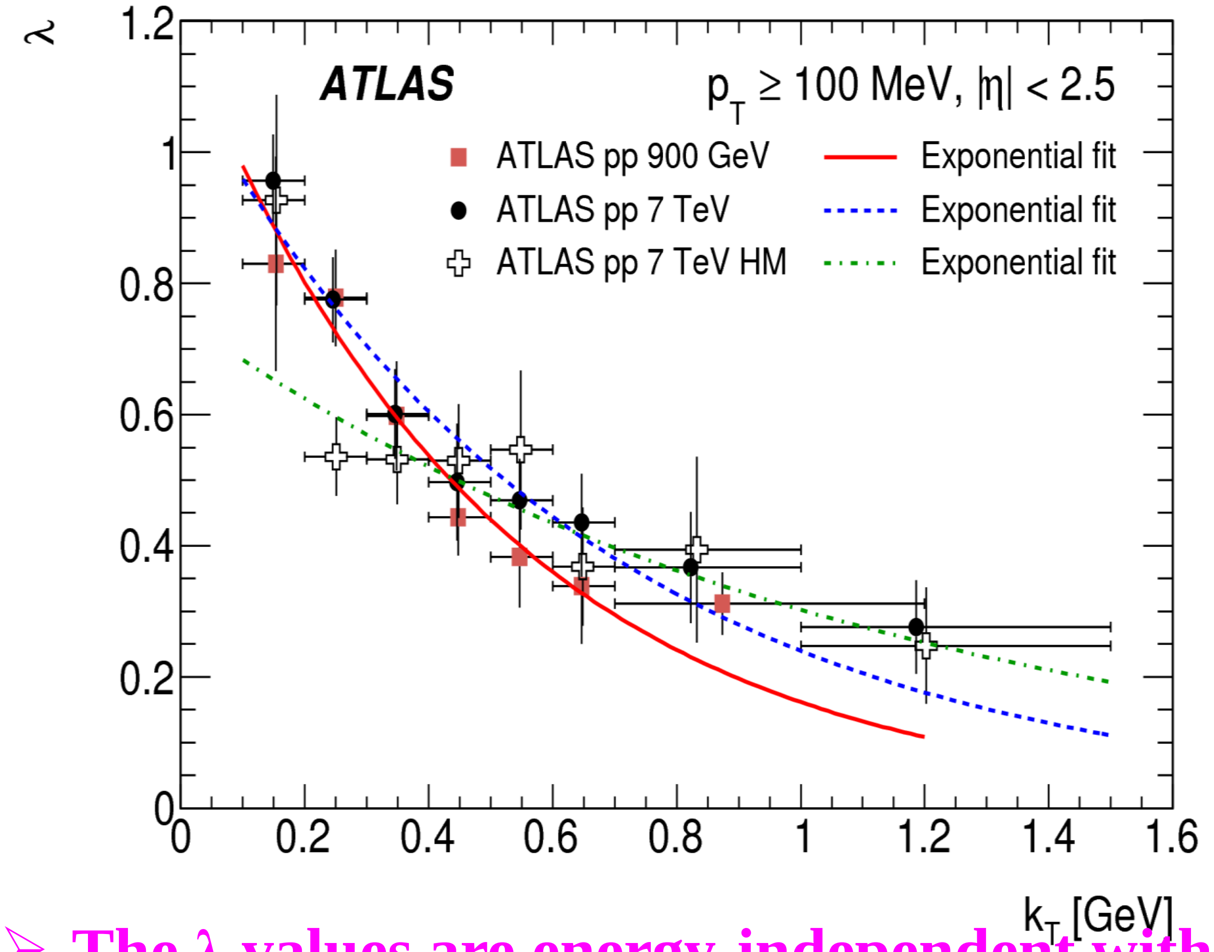

R distribution at 7 TeV

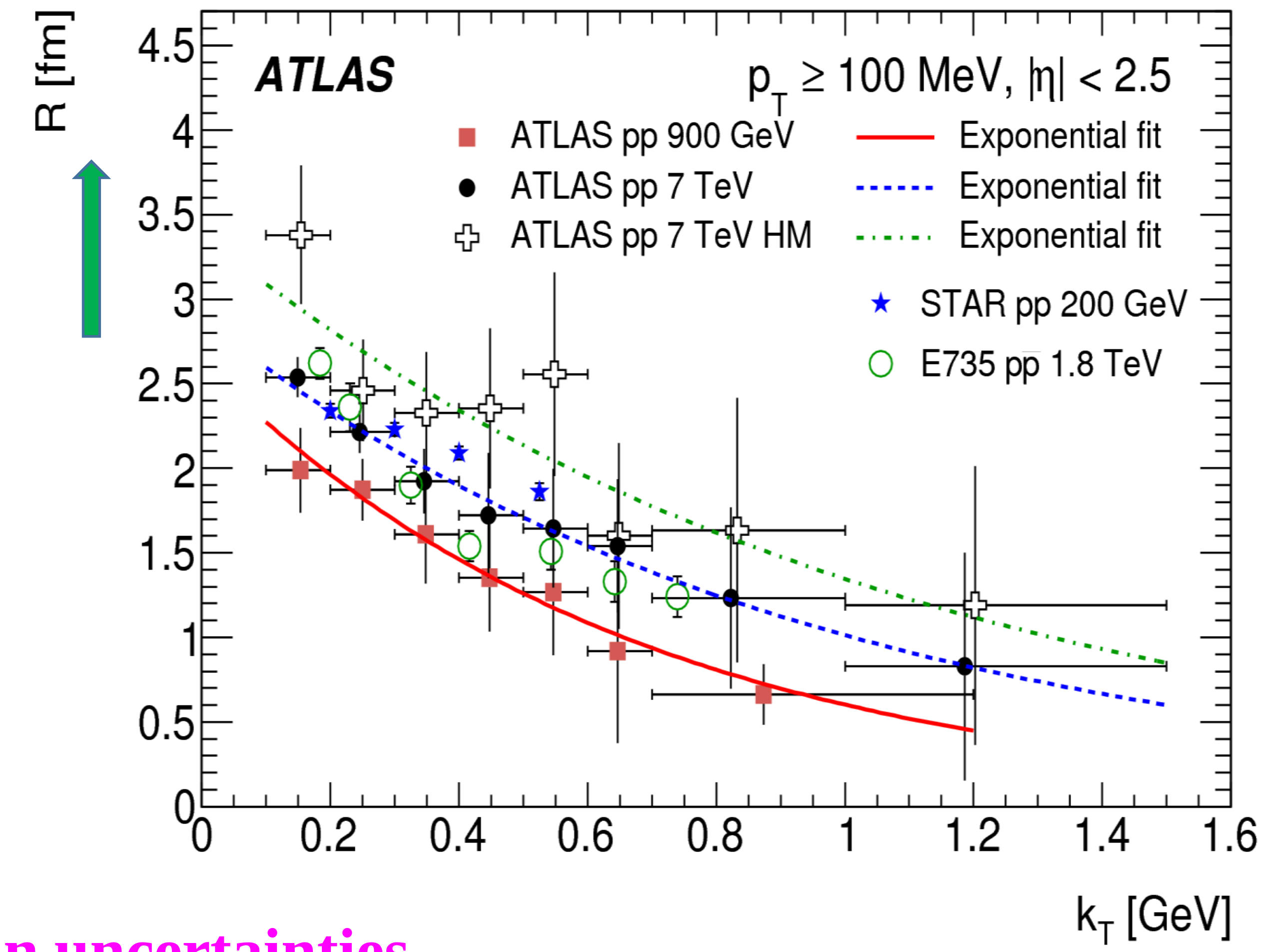

- **The λ values are energy-independent within uncertainties**
- **The R values increase with increasing multiplicity**
- **The λ and R values decrease exponentially with k_T**

k_T DEPENDENCE OF χ^2/NDF FOR (N_{CH}, k_T) INTERVALS

χ^2/ndf distribution at 13 TeV **HMT trigger** χ^2/ndf distribution at 13 TeV

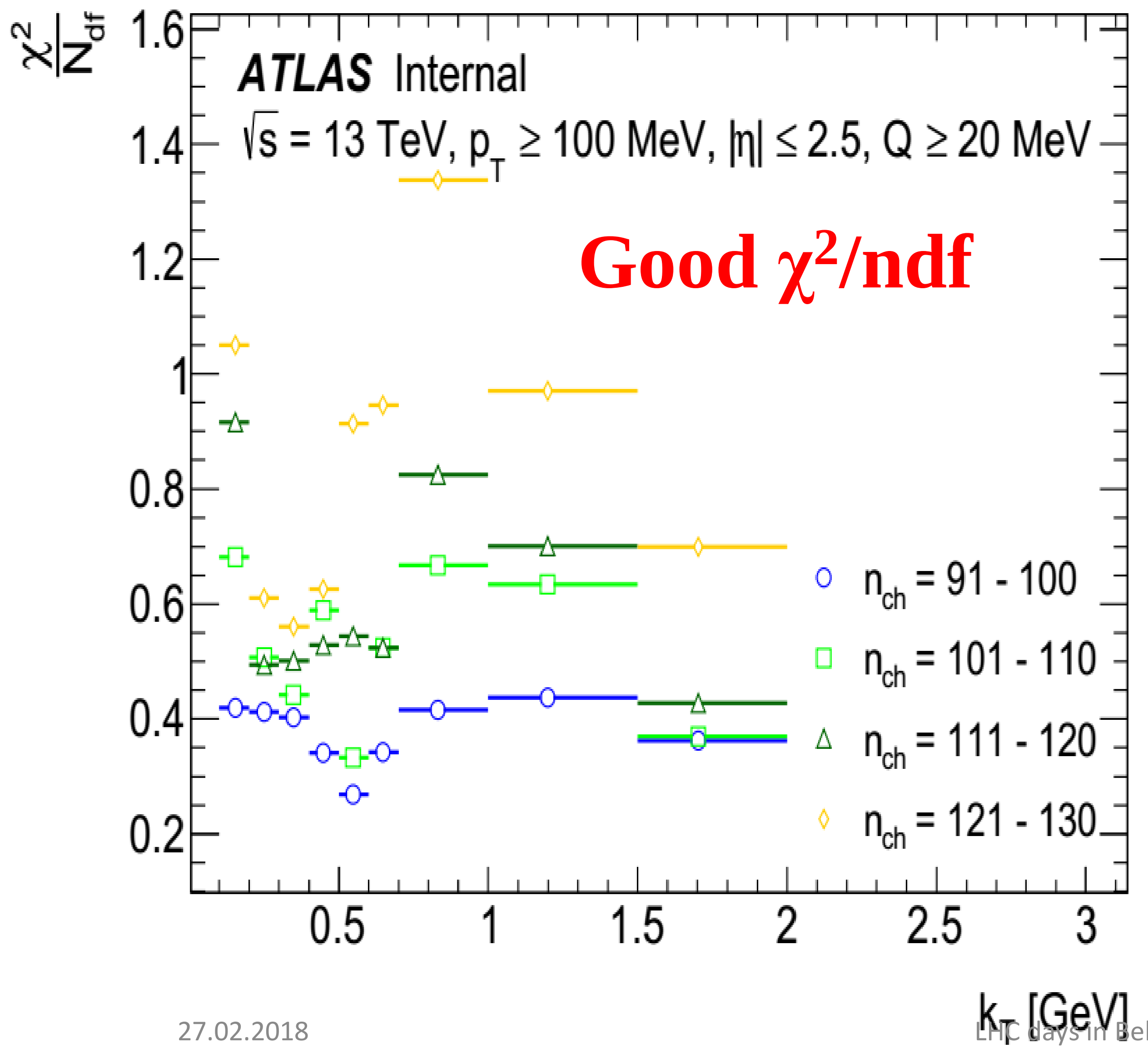

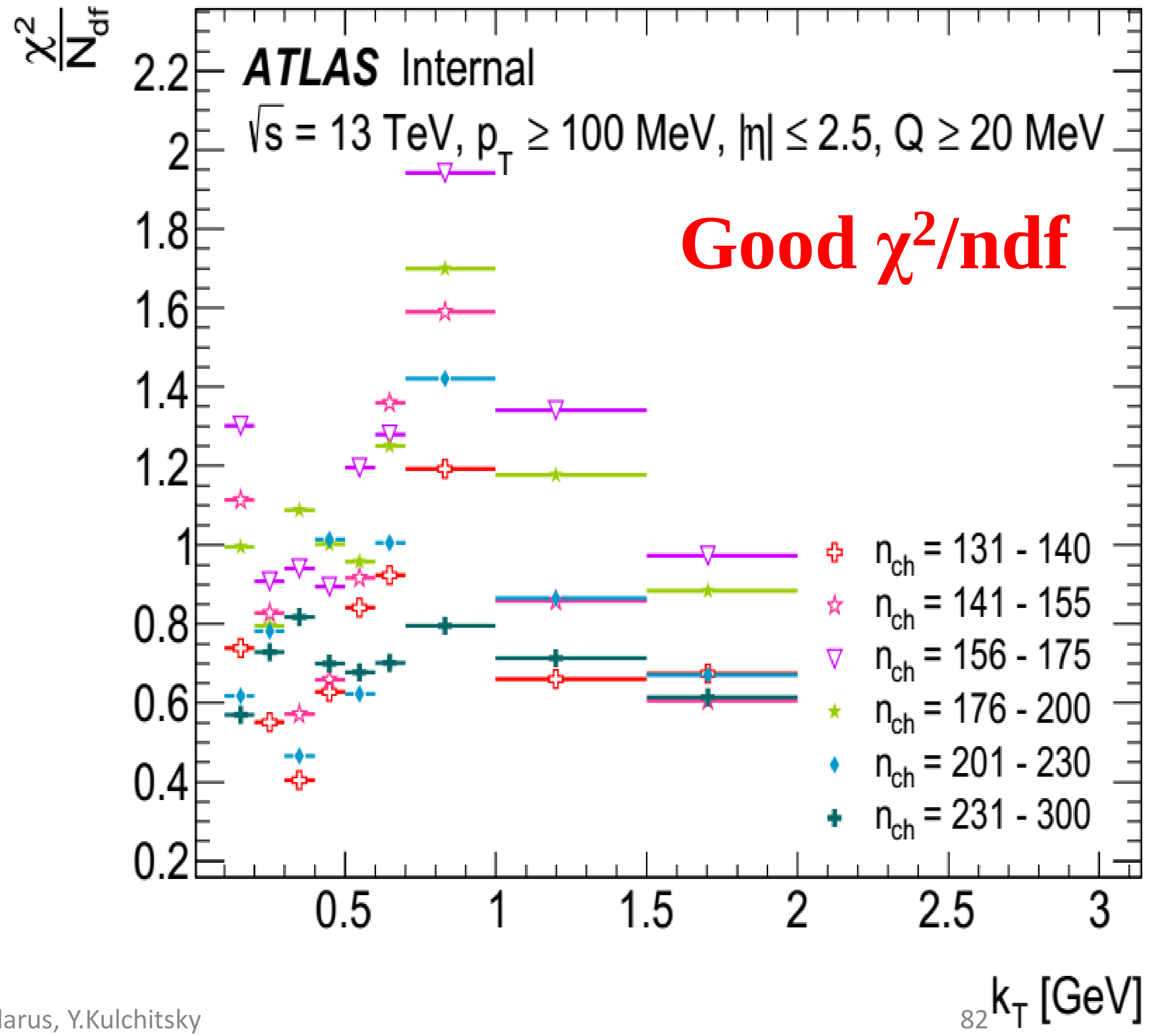

k_T DEPENDENCE OF BEC PARAMETERS

λ distribution at 13 TeV   **MB + HMT triggers**   R distribution at 13 TeV

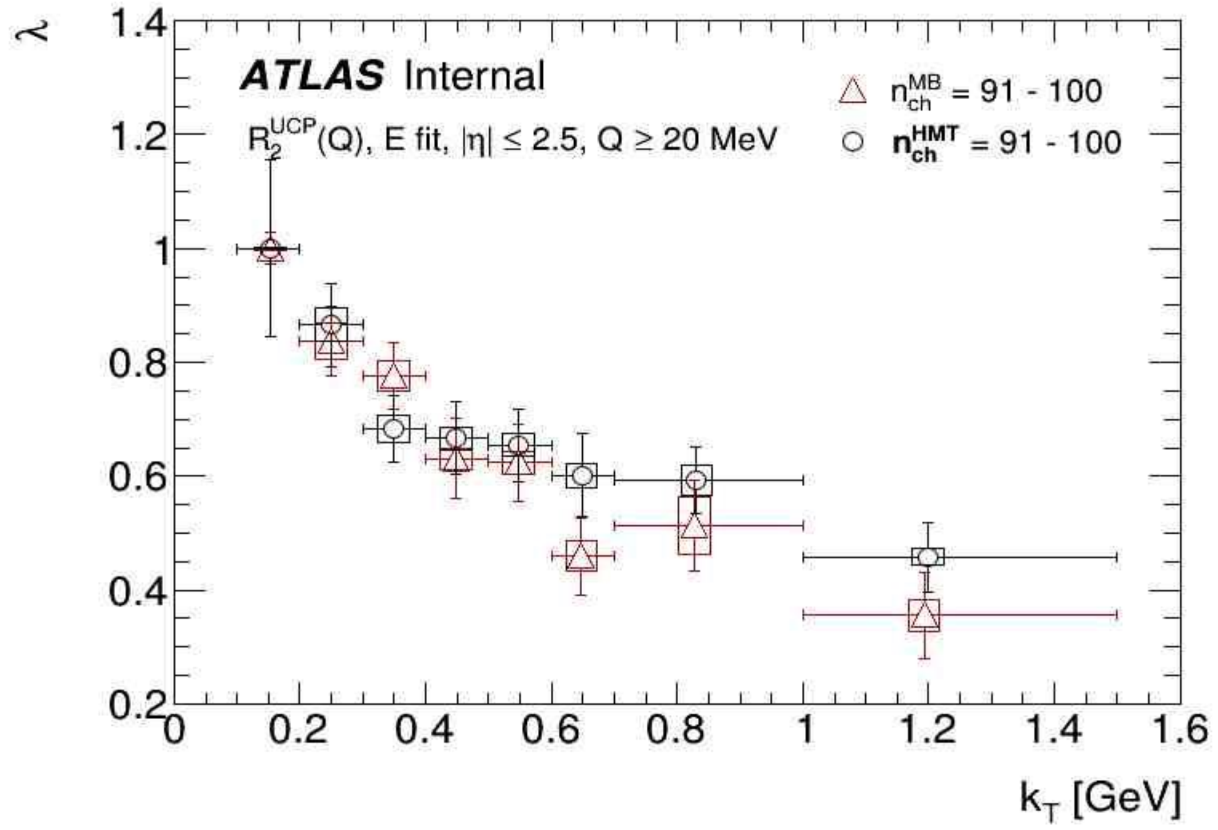

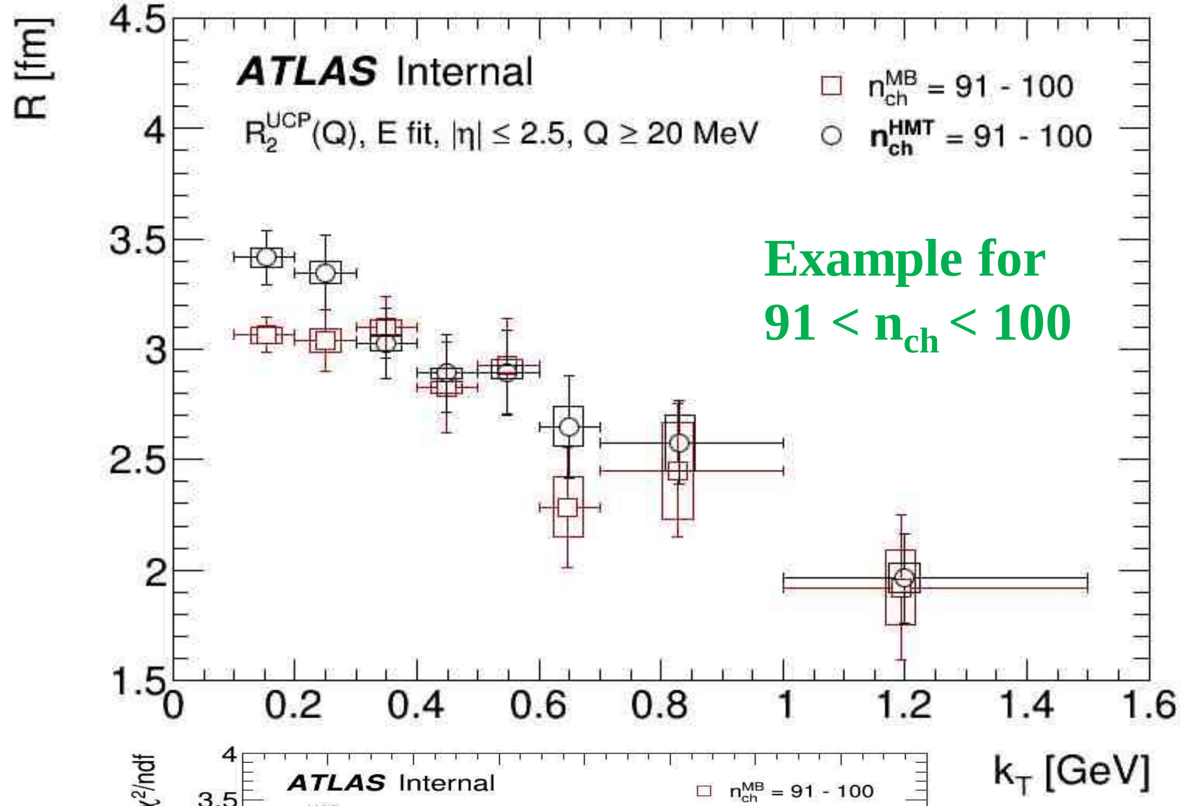

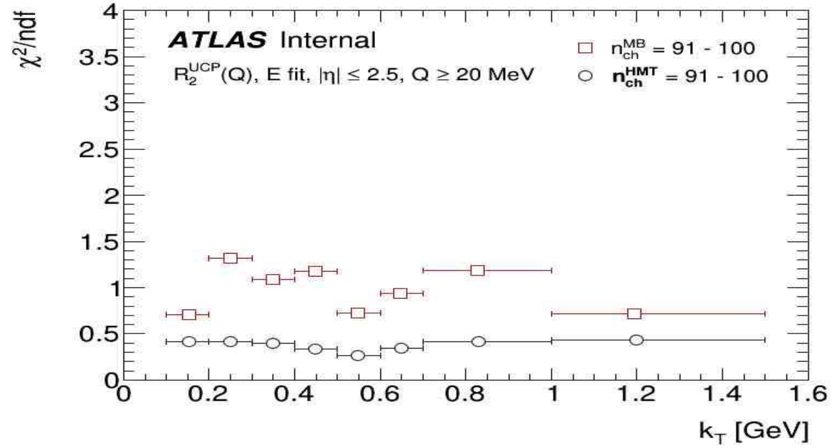

- Agreement between MB and HMT results
- The λ values decreases exponentially in dependence of k_T
- The R values decreases exponentially in dependence of k_T

k_T dependence of BEC parameters at 0.9 – 13 TeV

EPJC 75 (2015) 10, 466; ATL-COM-PHYS-2016-1621

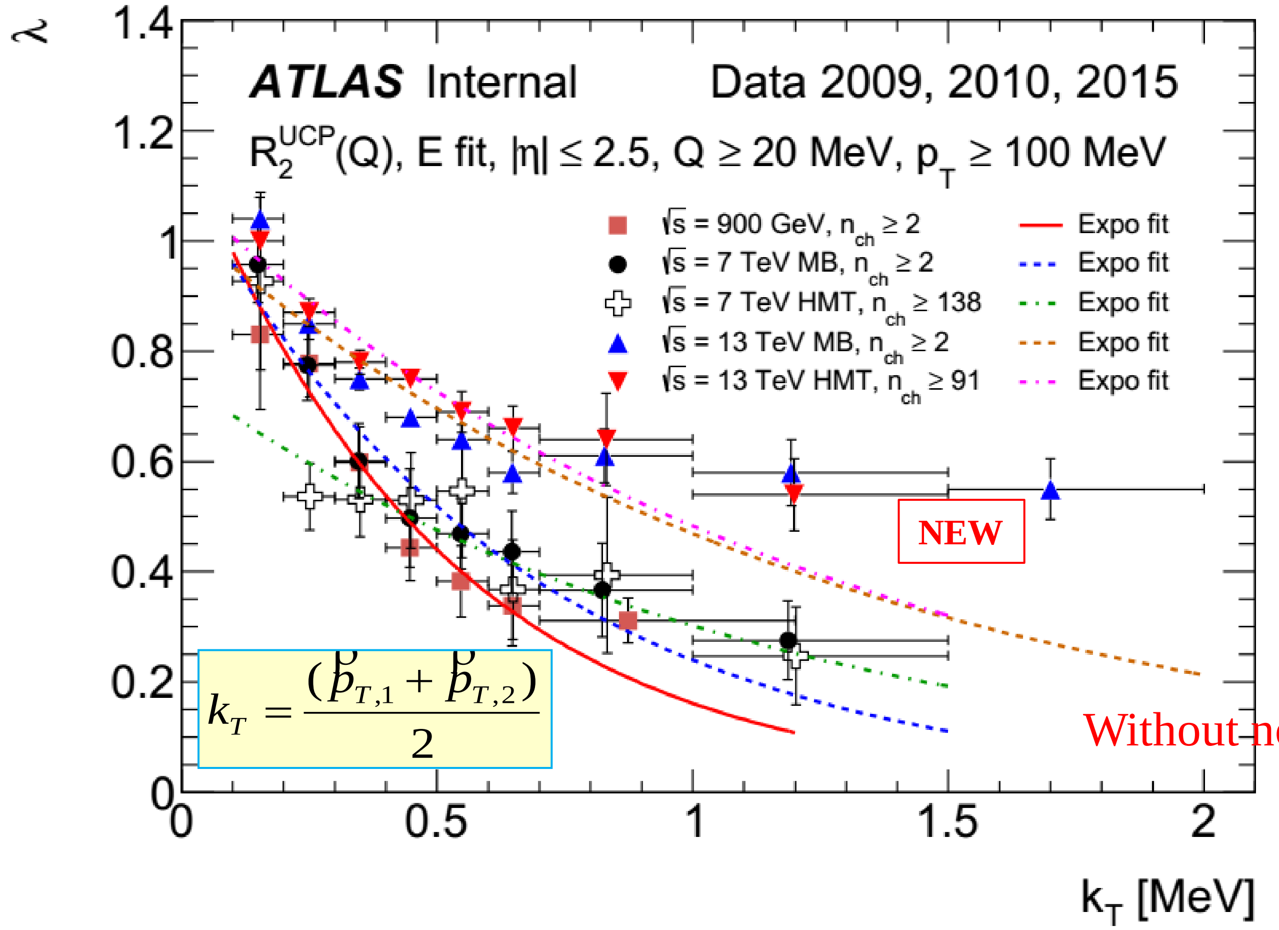

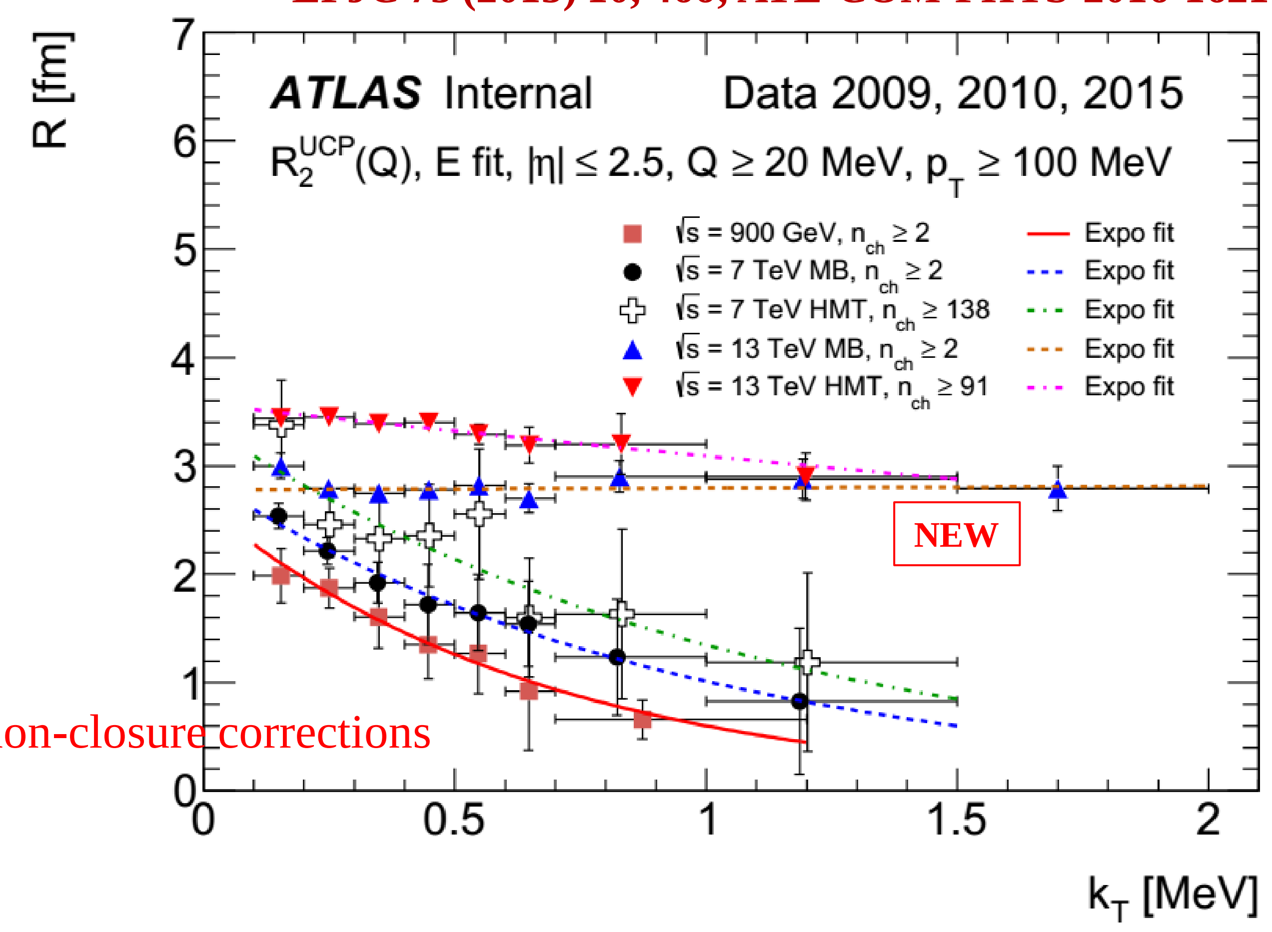

Without non-closure corrections

- The λ values are (trigger) multiplicity-independent within uncertainties at 13 TeV
- The R values increase with increasing multiplicity region (trigger)
- The λ values decrease exponentially with k_T
- The R values decrease exponentially with k_T for HMT events

RESONANCES STUDY AT 13 TEV

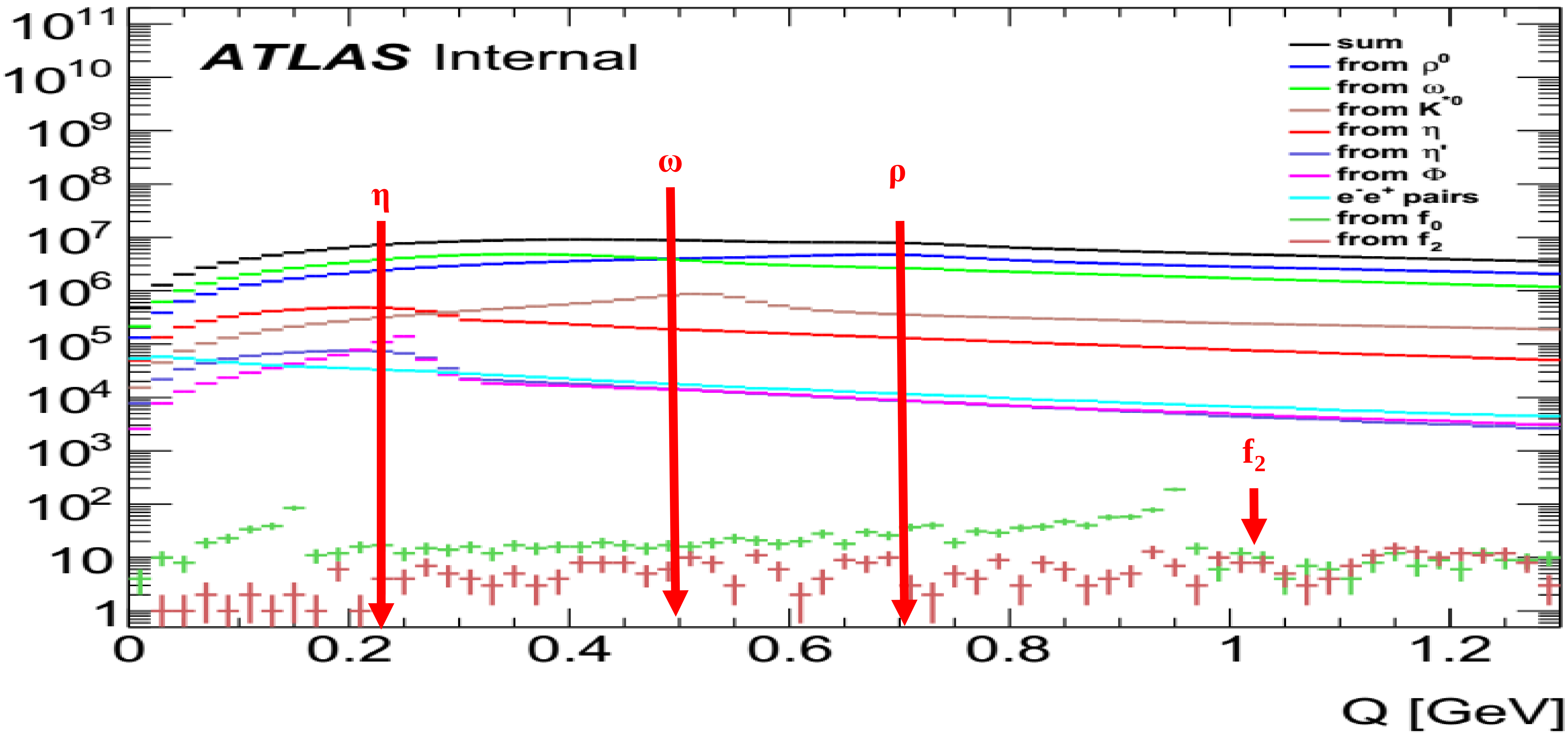

The Q spectrum generated by Pythia8 and the decomposition of its resonant part into leading contributions.

MULTIPLICITY DEPENDENCE OF χ^2/NDF FOR (N_{CH}, K_T) INTERVALS

χ^2/ndf distribution at 13 TeV

MB trigger

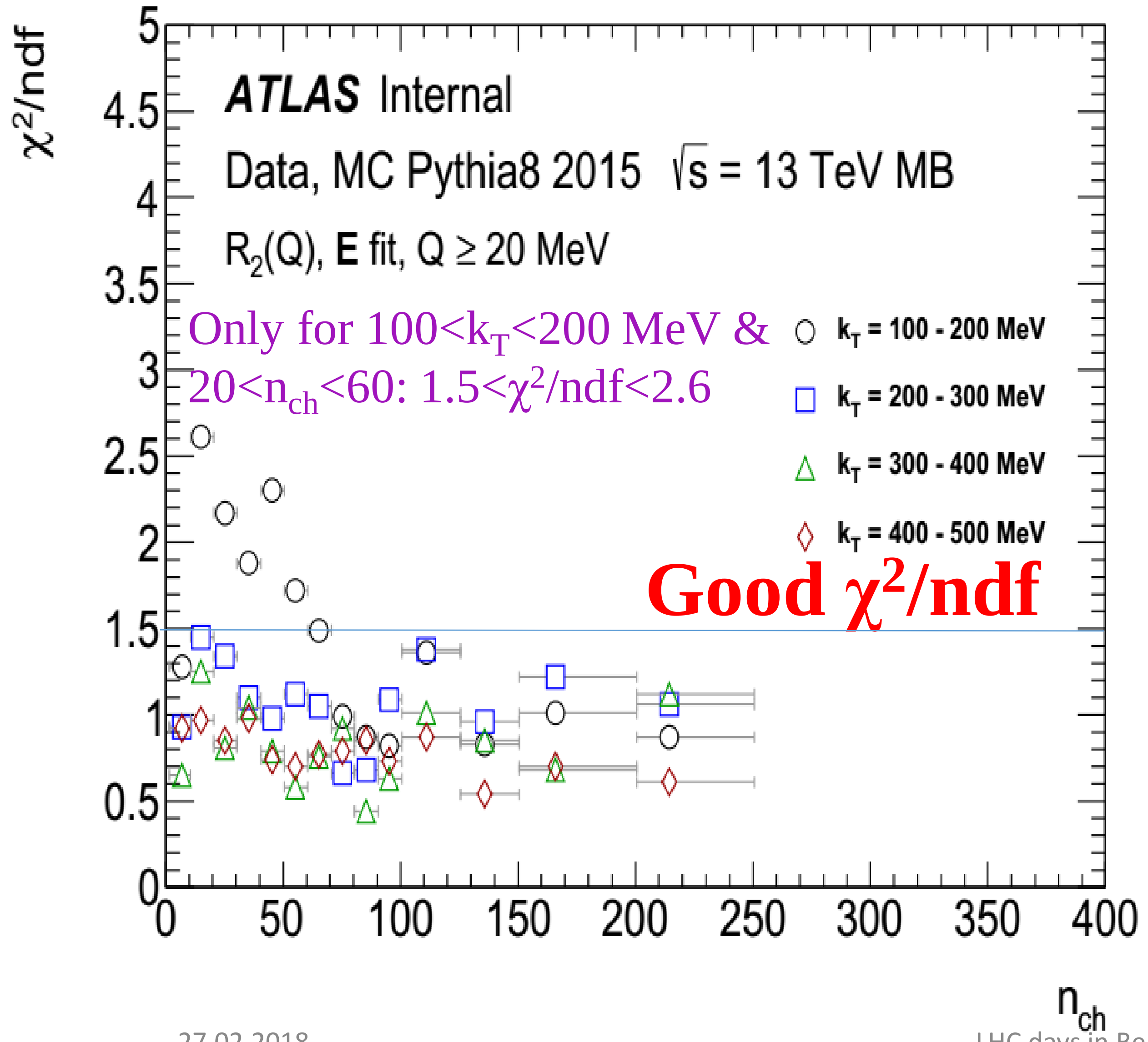

χ^2/ndf distribution at 13 TeV

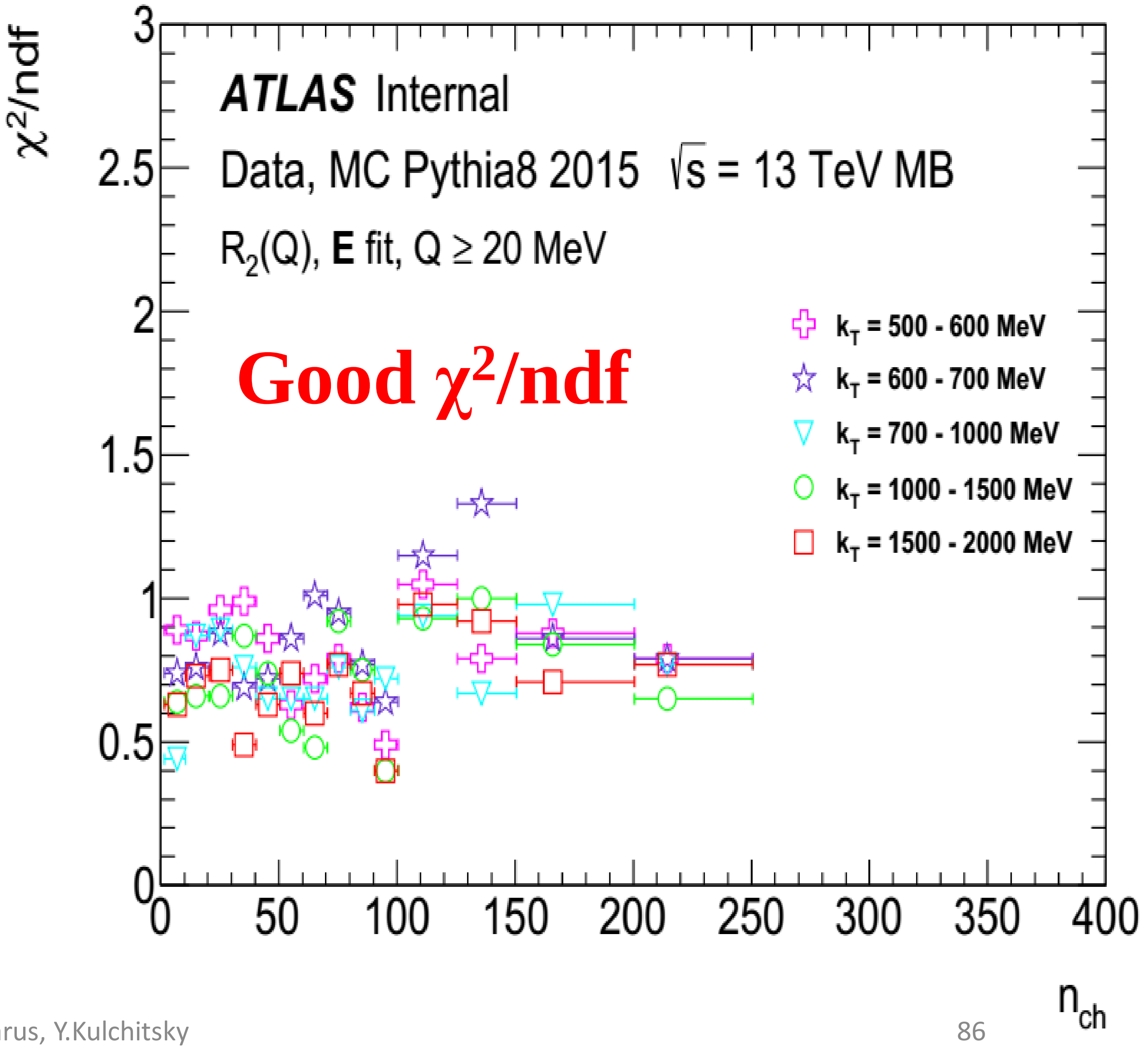

MULTIPLICITY DEPENDENCE OF χ^2/NDF FOR (N_{CH}, K_T) INTERVALS

χ^2/ndf distribution at 13 TeV **HMT trigger** χ^2/ndf distribution at 13 TeV